INFORMATION TO USERS

This manuscript has been reproduced from the microfilm master. UMI films the text directly from the original or copy submitted. Thus, some thesis and dissertation copies are in typewriter face, while others may be from any type of computer printer.

The quality of this reproduction is dependent upon the quality of the copy submitted. Broken or indistinct print, colored or poor quality illustrations and photographs, print bleedthrough, substandard margins, and improper alignment can adversely affect reproduction.

In the unlikely event that the author did not send UMI a complete manuscript and there are missing pages, these will be noted. Also, if unauthorized copyright material had to be removed, a note will indicate the deletion.

Oversize materials (e.g., maps, drawings, charts) are reproduced by sectioning the original, beginning at the upper left-hand corner and continuing from left to right in equal sections with small overlaps. Each original is also photographed in one exposure and is included in reduced form at the back of the book.

Photographs included in the original manuscript have been reproduced xerographically in this copy. Higher quality 6" x 9" black and white photographic prints are available for any photographs or illustrations appearing in this copy for an additional charge. Contact UMI directly to order.

UMI

A Bell & Howell Information Company
300 North Zeeb Road, Ann Arbor MI 48106-1346 USA
313/761-4700 800/521-0600

UPGRADING OF GOLD GRAVITY CONCENTRATES
A STUDY OF
THE KNELSON CONCENTRATOR

Liming Huang

**A thesis submitted to the Faculty of Graduate
Studies and Research in partial fulfillment of
the requirements for the Degree of Philosophy**

**Department of Mining and Metallurgical
Engineering, McGill University
Montreal, Canada**

0-612-29960-0

ABSTRACT

In recent years, the Knelson Concentrator has become the predominant unit used for primary gold recovery by gravity. However, its application potential as a cleaner in the final gravity concentration stage and its separation mechanisms have not been well studied. In most Canadian gold mills, rougher gravity concentrates produced by the Knelson (operating at 60 gravity acceleration or 'g') are further upgraded with shaking tables, non-centrifuge units operating at one 'g'. As a result, tabling results in significant gold losses (mainly fines). It is also labour intensive and represents a security risk because of the high gold content of the material being processed. The main objectives of this research, therefore, are to study the separation mechanisms of the Knelson Concentrator and to explore its potential application as a cleaner to supplement, or even to replace, tabling.

A methodology based on the use of synthetic feeds (tungsten, silica and magnetite) was designed to study the performance and mechanisms of a 7.5 cm Knelson. Four types of gangue were used, both fine and coarse silica and magnetite. The fluidization water flowrate was optimized for each gangue type, and the Knelson was then overloaded by feeding a high-grade feed. The extent of overload was found to be highly dependent on the size distribution and density of the gangue processed, from severe and immediate with coarse magnetite to non-existent with fine silica. A two-parameter model to describe the overload was derived, which showed a good fit with the experimental data.

Two separable bowls were designed to analyze the nature of the material recovered in the five grooves of the Knelson bowl. It was found that the densest minerals, such as tungsten and gold, were mainly recovered in the inner groove sections, closest to the rotating axis. The outer sections packed at the beginning of the recovery cycle and served mostly to distribute fluidization water evenly.

Three modified Knelson bowls, a cleaner bowl equipped with a filter at the bottom of each groove, the other two with different groove depth and fluidization water flowrate distribution, were tested using the synthetic feed methodology. Results generally confirmed the soundness of the basic designs of the conventional and cleaning bowls. The importance of superficial fluidization water velocity was also demonstrated.

Recovery of gold with the 7.5 cm Knelson from seven samples of gold table tails from different Canadian gold mills was tested. Recovery significantly increased when the coarser, largely barren fraction was removed prior to processing. Concentrate grade significantly increased, up to 60% Au, by feeding a magnetite "filler" prior to the recovery cycle, and removing it magnetically at the end of the test, to mimic the effect of the cleaner bowl.

RÉSUMÉ

Le Concentrateur Knelson, un centrifuge, est devenu l'appareil le plus utilisé pour la récupération gravimétrique de l'or, à l'étape du dégrossissage. Néanmoins, ni son fonctionnement fondamental, ni son potentiel comme appareil de nettoyage, ont fait l'objet d'études approfondies. Dans la plupart des concentrateurs canadiens, les concentrés primaires produit par Knelson (qui opère à une accélération centrifuge de 60 'g') sont nettoyés par table à secousse, un type d'appareil non centrifuge qui fonctionne donc à 1 'g', et qui ne peut donc pas récupérer tout l'or concentré par le Knelson, surtout dans les fractions granulométriques les plus fines. La table à secousse exige également beaucoup d'attention pour son opération et constitue un risque de vol, étant la valeur élevé du matériel qu'elle traite. Ce projet est consacré à l'étude des mécanismes de séparation du Knelson, éventuellement pour l'utiliser soit pour compléter le travail de la table à secousse, ou tout simplement la remplacer.

L'approche expérimentale a été fondée sur l'utilisation d'alimentation synthétiques de tungstène, silice et magnétique et d'un Knelson de 7,5 cm de diamètre. On a utilisé quatre types de gangue, de la silice et de la magnétique fines et grossières. Pour chaque type, nous avons d'abord déterminé le débit optimal d'eau de fluidisation, puis nous avons surchargé le Knelson en l'alimentant à haute teneur de tungstène. Cette surcharge, immédiate et très importante avec la magnétite grossière comme gangue, mais nulle avec la silice fine, a été décrite par un modèle de deux paramètres.

On a conçu deux bols séparables pour étudier la distribution du matériel récupéré dans ses cinq riffles. Les particules les plus denses, tungstène ou or, se retrouvent sur la face intérieure des riffles, en contact avec le flot de pulpe, tandis que la portion extérieure des riffle se remplit au début du cycle de récupération de matériel plus grossier mais stérile, et sert surtout à mieux distribuer l'eau de fluidisation.

Nous avons utilisé les mêmes alimentations synthétiques pour étudier trois versions modifiées du bol, un bol de nettoyage équipé d'un filtre au fonds de chaque riffle, un bol avec riffles moins profonds de 2 mm, et un bol dont la distribution de l'eau de fluidisation était différente. Les résultats ont confirmé le bien fondé du design du bol conventionnel et de nettoyage, et démontré l'importance d'une bonne distribution de l'eau de fluidisation.

Sept échantillons de rejet de table industriels ont été traités par Knelson pour en récupérer l'or fin. En éliminant par tamisage la fraction granulométrique plus grossière mais moins riche en or, on a pu augmenter considérable la récupération du Knelson. Pour obtenir une teneur de concentré plus élevée, jusqu'à 60% Au, un échantillon de magnétite a été pré-alimenté au Knelson pour remplir le fond des riffles, pour être séparé du reste du concentré à la fin de l'essai par voie magnétique.

摘要

近年来，奈尔森(Knelson)选矿机已成为一种重选选金粗选段的主要设备．然而，它在最终精选段用作精选设备的潜力以及它的分选机理尚未得到充分研究．在多数加拿大金选矿厂，奈尔森(以60倍重力加速度运转)产生的重选粗精矿由摇床进行精选．摇床是一种非离心力作用的设备，仅在一个重力加速度下工作．因而，摇床作业导致可观的金损失(主要是细粒金)．同时，摇床操作劳动强度较大，而且由于所处理之物料含金很高,从而导致金的管理不便．本研究的主要目的是：研究奈尔森选矿机的分选机理以及探讨其作为一种精选设备补充或取代现有摇床的应用潜力．

一种基于应用人工合成给矿(钨,石英,磁铁矿)的方法用来研究直径为7.5厘米奈尔森选矿机的操作及其分选机理．应用了四种脉石类型，即粗，细石英和磁铁矿．确定了四种脉石类型所需的最佳松散压力水量．进而，采用高品位给矿进行了奈尔森选矿机超载试验(即在分选器中集存过量的目的矿物而造成明显的尾矿损失)．超载效应的大小主要决定于所处理物料之粒度分布及比重．粗粒磁铁矿给料出现严重超载，而细粒石英给料几乎没有．建立了一个描述超载效应的两参数数学模型并能很好的拟合试验数据．

设计了两个能分开的分选器用以研究分选器五个槽沟中回收的物料性质．业已发现最重的物料例如钨,金主要积存于靠近旋转轴的内槽沟部分，外槽沟在选别周期的最初阶段就被充满，主要起着均匀分布松散压力水的作用．应用合成给矿对三个改进型分选器进行了试验，即在槽沟底部装有填料的精选分选器，不同槽沟深度的分选器以及不同压力松散水分布的分选器．所得结果肯定了常规分选器以及精选分选器的设计，并证明了压力松散水分布的重要性．

用7.5厘米奈尔森选矿机对加拿大7个金选厂的摇床尾矿进行了试验．当预先筛除粗而贫的粒级，回收率明显提高；当预先给入少量磁铁矿作为槽沟充填料，在试验完毕后再用磁选的办法分选出磁铁矿，精矿品位大大提高，达到60% Au．

ACKNOWLEDGEMENTS

This research would not have been completed without the essential contributions of the following individuals.

My supervisor, Professor A.R. Laplante, for his intelligence and wisdom, his excellent advice and constant encouragement throughout the research program. I am also very grateful to him for all his non-research help. My co-supervisor, Dr. Bryn Harris, for his erudite knowledge in hydrometallurgy, patient direction in the research work, as well as his wise advice while writing the thesis and publications. Professor J. A. Finch and Professor Z. Xu, for their patient instructions in courses and enthusiastic help for the research.

My wife, Zhongyi Shi, for her full understanding and support, especially for the January 1992 to August 1993 period when she was working and taking care of our two children in Beijing, China. My son, Hui Huang, for his successful completion of undergraduate studies in Beijing Polytechnic University and great progress in the study of computer science and engineering at Concordia University, during my studies. My daughter, Xuan Huang, for her firm support by investing great efforts in her studies at Westmount High School during my studies.

I also thank all of my colleagues in the Department of Mining and Metallurgical Engineering, McGill University, for their friendly help and cooperation, in particular Raymond Langlois and Michel Leroux, for their kind help in the laboratory and elsewhere. Last, I sincerely appreciate the financial support of the Natural Science and Engineering Research Council of Canada and Knelson Concentrator Inc.

TABLE OF CONTENTS

ABSTRACT i
RÉSUMÉ iii
ZHAIYAO v
ACKNOWLEDGEMENTS vi
TABLE OF CONTENTS vii
NOMENCLATURES xiii
LIST OF FIGURES xv
LIST OF TABLES xxi

CHAPTER 1 INTRODUCTION 1
1.1 Gold Gravity Concentrates 1
1.2 Objectives of the Study 2
  1.2.1 Physical Route 2
  1.2.2 Chemical Route 3
1.3 Structure of the Thesis 3

CHAPTER 2 GOLD AND GOLD ORE PROCESSING 6
2.1 General Description of Gold 6
2.2 Main Methods of Gold Ore Processing 9
  2.2.1 Gravity 9
  2.2.2 Gold Amalgamation 10
  2.2.3 Gold Flotation 12
  2.2.4 Gold Cyanidation 14

CHAPTER 3 RECOVERY OF GOLD GRAVITY CONCENTRATES AND THEIR FURTHER UPGRADING 18
3.1 Gravity Gold Recovery in South Africa 18
    3.1.1 Methods of Primary Gravity Recovery 18
    3.1.2 Upgrading of Gravity Concentrates 20
    3.1.3 Current Situation in South Africa 21
3.2 Gravity Gold Recovery in Canada 22
3.3 Non-Cyanidation Leaching Approaches 25
    3.3.1 Bromine 27
    3.3.2 Chlorine 29
    3.3.3 Iodine 30
    3.3.4 Thiocyanate 31
    3.3.5 Thiosulphate 32
    3.3.6 Thiourea 33
3.4 Conclusions 34

CHAPTER 4 THE KNELSON CONCENTRATOR 37
4.1 A Brief Description of Centrifuges Used in Mineral Processing 37
4.2 Characteristics of the Knelson Concentrator 42
    4.2.1 Basic Description 42
    4.2.2 Industrial Applications 46
    4.2.3 Industrial Performance 50
4.3 Description of the Φ7.5 cm Knelson Concentrator 53
4.4 Theoretical Considerations 55
    4.4.1 Centrifugal Force Acting on a Particle 55
    4.4.2 Terminal Settling Velocity 57
    4.4.3 Travel Time from Downcomer to Wall 60
4.4.4 Particle-Particle Interactions 62

CHAPTER 5 OVERLOADING THE KNELSON CONCENTRATOR 66
5.1 Introduction 66
5.2 Materials 69
5.3 Experimental Methodology 72
  5.3.1 Silica Tests 72
  5.3.2 General Test 73
  5.3.3 Operating the Knelson Concentrator 73
  5.3.4 Size Analysis 74
  5.3.5 Analysis of Tungsten Products 74
5.4 Results and Discussion 78
  5.4.1 Pure Silica Tests 78
  5.4.2 Preliminary Tests 79
  5.4.3 Overload Experiments 82
  5.4.4 Overload as a Function of Mass of the Average Diameter 84
5.5 Modelling the Overload 86
  5.5.1 Derivation of the Mode 86
  5.5.2 Size by Size Data and Fit of the Model 89
5.6 Conclusions 93

CHAPTER 6 THE DISTRIBUTION OF CONCENTRATE IN THE KNELSON CONCENTRATOR RINGS 94
6.1 Description of the Separable Bowl 94
6.2 Experimental Methodology 95
6.3 Results 99
  6.3.1 Test 1 99
  6.3.2 Test 2 102
  6.3.3 Test 3 105
  6.3.4 Test 4 108
  6.3.5 Photographic Evidence of the Concentrate Distribution 110

6.4 Discussion 114

6.4.1 Possible Separation Mechanisms of the Knelson Concentrator 114

6.4.1.1 At the Beginning of a Test, the Rings Are Completely Fluidized 114

6.4.1.2 As Soon as the Concentrate Bed Builds-up, It Is only Partially Fluidized 115

6.4.1.3 The Selective Recovery Begins Once the Initial Concentrate Bed Formed 115

6.4.2 Practical Implications 117

CHAPTER 7 KNELSON BOWLS WITH DIFFERENT CONFIGURATIONS 120

7.1 Objectives 120

7.2 Bowl#1 120

7.2.1 Features of the Bowl 120

7.2.2 Methodology 121

7.2.3 Test Results 122

7.2.4 Discussion 123

7.3 Bowl#2 125

7.3.1 Description of the Bowl 125

7.3.2 Testwork 125

7.3.3 Results and Discussion 126

7.4 Bowl#3 127

7.4.1 Description of the Bowl 127

7.4.2 Testwork 127

7.4.3 Results and Discussion 128

7.4.4 Superficial Fluidization Water Velocity 135

7.5 Conclusions 137

CHAPTER 8 UPGRADING OF GOLD TABLE TAILS 139
8.1 Introduction 139
8.2 Lucien Béliveau 141
  8.2.1 Description of the Mill 141
  8.2.2 Ore Characteristics 142
  8.2.3 Laboratory Testwork 143
  8.2.4 Test Results 145
  8.2.5 Discussion 145
8.3 Meston Resources 151
  8.3.1 Concise Description of the Mill1 151
  8.3.2 Laboratory Testwork 152
  8.3.3 Test Results 154
  8.3.4 Discussion 156
8.4 Hemlo Golden Giant Mine 162
  8.4.1 Concise Description of the Mill 162
  8.4.2 Laboratory Testwork 164
  8.4.3 Test Results 164
  8.4.4 Discussion 165
8.5 Snip Operations 169
  8.5.1 Concise Description of the Mill 169
  8.5.2 Laboratory Testwork 170
  8.5.3 Test Results 172
  8.5.4 Discussion 172
8.6 Les Mines Casa Berardi 176
  8.6.1 Concise Description of the Mill 176
  8.6.2 Laboratory Testwork 177
  8.6.3 Test Results 178
  8.6.4 Discussion 185
8.7 Les Aurbel Division Inc. 187

8.7.1 Laboratory Testwork 187
8.7.2 Test Results 189
8.7.3 Discussion 189
8.8 Resources MSV Inc. 189
8.8.1 Laboratory Testwork 189
8.8.2 Test Results and Discussion 189
8.9 Discussion 191
8.10 Summary 199

CHAPTER 9 CONCLUSIONS 202
9.1 Overall Conclusions 202
9.2 Claims for Original Research 205
9.3 Suggestions for Future Work 206

REFERENCES 208

APPENDIXES

Appendix 1-1 A Review of Gold Chlorination A1
Appendix 4-1 Settling Distance as a Function of Time A24
Appendix 8-1 Data of Lucien Béliveau Table Tails Processing A29
Appendix 8-2 Data of Meston Resources Table Tails Processing A36
Appendix 8-3 Data of Hemlo Table Tails Processing A42
Appendix 8-4 Data of Snip Table Tails Processing A47
Appendix 8-5 Data of Casa Berardi Table Tails Processing A52
Appendix 8-6 Data of Aurbel Division Table Tails Processing A58
Appendix 8-7 Data of Resources MSV Table Tails Processing A63

NOMENCLATURE

a	in Equation 4-1, centrifugal acceleration, $cm.s^{-2}$.
r	in Equation 4-1, rotating radius of a particle, cm.
ω	in Equation 4-1, angular velocity, $radian.s^{-1}$.
F_c	in Equation 4-2, centrifugal force acting on a particle, $g.cm.s^{-2}$.
d	in Equation 4-2, diameter of a particle, cm.
δ	in Equation 4-2, specific density of a particle.
ρ	in Equation 4-2, density of a medium.
V_t	in Equation 4-3, velocity at time t, $cm.s^{-1}$.
F_d	in Equation 4-4, inward drag force, $g.cm.s^{-2}$.
V_r	in Equation 4-4, velocity at radial distance r, $cm.s^{-1}$.
μ	in Equation 4-4, viscosity of a fluid medium, 0.01 $g.cm^{-1}.s^{-1}$ for water at 20°C.
V_0	in Equation 4-5, terminal settling velocity, $m.s^{-1}$, or $cm.s^{-1}$.
D_a	in Equation 4-6, specific density of particle a, $g.cm^{-3}$.
D_b	in Equation 4-6, specific density of particle b, $g.cm^{-3}$.
D_f	in Equation 4-6, specific density of a fluid medium, $g.cm^{-3}$.
d_a	in Equation 4-6, diameter of particle a, cm.
d_b	in Equation 4-6, diameter of particle b, cm.
t	in Equation 4-8, time taken for a particle to move from radius r_1 to r_2, s.
r_1	in Equation 4-8, radius 1, cm.
r_2	in Equation 4-8, radius 2, cm.
D^{o}_{a}	in Equation 5-1, weighted average diameter for an entire material, cm or μm.
γ_i:	in Equation 5-1, fraction yield, %.
D^{o}_{i}:	in Equation 5-1, fraction size, cm or μm.
M^{o}_{i}:	in Table 5-6, mass of a particle of average diameter, g.
W	in Equations 5-3 and 8-1,mass of tungsten (or gold) recovered in concentrate, g.

W_f	in Equations 5-3 and 8-1, mass fed to the Knelson Concentrator, g.
G_f	in Equations 5-3 and 8-1, feed grade of tungsten (or gold), %.
K	in Equations 5-5 and 8-1, erosion rate constant, g^{-1}.
W_c	in Equations 5-6 and 8-1, tungsten (or gold) collected at which overload begins, g.
W_o	in Equations 5-5 and 8-1, mass of feed corresponding to W_c, g
R	in Equations 5-9 and 8-1, recovery, %.
J_w	in Equation 7-1, superficial fluidization water velocity, $cm.s^{-1}$.
Q_w	in Equation 7-1, volumetric flowrate of fluidization water, $cm^3.s^{-1}$.
A_r	in Equation 7-1, section area of a ring or series rings, cm^2.
S	in Equation A4-2, settling distance, cm.
V_{ol}	in Equation A4-3, the volume of a spherical particle, cm^3.
Q	in Equation A4-3, coefficient of resistance, 0.4 for spherical particle.
F_{80}	in Table 8-9, the particle size at which 80% of the mass passes.
R_o	in Equation 8-1, the Knelson recovery at the beginning of the recovery cycle.

LIST OF FIGURES

Figure 3-1 SEM Back-Scattered Image of -25 μm Knelson Tail 26

Figure 4-1 Schematic Diagram of 800 x 600 mm Yunxi Centrifuge 38

Figure 4-2 Cross Section of the 76 cm Manual Discharge Knelson Concentrator 43

Figure 4-3 Cross Section of the Central Discharge Knelson Concentrator 45

Figure 4-4 Cross Section of the Variable Discharge Knelson Concentrator 46

Figure 4-5 Laboratory 7.5 cm Knelson Concentrator 54

Figure 4-6 Schematic Diagram of the 7.5 cm Knelson Concentrator 54

Figure 4-7 Travelling Time to Reach the Wall of the First Riffle 61

Figure 4-8 Settling Distance vs Settling Time in a Relatively Long Period 64

Figure 4-9 Settling Distance vs Settling Time in a Ralatively Short Period 65

Figure 5-1 SEM Back-Scattered Images for Spherical and Irregular Tungsten Particles 70

Figure 5-2 Mozley Separation of 25-38 μm Silica-Tungsten 76

Figure 5-3 Mozley Separation of -25 μm Magnetite-Tungsten 77

Figure 5-4 Pure Silica Recovery as a Function of Fluidization Water Flowrate .. 78

Figure 5-5 Effect of Fluidization Water Flowrate on Tungsten Recovery 79

Figure 5-6 Effect of Fluidization Water Flowrate on Concentrate Grade 80

Figure 5-7 Effect of Fluidization Water Flowrate on Tungsten Recovery for the Silica Gangue 81

Figure 5-8 Effect of Fluidization Water Flowrate on Tungsten Recovery for the Magnetite Gangue 82

Figure 5-9 Overload for Four Types of Gangue 83

Figure 5-10 Tungsten Recovery as a Function of the Mass of Gangue Particle, M_a^o 85

Figure 5-11 Overload with Fine Silica Gangue 90
Figure 5-12 Overload with Fine Magnetite Gangue 91
Figure 5-13 Overload with Coarse Silica Gangue 91
Figure 5-14 Overload with Coarse Magnetite Gangue 92
Figure 6-1 Separable Knelson Concentrator Bowl 96
Figure 6-2 Schematic Diagram of the Concentrate Split 98
Figure 6-3 Test 1: Ring-by-Ring Mass, Recovery and Grade (Feed: -425 μm silica) 100
Figure 6-4 Tungsten Size Distribution in Concentrate (Feed: -425 μm silica) 101
Figure 6-5 Concentrate Size Distribution of the Three Sections of Ring Four (Test 2) 103
Figure 6-6 Mass, Grade and Tungsten Distribution in the Three Sections of Ring Four (Test 2) 104
Figure 6-7 Size Distribution in Three Sections of the Concentrate (Test 3, all five rings combined) 107
Figure 6-8 Mass, Grade and Tungsten Distribution in Three Sections of the Concentrate (Test 3, all five rings combined) 107
Figure 6-9 Recovery and Grade vs Ring No (Test 4) 109
Figure 6-10 Size Analysis of First Four Tails (Test 4) 109
Figure 6-11 A Half Bowl of the Concentrate with -425 μm Silica Gangue 111
Figure 6-12 A Half Bowl of the Concentrate with -425 μm Magnetite 111
Figure 6-13 A Bottom View of a Piece of the Concentrate with -425 μm Silica Gangue (Fluidization water flowrate: 2.6 L.min^{-1}) 113
Figure 6-14 A Bottom View of a Piece of the Concentrate Obtained from -425 μm Magnetite Gangue 113
Figure 6-15 Two Pieces of the Concentrate with -425 μm Silica Gangue (Fluidization water flowrate: 4.9 L.min^{-1}) 114
Figure 6-16 Forces Acting on a Particle and the Possible Concentration Process 118
Figure 7-1 Schematic Diagram of Bowl#1 122

Figure 7-2 Concentrate Grade, Mass and Tungsten Recovery as a Function of Fluidization Water Flowrate for Bowl#1 and the Conventional Bowl (Feed: 950 g silica; 50 g tungsten) 124
Figure 7-3 The Effect of Magnetite Pre-feed on Bowl#1 Performance 124
Figure 7-4 Knelson Performance before and after Shaving 2 mm of the Riffle Ribs 126
Figure 7-5 Overload of Bowl#3 Compared to the Conventional Bowl (Test 1) .. 129
Figure 7-6 Overload of Bowl#3 Compared to the Conventional Bowl (Test 2) .. 129
Figure 7-7 Overload Tests of Bowl#3 Compared to Conventional Bowl 130
Figure 7-8 Two Halves of Bowl#3 with the Concentrate (Test 3) 132
Figure 7-9 A Piece of the Concentrate in First Ring with Bowl#3 (Test 3) 133
Figure 7-10 A Piece of the Concentrate in Fourth Ring with Bowl#3 (Test 3) 133
Figure 7-11 Grade and Tungsten Distribution in the Various Rings (Feed: 1900 g of -425μm silica and 100 g tungsten) 134
Figure 7-12 Grade and Recovery of Bowl#3 and the Conventional Bowl (Feed: 1900 g of -425 μm silica and 100 g tungsten) 134
Figure 7-13 Fluidization Water Hole Distribution and Superficial Fluidization Water Velocity for the Conventional Bowl and Bowl#3 (Total flowrate: 2.8 L.min^{-1}) 137
Figure 8-1 Grinding-Gravity Circuits of the Lucien Béliveau Mill (as of 1992) 142
Figure 8-2 Schematic Diagram of a B6 Falcon Concentrator 145
Figure 8-3 Results of the Knelson Concentrator -- Feed: Lucien Béliveau Table Tail 1 Diluted with Silica (4:1) 147
Figure 8-4 Results of the Knelson Concentrator-- Feed: Lucien Béliveau Table Tail 2 Diluted with Silica (4:1) 147
Figure 8-5 Results of the Knelson Concentrator -- Feed: Lucien Béliveau Total Table Tails (Undiluted) 148
Figure 8-6 Results of the Falcon Concentrator -- Feed: Lucien Béliveau Total Table Tails (Undiluted) 148

Figure 8-7 Grinding and Gravity Circuit of Meston Resources 153
Figure 8-8 Results of the Knelson Concentrator for Meston Original Table Tails 156
Figure 8-9 Size-by-Size Performance of Test 2 (Feed: Meston table tails diluted by -212 μm Silica 3:1) 157
Figure 8-10 Size-by-Size Performance of Test 3 (Feed: Meston -150 μm table tails) 157
Figure 8-11 Comparing Tests 1, 3 and 4 (Feed: Meston table tails) 158
Figure 8-12 Size-by-Size Recoveries of Tests 1 and 3 (Feed: Meston table tails) 158
Figure 8-13 SEM Image of +106 μm Knelson Concentrator Tails for Processing Meston Table Tails (1: gold; 2: arsenopyrite; 3: silica) 159
Figure 8-14 SEM Image of 38-53 μm Knelson Concentrator Tail for Meston Table Tails Processing (1: gold; 2: locked gold; 3: arsenopyrite; 4: pyrite; 5: silica) 159
Figure 8-15 The Hemlo Gravity Circuit Flowsheet 163
Figure 8-16 Size-by-Size Performance of Test 1 (Feed: Hemlo gold table tails) 166
Figure 8-17 Size-by-Size Performance of Test 2 (Feed: Hemlo -212 μm table tails) 166
Figure 8-18 Comparing the Three Hemlo Gold Tests (Feed: Gemeni table tails) 167
Figure 8-19 Evolution of Gold Losses in Tests 2 and 3 (Feed: Hemlo Gold -212 μm table tail, without and with magnetite pre-feed) 167
Figure 8-20 Simplified Diagram of the Snip Grinding/Gravity Circuits 171
Figure 8-21 Size-by-Size of the First Snip Test (Feed: coarse table tails) 174
Figure 8-22 Size-by-Size of the Second Snip Test (Feed: -212 μm table tails) 174
Figure 8-23 Evolution of the Tailing Grade for the Snip Tests 2 and 3 (Feeds: -212 μm table tails, without and with magnetite pre-feed) 175
Figure 8-24 Comparing the Three Snip Tests 175
Figure 8-25 Simplified Grinding/Gravity Circuit of Casa Berardi 178
Figure 8-26 Size-by-Size Performance of the First Casa Berardi Test (Feed: total

table tails) ... 180
Figure 8-27 Size-by-Size Performance of the Second Casa Berardi Test (Feed: -212 μm table tails) ... 180
Figure 8-28 Size-by-Size Performance of the Third Casa Berardi Test (Feed: -150 μm table tails) ... 181
Figure 8-29 Evolution of the Tail Grade for Casa Berardi Tests 2 and 4 ... 181
Figure 8-30 Comparing the Results of the Four Casa Berardi Tests ... 182
Figure 8-31 Frozen Concentrate of the Fourth Casa Berardi Test 4 Prior to Separation ... 182
Figure 8-32 Frozen Concentrate of the Fourth Casa Berardi Test 4 after Separation of the Two Halves ... 183
Figure 8-33 Close-up of Part of the Concentrate of a Ring (Casa Berardi Test 4) ... 183
Figure 8-34 and 8-35 Total Concentrate of Casa Berardi Test 4 before and after Magnetic Separation ... 184
Figure 8-36 Size-by-Size Performance of the First Aurbel Test (Feed: total table tails) ... 188
Figure 8-37 Comparing the Results of the Two Aurbel Tests ... 188
Figure 8-38 Recovery, Grade and Distribution for MSV ... 190
Figure 8-39 Evolution of Gold Losses without Magnetite Pre-Feed ... 194
Figure 8-40 Evolution of Gold Losses with Magnetite Pre-Feed ... 194
Figure 8-41 Fit of the Synthetic Ores to Equation 5-9 (parameters in Table 8-11) ... 197
Figure 8-42 Fit of the Table Tails Processing Data with Magnetite Pre-Feed to Equation 8-1 (Parameter in Table 8-1) ... 197
Figure 8-43 Fit of the Table Tails Processing Data without Magnetite Pre-Feed to Equation 8-1 (Parameter in Table 8-1) ... 198
Figure 8-44 K as a function of G_t ... 198
Figure A1-1 The Eh-pH Diagram for Aqueous Chlorine, 25 °C, $C_{T,Cl}=1 \times 10^{-4}$ M ... A4
Figure A1-2 Distribution Diagram for Chlorine Species at 25 °C

$[Cl^-] = 10^{-3}$ M, $C_{T,CL} = [Cl_2] + [HOCl] + [OCl^-]$ A4

Figure A1-3 Eh-pH Diagram for the System of Au-H_2O-Cl^- at 25°C
$[Au(III)] = 10^{-2}$ M, $[Cl^-] = 2$ M, $P_{Cl2} = 0.1$ atm,
$[HClO] = [ClO^-] = 6x10^{-3}$ M, $P_{O2} = P_{H2} = 1$atm A6

Figure A1-4 Chlorination Test Apparatus A17

LIST OF TABLES

Table 2-1 World Gold Mine Production 8
Table 3-1 Some Canadian Gold Gravity Circuits 24
Table 3-2 Non-Cyanide Lixiviants 27
Table 4-1 Metallurgical and Economic Impact of Knelson Industrial Applications 50
Table 4-2 Centrifugal Force (g.cm.s^{-2}) 57
Table 4-3 Terminal Settling Velocities (cm.s^{-1}) 58
Table 4-4 Particle Travel Time (second) from Downcomer to Wall 61
Table 5-1 Illustration of Contamination Problems 68
Table 5-2 Tungsten Size Distribution (as received) 69
Table 5-3 Size Distribution of Gangue Minerals 72
Table 5-4 Variance of Tungsten Separation by Mozley Table 75
Table 5-5 Effect of Gangue Size and Density on the Performance 83
Table 5-6 Recovery as a Function of the Average Diameter Mass 84
Table 5-7 Model Parameters for the Four Gangue Type 89
Table 6-1 Inside Dimensions of the Separable Bowl 95
Table 6-2 Size Distribution of the Gangue Minerals for Split Bowl Tests 96
Table 6-3 Overall Results of Test 1 100
Table 6-4 Overall Results of Test 2 102
Table 6-5 Content of the Three Sections of Ring Four (Test 2) 103
Table 6-6 Overall Results of Test 3 105
Table 6-7 Grade Variation (%W) along the Radial Direction, Ring by Ring ... 106
Table 6-8 Overall Results of Test 4 108
Table 7-1 Size Distribution of Magnetite as a Filler 122
Table 7-2 Comparing Bowl#1 to the Conventional Bowl 123

Table 7-3 Hole Distribution for Both the Conventional Bowl and Bowl#3 127

Table 7-4 Concentrate Size Distributions of Silica and Magnetite Gangue 131

Table 8-1 A Summary of Gold Table Tails Processed 140

Table 8-2 A Summary of the Test Results for L. Béliveau Table Tails 146

Table 8-3 Results of the Knelson Concentrator Tests for Meston Resources ... 155

Table 8-4 Results of the Knelson Concentrator Tests for Hemlo Gold Mines .. 165

Table 8-5 Results of the Knelson Concentrator Tests for Snip Operation 173

Table 8-6 Results of the Knelson Concentrator Tests for Les Mines Casa Berardi 179

Table 8-7 Results of the Knelson Tests for the Aurbel Table Tail Sample 187

Table 8-8 Results of the Knelson Concentrator Test for MSV 190

Table 8-9 Properties of the Table Tails Processed 191

Table 8-10 Recovery (%) of the Table Tails Tests 192

Table 8-11 Parameters of Equations 5-9 (Synthetic Feeds) and 8-1 (Table Tails Feeds) 195

CHAPTER 1 INTRODUCTION

1.1 Gold Gravity Concentrates

Gravity concentration was the dominant mineral processing method for about two thousand years, and it is only in the twentieth century that its importance has declined, with the development of such processes as flotation, magnetic separation and leaching (Burt, 1984). Gravity concentration is still the main method to treat most iron, tungsten, and tin ores, beach sands, and some rare metal ores such as tantalum and niobium. Gravity also plays an important role in the production of gold because of its high specific density (19.3) and natural occurrence as liberated species.

The gold concentrates produced by gravity equipment such as Knelson Concentrators, jigs and spirals are called gravity concentrates, and are normally pumped to a secured area, the gold room, for further upgrading. The tails and middlings of the gold room cleaner are also concentrates of a sort, as they generally contain liberated gold at a significantly greater concentration than in the ore itself.

Upgrading of the gold is achieved by rejecting gangue minerals and tramp metals (steel and copper) whilst retaining free gold particles. For gold-bearing sulphide ores, the main gangue minerals in gold gravity concentrates are pyrite and arsenopyrite, with small amounts of magnetite. For oxide ores, the gold concentrates may contain some heavy minerals, such as cassiterite, magnetite, ilmenite, rutile, zircon and monazite (Marsden and House, 1992).

Tramp steel can be rejected by magnetic separation, and tramp copper, usually blasting wire, can be washed out of the final concentrates using nitric acid. Gangue minerals, however, are typically rejected using gravity methods. This proves particularly challenging for higher density minerals, such as sulphides and some oxides.

1.2 Objectives of the Study

1.2.1 Physical Route

In Canadian operations, all gravity concentrates are further upgraded using shaking tables. These tables typically yield gold recoveries between 75 and 90%. The gold losses are due to incomplete liberation only in part, and in fact, result mostly from fines and flakes (i.e. particle size and morphology). Fines often float to the tails (i.e. table flotation), whereas flakes tend to report with the heavy minerals in the middlings. When a table processes the concentrate from a Knelson Concentrator, recoveries can be particularly low, because the table, with a gravity acceleration of only 1 'g' (9.8 $m.s^{-2}$), cannot recover all the gold originally recovered by the Knelson Concentrator, which operates with a theoretical acceleration of 60 'g' (588 $m.s^{-2}$). Furthermore, table operation is labour intensive, which creates a security risk because of the high gold content of the material being processed. Hence, there is a strong incentive to supplement or even replace tables by a unit which requires little or no supervision, such as an automated Knelson CD.

One logical candidate for this duty is the Knelson Concentrator itself, whose efficiency for primary recovery is well documented (Laplante et al, 1990; Laplante, 1993). However, before the Knelson Concentrator can be proposed for cleaning applications, it is necessary, ideally, to develop a better understanding of how it works -

i.e. what are the important mechanisms that are responsible for selectivity.

Two additional challenges must be met. First, the gangue is not as easily rejected, since it generally has a much higher specific density. Second, much higher concentrate grades are targeted, 40-70% Au rather than the 0.5 to 3% of most primary concentrates. It follows that the effect of both the specific density and size distribution of the Knelson Concentrator feed should be well characterized and understood in order to assess the impact of the coarser, denser feed. Further, factors capable of lowering concentrate grade, such as short circuiting of feed into the concentrate at the beginning of the recovery stage, require investigation.

1.2.2 Chemical Route

For the further upgrading of high grade table concentrates, the traditional approach is smelting. The high grade of the furnace feed, obtained at the cost of recovery during tabling, minimizes smelting costs. However, smelting still remains expensive, environmentally costly and incapable of separating gold from silver, whose losses can be significant. Alternatively, the production of very pure gold from gravity concentrates by hydrometallurgy rather than pyrometallurgy could be attractive. First, smelting and traditional refining would be avoided, and second, gold could be separated from silver. Hydrometallurgical methods to replace smelting for producing very pure gold from high grade gold gravity concentrates are explored in Appendix 1-1; they are presented in an appendix, since they do not really constitute part of the fundamental study which comprises this thesis.

1.3 Structure of the Thesis

The thesis consists of 9 chapters.

CHAPTER 1 introduces the background of the project, its objectives, and the structure of the thesis.

CHAPTER 2 summarizes the types of gold ores, the main processing routes, including gravity separation, amalgamation, flotation and cyanidation.

CHAPTER 3 describes gold gravity separation and further upgrading primary concentrates both in South Africa and Canada. Some possible non-cyanide leaching alternatives are also reviewed.

CHAPTER 4 introduces the Knelson Concentrators, from the laboratory unit to the largest industrial models. Some theoretical considerations are discussed.

CHAPTER 5 presents overload results of the Knelson Concentrator using synthetic ores (tungsten to mimic gold, magnetite to mimic pyrite). The optimum ranges of fluidization water flowrate for different gangue minerals are first determined. Overload as a function of particle size and specific density is discussed. Finally, a two-parameter overload model is derived and tested.

CHAPTER 6 first presents a separable modified Knelson Concentrator bowl, from which concentrate can be recovered after freezing. It was used to determine spatial distribution of gangue and tungsten within the riffles. These results shed much light on the operating mechanisms of the Knelson Concentrator.

CHAPTER 7 shows some results obtained with the Knelson Concentrator bowls having different features, including a cleaning bowl, a shallower riffles bowl, and a bowl with a different distribution of fluidization water.

CHAPTER 8 summarizes the results of processing seven different gold table tails taken from Canadian gold mills. Different processing ways achieved quite different results. A method to obtain very high grade concentrate is proposed and tested.

CHAPTER 9 presents overall conclusions, claims to original knowledge, and some suggestions for future work.

CHAPTER 2 GOLD AND GOLD ORE PROCESSING

2.1 General Description of Gold

Gold is the most noble of metals. Its terrestrial abundance is 0.005 ppm, approximately equal to that of platinum, the adjacent element in group VIII (Boyle, 1987). The electron configuration of the gold atom is $1s^2 2s^2 2p^6 3s^2 3p^6 3d^{10} 4s^2 4p^6 4d^{10} 4f^{14} 5s^2 5p^6 5d^{10} 6s^1$. Gold forms M^{III} complexes. With its higher electronegativity, gold can obtain an adequate share of electrons from a smaller number of ligands and occurs more commonly in 4 co-ordination, such as $AuCl_4^-$ and $AuBr_4^-$ (Heslop and Robinson, 1960). Gold has a density of 19.34 $g.cm^{-3}$ at 20 °C. Its melting point and boiling point are 1063°C and 2699°C, respectively. With the highest ductility and malleability among metals, one ounce (31.103 g) of gold can be beaten out to 300 square feet (27.87 m^2), yielding a sheet thinner than 0.000004 inch (0.1 μm) (Puddephatt, 1978; Louis, 1894).

Gold is not attacked by any of the ordinary acids and alkalies except selenic acid. It can be dissolved by aqua regia (25% HNO_3, 75% HCl) and by hydrochloric acid in the presence of hypochlorite or iron (III) as oxidant (Puddephatt, 1978). It is also well known that the following reagent solutions are able to react with gold: bromine, chlorine, cyanide, iodine, thiocyanate, thiosulphate and thiourea (Swaminathan et al, 1993).

Gold was probably the first metal discovered by mankind as nuggets in soils and alluvials. Undoubtedly, ancient people were attracted by its intrinsic beauty, great malleability and ductility, which made its processing with relatively primitive tools easy.

The use of gold can be dated back 3050 BC. In Egypt, during the reign of Menes, gold was used as a means of currency, either as grains or bars. Finely worked gold ornaments originating from about 2700 BC have been excavated in what was then Mesopotamia and is now Iraq (Marsden and House, 1992).

The main usage of gold is for jewellery, accounting for 67% of total consumption. Other uses are: 5% for electronics, 2% for dentistry, 2% for industrial, 1% for metals, 5% for coins, and 19% for bar hoarding (Marsden and House, 1992).

Total world gold production in 1993 was 2281 tonnes, the main producers being South Africa, United States, Australia, C.I.S., Canada and China as shown in Table 2-1 (Metals and Minerals Annual Review, 1994).

Although 40 gold-bearing minerals are reported, only native gold and electrum are common. In nature, gold occurs predominantly in the native state or as a major constituent of various alloys containing mainly silver, copper or platinum. Gasparrini points out that at atomic silver: gold ratios greater than 1:1, the mineral should be called kustelite; this corresponds to a silver content (by weight) of 36% or higher (Gasparrini, 1993). For silver contents lower than this value, the mineral is called electrum. A complete substitutional series probably exists from gold through electrum, kustelite (aurian silver), to native silver. A term commonly used to express the purity of bullion is fineness (note: it is different from karat, 1 K = (100/24)%), defined by (Gasparrini, 1993; Boyle, 1968; Marsden and House, 1992):

$$\mathit{Fineness} = \frac{1000(wt\%\,Au)}{wt\%\,Au + wt\%\,Ag} \qquad 2\text{-}1$$

In placer deposits, gold appears mainly as nuggets, grains and scales. The gold content of most natural gold grains varies from 85% to 95% (Marsden and House, 1992).

TABLE 2-1 World Gold Mine Production (in tonnes)

Country	1991	1992	1993
South Africa	601.1	614.1	619.5
US	296.0	329.1	336.0
Australia	236.2	243.5	247.2
CIS	252.0	237.0	244.0
Canada	176.6	160.4	150.9
China	110.0	118.0	127.0
Brazil	78.6	76.5	75.7
Papua New Guinea	60.8	71.2	61.8
Indonesia	18.4	40.4	46.3
Ghana	27.3	33.3	41.4
Chile	33.0	39.3	39.5
Philippines	30.5	27.2	28.0
Colombia	30.7	29.9	26.4
Sum	1,951.2	2,019.9	2,043.7
Other Latin	66.1	67.4	83.0
Other Africa	61.2	64.6	67.3
Other Asia	22.6	24.8	27.5
Europe	32.3	25.3	25.6
Other Oceanic	10.3	14.3	15.0
Rest of World	17.0	21.0	19.0
Total	2,161	2,237	2,281

There are different ways to classify gold-bearing ores. According to their composition and processing, gold ores can be classified as placers, free milling ores, oxidized ores, silver-enriched ores, iron sulphides, arsenic sulphides, copper sulphides, antimony sulphides, tellurides and carbonaceous ores (Marsden and House, 1992).

2.2 Main Methods of Gold Ore Processing

2.2.1 Gravity

Because of its high specific density and its natural occurrence in ancient times, gold was mainly recovered by gravity separation from placer-type deposits. Recovery of gold by gravity concentration dates back 6,000 years ancient Chinese, Egyptian and Greek civilisations (Puddephatt, 1978; Turner, 1991). Gold mining in Egypt started with alluvial workings and was followed by shallow underground vein mining in Nubia in about 1300 B.C.. The Romans used a sluicing technique, whereby broken rock was washed through channels containing prickly shrubs which caught the gold (Marsden and House, 1992).

In South Africa, most active gold mines are centred around the Witwatersrand Basin. In the early days, the ores were passed over mercury coated copper plates placed after stamp mills and later after tube mills. The plates were later replaced by corduroy cloths on sloping tables. The concentrate was treated on a shaking table prior to amalgamation in barrels. Gravity concentration and amalgamation of gold in milling circuits was retained after the introduction of the cyanide extraction process, and yielded between 15 and 60% of the total production (Burt, 1984). Amalgamation was eventually eliminated because of health considerations, and gravity recovery has virtually disappeared for security reasons and due to the increased efficiency of carbon circuits (Laplante, 1995).

In the rest of the world, the same evolution from amalgamation to cyanidation took place. Gravity recovery, however, is still extensively used, and has in fact experienced a resurgence in popularity due to the advent of the Knelson Concentrator (Darnton et al, 1995; Hart and Hill, 1995; Poulter et al, 1995; Cloutt, 1995).

What are the advantages of applying gravity concentration in gold recovery? By removing gold from the pulp circulating through the mills, the amount of gold locked up behind the mill liners is considerably reduced; selective grinding can be applied to the pyritic concentrate to ensure the release of enclosed gold particles without overgrinding; the reduced gold content of the cyanidation feed (by approximately 50%) results in a lower concentration in the cyanide solution, which has certain benefits in filtration and precipitation. The loss of gold-bearing solution as a result of imperfect washing on the filters (0.3-0.5%) is diminished (Burt, 1984; Bath, 1973; Loveday,1982). Fine particles of osmiridium are also recovered when present. There is no doubt that gravity concentration is an economical, pollution-free method compared to other methods, especially amalgamation and cyanidation.

Final gold gravity concentrates are generally smelted to remove base metals and other impurities in order to produce a gold-silver bullion containing typically more than 95% precious metals. The smelted product, doré bullion, is suitable for direct sale and/or for further refining.

The introduction of CIP and CIL circuits (see section 2.2.4) has significantly increased the efficiency of dissolved gold recovery, and, at least in South Africa, has led to the perception that gravity recovery is no longer attractive. However, recent industrial data from Australia seems to suggest otherwise, as increases in overall recovery of 0.92%, an annual cost saving of over $350,000 for cyanide, and elution plant savings of $400,000 have been reported (Cloutt, 1995). A more complete survey of the Knelson-based gravity circuits is presented in Chapter 4.

2.2.2 Gold Amalgamation

If the surface of a gold particle is clean, it can be trapped by clean mercury. Amalgamable gold is said to be "free milling" (Pryor, 1965), but this is incorrect terminology since free milling traditionally refers to cyanidation recovery, which is normally much higher than that of amalgamation. Amalgamation is a concentrating process in which metallic gold or silver, or an alloy of the two, passes preferentially across a water mercury interface, after which the metal-laden mercury (amalgam) is obtained (Taggart, 1945).

Mercury has a tendency to combine with many metals, e.g. Na, Zn, K, Ag and Au, to produce amalgams. However, several transition metals, e.g. Fe, cannot be amalgamated. As mercury diffuses into a gold particle, $AuHg_2$ is first formed, then Au_2Hg and Au_3Hg follow (Taggart, 1945; Sun, 1985).

Various amalgamation units can be used: plates, inclined at 8°, either stationary, or oscillating with a small amplitude, and coated with silver; pocket amalgamators (liquid and amalgams are held in a pocket onto which the pulp to be amalgamated flows); and grinding amalgamators, which are used for the ores in which the gold is difficult to amalgamate, because it is either very fine, or locked with other minerals. The usual apparatus is the amalgamating barrel (Taggart, 1945). Gold particles in the size range of 0.1-1 mm (-0.03 mm particles are easily floated away), a pulp density of 10 to 25% solids would make the plate amalgamation more effective (Sun, 1985).

An amalgam which contains significant concentrations of mercury must be treated prior to smelting to gold bullion. Retorts are operated under a slightly negative pressure and mercury vapour is usually fumed into a water condensation system. The vapour is cooled rapidly to below the boiling point (375°C) and the liquid mercury is collected under water to avoid re-evaporation. Retorting of amalgams yields a mercury-free product in the form of "sponge' gold, which can be treated directly by smelting for the removal of residual base metal impurities (Marsden and House, 1992; Pryor, 1965).

Mercury is highly toxic and has a cumulative physiological effect; therefore, amalgamation has not been tolerated in the Canadian gold industry since the early 1970s.

The widespread use of the amalgamation, especially in developing nations such as Bolivia, Chile, Zimbabwe, Dominican Republic, Ghana, Kenya, Zambia, China, India, Indonesia, Malaysia and the Philippines has been documented, and environmental and health problems are likely to persist for decades to come (Blenkinsop, 1990; Campbell and Pitfield, 1991; Cramer, 1990 and Neisser, 1993).

2.2.3 Gold Flotation

Gold has a good natural floatability. In the remote past (fifth century B.C.), gold grains were separated from sands by means of goose feathers coated with grease, the gold grains attaching to the surface of the feathers (Glembotskii, 1963).

In most base metal mineral processing plants, gold is generally floated into copper and lead concentrates, and is recovered during metallurgical processing as a by-product. This is not the case for zinc concentrates, which clearly creates an incentive for gravity recovery ahead of zinc flotation circuits (even when a copper concentrate is first produced, some GRG reports to the zinc circuit). For gold that is associated with pyrite, a gold-bearing pyrite concentrate can be produced by flotation. The concentrate is then either reground or pressure-oxidized and then cyanided. Gold flotation can also be used as a supplement of gravity for gold fines and flakes easily lost during gravity separation (Wang and Poling, 1983).

However, by far the most common interface between gold flotation and gravity is the use of gravity recovery in grinding circuits ahead of flotation in order to increase overall gold recovery and to recover it into a higher-value product (payment in excess of 99% for gold bullion, as opposed to 92-95% for gold recovered into flotation concentrates).

The flotation of auriferous sulphides, particularly pyrite, is of great importance in gold mines in South Africa and Australia. In South Africa, more than 60 million tonnes of ore are processed annually in flotation plants to recover auriferous pyrite. One of the main reasons for floating pyrite is for the manufacture of sulphuric acid, mostly used for the leaching of uranium. The calcines produced from the roasting of pyrite are cyanide-leached to recover gold (O'Connor and Dunne, 1991).

Gold flotation investigations, in South Africa, also focused on the flotation and separation of uranium, gold and pyrite (Lloyd, 1981; Kok, 1975; Stassen, 1991). The flotation of a gold gravity concentrate with a frother and dithiophosphate resulted in a gold recovery of 98%, the flotation concentrate could be smelted directly to yield a bullion averaging 87% Au; a belt gold concentrate with 2.5 $kg.t^{-1}$ Au was enriched to 7.3% Au by flotation with a recovery of 87% (Lloyd, 1981).

More recently, selective ion flotation of gold has been investigated (Galvin et al, 1992). The flotation of gold and silver cyanide anions with cetyltrimethylammonium bromide as a surfactant collector exhibited a significant selectivity for gold even though the concentration of silver cyanide was much higher than that of gold cyanide.

The role of flotation in gold recovery has recently been investigated and discussed (Jackman and Williams, 1995; Lins and Adamian, 1993). The objectives and the modes of application depend on the ore types, the gold associations, other valuable metals, market considerations and environmental requirements.

In Australia, it has been shown that flotation columns can recover significantly more gold than mechanical cells, in tests with a new collector, Karbochem, SK5 (O'Connor and Dunne, 1991; Subramanian, 1988). Recovering fine gold particles from tailings by column flotation in South Africa might save some lower gold grade mines from closure (Franzidis, 1991). In Canada, column flotation has also demonstrated its ability in roughing. Under the optimum operating conditions, column roughers can achieve much higher rougher concentrate grades than those obtained by mechanical flotation cells (Furey, 1990)

Flash flotation, with a retention time of 1-3 minutes, improved the recovery of 30-100 μm gold particles from cyclone underflow or the discharge of a ball mill (McCulloch, 1990). It has been proved that the installation of large flash cells in gold mines in Australia, Ghana and New Zealand greatly improved productivity (Bourke, 1995). There was significant coarse liberated gold in the circulating load of a ball mill that might not be readily floated. Recovering gold from the cyclone underflow by the installation of the Knelson Concentrator improved the recovery of coarse gold particles ahead flotation circuits (Putz, 1994).

2.2.4 Gold Cyanidation

Gold cyanidation has been the most important method of gold extraction from gold ores since its first commercial application in 1889.

The dissolving action of cyanide solutions on metallic gold was known as early as 1783; solutions obtained by dissolving gold in cyanide solution were used by Elkington to prepare the bath used for electroplating gold. In October 1887, British Patent No. 14174 entitled "Process of Obtaining Gold and Silver from Ores" was issued. The discovery was made by John Atewar MacArthur, who was a chemist-metallurgist, supported and assisted by Robert and Willian Forrest, two brothers practising medicine in Glasgow (Habashi, 1987; Mellor, 1923).

The process, which became known as cyanidation, in reference to the alkali cyanide reagent used, immediately achieved industrial success in New Zealand in 1889 and in South Africa in 1890 (McQuiston and Shoemaker, 1975; Habashi, 1987), and almost completely replaced the chlorination method. In 1903, MacArthur was awarded the first medal of The Institution of Mining and Metallurgy in London. The cyanidation process was responsible for doubling gold production in the world in two decades.

> Faraday described the dissolution mechanisms as follows: "Air voltaic circles are formed in their cases, and the gold is dissolved almost exclusively under their influence. When one piece of gold leaf was placed on the surface of a solution of cyanide of potassium, and another moistened on both sides was placed under the surface, both dissolved; but twelve minutes sufficed for the solution of the first, while more than twelve hours were required for the submerged piece......" (Habashi, 1987). Thus, the role of oxygen was discovered very early on.

Generally, the ground ore is leached in agitated tanks, using lime (to maintain pH of the solution in the range of 10.5 -12) and cyanide (normally sodium cyanide) at a concentration of 20-200 ppm. In most cases, the leach liquors obtained by agitation leaching contain about 2-10 ppm of gold, and those obtained by heap leaching of low grade ores usually less than 1 ppm. The main chemical reactions of cyanidation are as follows (Prasad et al, 1991; Piret et al, 1991):

$$4Au + 8NaCN + O_2 + 2H_2O = 4NaAu(CN)_2 + 4NaOH \qquad (2\text{-}2)$$

or

$$4Au + 8CN^- + O_2 + 2H_2O = 4Au(CN)^-_2 + 4OH^- \qquad (2\text{-}3)$$

$$2Au + 4CN^- + O_2 + 2H_2O = 2Au(CN)^-_2 + H_2O_2 + 2OH^- \qquad (2\text{-}4)$$

It used to be that the leached pulp underwent counter-current decantation (CCD) or filtration using drum or belt filters. The precious metal values were finally cemented from the pregnant liquor using zinc dust (the Merrill-Crowe process), or (more seldom) were electrodeposited through electrowinning. The Merrill-Crowe process was introduced commercially for the treatment of cyanide leach solutions in 1890 (Rose, 1937). Some fundamentals of gold cementation were described by Adamson (1972). According to Barin et al (1980), the overall reaction of cementation is:

$$Zn + Au(CN)_2^- + H_2O + 2CN^- \rightarrow Zn(CN)_4^{2-} + OH^- + Au + \tfrac{1}{2}H_2 \qquad (2\text{-}5)$$

When slimy ores are leached, filtration to prepare clear solutions becomes an expensive operation; for this reason, the so-called carbon-in-pulp (CIP) process was developed. After agitation cyanidation, carbon is added to the pregnant pulp. When the adsorption of aurocyanide unto carbon is complete, the pulp is screened to separate the gold-laden carbon for washing and desorption. The process has the advantage of eliminating the expensive filtration operation needed in the case of the Merrill-Crowe process (Habashi, 1987) and savings of 20 to 50% can be obtained. Dissolved gold recovery is also higher than with counter-current filtration. Another variation is carbon-in-leach (CIL), in which carbon is put into the pulp during the cyanidation leach. It is especially appropriate for ores containing carbonaceous material, as dissolved gold is immediately adsorbed by the carbon pellets rather than the carbonaceous matter in the ore (Sorensen, 1984).

The loaded carbon must be treated by an elution step (sometimes referred to as 'stripping') to desorb the gold suitable for the final gold recovery by electrowinning or zinc precipitation. The method of desorption can be the atmospheric Zadra process, the alcohol stripping process, the high-pressure stripping process, the Anglo-American stripping process or the Micron gold desorption process (Yannopoulos, 1991; Harris, 1991).

Electrolysis can be used for the extraction of metals from either aqueous solutions or molten salts, known as electrowinning, and for the purification of crude metal obtained by other extraction routes, known as electrorefining (Bodsworth, 1994). Electrowinning of gold from dilute pregnant solution was developed by Zadra (1950), who proposed and tested a cathode compartment packed with steel wool in a cylindrical cell. The extensive surface of the cathode allowed an acceptable rate of gold electrowinning from dilute pregnant solutions. A modern electrowinning cell is rectangular, and has pervious cathodes packed with steel wool and stainless steel mesh anodes (Zadra 1950, Yannopoulos, 1991).

The mechanism of electrolytic deposition of gold probably proceeds by the adsorption of aurocyanide at the cathode, followed by reduction of the adsorbed species, as follows (Marsden and House, 1992; Kuhn, 1978):

$$Au(CN)^-_2 \leftrightarrows AuCN_{ads} + CN^- \quad (2\text{-}6)$$

$$AuCN_{ads} + e \leftrightarrows AuCN^-_{ads} \quad (2\text{-}7)$$

The reaction step is then followed by the dissolution of the reduced species:

$$AuCN_{ads} \leftrightarrows Au + CN^- \quad (2\text{-}8)$$

CHAPTER 3 RECOVERY OF GOLD GRAVITY CONCENTRATES AND THEIR FURTHER UPGRADING

3.1 Gravity Gold Recovery in South Africa

The gold particles in Witwatersrand ore in South Africa are usually smaller than 300 μm (Burt, 1984). The ore types are not much different from one mine to another; thus, significant operating knowledge and experience has been built up over the years and there is considerably less risk in selecting a gold recovery process route. The vast majority of gold mines in South Africa are founded by one or other of the mining groups, Anglo American, Gengold, J.C.I., Rand Mines or Goldfields (Lindeman, 1992).

3.1.1 Methods of Primary Gravity Recovery

In South Africa, in the early 1980s, 70% of gold mills still used gravity concentration followed by barrel amalgamation of the concentrates, particularly where the grade was high (Weiss, 1985). Many of the gravity devices used in the gold industry were created in South Africa (Adamson, 1972), these being Johnson cylinders, belt concentrators or plane tables. Although, as of 1996, virtually no gravity recovery is now practiced in South Africa, it is worthwhile to review the evolution of gravity circuits over the years.

Johnson Cylinder: It consists of a slowly rotating cylinder, 0.91 m in diameter by 3.66 m long, with its axis sloping at about 10%. The discharge from a tube mill flows through the interior of the cylinder, which is lined with corduroy cloth to trap the high density constituents in the pulp. The concentrate is washed out at the apex of the revolution into a regrinding circuit or the recovery house.

Belt Concentrator: This device was created in 1949. It is a slow moving endless rubber belt, 1.52 m wide, riffled in a similar manner as the corduroy cloth. The belt slopes downwards at an angle of 12°, but moves upwards at a rate up to 0.38 m per minute. The mill pulp flows down over the riffles which collect a concentrate of gold and pyrite. The concentrate moves countercurrent to the flow of pulp, is washed out of the riffles from under the head pulley and taken to the clean-up room for amalgamation.

Plane Table: The plane table consists of an inclined steel or wooden table, 1.52 m long and 1.07 m wide, sloping between 8-12°, with a step halfway down the table. The deck is covered with two sections of riffled rubber matting of the same type used as a substitute for corduroy cloth, but with the riffles running longitudinally instead of transversely. As the pulp flows over the table, gold concentrates in the troughs of the rubber matting.

Other types of gravity concentrators are:

Cylindrical Concentrators: This was a modified type of Johnson cylinder using riffled rubber mats instead of corduroy cloth to line the interior of the cylinder. This apparatus was used as a primary concentrator, and the concentrate from three units was re-treated on an endless moving belt concentrator prior to amalgamation in the recovery plant.

Jigging: Although sporadic experiments were conducted with several types of jigs, no economically satisfactory results were obtained until 1960. During the sixties, two new gold plants used jigs with the objective of eliminating corduroy concentrators. Jigs occupied less floor space, and those used were the Yuba Richards mineral jig, which comprises two cells, each 1.07 square meter, fitted with fixed screens and rubber diaphragms to provide the necessary pulsations.

3.1.2 Upgrading of Gravity Concentrates

In South Africa, Johnson cylinder drums were generally used as the primary concentrators followed by re-dressing on endless riffle belts. This yielded concentrates assaying typically 6-22 $kg.t^{-1}$ gold (Davidson, 1978). There were several methods to recover gold from these concentrates, mainly tabling and amalgamation. Most gold gravity concentrates, however, were traditionally treated by amalgamation (Lindeman, 1992). In 1990, more than two thirds of the gold was treated in this way because of its simplicity (Piret, et al., 1991). During the 1970s, intensive cyanidation and chlorination to recover gold from these gravity concentrates were also investigated and developed.

Intensive Cyanidation

Since amalgamation and retorting are much more labour intensive and hazardous than cyanidation, and conventional cyanidation has a slow leach rate, the so-called "intensive cyanidation" process had been developed in South Africa (Dewhirst et al, 1984; Davidson, 1978). This technique uses a high cyanide dosage (up to 50 $kg.t^{-1}$), oxygen sparging and vigorous agitation to tackle the high gold content and coarse particle concentrates. The gold content of the concentrates ranged from 6 to 22 $kg.t^{-1}$. The proposed principal flowsheets are: (i) cyanidation-electrowinning for lower grade gold concentrates; (ii) flotation followed by smelting of the concentrate and cyanidation-electrowinning of the tails for higher grade gold concentrates. Intensive cyanidation can yield up to 99.9% gold extraction in four hours.

Two plants in South Africa using intensive cyanidation to substitute for amalgamation, Western Holdings and East Gold Plant of Vaal Reefs Exploration and

Mining Company Limited, were commissioned in 1971 and 1981, respectively (Dewhirst et al., 1984). The main advantages of intensive cyanidation compared to amalgamation were found to be 2-4% higher gold extraction, and the elimination of pollution due to mercury losses. However, intensive cyanidation resulted in two new problems, high cyanide consumptions and the impact of increased cyanide discharge to the environment. Intensive cyanidation needs a relatively large amount of gravity gold concentrate to achieve continuous operation. This is not a problem in South Africa, where many mines produce in excess of 40 t of gold yearly. In Canada, however, most mines produce less than 5 t of gold yearly. Therefore, intensive cyanidation is not an ideal alternative to upgrade gold gravity concentrates in Canada.

Chlorination

Laboratory and pilot experiments carried out by the Anglo American Research Laboratory have shown that the wet chlorination process could recover gold with 999.5 parts per thousand gold fineness from gravity concentrates (Finkelstein et al, 1966). Before chlorination, a gravity concentrate containing 6% Au was first roasted at 800 °C; 97% of the sulphur was removed, and the iron sulphides were converted to hematite, which is not appreciably attacked by either chlorine or hydrochloric acid solutions. After filtration, 99.5% of the gold was recovered and 90% of the silver remained with the calcine in the form of silver chloride. Chlorinated pregnant solutions were treated with sulphur dioxide to precipitate gold. The gold concentrates must be roasted prior to chlorination because chlorine attacked almost all the pyrite and tramp iron, resulting in a long leach time (>10 hours) and higher chlorine consumption. It seems that if a very high grade of gravity concentrate, for example 50% gold, is treated by chlorination, the method might be attractive, especially if the roasting step is omitted.

3.1.3 Current Situation in South Africa

The status of gold recovered by gravity has changed appreciably in recent years in the gold mills of South Africa (Laplante, 1995). Gold gravity circuits almost disappeared because of the lack of perceived benefit and the security risk of the gravity separation. The lack of perceived benefit is in part due to very aggressive flowsheets, typically an acid leach to recover uranium followed by neutralisation and cyanidation/CIP. Pyrite is then floated from the cyanidation tail, roasted to produce sulphuric acid (used to dissolve uranium), and the calcine is cyanided again. The double cyanidation step suggests that little additional recovery, if any, can be achieved by an upstream gravity circuit.

However, gravity separation has not completely disappeared, still being used as an auxiliary to recover platinum group elements from the Merensky Reef Ores. Further, the need to reduce milling costs (hence flowsheet complexity) and the worsening of the gold theft problem (despite the removal of gravity recovery) may herald a new era of gold recovery in South Africa.

3.2 Gravity Gold Recovery in Canada

With its immense mineral potential, gold camps in Canada have sprung up from Vancouver Island in the West to Newfoundland in the East. Well over 100 new exploration projects were under evaluation or in development in the late 1980s (Anderson, 1989). The major areas of gold production in Canada are in Québec, Ontario, British Columbia, and some gold mines operating in the North West Territories.

Unlike South Africa, where ore characteristics (quartz pebble conglomerates and quartzites) vary little from one mine to another, new mines in North America can exhibit considerable variations in mineralogy, and require careful test work for flowsheet selection. As a result, gravity recovery is comparatively easier to justify (Lindeman and Nendick, 1992).

CHAPTER 3 RECOVERY OF GOLD GRAVITY CONCENTRATES AND THEIR FURTHER UPGRADING

The major methods for gold recovery from Canadian ores are cyanidation, flotation and gravity. Where there are economic quantities of relatively coarse gravity recoverable gold, gravity concentration is incorporated either within, or immediately after, the grinding circuit. Where gold is essentially locked-up within non-cyanacide sulphides, then preconcentration of the sulphides by flotation is followed by a fine regrind and cyanidation of the flotation concentrate. Where the gold is fine grained and is both free and associated with sulphides, then cyanidation of the total ore, with or without gravity concentration preceding it, is required.

The new equipment developed in South Africa such as the plane table or Johnson cylinder is not used in Canada (Burt, 1984). Rather, primary gold gravity concentrates are produced by Knelson Concentrators and/or jigs, with a gold content between 0.1 and 5%. A few mills also use sluices, such as Meston Resources, or the spirals, such as Lucien Béliveau. This gravity stage can be called the primary stage, and is generally characterised by treatment of all the circulating load at low recovery with a jig, and a part of the circulating load at high recovery with a Knelson Concentrator. The metallurgical performance of a few Canadian gold gravity circuits is summarized in Table 3-1 (adapted and amplified from Wells and Patel, 1991; Bissonnette and Ladouceur, 1991; Coté et al, 1978; Giancola et al, 1995; Carter, 1992; Giancola et al, 1995; Honan and Luinstra, 1996; Hope et al, 1993).

The success of gravity circuits in Canadian gold mills is based on an increase of overall recovery of about 3% for less than 3% of total plant installed costs (Wells and Patel, 1991).

The primary concentrate is commonly accumulated for weekly treating on a Wilfley, Deister or Gemini table to produce a final concentrate, with the recycle of middlings. This gravity stage can be called secondary stage; it yields a concentrate of about 50% Au on average. Table recoveries are in the range of 80-95%.

TABLE 3-1 Some Canadian Gold Gravity Circuits

Name	Location	Capacity (t per day)	Head Grade ($g.t^{-1}$, Au)	Gravity Equipment	Gravity Recovery (%)	Conc. Grade (Au%)
Dome	Timmins Ontario	3000	3-8	Jig (replaced by KC), table	40-50	40-80
Campbell Red Lake	Balmertown Ontario	1000	20	Jig (replaced by KC) table, spiral	50	80
Golden Giant	Marathon Ontario	3000	12	Jigs and later a KC	30	75
Kidd Creek	Timmins Ontario	500	n/a	Jig, table	40	n/a
Johnny Mountain	British Colombia	n/a	n/a	Jig, table	22	65
Meston	Chibougamau Québec	1000	9	PS, KC, table	35-40	50-60
Jolu	Saskatoon Saskatcheman	500	12	Jig, table	n/a	65
Casa Berardi	La Sarre Québec	2000	8	KC, table	25	n/a
Snip Operations	British Colombia	500	30	Jig, table	35-40	50
Resources MSV Inc.	Chibougamau Québec	2500	4	Jig (later replaced by KC), table	20	80
Lucien Béliveau	Val d'Or, Québec	1070	2.5-4.5	KC, spiral, table	25	50
Agnico-Eagle (div.laRonde	Cadillac Québec	1800	10	KC, table	20-25	n/a
East Malartic	Malartic Québec	1800	10	KC, table	40	85

n/a: not available; PS: pinched sluice; KC: Knelson Concentrator; FC: flash cell

Gold losses during tabling are due to incomplete liberation in part, but are mainly attributed to gold fines and flakes, most of which are washed away to table tails before they can settle in the riffles.

The final gold concentrate is loaded into a furnace to produce bullion containing 90-98% gold plus silver. This can be identified as the third upgrading stage.

For all the gravity circuits described in Table 3-1, table tails are produced. These tails are characterized by high gold content (~1000-4000 $g.t^{-1}$) and a relatively high proportion of free gold fines. At present, in most of the plants, the table tails are recycled to the grinding circuit. As a result, a great portion of the gold value is diluted again to be sent to cyanidation or flotation.

Compared to Canadian standards, many South African gold mines are extremely large (>500,000 tr. oz (15552 kg) per year). Most Canadian mills produce gold from 50,000 (1555 kg) to 300,000 tr. oz. (9331 kg) per year, with only a very few producing more than 150,000 tr. oz. (4666 kg) per year (none outside Ontario except Lupin, North West Territories, and Doyon, Québec). As a result, typical daily production of primary gravity concentrates is around 1 tonne. The preferred choice at present is to treat by tabling, because intensive leaching would be more appropriate for daily productions of 10 tonnes and more (of primary gravity concentrates), typical of the South African mines. The possibility of using the Knelson Concentrator, substituting for or supplementing the shaking table to obtain high gold concentrates, and then, to produce pure gold from these gold concentrates by chlorination and cementation, or other feasible non-cyanide leaching routes, would be very attractive.

3.3 Non-Cyanide Leaching Approaches

Some gravity gold concentrates, especially second stage table tails, contain a high portion of gold fines and gold flakes, which makes them difficult to upgrade with high recovery using gravity separation. Figure 3-1 shows a SEM image of minus 25 μm laboratory Knelson Concentrator tails that was obtained by reprocessing Meston table tails. From the photograph, it can clearly be seen that all the lost gold fines (white colour) are free gold particles, and that some of them are very fine, < 10 μm. For these very fine gold particles, direct non-cyanide leaching could be a feasible approach (Huang et al, 1993).

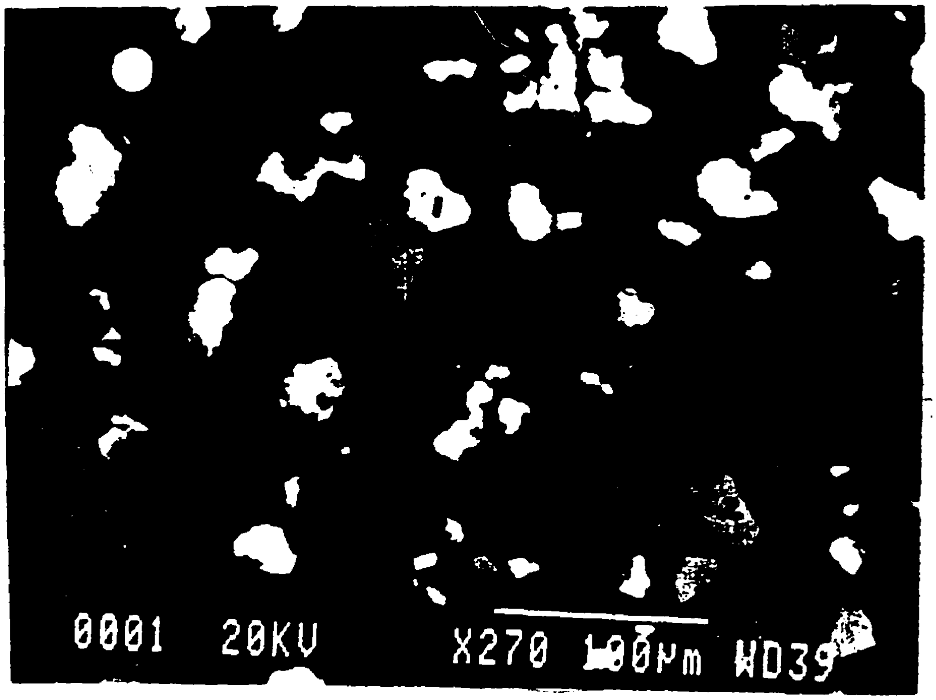

SEM: Meston Table tail → lab KC
Tail (-25 μm) 1. gold 2. arsenopyrite

FIGURE 3-1 SEM Back-Scattered Image of -25 μm Knelson Concentrator Tail for Meston Table Tail Processing (1: gold 2: arsenopyrite 3: pyrite 4: silica)

Due to the inherent disadvantages of toxicity and long residence time for conventional cyanidation (sometimes, more than 72 hours are needed), several other lixiviants have recently been investigated. These are bromine, chlorine, iodine, thiocyanate, thiosulphate and thiourea. Their major features, compared with cyanidation, are described in the following sections, and are summarized in Table 3-2.

TABLE 3-2 Non-Cyanide Lixiviants

Lixiviant	Formula	pH range	Auxiliary chemical	Comments	Applications
Bromine	Br_2	3-7	NaBr, KBr, NaCl	Fast rate, easy to regenerate, corrosive fumes, attack sulphides, high consumption	Roasted gold-bearing sulphide ore or conc. and black sand
Chlorine	Cl_2	<2.0	OCl^-, Fe^{3+}	Attack sulphides, carbon, organics, corrosive	Roasted gold ore or conc. or refractory ore pre-treatment
Iodine	I_2	2-10	Iodide	Fast rate, insensitive to sulphides, easy to regenerate, high consumption and costly	Limited to fundamentals using pure gold
Thiocyanate	MCNS (M-NH_4, Na, ..)	<3.0	Oxidant, MnO_2, Fe^{3+}	Insensitive to sulphides, fast rate, easy to generate, high consumption	Gold-bearing sulphide ore or conc.
Ammonium thiosulphate	$(NH_4)_2S_2O_3$	>7	Stabilizer: SO_2, sulphite catalyst: Cu^{++}	Non-toxic, high consumption	Copper or manganese-bearing gold ore or conc.
Thiourea	$(NH_2)_2CS$	<2.0	Oxidant, Fe^{3+}, H_2O_2, $KMnO_4$	Insensitive to sulphides, less toxic, fast rate, high consumption	Gold-bearing sulphide ore and conc.

3.3.1 Bromine

Bromine has the fastest dissolution rate for gold among the alternative lixiviants. Bromine is easy to regenerate, but has a high vapour pressure, with very corrosive fumes. It exhibits a high consumption in the presence of sulphide minerals since it is a powerful oxidant. Therefore, it is suggested that all constituents present in the lower oxidation states should be preoxidized to their highest oxidation states, for example by roasting (Michaelis, 1987; Rose, 1984; Prasad, Biney and Pizarro, 1991; Pesic and Sergent, 1991; Sergent and Dadgar, 1990).

Many of the reactions of bromine are associated with its oxidizing power as:

$$\tfrac{1}{2}Br_2 + e \rightleftarrows Br^- \qquad E^\circ = 1.065\ V \qquad (3\text{-}1)$$

Therefore, bromine is capable of oxidizing a variety of materials which are less electronegative. It is a stronger oxidant than ferric iron or dilute nitric acid, but weaker than oxygen or ceric sulphate (Jolles, 1966). The dissolution of gold in bromine solutions is an electrochemical process (Dadgar, 1989) as illustrated by:

$$Au = Au^{3+} + 3e \qquad E^\circ = 1.50\ V \qquad (3\text{-}2)$$

$$2H_2O = O_2 + 4H^+ + 4e \qquad E^\circ = 1.23\ V \qquad (3\text{-}3)$$

$$H_2 = 2H^+ + 2\ e \qquad E^\circ = 0\ V \qquad (3\text{-}4)$$

When gold is dissolved in bromine solutions, the following reaction takes place (Dadgar, 1989):

$$Au + 4Br^- = AuBr^-_4 + 3e \qquad E^\circ = 0.87\ V \qquad (3\text{-}5)$$

In Geobrom 3400 (a proprietary stabilized form of soluble bromine) solutions, the overall reaction of gold dissolution can be expressed as (Dadgar, 1989):

$$2Au + 3HOBr + 5Br^- + 3H^+ = 2AuBr^-_4 + 3H_2O \qquad (3\text{-}6)$$

According to reaction 3-6, gold is first oxidized to Au^{3+} by HOBr, and then forms a stable complex, $AuBr_4^-$ with bromine.

Bromine has been successfully used to leach flotation concentrates (Dadgar, 1989) and black sand concentrates (Dadgar et al, 1990). Due to the higher contents of carbon (10-13%) and sulphur (12-15%), flotation concentrates containing about 300 $g.t^{-1}$ Au were roasted at 670-750°C before leaching. Using 4 $g.L^{-1}$ Geobrom 3400 at a pH range of 5.0-6.0, 98% of the gold was extracted within 2 hours.

A black sand with a grade of 6 $kg.t^{-1}$ Au, consisting predominantly of magnetite, and hematite, as well as a small amount of nickel, manganese, chromium and titanium, was tested. When an oxidation-reduction potential (ORP) of 800-900 mV was maintained, extraction reached a maximum after 6 hours. To extract ~95% Au from such a high grade concentrate, a ratio of 14 g Geobrom to 100 g of the concentrate was required (Dadgar et al, 1990).

It is very difficult for bromine to leach gold from gold gravity concentrates with high sulphur contents without pre-roasting, which has been shown by some exploratory tests conducted at McGill University. Since Geobrom reacts vigorously with sulphides, the Eh value of the system dropped sharply, from an initial 604 mV down to a final 182 mV. After 6 hours leaching, the extraction of gold was only about 1%, whereas it was 95% for a South African tail with a low sulphide content. If sulphide concentrates are roasted prior to leaching, the sulphur dioxide released would have to be captured to avoid environmental problems.

3.3.2 Chlorine [1]

Direct chlorine leaching of gold is normally carried out at pH <2.0. It can also be used as a pretreatment for refractory gold ores where fine gold particles are released from sulphide minerals, while carbonaceous material and humic acid are oxidized or rendered inactive (Guay and Peterson, 1973; Guay, 1980; Scheiner, 1971). Gold is separated from silver (which is present as insoluble chloride) by simple filtration (Finkestein et al, 1966; Yen, Pindred and Lam, 1990; Li et al, 1992; Seymour and Ramadorai, 1988).

---

[1] Please also see Appendix 1-1.

Like bromine, gaseous chlorine is pungent and an irritant, and measures must be taken for preventing its leakage. Chlorine is also a strong oxidant, and in most cases, sulphur-bearing gold ores or concentrates must be roasted prior to chlorination in order to reduce chlorine consumption. However, chlorine is preferred over bromine for treating concentrates with a high gold content (>50% Au) because pure gold is much more easily recovered from chloride solutions by precipitation and silver is easily separated from gold as an insoluble silver chloride leach residue.

It has been shown that the rate of gold dissolution in chlorine solutions is markedly accelerated in the presence of chloride ions (Putnam, 1944). The first reaction between gold and chlorine is the formation of aurous chloride which is not only insoluble but also metastable:

$$2Au + Cl_2 \rightarrow 2AuCl \tag{3-7}$$

The dissolution rate of gold is therefore controlled by the rate at which the insoluble aurous chloride film is removed from the surface by the following reactions:

$$AuCl + Cl^- \rightarrow AuCl^-_2 \tag{3-8}$$

$$AuCl + Cl^- + Cl_2 \rightarrow AuCl^-_4 \tag{3-9}$$

3.3.3 Iodine

Iodine forms the most stable gold complexes of all the halogens. It is claimed that iodine does not adsorb to any great extent on gangue minerals (Jacobson and Murphy, 1987), and is easily regenerated (Prasad et al, 1991; Qi and Hiskey, 1988). It is also claimed that the excessive consumption and high cost of iodine are the main reasons that it could not compete with cyanide (Prasad et al, 1991). At ambient temperature, gold dissolution by a mixture of iodine and iodide is strongly dependent on the iodide concentration (controlling the oxidation half-cell) and the iodine concentration (controlling the reduction half-cell) (Davis et al, 1993).

In iodine leaching of gold, the iodide ion acts as a complexing agent and the iodine as the oxidant. The triiodide ion can serve as an oxidant. The reactions are as follows (Davis and Tran, 1991):

$Au + 2I^- = AuI^-_2 + e^-$ anodic (3-10)

$I^-_3 + 2e^- = 3I^-$ cathodic (3-11)

$2Au + I^- + I^-_3 = 2AuI^-_2$ overall (3-12)

Iodine leaching is insensitive to pH over the range pH 2-10 (Qi and Hiskey, 1991). However, few applications of iodine leaching of gold concentrates have been reported; most studies have been limited to examining process fundamentals using pure gold.

3.3.4 Thiocyanate

In acidic solution (pH 1-2), using pyrolusite (63.2% MnO_2) as an oxidant and ammonium thiocyanate (NH_4CNS, low toxicity) as the leachant, a new leach method for gold and silver extraction was proposed by Pang et al (1992). For a sulphide concentrate containing 59 g.t $^{-1}$ Au and 34.8% S, after 7 hours of leaching, gold extraction was 99% (Pang et al, 1992, Swaminathan et al, 1993). The consumption of thiocyanate was higher than that of cyanide and thiourea, but lower than that of thiosulphate. The reaction sequence was considered to be:

$$MnO_2 + 4H^+ + 2e \rightarrow Mn^{2+} + 2H_2O \qquad (3\text{-}13)$$

$$Au + 2CNS^- \rightleftarrows Au(CNS)_2^- + e \qquad (3\text{-}14)$$

When the pH is <4.0, the following reactions take place:

$$MnO_2 + 4H^+ + 4CNS^- \rightarrow Mn(CNS)_2 + 2H_2O + (CNS)_2 \qquad (3\text{-}15)$$

$$(CNS)_2 + 2Au + 2CNS^- \rightleftarrows 2Au(CNS)_2^- \qquad (3\text{-}16)$$

Using pH-potential diagram methodology, Broadhurst and Preez studied the thermodynamics of gold dissolution in the acidic iron/thiocyanate/sulphate/water system (Broadhurst and Preez, 1993). They claimed that this thermodynamic study is useful for predicting the feasibility and optimum experimental parameters of gold dissolution in the above system.

Exploratory tests have been carried out at McGill University, and showed that using 106 $kg.t^{-1}$ ammonium thiocyanate and MnO_2 as an oxidant, more than 80% of the gold was extracted from Meston table tails assaying 3.5 $kg.t^{-1}$ Au after 6 hours of leaching. It was concluded that thiocyanate might be a promising leachant for gravity gold concentrates, although appreciable further work is necessary.

3.3.5 Thiosulphate

The thiosulphate leach is nontoxic. Since it has the capacity to reduce manganese dioxide and also has to use copper ion as a catalyst, the thiosulphate leach is suitable for treating copper-bearing or manganese-bearing gold ores (Zipperrian and Raghavan, 1988; Jiang and Chen, 1990).

The thiosulphate leach is conducted in alkaline medium, at an optimum temperature range of 50-60°C. Because thiosulphate itself can be consumed in an oxidizing medium, SO_2 or sulphite must be added to the leach system as a stabiliser (Hu and Gong, 1991). Under the conditions of 22% thiosulphate, 7% NH_3 and 1.5% $CuSO_4$, the extraction of gold from rhyolite was about 90% after 3 hours of leaching at 60°C (Zipperian and Raghavan, 1988):

The main reactions during thiosulphate leaching are as follows (Zipperian and Raghavan, 1988).

$$2Au + \tfrac{1}{2}O_2 + 4S_2O_3^{2-} + 2H^+ \rightarrow 2Au(S_2O_3)_2^{3-} + H_2O \qquad (3\text{-}17)$$

$$Au + 5S_2O_3^{2-} + Cu(NH_3)_4^{2+} \rightarrow Au(S_2O_3)_2^{3-} + 4NH_3 + Cu(S_2O_3)_3^{5-} \qquad (3\text{-}18)$$

From an environmental standpoint, thiosulphate leaching has a definite advantage over cyanide. It is suitable for treating gold-bearing copper ore, but has a higher consumption than cyanide.

3.3.6 Thiourea

Thiourea has a lower toxicity than cyanide, although it has been claimed that this reagent might be a carcinogen (Sax, 1975; DeVries and Hiskey, 1992), faster gold dissolution rates, higher selectivity and lower sensitivity to base metals or impurities (Farinha et al, 1992; Raudsepp and Allgood, 1987; Huyhua et al, 1981; Deschenes, 1986). However, thiourea is sensitive to variations in experimental conditions. The optimum pH range is 1.0-2.0.

The overall formation constant of the gold (I) thiourea complexes is as follows (Huyhua and Gundiler, 1984).

$$Au^+ + 2NH_2.CS.NH_2 = Au(NH_2.CS.NH_2)_2^+ \qquad pK_f = -21.03 \qquad (3\text{-}19)$$

In the presence of an oxidant, thiourea is oxidized to form a number of products, the first step being the formation of formamidine disulphide. The redox potential of the thiourea/formamidine disulphide system is described by the following equation (Preisler and Berger, 1947).

$NH_2(NH)CSSC(NH)NH_2 + 2H^+ + 2e \rightleftharpoons 2NH_2.CS.NH_2 \quad E^\circ = 0.42\ V$ (3-20)

It has been demonstrated that formamidine disulphide is an active oxidant for gold and silver dissolution (Huyhua and Gundiler, 1984).

The hydrolysis or degradation of thiourea by oxidation is a critical limitation in the applicability of acidic thiourea solutions. To reduce the consumption of thiourea and to avoid passivation, it is necessary to find a suitable oxidant (Yannopoulos, 1991). Ideally, oxidants should be non-complexing and stable, and should prevent degradation of thiourea and increase the dissolution rate of gold.

For a pyrite concentrate with 65 $g.t^{-1}$ Au and 1% Cu, the optimum thiourea leach conditions were 5 $g.L^{-1}$ thiourea, 15 $g.L^{-1}$ sulphuric acid, 40°C and 40% solids. After two-stage leaching of the concentrate, each of two hours, 96% gold extraction was obtained (Raudsepp and Allgood, 1987). For the pilot test (750 $g.h^{-1}$), gold extraction was 94.4% with a reagent consumption of 1.9 $kg.t^{-1}$ thiourea, 11 $kg.t^{-1}$ H_2SO_4, 1.7 $kg.t^{-1}$ H_2O_2 and 3.2 $kg.t^{-1}$ SO_2 (Raudsepp and Allgood, 1987).

3.4 Conclusions

Gravity separation has been an important method of gold recovery for thousands of years. There is no doubt that it is an economical, pollution-free method, especially when compared to cyanidation. It is still extensively used in the world and has experienced a resurgence in popularity because of the advent of the Knelson Concentrator. It can be expected that gold recovery by gravity separation will continue to play an important role, especially for small and middle sized gold mines.

Most of the gravity equipment used in the gold industry was originally created or first used for gold in South Africa, such as the Johnson cylinder, belt concentrator, plane table, cylindrical concentrator and jig. However, the situation has greatly changed in recent years in that the gravity circuits in gold ore processing in South Africa have almost disappeared. This is partly because the technology of acidic leach-cyanidation-flotation-calcination-cyanidation is very suitable to treat the gold-uranium-PGM ores with a high throughput, and the application of CIP and CIL circuits has significantly increased the efficiency of recovering of dissolved gold. Intensive cyanidation and chlorination-precipitation for the further upgrading of gold gravity concentrates also virtually disappeared with the decline of gold gravity concentration.[2]

Compared to South Africa, most Canadian gold mines are much smaller, only one tenth to one fourth in size, but there are economic quantities of relatively coarse gravity recoverable gold in many mines. In most of the Canadian gold gravity circuits, primary gold concentrates with 0.2 - 5% gold are produced by Knelson Concentrators or jigs. There is a trend of replacing jigs by Knelson Concentrators. The primary concentrate is accumulated and treated daily by a shaking table to produce a concentrate with a gold content of 40-80% for smelting. The tabling operation is labour intensive, a security risk, and expensive (with gold contents in the table tails as high as 1000-4000 $g.t^{-1}$), especially when the primary concentrates are produced with the Knelson Concentrator. Exploiting the use of the Knelson Concentrator as a cleaner to replace or supplement shaking tables promises to be very attractive.

For the third stage (smelting), the high grade of the furnace feed is obtained at the cost of recovery during tabling. Smelting is expensive, cannot separate silver from gold, as well as having environment problems due to the release of sulphur dioxide. Intensive cyanidation is not suitable for Canadian gold mines because of the small quantity of the concentrate produced, typically 1 tonne per day, making its operation

---

[2] It is still being used in a few plants outside South Africa

difficult to justify. Therefore, chlorination, an alternative which can treat high grade gold gravity concentrates to produce very pure gold and separate silver. is a promising alternative.

Other non-cyanide lixiviants could also be options to treat gold gravity concentrates. However, their consumption and reactiveness to sulphides have to be evaluated. It seems that thiocyanate, thiourea, thiosulphate and iodine might be possible choices for the treatment of gold concentrates with high gold (0.5-5%) and sulphur (25-40%) contents. Exploratory tests conducted at McGill University have shown that using ammonium thiocyanate and MnO_2, after a 6-hours leach, 80% of the gold was extracted from Meston table tails, which contained 3.6 $kg.t^{-1}$ of gold and high contents of sulphides. Bromine and chlorine are likely to result in excessive consumption, although chlorine would be the reagent of choice for very rich (50%) gold concentrates and low sulphur contents.

In Canada, for the primary stage of upgrading, there is a trend for jigs to be replaced by the Knelson Concentrator; for the secondary stage, upgrading is likely to remain gravity, but tabling will be supplemented or replaced by Knelson Concentrators. This research work focuses on physical upgrading, through a study of the Knelson Concentrator. For final upgrading, an exploratory investigation of chlorination will be conducted in the future.

CHAPTER 4 THE KNELSON CONCENTRATOR

The Knelson Concentrator operates on the principle of centrifugal force. It is appropriate, therefore, to conduct a brief review of centrifugal concentration prior to the advent of the Knelson Concentrator.

4.1 A Brief Description of Centrifuges Used in Mineral Processing

Centrifugal concentration has been proved an effective technique for recovering fine or ultra-fine heavy minerals for many years. In centrifugal concentration, the centrifugal force acting on a particle can be much greater than the acceleration of gravity; as a result, the settling velocity of particles increases greatly. The higher the centrifugal intensity (the centrifugal acceleration over gravity acceleration, often noted 'g'), the finer the particles that can be recovered.

One of the traditional centrifuges extensively used in the Chinese mineral industry is "Yunxi Centrifuge" developed by the Yunnan Tin Corporation of China in the early 1960s. It is a horizontal unit aimed at effectively recovering very fine cassiterite particles. For tin ore slime, the suitable feed size is -0.074 mm, and the recoverable cassiterite particle size is 10 μm (Sun, 1982). The main body of the equipment is a drum; its diameter progressively increases toward the discharge end with an angle 3 - 5°. The slurry is fed into the drum, heavier particles settling down on the drum surface as a concentrate, and lighter particles are continuously discharged as a tail. It is a batch, or rather, a semi-batch machine, much like the Falcon Concentrator (to be described later), its feeding and concentrate washing periods being automatically controlled, as shown in Figure 4-1.

About 1000 such units were installed in tin, tungsten and iron ore plants in China (Fan, 1991). Appropriate centrifugal intensities are 102 'g', 51 'g' and 30 'g' for industrial equipment with diameters of 400 mm, 800 mm, and 1600 mm, respectively. The unit has a rather low capacity e.g. about 30 tonnes per day for a Φ 800 x 600 mm unit.

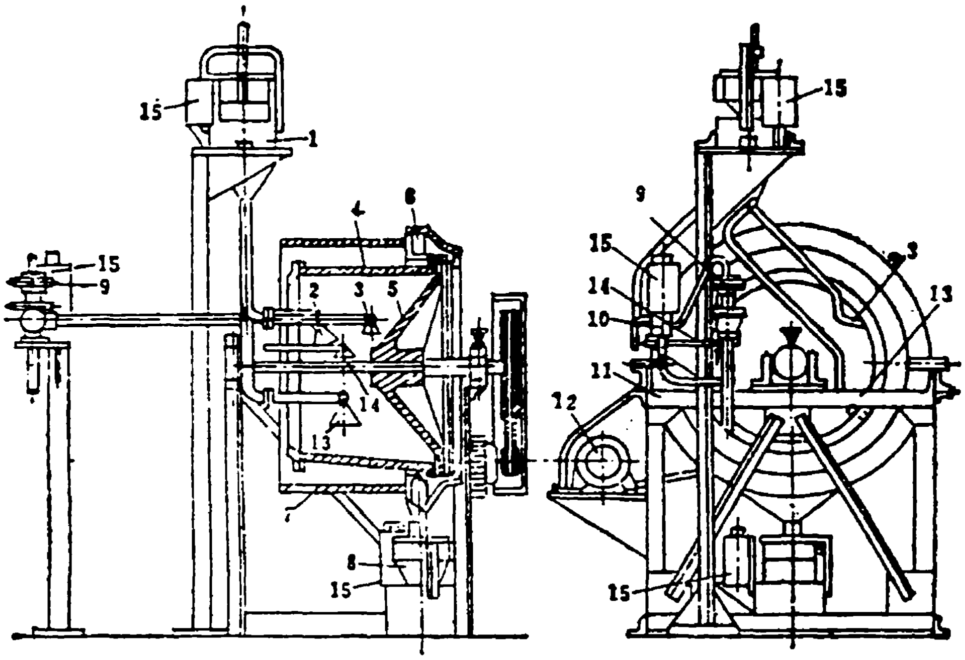

FIGURE 4-1 Schematic Diagram of Φ 800 x 600 mm Yunxi Centrifuge (Sun, 1982) 1: feed tank; 2: feed tube; 3: upper nozzle; 4: drum; 5: drum bottom; 6: feed tube; 7: security shield; 8: splitter; 9: diaphragm valve; 10: two-way valve; 11: frame; 12: motor; 13: lower nozzle; 14: washing water; 15: electromagnet.

In the late 1980s, a continuous centrifuge with a much higher rotation speed was developed by the Beijing General Research Institute of Mining and Metallurgy, China (Lu, 1990). It is also a horizontal unit, and works in a similar way to the Yunxi centrifuge. A Φ 600 x 240 mm centrifuge has a centrifugal intensity of 653 'g'. It is particularly suitable for treating ultra-fine particles (-40 μm), and recovers cassiterite fines down to 3 μm, but with a limited capacity of about 400 $kg.h^{-1}$.

The Kelsey Centrifugal jig is a gravity device utilizing the principles of the conventional jigs, but at an acceleration of 60 'g'. Its vertical rotational axis coincides with a downcomer used for feeding. Material then flows upwards on top of a series of hutches distributed cylindrically. Heavy particles are recovered in the hutches and flow outward to a concentrate launder. Light particles flow past the hutches to the top of the unit, to a tailings launder. Recent progress and applications of Kelsey jigs were reported by Beniuk et al (1994). The first commercial J650 Kelsey jig in the world was installed at Renison Limited, Australia, and two J1300 models were also prepared for the same mine. The results obtained show the Kelsey jig's superiority to historical performance with a shaking table. It was predicted that the equipment would have the potential to replace conventional gravity equipment, like shaking tables, to recover fine particles at a higher enrichment ratio and a lower cost. The unit was also briefly tested at Rio Kemptville Tin Mine. Higher recovery and grade were achieved at much higher throughput than the traditional electrostatic separators and shaking tables, and the Kelsey was less sensitive to changes in feed grade (Wyslouzil, 1990).

The Falcon Concentrator is also a vertical axis centrifuge. The rotating drum of the Falcon is smooth and there is no fluidization water flow (as provided in the Kelsey jig or the Knelson Concentrator). The feed is introduced via a central pipe to the impeller zone, then further accelerated as it flows on the inner wall of the rotor (McAlister, 1992). The lower half of the rotor is conical, with an angle of 8-14°, and is called the migration zone. The upper section, identified as the retention zone, is cylindrical. The Falcon has a high centrifugal intensity; e.g. the B6 laboratory Falcon has a rotational speed of 1950 rpm with an acceleration of 340 'g'. The Falcon is particularly suitable for recovering very fine particles on account of its high 'g's.

A B6 Falcon was systematically investigated using synthetic ores and Meston's flotation tails as well as Agnico-Eagle division LaRonde samples at McGill (Buonvino, 1993, Laplante et al, 1993). The results showed that the most important parameters affecting the Falcon's performance were the specific density and the size distribution of the material processed. The concentrate bed built up very quickly and recovery occurred predominantly on the surface via capture cites. Particles reported to the bed in two different ways: coarse particles were captured because they buried in the concentrate bed, and finer particles were captured when they lodged between the interstices created by the coarse particles. Four recovery phases were suggested: initial unselective recovery, optimum recovery, rapidly dropping recovery, and stable and near-zero recovery.

Potential industrial gold applications of the Falcon Concentrator include scavenging conventional gravity and cyanidation circuit tailings, cleaning gravity concentrate, scavenging flotation tailings (McAlister, 1992; Lins et al, 1992). It was reported that a semi-batch Falcon having a 6 in (15.2 cm) diameter bowl was used in the study of ash and sulphur rejection from coal (Honaker et al, 1995). The rotation speed of the bowl was 2000 rpm, yielding a centrifugal intensity of 300 'g'. The results showed that the Falcon was generally more efficient for this purpose than the traditional technology, flotation, which was only more efficient when the fine coals contained a small fraction of middling particles. A continuous C20 Falcon Concentrator was tested at Iron Ore Company of Canada Ltd. (Laplante et al, 1993). The results showed that the C20 Falcon eliminated concentrate bed overloading and the original bed dilution of the batch unit; however, upgrading was severely reduced, especially in the fine size range.

The Multi-Gravity Separator (MGS) is a continuous centrifugal device capable of processing very fine particles developed in recent years. It can described as the horizontal concentrating surface of a conventional shaking table wrapped in a drum and rotating rapidly. It was claimed that a double drum MGS produced a 40% tin concentrate with a recovery of 70% from a feed 83% finer than 75 microns and assaying 0.9% tin, at a feed rate 2.3 $t.h^{-1}$ (C 900 Multi-Gravity Separator booklet). The same results were obtained with a shaking table, but with a feed rate of only 0.19 $t.h^{-1}$. Recently, it was reported that using a MGS, a concentrate containing 50% Cr_2O_3 was obtained with a recovery of 72% from ore ground to 80% -100 μm (Belardi et al, 1995).

Depending on the nature of the material processed, the drum speed can be varied between 90 and 150 rpm, giving centrifugal intensities of 5.5 to 15.1 at the drum surface. The lower 'g's are suitable for the separation of high density materials from low density gangue, such as for tin ores. The high 'g's are required to separate minerals with a smaller density differential, particularly in the finer size range (Chan et al, 1991, Traore et al, 1995).

The working surface of the MGS is similar to slime shaking tables, but is much more effective, especially for processing narrowly-sized fine material, such as fine tantalum minerals. For the special purpose of recovering -30 μm tantalum, four types of centrifuges, the Knelson, the Falcon, Kelsey Jig and MGS, were tested. Results showed that the Knelson and Kelsey were incapable of recovering the very fine particles; the MGS was superior to the Falcon as well as to the existing equipment (Bartles Concentrator) at Tanco (Burt et al, 1995). The optimum recovery of the MGS was about 60%, 25-30% for the Bartles Concentrator, and less than 40% for the Holman table. Tests with the Falcon Concentrator for the same material were carried out at McGill University (McGuiness and Anonychuk, 1994). The results showed that to achieve a recovery higher than 35%, several passes through the Falcon, e.g. 3 times, were required, producing only moderate upgrading. For processing -40 μm material, size-by-size recoveries of the MGS were much higher than those of the Falcon (Burt et al, 1995).

4.2 Characteristics of the Knelson Concentrator

4.2.1 Basic Description

Since the first unit was commissioned in 1980, more than 800 Knelson Concentrators with different specifications have been installed in over 60 countries (Knelson and Jones, 1994). In recent years, the Knelson Concentrator has become the preferred gravity device to recover free gold. Compared to other centrifuges, it possesses quite different features either in design or separation mechanisms.

One unique feature of the Knelson Concentrator is its riffle construction and tangential fluidization water flow in the separating bowl, which partially fluidizes the concentrate bed. As a result, the unit can achieve high recovery over a wide size range. Industrial recoveries of gravity recoverable gold have been measured as high as ninety percent. Recovery is strongly influenced by feed rate and gangue density.

Knelson Concentrators have a large throughput capacity, e.g. a Φ 76 cm Knelson Concentrator can treat up to 40 tonnes of material per hour (Knelson and Jones, 1994). Locating the Knelson within the grinding circuit can eliminate the need for other gravity recovery devices (Banisi, et al, 1991). Another advantage of the Knelson is its ability to treat a wide size range of material without desliming, something most other centrifuges cannot do.

Twelve models of the Knelson Concentrator are currently available, from 7.5 to 76 cm (Knelson, 1988 and 1992). Knelson Concentrators can be classified into the Manual Discharge, Centre Discharge (CD), and Variable Discharge models (Knelson and Jones, 1994). Presently, a Φ 122 cm CD model is in its final test stage (Laplante, 1995).

The Manual Discharge Knelson (Figure 4-2) is especially suitable for the recovery of very low grade high density particles, typically on account of the limited concentrate volume. It develops a centrifugal intensity of 60 'g', and can process feeds finer than

6 mm. The feed is introduced to the bottom of the bowl by gravity through a downcomer. The feed requires only enough water for transport, and any density from 0 to 70% solids can be handled without any detrimental effect on operating efficiency.

Under the effect of the centrifugal force field, the heavy particles will report to the riffles as concentrate, whereas gangue minerals will flow to the outer rim as tails. The centrifugal force that would cause packing of material in the rings is partially offset by the fluidization water. The water jets are tangentially injected into the bowl from small holes on the Knelson Concentrator bowl in a direction opposite to the bowl's rotation.

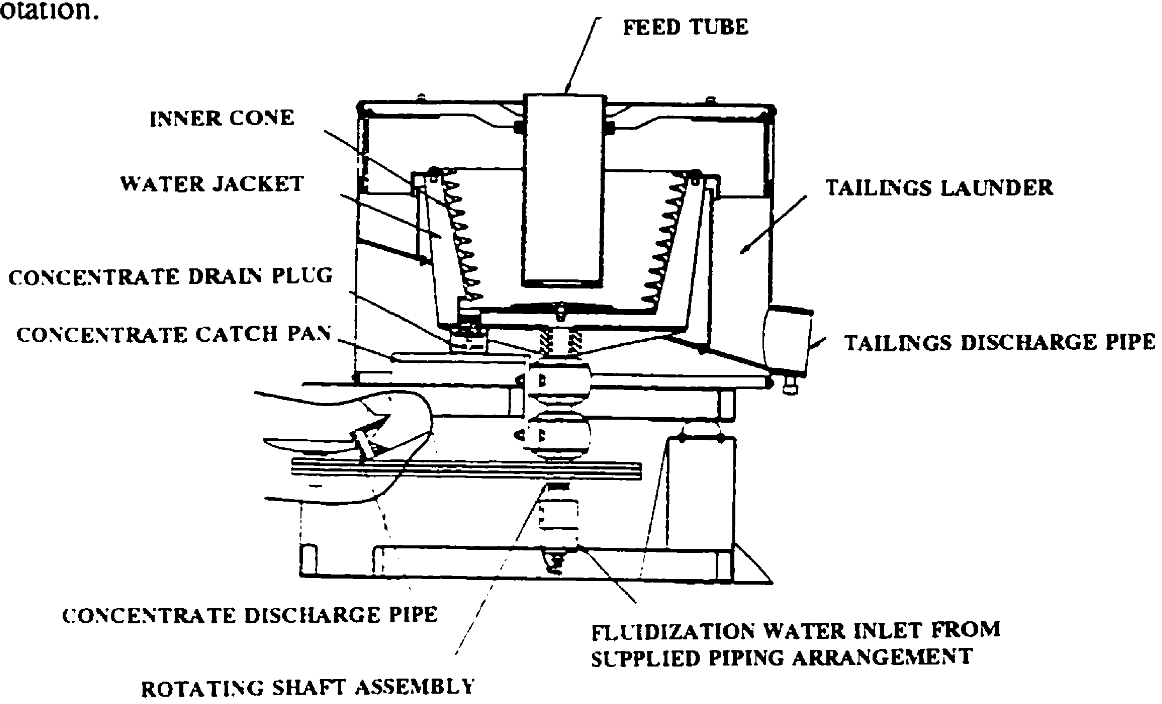

FIGURE 4-2 Cross Section of the Φ 76 cm Manual Discharge Knelson Concentrator (Knelson and Jones, 1994)

The resulting fluidized bed behaves as a heavy liquid whose density is that of the pulp, and hindered settling conditions prevail. It is in this constantly agitated environment that concentration takes place with the particles of higher specific density displacing the lighter ones.

Very high concentration ratios can be achieved, even above 500, at little or no loss of recovery. The Manual Discharge Knelson is a batch machine. The feed must be interrupted (normally, the Knelson Concentrator is simply by-passed during this operation) while concentrate removal takes place. This takes from 5 to 10 minutes, and is accomplished by unlocking an access door, removing a drain plug and flushing the concentrate to a secure gold room via a pipeline or into a container.

The manual discharge of its concentrate makes frequent flushing difficult, yielding loading cycles of two hours or more. Although virtually no gold operation can boast gold feed grades that would overload the Knelson over such recovery cycles, loss of recovery due to concentrate bed erosion, which will be discussed later, should require shorter recovery cycles. Another drawback of manual discharge is the security risk entailed.

The Knelson Concentrator requires little maintenance. It is sturdy and has only one moving part, the rotor. Its drive shaft passes through two pillow-block bearings, wetted surfaces are made of stainless steel, and the concentrating bowl is moulded in wear-resistant polyurethane.

The CD (central discharge) model (Figure 4-3) can be totally automated and integrated into any existing computerized circuit. It is manufactured in three production sizes, i.e., Φ 30 cm, Φ 50 cm and Φ 76 cm. There are three important improvements over the Manual Discharge Model: the shape of the concentrating bowl, the addition of a dual purpose hub directly below the bowl, and a feed deflector below the point of feed injection.

The removal of concentrate can be accomplished automatically in less than two minutes. The feed is first diverted (generally to a cyclone pump sump or ball mill), the fluidization water flowrate and the speed of rotation are reduced. The concentrate is then flushed from the concentrating rings past the feed deflector and piped directly to a secure gold room. Installations of the CD Model have been made in Canada, USA, Australia, Indonesia and Ghana.

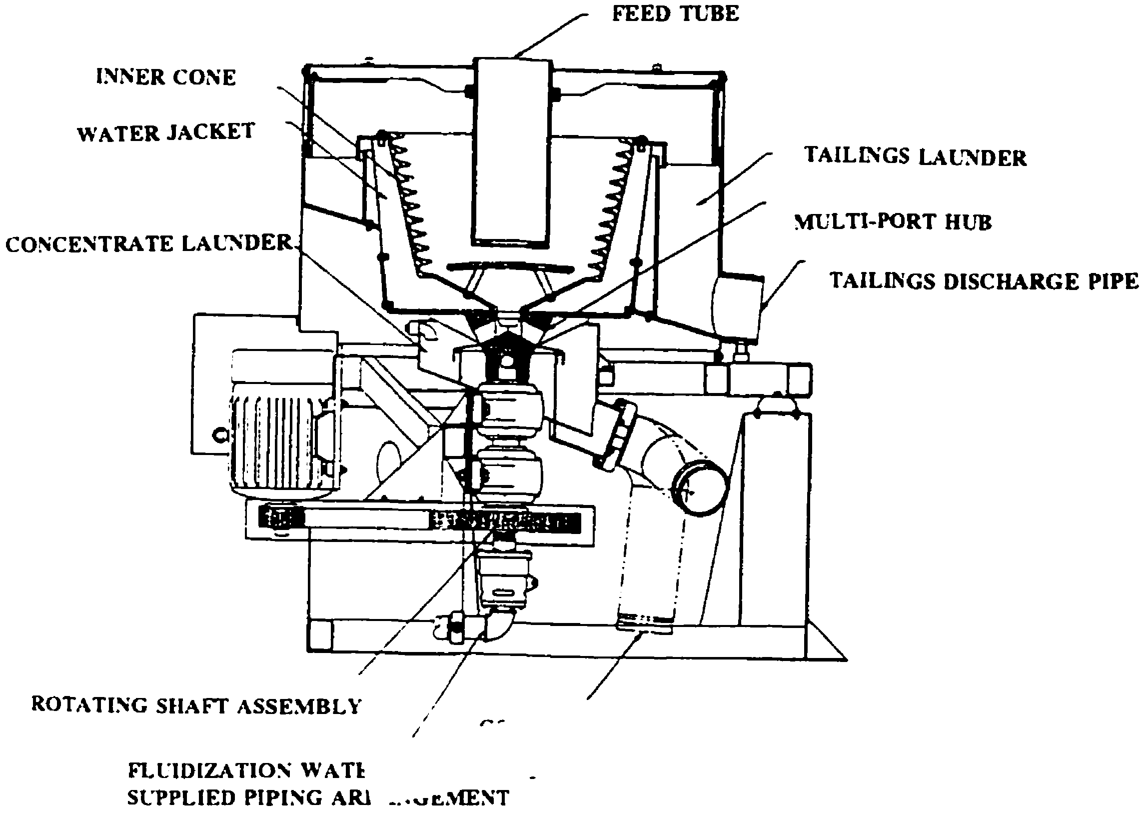

FIGURE 4-3 Cross Section of the Central Discharge Knelson Concentrator (Knelson and Jones, 1994)

The Variable Discharge Model is a continuously operating Knelson Concentrator still at the prototype stage (Figure 4-4). It has been specially designed for the base metal and coal industries, for yields of a few percent rather than much less than one percent, as appropriate with precious metals. The unit has been tested to separate the fine fractions of sulphides and ash from coal. Tests have been carried out by the CANMET (Canadian Centre for Mineral and Energy Technology) testing facility at Devon, Alberta, and very positive results were obtained (Knelson and Jones, 1994).

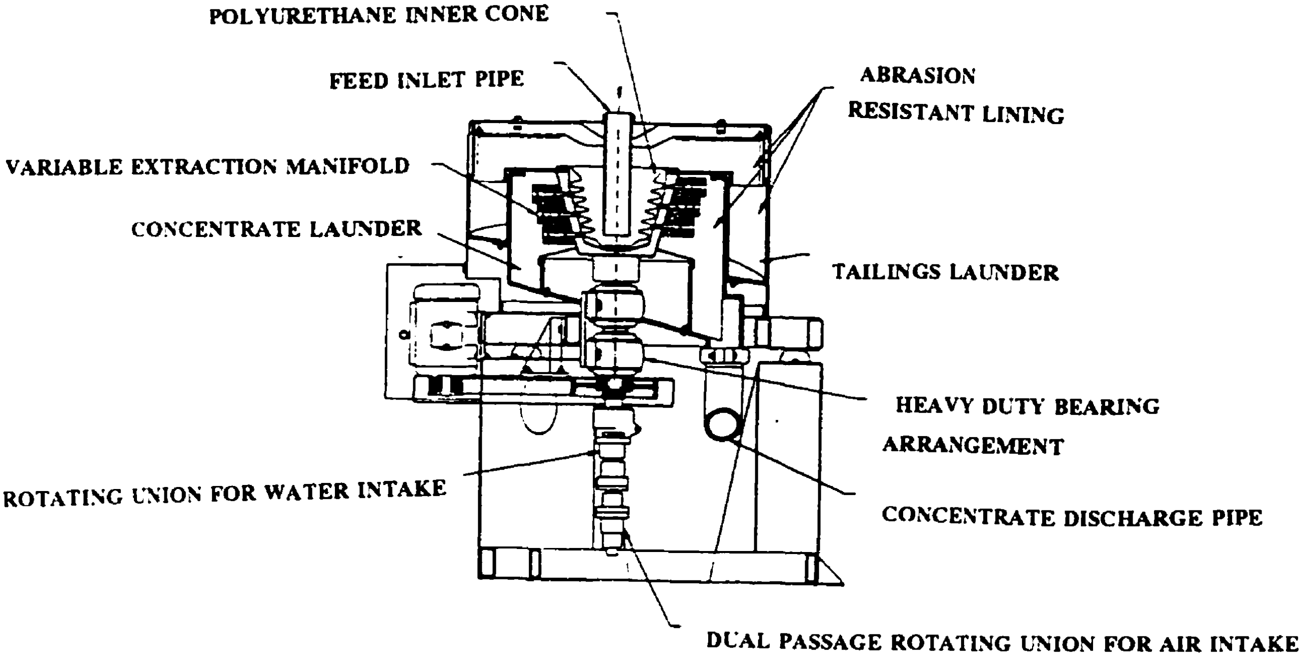

FIGURE 4-4 Cross Section of the Variable Discharge Knelson Concentrator (Knelson and Jones, 1994)

4.2.2 Industrial Applications

In North America, the two units of gravity separation that dominate gold recovery in grinding circuits are the Knelson and jig. Since the Knelson is much simpler to operate and can achieve at least similar gold recoveries, even when processing only part of the circulating load (Vincent, 1996), it has become the most logical choice for gold recovery by gravity separation.

Although the Knelson was originally designed for alluvial operations, hard-rock applications make up the majority of the existing user base. This can be explained by the behaviour of gold in grinding circuits, low breakage kinetics because of its malleability, and high recovery to cyclone underflows because of its density (Banisi, 1991). As a result, gold builds up in very large circulating loads in grinding-classifying circuits (Banisi, 1991; Poulter et al, 1995). If this liberated gold can be recovered in time, the over-grinding, flattening and tarnishing of the fresh surfaces would be avoided. In the meantime, since coarse free gold is recovered by gravity before cyanidation, the efficiency of cyanidation can also be improved.

A bleed extracted from cyclone underflow and processed with a Knelson was first applied at Les Mines Camchib Inc. (now Meston Resources) mill, where gravity recovery increased total gold recovery by about 3% (The present flowsheet is shown in Figure 8-7). The Knelson Concentrators recovered around 90% of the gravity-recoverable gold that was captured by the sluices (Laplante, 1987). The concentrate produced by the Knelson is generally sent to a shaking table, where a smeltable gold concentrate is achieved. The tails of the Knelson are normally recycled to the hydrocyclone feed or sent to the cyanidation section.

Generally, the benefits of gravity recovery are an increase in metallurgical recovery (e.g. recovering more gold), an increase in economic recovery (i.e. recovering gold into a higher-value product) and a decrease in capital and/or operating costs. For alluvial operations, where gravity is the sole recovery method, increases in metallurgical recovery can be spectacular, but are generally not well documented.

At Lac Minerals (now Barrick Gold) Est Malartic Division, north western Quebec, a massive sulphide copper/gold ore, the mill operation has been improved by the installation of the Knelson Concentrator (Hope et al, 1995). After a 76 cm Knelson replaced the Denver jig, the gold recovered by gravity separation was enhanced from 10.8% to 40% with an enrichment of 1000 in only a single stage. The concentrate was upgraded by a Gemini table, which replaced the original Wilfley table, and the recovery of tabling was enhanced from 50-60% to 95% with a concentrate grade of 85% Au.

Improvements in metallurgical recovery ahead of flotation will be more modest, because flotation can recover liberated gold reasonably well (Jackman and Williams, 1995). Nevertheless, increases in total recovery of 1 to 3% are routinely claimed, and are economically extremely significant (Darnton et al, 1995; Hart and Hill, 1995; Poulter et al, 1995; Cloutt, 1995). Recovering gold into a gravity concentrate that can be smelted results in a quick (generally less than one month) and high payment (generally more than 99% of gold value), as opposed to gold recovered into a flotation concentrate, which is typically paid for at 95 to 98% of its value after 3 to 6 months for copper concentrate. Gold recovered into zinc concentrates is often not credited at all. When flotation tails are cyanided, the major economic impact of gravity recovery is to maximize economic, rather than metallurgical recovery. As a result, gravity recovery ahead of flotation is generally advisable, in particular when significant gravity recoverable gold is present.

Ahead of cyanidation circuits, the economic impact of gravity is more difficult to assess. For example, at the Hemlo Golden Giant mill, it is claimed that no increase in metallurgical recovery was detected, even though the gravity circuit yields approximately 25% of the site production, and a significant decrease in carbon stripping costs should have justified installing the gravity circuit (Honan and Luinstra, 1996).

At Montana Tunnels gold mine in the United States, the intermittent loss of free gold has been observed in the flotation tails since the mill started up. A comprehensive research program led to a gravity circuit being installed at the cyclone underflow (two 76 cm Knelson Concentrators for processing the undersize of a Tyler doubledeck screen, Darnton et al, 1992). The primary objectives of reducing the loss of coarse gold during flotation and increasing the amount of payable gold in a cost-effective manner was achieved. Furthermore, circuit expansion and relocation will allow an estimated 50% increase in gravity gold production, while significantly reducing overall unit costs of production (Darnton et al, 1995).

The Australian experience is more conclusive, presumably because cyanidation solution chemistry is more challenging (with concentrations of dissolved solids that can exceed 100,000 ppm[1]). As a result, not only are costs associated with cyanide consumptions and those of carbon reduced, but increases in metallurgical gold recoveries, generally in the order of 1%, were claimed (Cloutt, 1995).

Rosebery Mine, West Coast of Tasmania, Australia, used to be a base metals sulphide mine, but now it must be considered as a zinc/gold mine, since 65% of its income is generated from zinc and 14% generated from gold (Poulter et al, 1995). During the late 1980s, a conventional gravity plant equipped with spirals and shaking tables was commissioned. Recovery of gold to doré via the gravity plant on average was less than 10% of the gold in the feed. A 76 cm Knelson Concentrator was installed in 1993, and a double screen deck, consisting of 5 mm and 2 mm screens, was installed to cut the total throughput to about 200 $t.h^{-1}$ cyclone underflow. Minus 2 mm material was fed to the Knelson Concentrator. As a result, 15-20% of gold in feed was recovered during the trial period, February 1993, and 31% of the gold in the feed was recovered during April and May of the same year. A new central discharge (CD) Knelson Concentrator was installed in March 1994, and it is expected that more than 30% of the gold in feed will be recovered in the gravity circuits.

Some typical examples of metallurgical and economic impact of the Knelson industrial applications are summarized in Table 4-1 (Hope et al, 1993; Darnton et al, 1995; Honan and Luinstra, 1996; Cloutt, 1995)

---

[1] at the Paddington and Ora Banda Mines, Laplante, 1995.

TABLE 4-1 Metallurgical and Economic Impact of Knelson Industrial Applications

Plant	Unit Location and Performance	Rationale
Meston Resources Chibougamau, Québec	35-40% recovery from pinched sluices concentrate, 76 cm Knelson concentrate upgraded in 19 cm Knelson	Increase in economic* and metallurgical recovery of at least 3%
Agnico-Eagle (division LaRonde), Cadillac, Québec	20-25% recovery from screened cyclone underflow	Increase in economic recovery*
Barrick, East Malartic, Québec	Gravity recovery increased from 11% to 40% from screened cyclone underflow	1000-fold enrichment in a single Knelson stage, increase in economic recovery*
Hemlo Golden Giant, Marathon, Ontario	30% recovery from screened cyclone underflow	Reduction in carbon stripping costs
Montana Tunnels, United States	From screened cyclone underflow	4.3% total recovery increase, coarse gold losses and overall unit costs were reduced
Rosebery Mine, West Coast, Tasmania, Australia	From screened cyclone underflow, gravity recovery increased from 10% to 30%	Became a zinc/gold mine as 14% income generated from gold after Knelson installation
St Ives Gold Plant, Western Australia	From screened cyclone underflow	1% total recovery increase, elution saving, CIP cyanide saving, operating costs saving

* ahead of flotation

4.2.3 Industrial Performance

Most industrial reports of Knelson operations shed little light on the unit's actual performance. For example, few data are ever published about stage size-by-size recovery, or about the progression of overload over the duration of a full recovery cycle. Most detailed evaluations of industrial Knelson performance have been performed at

McGill (Lui, 1989; Laplante and Shu, 1992; Putz, 1994; Vincent, 1996).

An important concept when evaluating gold gravity recovery is that of "free", or more specifically gravity-recoverable gold (GRG). Here, GRG is defined as the portion of gold in the ore that reports to a low yield (<1%) gravity concentrate and could, in principle, be upgraded to a smeltable concentrate (Woodcock, 1994).

Meston Resources (Les Mine Camchib Inc.)

The testwork was designed to answer the following important questions of plant Knelson performance:

- Up to what size can gold be recovered?
- How long should a cycle be before the Knelson Concentrator becomes overloaded?
- What would be an optimum pressure for fluidization water (Lui, 1989)?

The results showed that in the gravity circuit, 39-42% of the total gold recovery with an enrichment ratio 27,000:1 was achieved. The 76 cm rougher Knelson achieved 58-71% total gold recovery with an upgrading ratio of 330-480. The optimum fluidization water pressure was about 73 kPa; a 90 minutes recovery cycle did not overload the Knelson. The recoveries of the 76 cm and 19 cm Knelson (the second, a cleaner for the first) slightly increased with decreasing particle size, at least down to 38 μm. In the gold room, 90% recovery, with an enrichment ratio of 5.9, was achieved with the 19 cm Knelson.

In June 1989, samples of the primary gravity concentration circuit were taken again and tested at McGill University (Laplante and Shu, 1992). This time, the study focused on the performance of a 76 cm plant Knelson operated at a fluidization water flowrate of 80 kPa (12 psi) and at a feed rate of 25 $t.h^{-1}$, higher than that previous studies of the same circuit. The results showed that 50% of the gold recovered by the laboratory

Knelson from the plant Knelson tails was GRG. This was attributed to the high feed rate of the plant Knelson, and also to the superior performance of the laboratory Knelson as a "perfect separator" to measure GRG (the previous testwork was performed with a Mozley Table Separator). It was found that a cycle time of up to 2 hours did not decrease gold recovery, and a significant proportion of the gold recovered was below 300 μm.

Golden Giant Mine of Hemlo Gold Mines Inc.

In this research work, a 7.5 cm laboratory Knelson was used to recover GRG from the high grade primary cyclone underflow of the Golden Giant Mine. The sample contained about 150 g.t^{-1} Au, 8% sulphides, with a specific density of 3.2 g.cm^{-3}. Feed rate, density, size distribution and fluidization water flowrate were systematically tested (Laplante et al, 1996).

The results showed that the Knelson's efficiency was affected mainly by feed specific density and rate. High feed rate had a negative effect on fine gold recovery, and high feed specific density had a negative impact on the recovery of the middle size range material. Fluidization water spanning 15-40 kPa did not significantly affect performance. The variation of feed size distribution over a wide range did not have a deleterious effect on performance for material with a specific density of 2.8 g.cm^{-3}. For material diluted with 212 μm silica, the best performance was achieved at a feed rate of 0.3-0.6 kg.min^{-1}, with fluidization water flowrate of 33 kPa.

Lucien Béliveau Mill

A laboratory Knelson was used to evaluate two gravity circuits of the Lucien Béliveau Gold Mill, Val d'Or, Québec. The initial circuit consisted of a 76 cm Knelson. Later, a hydroseparator and a spiral were installed, with the hydroseparator underflow feeding the spiral and the spiral tailings and hydroseparator overflow reporting to a 51 cm Knelson (Putz, 1994; Putz et al, 1993).

The results showed that gold recovery in the 76 cm Knelson averaged 45%. Gold recoveries were relatively higher in all size fractions greater than 38 μm. Below 38 μm, gold recovery dropped to 22%. The hydroseparator and spiral decreased the Knelson's recovery to less than 17%, which was attributed to the spiral recovering much of the GRG ahead of the Knelson. It was found that there was significant coarse gold in the grinding circuit that was too coarse to float in the flash flotation cell, and that should be recovered by the 76 cm Knelson in the ball mill discharge or cyclone underflow streams.

4.3 Description of the Φ 7.5 cm Knelson Concentrator

Figures 4-5 and 4-6 show a photograph and a schematic diagram of the 7.5 cm (the diameter of the top ring) Knelson concentrator. Its throughput capacity can be as high as 50 kg per hour (3" Knelson Concentrator Manual, Knelson International Sales Inc.). The cross section of the bowl and the internal geometric parameters are detailed in Chapter 6.

The basic structure of laboratory Knelson Concentrator is similar to that of the industrial models. It is a batch machine. The bowl can be conveniently tightened just by turning it anticlockwise and released by clockwise rotation. The required fluidization water flowrate or pressure can be easily adjusted with a valve. Material is fed to the concentrator through a vibrating feeder, or manually (for low feed weights).

Because the diameter of the holes in the bowl is around 0.3 mm, they may be penetrated by some heavy particles that will then enter the pressurized water jacket (especially when processing materials 100% finer than 300 μm). At the end of a test, this material must be collected and added to the concentrate.

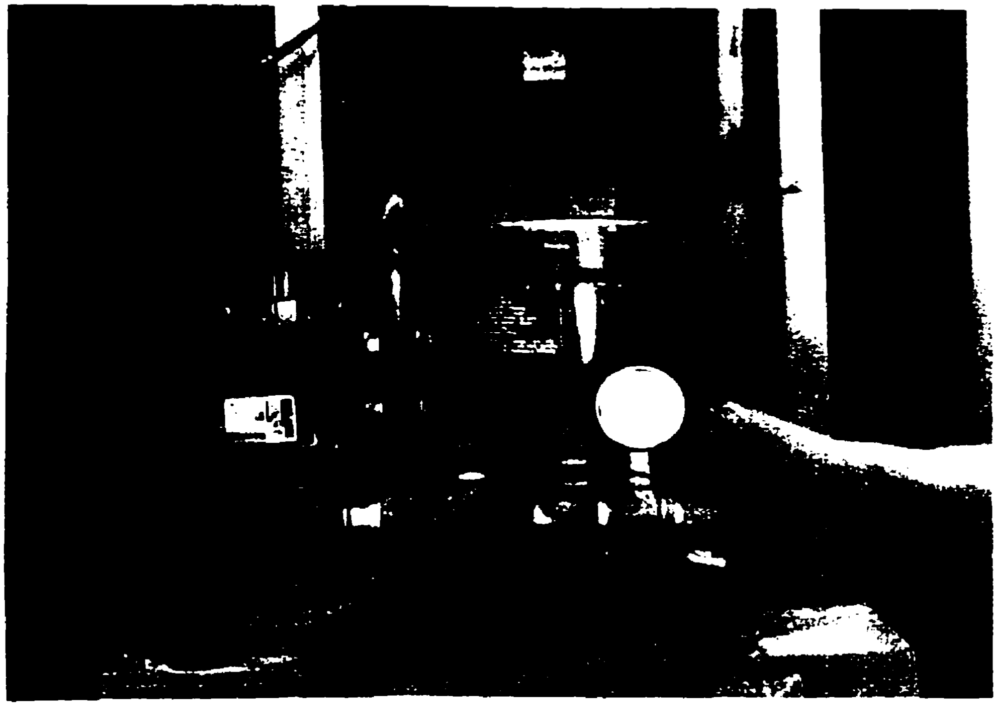

FIGURE 4-5 Laboratory Φ 7.5 cm Knelson Concentrator

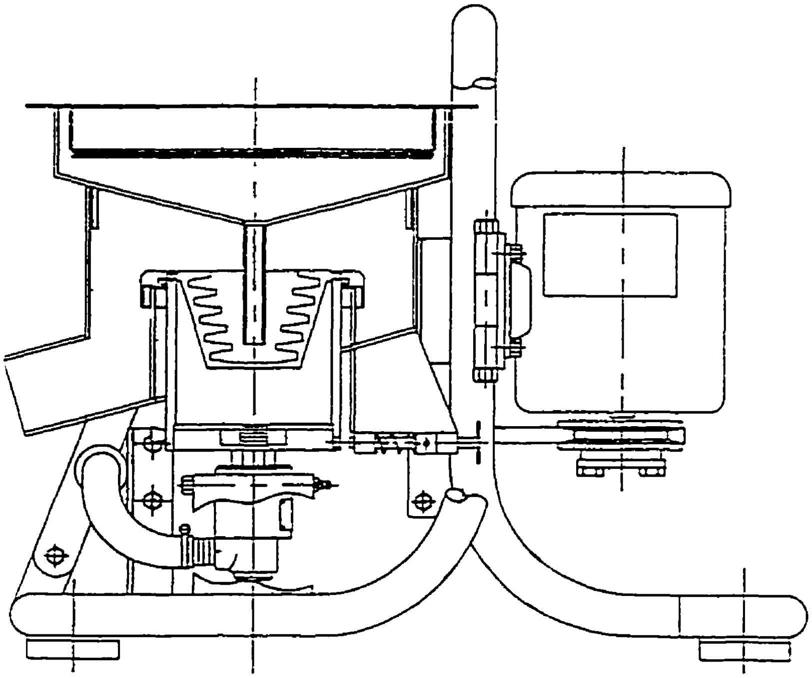

FIGURE 4-6 Schematic Diagram of the Φ 7.5 cm Knelson Concentrator

The traditional technique to determine the amount of free gold in a sample is amalgamation, but it suffers from health hazards. Mercury can form an amalgam with the gold which is on the surface of another mineral, but it would not be recovered by the Knelson Concentrator. Gold flakes and very fine gold will be recovered by amalgamation, but not by the Knelson Concentrator. Conversely, tarnished gold or gold particles coated by other substance will not be amalgamated, but will report to the Knelson concentrate. In many cases, the laboratory Knelson Concentrator recovery of gold approaches that of amalgamation, typically 95% of it (Woodcock, 1994; Putz, 1994; Banisi, 1991), and therefore, the laboratory Knelson can be considered as the most efficient gravity unit to analyze the GRG of gold samples at present.

4.4 Theoretical Considerations

4.4.1 Centrifugal Force Acting on a Particle

Centrifugal fields can be generated in two different ways. First, a fluid can be introduced at a high tangential velocity into a cylinder or conical vessel such as a hydrocyclone. Generally, the larger and heavier particles will be collected near the wall of the separator, and the smaller and lighter particles will be taken off through an outlet near the axis of the vessel. The other way is the use of a centrifuge. In this case, a fluid is introduced into a rotating bowl and it is rapidly accelerated. All the fluid tends to rotate at a constant angular velocity, ω, and a forced vortex is established. The tangential velocity is directly proportional to the radius at which the fluid is rotating (Coulson and Richardson, 1991).

In most practical cases, when a particle is moving in a fluid under a centrifugal field, gravitational effects will be comparatively small and, therefore, can be neglected. The equation for the particles in the centrifugal field will be similar to that for the motion in the gravitational field, except that the gravitational acceleration 'g' must be replaced by the centrifugal acceleration, $r\omega^2$ (Coulson and Richardson, 1991).

The centrifugal acceleration is given by,

$$a = r\,\omega^2 \tag{4-1}$$

For the laboratory Knelson Concentrator, substituting r = 2.51 cm (the distance from the middle to the centre of the third ring), rpm = 1462, the centrifugal intensity is about 60 'g'.

Assuming all particles to be spherical, the centrifugal force, the main force acting on a particle in the Knelson Concentrator, is equal to:

$$F_c = \frac{\pi}{6}\, d^3\, (\delta-\rho)\, r\,\omega^2 \tag{4-2}$$

or

$$F_c = \frac{\pi}{6}\, d^3\, (\delta-\rho)\, \frac{v_t^2}{r} \tag{4-3}$$

where

F_c: centrifugal force acting on a particle, g.cm.s^{-2}

d: diameter of a particle, cm

δ: specific density of a particle, g.cm^{-3}

ρ: density of a medium, g.cm^{-3}

r: rotating radius of a particle, cm

ω: angular velocity, radian.s^{-1}

v_t: velocity at time t, cm.s^{-1}

Centrifugal forces for particles with different sizes and densities are shown in Table 4-2, for the five rings of the Knelson Concentrator (of different diameters).

TABLE 4-2 Centrifugal Force (g.cm.s^{-2})

Ring		Particle size (cm)								
		0.0015			0.003			0.005		
No.	D_3 (cm)	Silica	Magnetite	Tungsten	Silica	Magnetite	Tungsten	Silica	Magnetite	Tungsten
5	5.0	0.0002	0.0004	0.0019	0.0014	0.0033	0.0152	0.0063	0.0153	0.0702
4	4.4	0.0002	0.0004	0.0017	0.0012	0.0029	0.0133	0.0056	0.0135	0.0618
3	3.8	0.0001	0.0003	0.0014	0.0010	0.0025	0.0155	0.0048	0.0117	0.0533
2	3.2	0.0001	0.0003	0.0012	0.0009	0.0021	0.0097	0.0041	0.0098	0.0449
1	2.6	0.0001	0.0002	0.0010	0.0007	0.0017	0.0079	0.0033	0.0080	0.0365

D_3 is the diameter of the inner rim of a ring in the Knelson bowl (also see Chapter 6).

4.4.2 Terminal Settling Velocity

The main forces acting on a particle inside the Knelson Concentrator are centrifugal force and axial drag force.

For the drag force, Stokes (Stokes, 1901; Kelly and Spottiswood, 1982) assumed that, under laminar flow conditions, the drag force on a spherical particle was entirely due to viscous forces within the fluid, and can be described as,

$$F_d = 3 \pi d v_r \mu \qquad \text{4-4}$$

where

F_d: inward drag force, g.cm.s^{-2}

v_r: velocity at radial distance r, cm.s^{-1}

μ: the viscosity of the fluid medium, 0.01 g.cm^{-1}.s^{-1} for water at 20 °C

If the effect of the fluidization water and other forces on the particle are not considered, the particle reaches its terminal settling velocity when F_c equals F_d. The equation of the terminal settling velocity can be derived by combining Equations 4-2 and

4-4. Because we mainly consider the behaviour of fine particles, Stokes' equation will be used to approximate the terminal settling velocity in a centrifugal field by substituting $r\omega^2$ for 'g', as shown in Equation 4-5 (Coulson and Richardson, 1991; Sun, 1982).

$$V_o = \frac{d^2\,(\delta-\rho)}{18\,\mu}\,r\,\omega^2 \qquad \text{4-5}$$

The terminal setting velocity of the particles of Table 4-2 is shown in Table 4-3.

TABLE 4-3 Terminal Settling Velocities (cm.s^{-1})

Ring		Particle Size (cm)					
		0.0015			0.003		
No.	D_3 (cm)	Silica	Magnetite	Tungsten	Silica	Magnetite	Tungsten
5	5.0	1.2	2.9	13.4	4.8	11.7	53.6
4	4.4	1.1	2.6	11.8	4.3	10.3	47.2
3	3.8	0.9	2.2	10.2	3.7	8.9	40.8
2	3.2	0.8	1.9	8.6	3.1	7.5	34.3
1	2.6	0.6	1.5	7.0	2.5	6.1	27.9
Ring		Particle Size (cm)					
		0.005			0.01*		
No.	D3 (cm)	Silica	Magnetite	Tungsten	Silica	Magnetite	Tungsten
5	5.0	13.4	32.6	148.9	53.7	130.2	595.8
4	4.4	11.8	28.6	131.1	47.3	114.6	524.3
3	3.8	10.2	24.7	113.2	40.8	99.0	452.8
2	3.2	8.6	20.8	95.3	34.4	83.3	381.3
1	2.6	7.0	16.9	77.4	27.9	67.7	309.8

* only as reference data since this size is above that for which Stokes equation can be used.

For a given particle the terminal settling velocity increases from riffles 1 to 5, as the ring diameter increases.

Consider two mineral particles of densities D_a and D_b and diameters d_a and d_b, respectively, falling in a liquid of density D_f at exactly the same terminal settling velocity. In the case of free settling, Stokes' law, applicable to particles <50 μm, and Newton's law, applicable to particles >0.5 cm, can be used as shown in Equation 4-6 and 4-7. For the particles in the intermediate size range, a similar equation can be used, but its exponent varies from 0.5 -1.0.

Stokes' law:

$$\frac{d_a}{d_b} = [\frac{D_b-D_f}{D_a-D_f}]^{\frac{1}{2}} \qquad 4\text{-}6$$

Newton's law:

$$\frac{d_a}{d_b} = \frac{D_b-D_f}{D_a-D_f} \qquad 4\text{-}7$$

Let a = silica or magnetite, b = tungsten, f = water, from Equation 4-6, we can obtain: $d_{silica}/d_{tungsten}$ = 3.33, and $d_{magnetite}/d_{tungsten}$ = 2.14. If we take a 15 μm spherical tungsten particle as an example, the equal settling silica particle is 50 μm, and the equal settling magnetite particle is 32 μm.

For the hindered settling case, the resistance to fall is mainly due to the turbulence created, and Newton's law can be used, replacing D_f with D_p (pulp density) (Wills, 1992). For example, if the pulp density is 1.6 g.cm^{-3}, $d_{silica}/d_{tungsten}$ = 16.9, and $d_{magnetite}/d_{tungsten}$ = 5.2.

For the case of free settling, all the silica particles larger than 50 μm will settle faster than tungsten particles whose diameter is equal to or smaller than 15 μm. For the case of hindered settling, at a pulp density of 1.6 $g.cm^{-3}$, all the silica particles larger than 253 μm would settle faster than 15 μm tungsten particles. This could suggest that the fine tungsten particles are very poorly recovered in the Knelson Concentrator. However, this is not the case, and most of the fine tungsten particles can be effectively recovered from silica even though some silica particles are greater than 300 μm. The terminal settling velocities alone cannot explain this well, even when hindered settling is considered. Therefore, the ability of the Knelson to recover fine gold is based on other mechanisms, such as particle-particle collision and percolation or consolidation trickling.

4.4.3 Travel Time from Downcomer to Wall

In a centrifugal field, the time taken for a particle to move to radius r_2 from an initial radius r_1 is given by (Coulson and Richardson, 1990; Sun, 1982):

$$t = \frac{18\,\mu}{d^2\,\omega^2\,(\delta-\rho)}\ \ln\left(\frac{r_2}{r_1}\right) \qquad 4\text{-}8$$

Assuming that particles are tossed outward from the edge of the downcomer bottom, and the space out of the downcomer is fully occupied by slurry, the time for a particle to travel to the riffle wall can be calculated. The bottom of the downcomer is equal in height to the middle of the first ring. The diameter of the downcomer is 1.0 cm (r_1 = 0.5 cm), and the diameter of the inner wall of the first riffle is 2.6 cm (r_2 = 1.3 cm). The calculated time for particles to travel to the inner wall of the first riffle is summarized in Table 4-4 and plotted in Figure 4-7.

From Table 4-4, it can be seen that for particles of equal diameter, the travelling time needed to reach the wall for silica is 11.1 times longer than that of tungsten, and 5 times longer than tungsten for magnetite. It is easy to understand that the separation of tungsten from silica should be much easier than from magnetite. Again, from Equation 4-8, it can be found that a 50 μm silica particle will take the same time as a 15 μm tungsten particle, 0.12 second, to reach the inner wall of the first riffle. Again, it is concluded that selectivity (i.e. gangue rejection) in a Knelson cannot be achieved on the basis of terminal velocities alone.

TABLE 4-4 Particle Travel Time (second) from Downcomer to Wall

Size (μm)	Silica	Magnetite	Tungsten
10	4.45	1.83	0.401
20	1.12	0.46	0.100
30	0.49	0.20	0.045
40	0.28	0.11	0.025
50	0.18	0.07	0.016

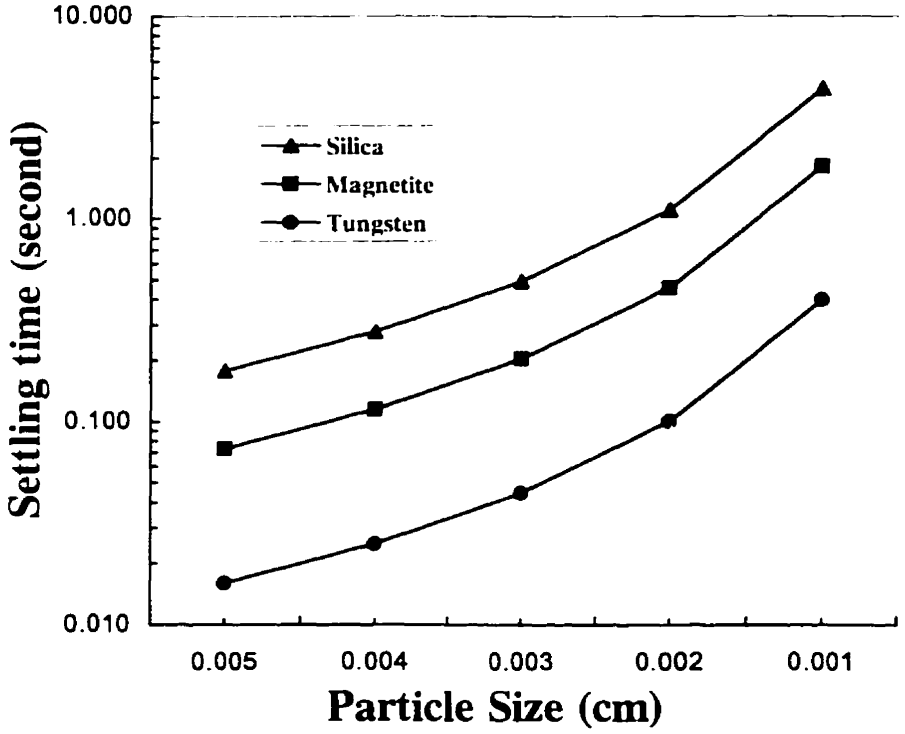

FIGURE 4-7 Travelling Time to Reach the Wall of the First Riffle

4.4.4 Particle-Particle Interactions

The above discussion makes it plain that reported Knelson performance--the ability to recover non-spherical gold particles finer than 25 μm from silica/sulphide gangue, some coarser than 100 μm, must rely on separation mechanisms less size-dependent than terminal settling velocities.

Initial acceleration is size independent (Kelly and Spottiswood, 1982), but as Figures 4-8 and 4-9 show[2], over the same acceleration time, fine tungsten (15 μm in diameter), cannot settle more rapidly than 300 μm magnetite and 1000 μm silica gangue particles, over time periods longer than about 0.0021 and 0.0031 second, respectively (Appendix 4-1). In a shorter time period, even a 50 μm tungsten particle settles only marginally more than the coarser, lighter particles. Yet, both laboratory and plant Knelson Concentrators can recover flaky gold finer than 25 μm from gangue that contain silica coarser than 1000 μm and magnetite (or sulphides of similar density) coarser than 300 μm (Laplante et al, 1990, 1994; Laplante and Shu, 1992).

Clearly, the separation mechanisms that makes the separation possible must incorporate a longer settling time for the finer particles. This is achieved in an environment of high particulate concentration, in which collisions between particles are frequent, especially for coarser particles. Finer particles can settle for longer time intervals than coarser ones between collisions. Bed packing (which would make even finer particle motion impossible) is prevented by both fluidization water and the flow of slurry, which create a shear rate resulting in a dispersion pressure that pries the concentrate bed apart (the Bagnold effect or force, Bagnold, 1954). Inter-particulate movement also facilitates the settling of finer, heavier particles through the bed of coarser particles, a phenomenon described as stress-induced percolation (Bridgwater et al, 1969, 1971; Masliyan, 1969).

---

[2] Figure 4-9 is a blowup of the bottom left of Figure 4-8.

The principles of fine dense particle percolation that would enable gold to report to a concentrate zone operate in hydrocyclones. Because very high GRG recoveries to cyclone underflows, in excess of 99%, have systematically reported (Laplante et al, 1994, Banisi, 1991, Poulter et al, 1995, Woodcock, 1994), it is legitimate to assume that GRG will report to the concentrate zone in the plant Knelson Concentrators. This first hypothesis will be ratified in this work. The ability of the Knelson Concentrator to store GRG in the concentrate zone will dictate its potential as a cleaner, as prolonged recovery cycles would then inevitably result in high concentrate grades. Intuitively, at some point the ability of the unit to "store" more concentrate will be exceeded, and severe overload will ensue. This will be investigated in the next chapter.

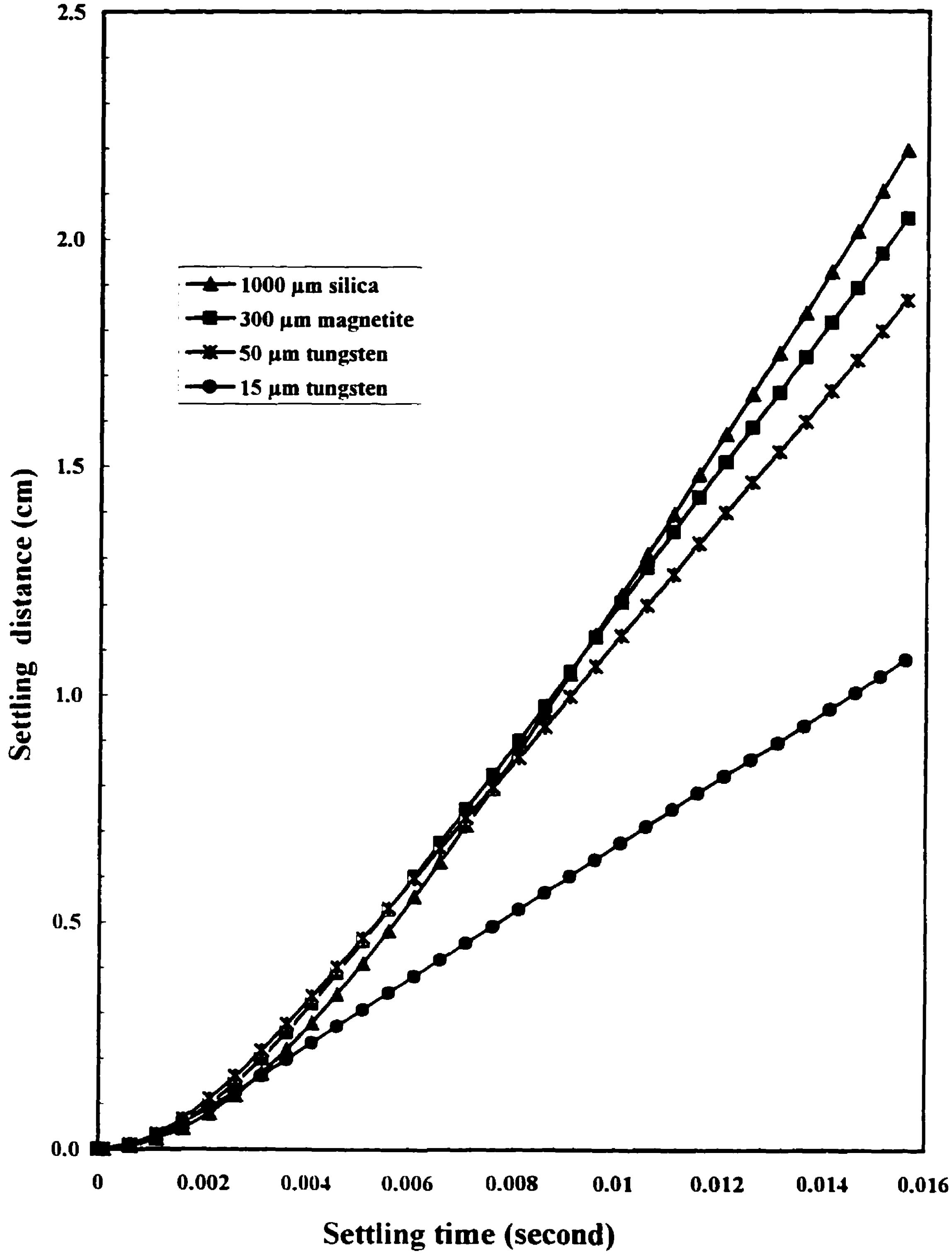

FIGURE 4-8 Settling Distance vs Settling Time in a Relatively Long Period

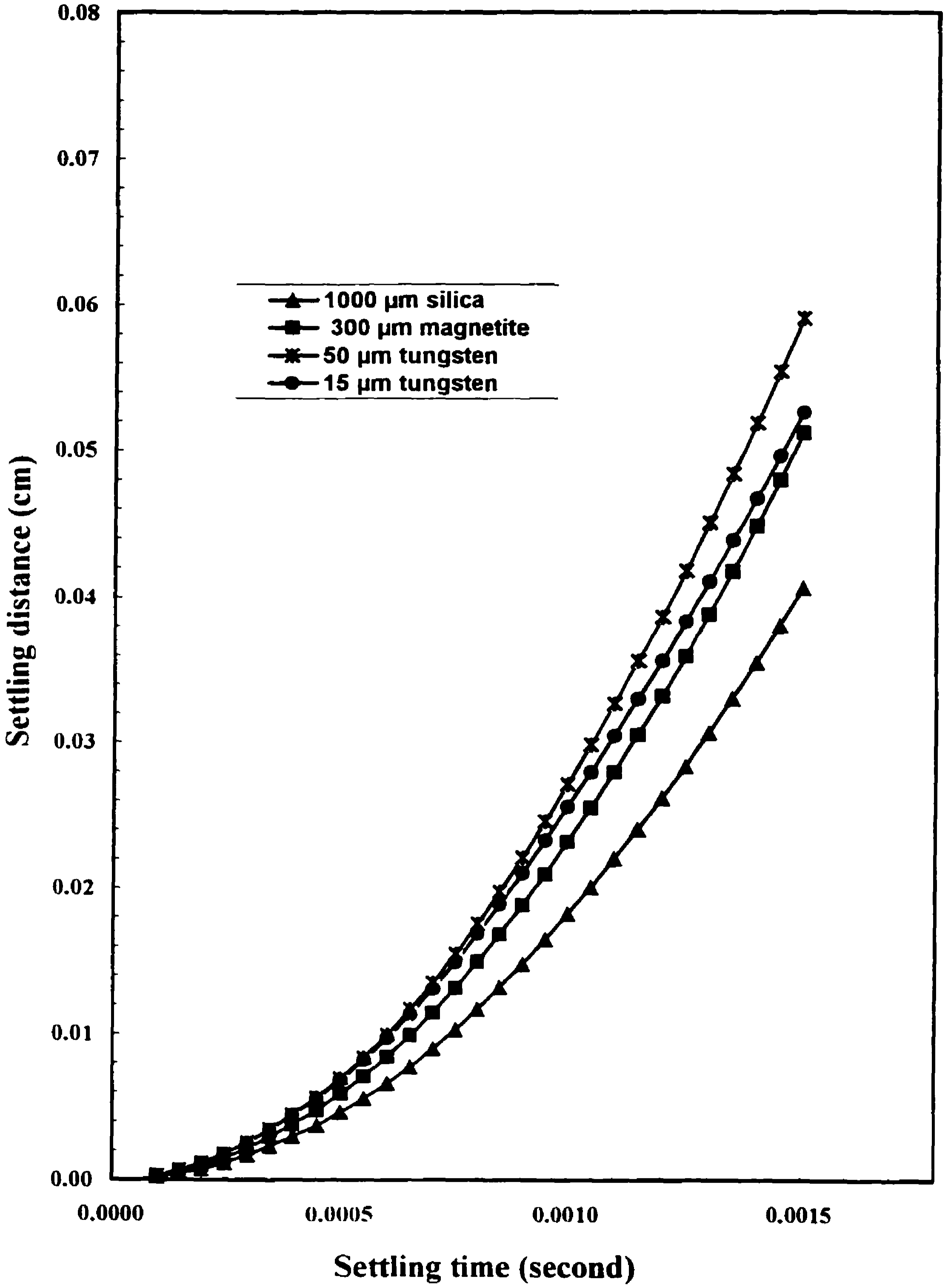

FIGURE 4-9 Settling Distance vs Settling Time in a Relatively Short Period

CHAPTER 5 OVERLOADING THE KNELSON CONCENTRATOR

5.1 Introduction

Although many types of shaking table can be used (e.g. Wilfley, Deister) as a final cleaner for gold gravity concentrates, the Gemeni is rapidly becoming a favourite, possibly because of its grooves (rather than riffles), which minimize the exposure of gold particles to air and consequently their risk of floating (especially when the table water contains collectors). The grooves also direct the concentrate to the end of the table, a feature that even the riffles of classical tables do not achieve. As a result, users also report very stable operation, unlike that of classical tables, whose concentrate band is difficult to control. However, since the Gemeni operates only at 1 'g', it is reasonable to suspect that some of the gold recovered in the primary unit will be lost in the table tails, especially if the primary recovery unit operates at several 'g'.

These considerations prompted the launching of a test program at McGill aimed at producing very high concentrate grades with the Knelson Concentrator, either to replace or to supplement table operation. Unlike earlier work on the unit (Laplante et al, 1995), it was decided to use synthetic feeds rather than high grade gold ores. Synthetic materials are occasionally used to study or demonstrate gravity processes; an early application was reported by Gaudin (1939), and a later application was described by Guest and Dunne (1985). The obvious advantage is that synthetic feeds can be totally liberated, and their size distribution, shape, density and grade can be controlled (Guest and Dunne, 1985). More recently, colour-coded synthetic tracers of carefully controlled density have been used, some quite coarse, to be recovered manually (Ayat and Leonard, 1987). They are particularly useful when adjusted to very small density increments, typically to characterize the performance of dense medium separators such as the Tri-Flo (McGuinness, 1994) or jigs. Two families of densities are usually targeted, one between 1.3 and 2.2 g.cm^{-3} for coal applications (Davis et al, 1985) and a second between 2.0 and 4.0 g.cm^{-3} for light/heavy mineral separations. Other applications of synthetic tracers may not be so 'high tech': Blowers (Blowers, 1992) proposed the use of copper wire cut and hammered to look like gold flakes to test the ability to pan gold. Flattened lead shot has also been used for a preliminary evaluation of the Knelson Concentrator (Forssberg and Nordquist, 1986).

For gold gravity studies, there are at least another three additional benefits for the use of synthetic ores. First, when trying to achieve high concentrate grades with a fixed concentrate mass (usually around 100 to 200 g), the use of gold would be cost prohibitive. Second, the risk of contamination for parallel work with much lower head grades, which would be severe with high grade gold samples, is eliminated. This is illustrated in Table 5-1, which shows such an occurrence, for at least four tests, with a low grade ore following a single test with a high grade feed (a table tail sample, see Chapter 8).

Note that only for the fourth sample is contamination so severe as to be readily detectable. For the other tests, a careful experimental procedure (Woodcock, 1994) has been developed to bring sampling and assaying errors down to 0.003 oz.st^{-1} (0.09 g.t^{-1}) on low-grade gravity tailings and make contamination detection possible.

TABLE 5-1 Illustration of Contamination Problems

Feed	Date	Grade, oz.st^{-1}	
		Contaminated[1]	Uncontaminated
Sample 1, stage 1	1-2-94	0.020	0.010
Sample 2, stage 1	1-2-94	0.031	0.005
Sample 3, Stage 3	5-2-94	0.030	0.022
Sample 4, Stage 3	5-2-94	0.090	0.015

Reverse contamination has also been observed at McGill (i.e. SEM work with natural ores showing spherical tungsten particles that were used in previous tests with synthetic feeds), but carries no ill effects and reinforces amongst the research team the need for extreme care to prevent contamination.

Third, the use of a tracer with a controlled shape can shed light on the behaviour of gold particles with much flakier shapes, when compared to that of tungsten particles of the same size and nearly the same density.

Because the Knelson is a batch unit, it is likely to overload if fed too much gold. For primary recovery, from feeds of 1-100 g.t^{-1}, this is highly unlikely, and indeed has not been detected in plant work (Lui, 1989; Shu, 1992; Putz, 1994). However, cleaning applications, with head grades of typically 5,000-50,000 g.t^{-1}, are far more likely to experience overload. This is best studied by dynamic tests of the Knelson performance- i.e. sampling the Knelson tails as a function of time (or mass fed). This will be the focus of this chapter.

---

[1] Contamination was traced to the use of contaminated sampling equipment and screens; the tests were then performed again with de-contaminated equipment to estimate the correct head grade.

5.2 Materials

Tungsten

If 200 g of gold is required to conduct a gravity test, it would cost over $Can 3,000! In this research work, fine metallic tungsten was, therefore, chosen to mimic the behaviour of gold. Its density (19.3 g.cm^{-3}) is identical to that of pure gold, and is therefore slightly higher than that of the gold-silver alloys normally encountered in most deposits (whose density varies from 13 g.cm^{-3} for Ag_2Au, kustelite, to 17 for Au_2Ag, electrum) (Wells and Patel, 1994; Laplante, 1994).

The tungsten (>99.9% W) was obtained from GTE Sylvania Products Corporation, U.S.A. Product #1 was in the size range of -75 +40 μm, mostly with irregular shapes; product #2 was -40 μm, in predominantly spherical shapes. Scanning electric microscope (JEOL JSM-840A) images of these two products are shown in Figure 5-1.

For easier analysis by gravity separation, the tungsten particles of the -25 μm fraction were further classified with a Warman cyclosizer to remove -8 μm particles. The size distribution of the original tungsten products is shown in Table 5-2. The objective of choosing such a size range of tungsten was to study the behaviour of fine gold particles.

TABLE 5-2 Tungsten Size Distribution (as received)

Size, μm	Coarse Granular	Fine Spherical
+53	71.3	0.1
37-53	27.9	20.8
25-37	0.7	49.9
0-25	0.1	29.2
Total	100.0	100.0

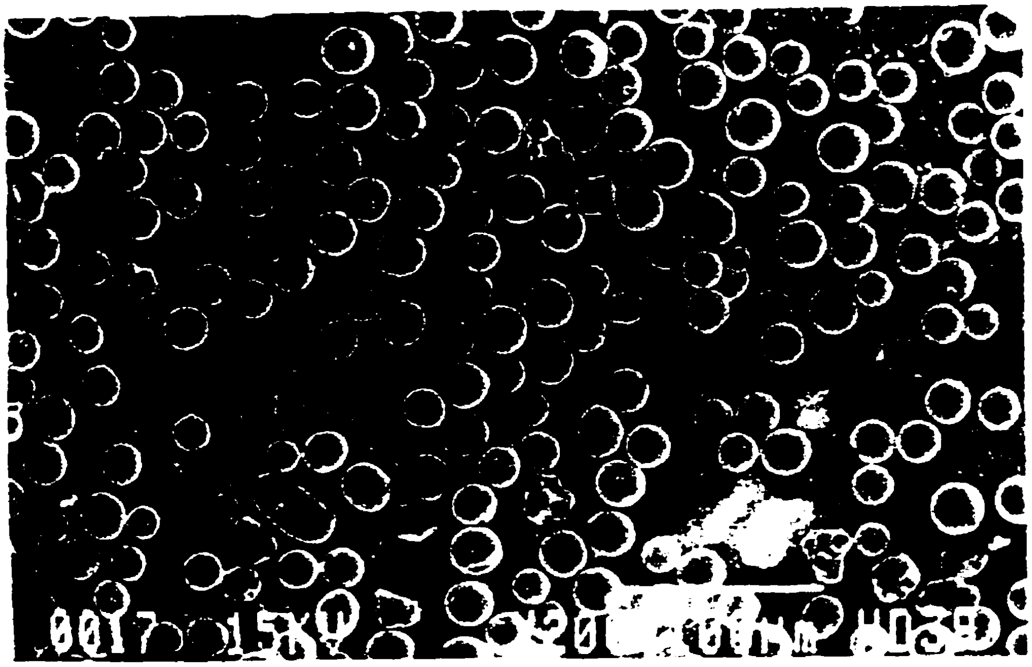

A. spherical particles

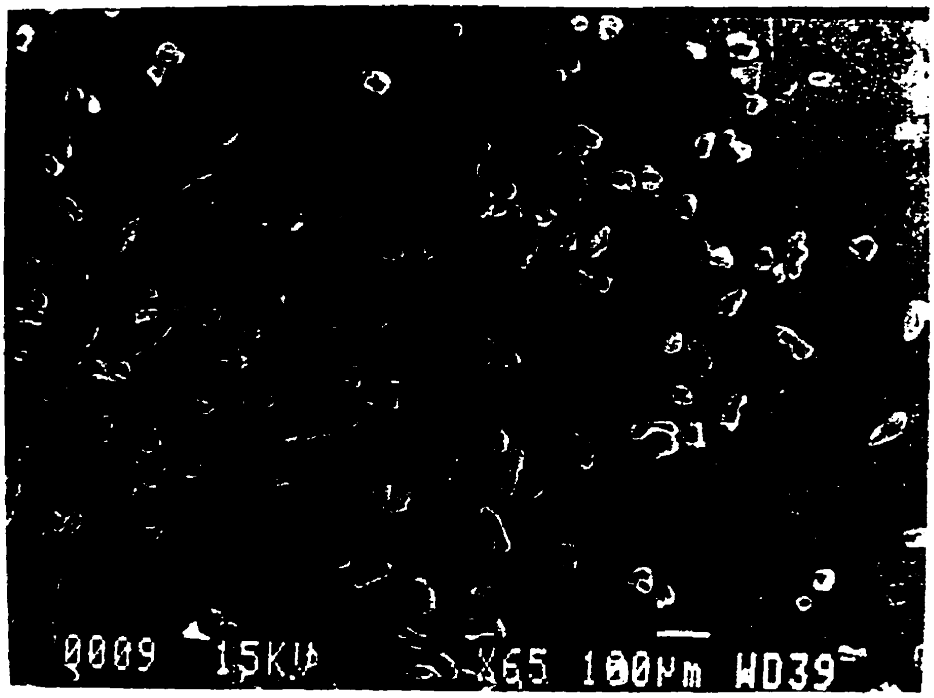

B. irregular shapes

FIGURE 5-1 SEM Back-Scattered Images for Spherical and Irregular Tungsten Particles

Magnetite

Magnetite is physically stable and relatively inert, chemically. It was used as a substitute for the main gangue mineral of gold gravity concentrates, pyrite. The two minerals have approximately specific density, around 5.0[2]. The substitution makes it easier and more convenient to separate tungsten by both gravity and magnetic separation methods from a mixture of tungsten and magnetite (compared to a mixture of tungsten and pyrite).

The magnetite used in the tests was obtained from the cobber concentrate of the Iron Ore Company of Canada, and further cleaned with a Davis Tube or hand magnet.

Silica

Silica (with a specific density of 2.65) was obtained from Unimin Canada Ltd. Different sizes were prepared by grinding in a laboratory porcelain ball mill and screening on a Rotap.

Two types of size distributions of gangue minerals were chosen. That of the coarse gangue was based on the actual size distribution of the gold table tails at Meston Resources (Liu, 1989). The fine size distribution was that of the -212 μm fraction of the Meston Resources' roughing Knelson concentrate. The size distributions are shown in Table 5-3.

---

[2] Although magnetite has a specific density of about 5.25, the sample used, with a silica content of about 5%, had a slightly lower specific density.

TABLE 5-3 Size Distribution of Gangue Minerals

Size		Mass (%)	
Mesh	μm	Fine Size	Coarse Size
20	+850		9.86
30	600-850		10.85
40	425-600		9.94
50	300-425		13.72
70	212-300		12.87
100	150-212	5.30	15.26
140	106-150	15.90	11.34
200	75-105	44.67	7.88
270	53-75	17.49	4.45
400	38-53	9.22	2.99
500	25-38	4.68	0.53
-500	-25	2.74	0.31
Total		100.00	100.00

5.3 Experimental Methodology

5.3.1 Silica Tests

To determine the ability of the Knelson Concentrator to capture silica as a function of fluidization water flowrate, five single sizes of silica, 212-300 μm, 150-212 μm, 105-150 μm, 75-105 μm, 38-53 μm and -25 μm were tested. For each test, 50 g of the sample was fed to the Knelson at a very low feed rate, 50 g.min^{-1}, in order to understand the basic behaviour of silica when the grooves of the Knelson bowl are completely fluidized. Tails and concentrate were collected, dried and then weighed.

5.3.2 General Test

The tungsten was mixed with silica for the low density experiments and with magnetite for the high density tests. The tungsten content in the mixtures was kept at 5% by mass.

First, the optimum fluidization water flowrate was determined with the four gangue materials tested, each with a feed of 950 g gangue and 50 g of tungsten. Second, the Knelson Concentrator was fed with 3800 g of gangue and 200 g of tungsten at the optimum fluidization water flowrate determined in preliminary tests to produce an overload. Overload is defined here as an obvious progressive decrease of the Knelson concentrator performance when too much of the heavy phase is recovered in its bowl. Correspondingly, a significant increase in the tungsten content of the tails is then observed.

Tungsten analysis was performed mainly on four size classes, 0-25, 25-37, 37-53 and 53-75 μm. However, because a few tungsten particles might report to the 75-106 μm fraction, this size of the material was also analyzed, and when recovered, it was added to the 53-75 μm fraction.

Tungsten recovered by gravity was cleaned with a hand magnet. For every test, the entire concentrate was analyzed. For the overload tests, the complete tails, sequentially extracted into 9 or 10 samples, were also analyzed. Samples were weighed with an AD Electronic scale.

5.3.3 Operating the Knelson Concentrator

During the entire research program, the following steps were used to operate the Φ7.5 cm Knelson Concentrator:

a) Run the Knelson Concentrator without feeding solids, apply suitable feed wash water, adjust valves to achieve the required fluidization water flowrate by reading the pressure meter, and measure the water flowrate (weighed timed samples).

b) Feed the material with the vibrating feeder or manually (for limited feed mass) at the feed rate required, normally in the range of 250-600 grams per minute.

c) Collect all the tails or take representative samples according to test requirements.

d) After feeding all material, take off the feed hopper and wash the tails launder.

e) Reduce the fluidization water flowrate by half, and then completely switch off at the same time as the Knelson motor is turned off.

f) Completely wash out the concentrate from the bowl and combine all the solids collected from the water jacket and the tails launder (the solids left in step (e)).

g) Decant the water of concentrate and filter tails samples; dry, screen and analyze each size class, with the MGS for synthetic ores, or by fire assay for actual gold samples (at the mine site assay laboratory).

5.3.4 Size Analysis

For fine material, tails samples were wet screened first with a 25 μm screen, and the oversize was dry screened on a Rotap for 20 minutes. The tail samples obtained from coarse feeds and all the concentrates were only dry screened.

5.3.5 Analysis of Tungsten Products

A Mozley Laboratory Separator (MLS) was used to separate tungsten from mixtures size by size. The basic operating conditions were as follows: slope: 1.75°; frequency: 90 rotations per minute; amplitude: 8.9 cm. Residual magnetite in the tungsten recovered with the MLS was removed by a hand magnet. The tungsten was then considered to be pure, and was weighed with an AD Electronic scale.

Using 5 g of tungsten and 25 g silica, both of 25-38 μm, the variance of the MLS separation was estimated and is shown in Table 5-4.

TABLE 5-4 Variance of Tungsten Separation by Mozley Table

No.	Tungsten (g)	Recovery (%)	Variance Analysis
1	4.86	97.20	Mean: 96.64% Standard Deviation: 0.81% Test Number: 5 Relative Standard Deviation: 0.84%
2	4.80	96.00	
3	4.77	95.40	
4	4.85	97.00	
5	4.88	97.60	
Average	4.83	96.64	

The 25-38 μm tungsten-silica and tungsten-magnetite mixtures (before and after separation) on the MLS flat tray are shown in Figure 5-2 and Figure 5-3, respectively.

A. before separation

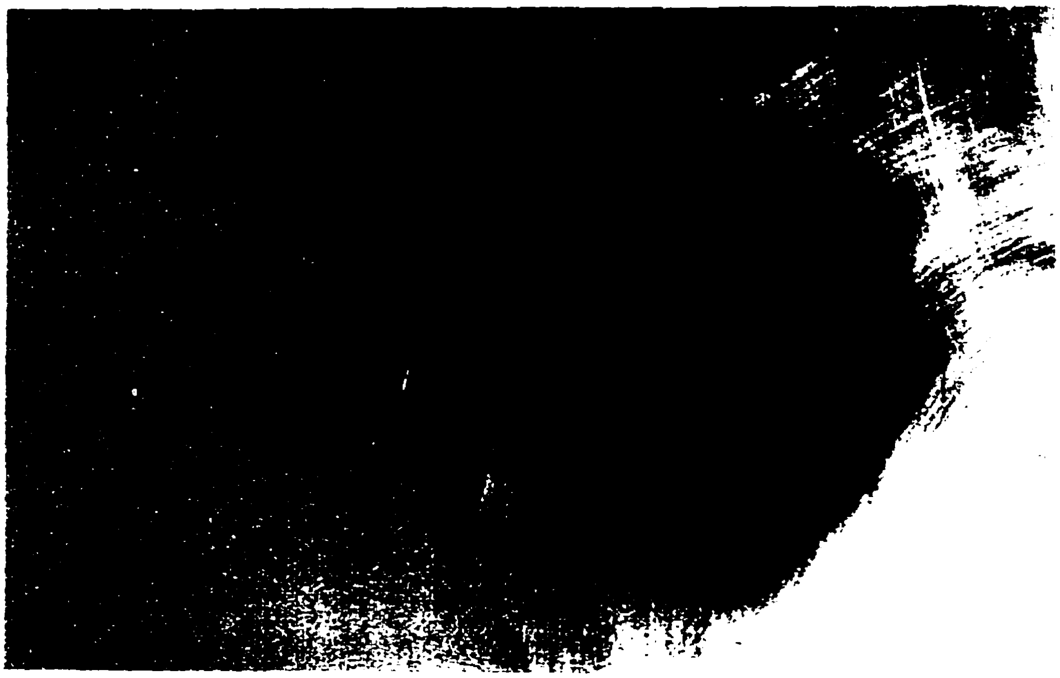

B. after separation

FIGURE 5-2 Mozley Separation of 25-38 μm Silica-Tungsten

A. before separation

B. after separation

FIGURE 5-3 Mozley Separation of -25 μm Magnetite-Tungsten

5.4 Results and Discussion

5.4.1 Pure Silica Tests

The results of the preliminary tests with pure monosized silica are shown in Figure 5-4. Silica particles coarser than 105 μm have a much higher probability of being collected in the bowl, even at a water flowrate as high as 13.7 L.min^{-1} (corresponding to about 54 kPa). About 90% of the -25 μm and 38-53 μm silica particles were rejected into the tails at the flowrate of 6.0 L.min^{-1} and 8.0 L.min^{-1}, respectively. Silica particles in the size range of 75-105 μm had an intermediate behaviour: at a water flowrate of 11.0 L.min^{-1}, 45% were recovered by the Knelson. A normal range of water flowrate is 3-5 L.min^{-1}, at which only the finest silica was rejected by the action of fluidization water for the situation of pure silica.

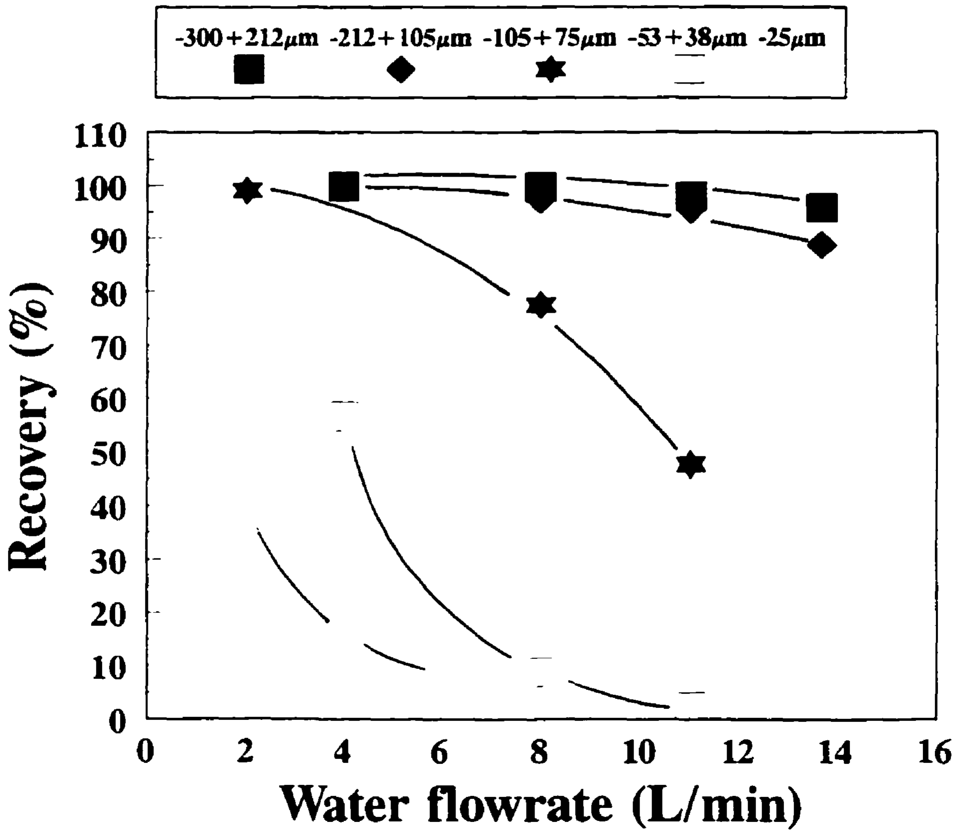

FIGURE 5-4 Pure Silica Recovery as a Function of Fluidization Water Flowrate

5.4.2 Preliminary Tests

Overall Effect of Water Flowrate on Performance

Figures 5-5 and 5-6 show the effect of fluidization water flowrate on tungsten recovery and grade for each of the four gangue types. As expected, the optimum fluidization flowrate increased with an increase in gangue density and/or coarseness.

The optimum fluidization water flowrate for the different gangue types with different size distributions was found to be:

Fine silica 1.8 L.min^{-1}

Fine magnetite 4.1 L.min^{-1}

Coarse silica 3.2 L.min^{-1}

Coarse magnetite 5.3 L.min^{-1}

These figures are accurate within ±0.3 L.min^{-1}.

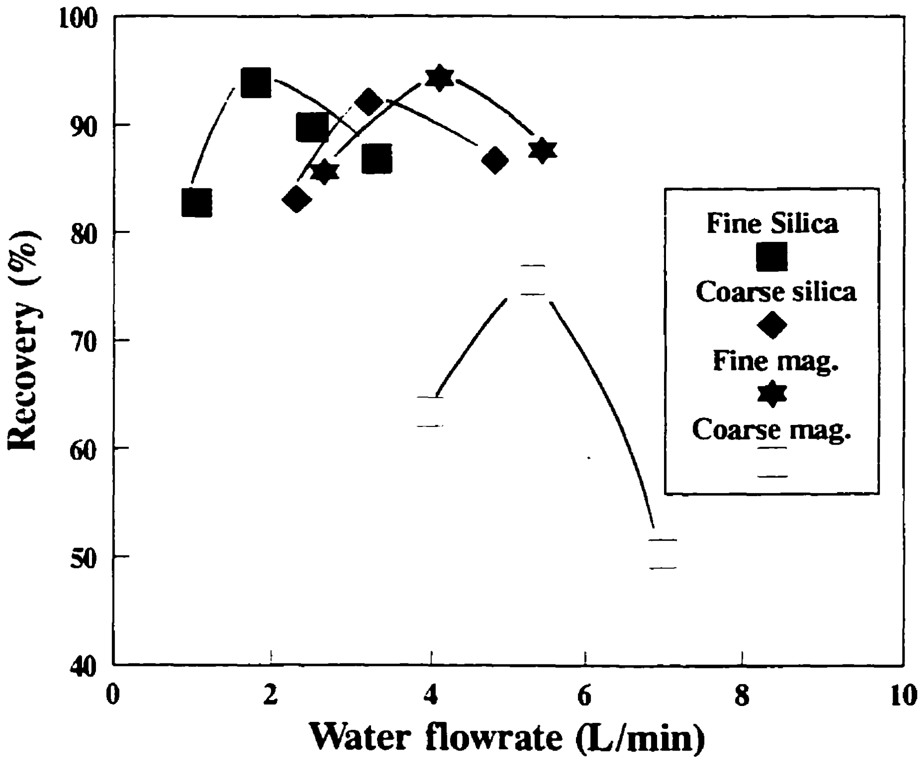

FIGURE 5-5 Effect of Fluidization Water Flowrate on Tungsten Recovery

Tungsten recovery was high for three of the four gangue types (Figure 5-5). With the fine silica gangue, the concentrate grade was, in fact, acceptable for smelting, but not for the three others (Figure 5-6).

Except for the coarse magnetite gangue, the effect of fluidization flowrate was limited, as found by Laplante, Shu and Marois (Laplante et al, 1995), with the same 7.5 cm diameter unit. This is critical for gold recovery, since operators have no readily observable indicator of performance (unlike with a shaking table or a flotation cell).

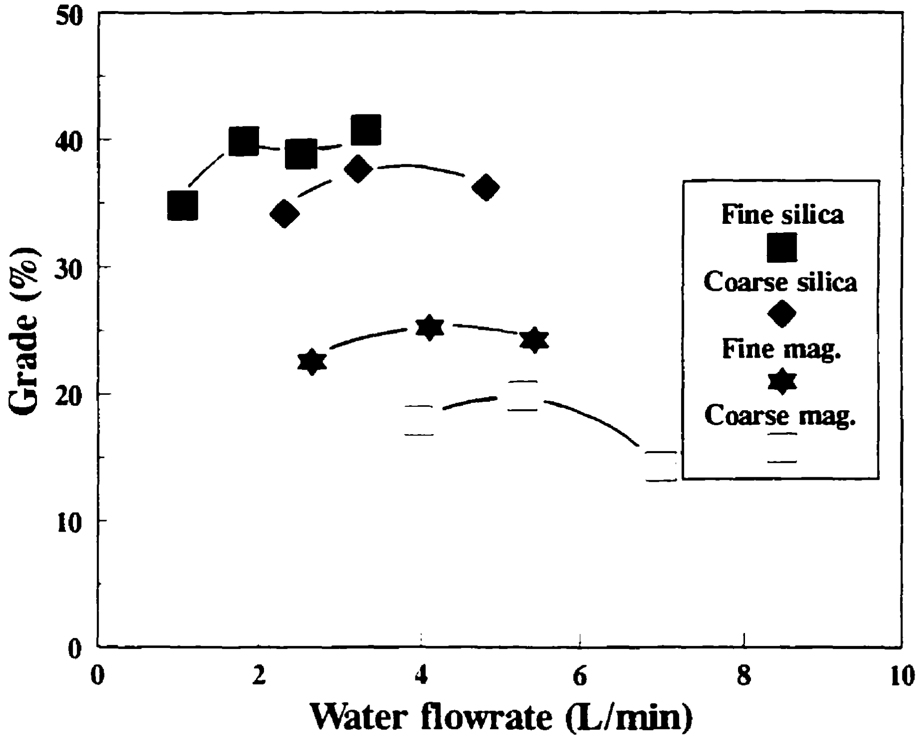

FIGURE 5-6 Effect of Fluidization Water Flowrate on Concentrate Grade

Effect of Water Flowrate on Size-by-Size Performance

Results are presented here as recovery of +37 μm ('coarse' angular particles), inclusive of the 53-75 and 37-53 μm classes; 25-37 μm tungsten (spherical particles) and 8-25 μm tungsten (fine spherical particles). Recovery is based on the amount of tungsten added to the Knelson Concentrator feed, as tail samples were not analyzed. Figures 5-7 and Figure 5-8 show the recovery of the three size classes as a function of fluidization water flowrate, for the silica and magnetite gangue, respectively.

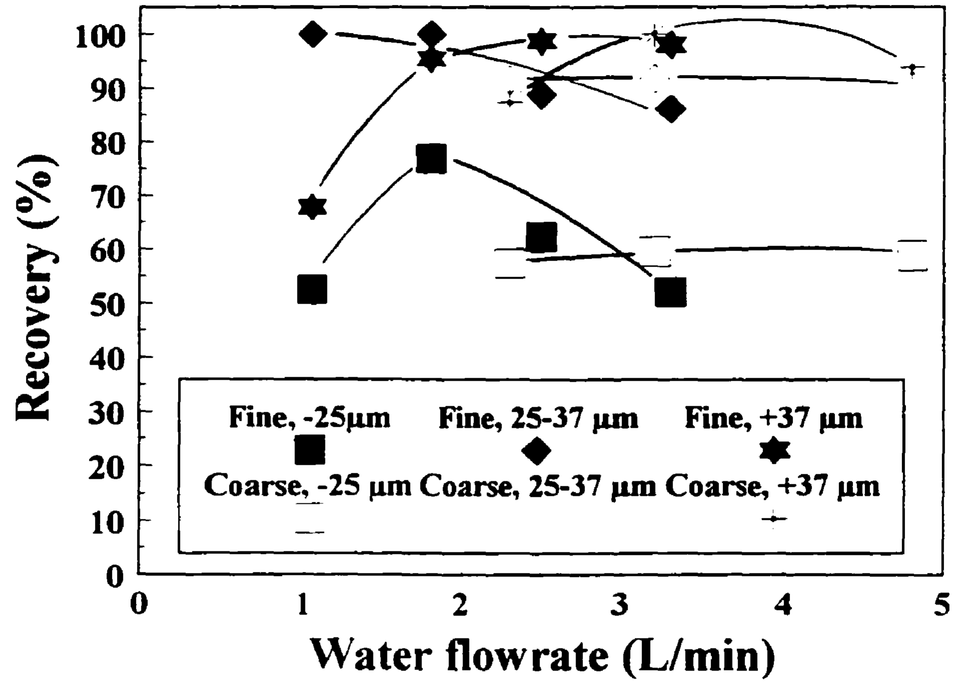

FIGURE 5-7 Effect of Fluidization Flowrate on Tungsten Recovery for the Silica Gangue

Figure 5-7 shows that with silica gangue, recoveries were high except for the -25 µm fraction. For the coarse gangue, recovery increased with tungsten size. However, for the fine gangue, the tungsten recovery of the 25-37 µm fraction is slightly higher than that of +37 µm fraction at the lowest fluidization flowrate. This drop in coarse tungsten recovery can be attributed to the lower concentrate bed expansion, which is inadequate for trickling of the coarser particles. The magnitude of this phenomenon becomes more important as the size of the trickling particles approaches that of the bed (Bridgwater, 1983), thereby reducing trickling velocity.

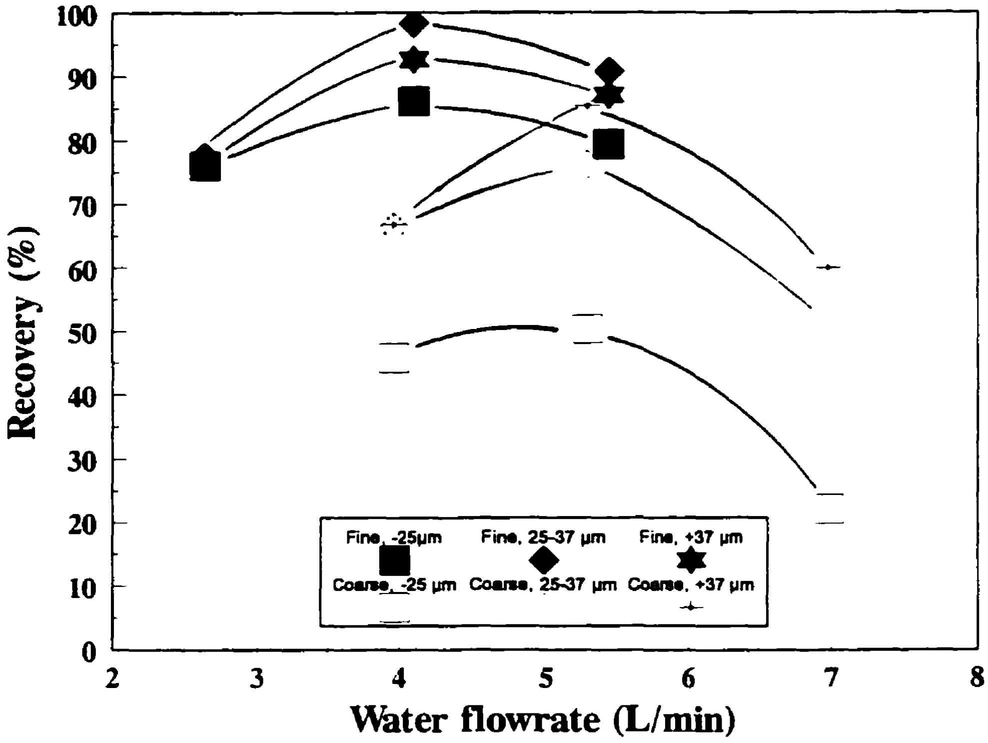

FIGURE 5-8 Effect of Fluidization Water Flowrate on Tungsten Recovery for the Magnetite Gangue

With the magnetite gangue, Figure 5-8 shows that recoveries were lower than those of silica. It also can be seen that tungsten recoveries are sensitive to gangue and tungsten particle size. The effect of tungsten particle size is particularly critical at around 25 μm i.e. the recovery of the +25 μm and -25 μm tungsten is markedly different.

5.4.3 Overload Experiments

Table 5-5 and Figure 5-9 summarize the overload testwork. In this research, overload was defined when ratio of the incremental tails grade over the feed grade increased above 10%. When the ratio reaches 100%, total overloading has taken place, and the quantities of tungsten fed and lost are equal. When overloading is severe, part of the concentrate bed can be sheared away, and the tails to feed grade ratio may exceed 100%.

TABLE 5-5 Effect of Gangue Size and Density on the Performance

Size → Mineral ↓	Coarse gangue		Fine gangue	
	R (%)	G (%)	R (%)	G (%)
Magnetite	31.2	27.9	94.4	57.8
Silica	76.8	62.6	99.4	75.8

R: recovery G: grade

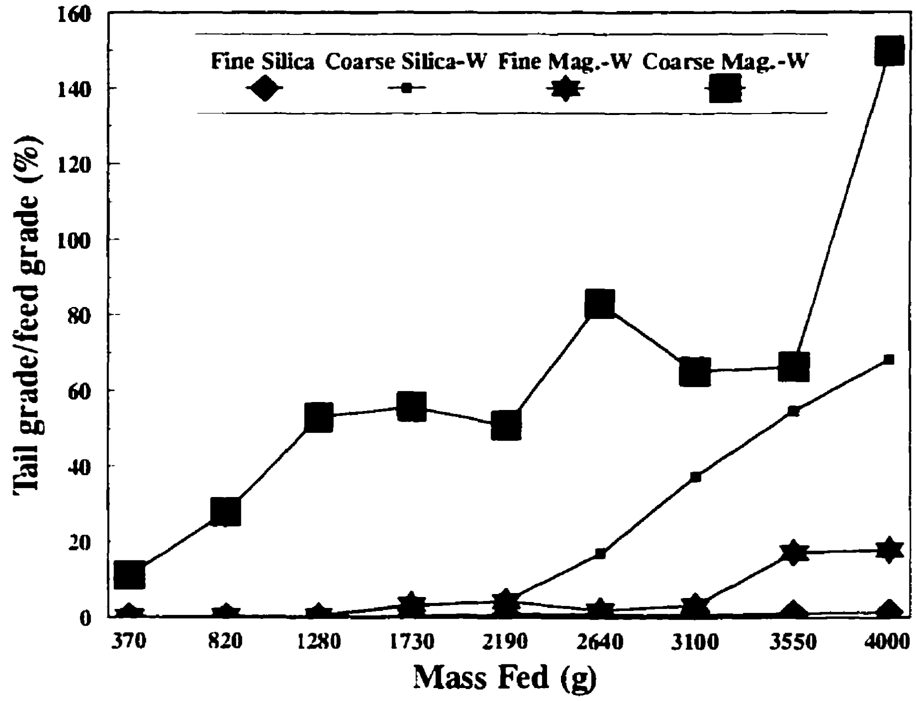

FIGURE 5-9 Overload for Four Types of Gangue

From Figure 5-9, it can be seen that with the coarse magnetite gangue, there was immediate overload; overload became severe in the second half of the test. No overload was observed in the case of fine silica. The fine magnetite gangue yielded good performance, with only a slight increase in tail grade near the end of the load cycle, for excellent overall recovery and concentrate grade. Coarse silica yielded no overloading (too small to be correctly called overload) for about half of the test, but a significant increase in tail grade midway through the test, followed by actual overload.

5.4.4 Overload as a Function of Mass of the Average Diameter

According to Equations 4-2 and 4-5, when the rotation of the machine is kept constant, the centrifugal force and the terminal settling velocity are only dependent on the diameter and the density of the material processed. The weighted average diameter of a full size distribution can be calculated according to Equation 5-1.

$$D_a^o = \frac{100}{\sum \frac{\gamma_i}{D_i^o}} \qquad \text{5-1}$$

where,

D^o_a: weighted average diameter of the gangue, cm or μm

γ_i: fraction yield, %

D^o_i: fraction size, cm or μm

Recovery can then be related to the mass of a particle of average diameter, M_a^o: These data are presented in Table 5-6.

TABLE 5-6 Recovery as a Function of the Mass of Gangue Particles D^o_a

	Fine Silica	Coarse Silica	Fine Magnetite	Coarse Magnetite	Tungsten
D_a^o (μm)	57	147	57	147	26
M_a^o (g)	$2.6*10^{-7}$	$44*10^{-7}$	$4.8*10^{-7}$	$81.4*10^{-7}$	$1.8*10^{-7}$
Tungsten recovery (%)	99	77	94	31	

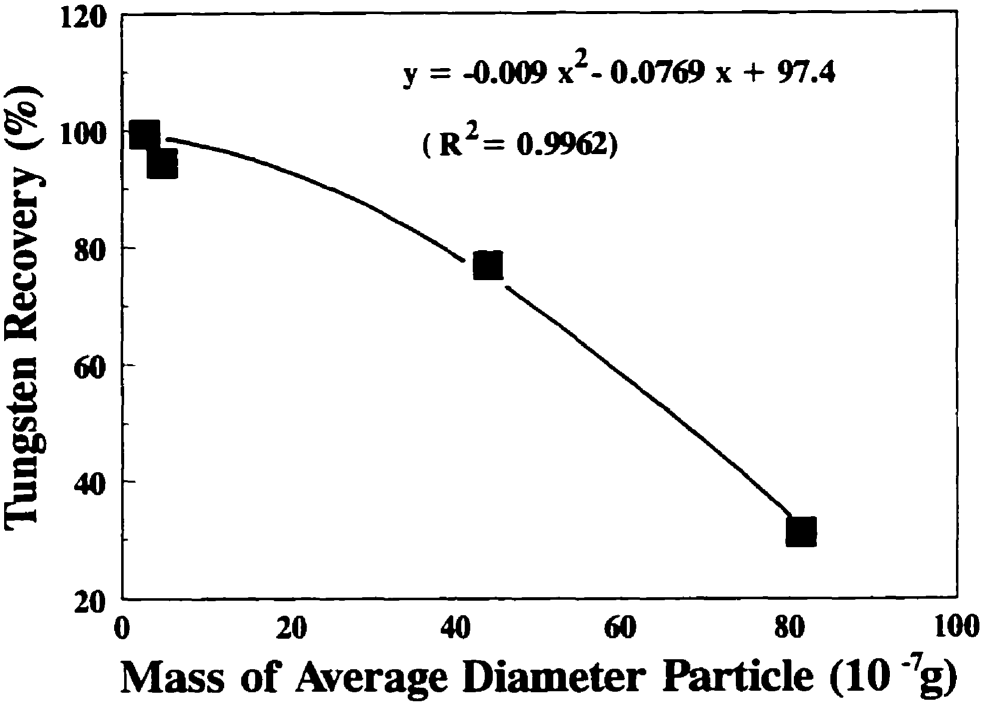

FIGURE 5-10 Tungsten Recovery as a Function of the Mass of Gangue Particle, M_a^o (overload tests)

The mass of the average diameter particle of the fine silica feed was very close to that of tungsten and, in this case, overload did not happen at all. The mass of the average particle of the fine magnetite was slightly higher than that of the tungsten, resulting in light overload. The mass of the average diameter particle of the coarse silica was 25 times that of tungsten, with the result that serious overload occurred. Finally, the mass of the average diameter particle of the coarse magnetite was 46 times that of tungsten, and not only did severe overload occur, but also the concentrate bed which had already formed was partially eroded away at the end of the test. An obvious practical implication of this test work is that when gold is to be recovered from high density gangue, careful, and possibly fine, screening of the feed is essential.

5.5 Modelling the Overload

5.5.1 Derivation of the Model

A relationship such as the one shown in Figure 5-10 is somewhat arbitrary. For example, it does not take into account the mass of material fed (which significantly affects tungsten recovery for the two coarse feeds). Nor does it describe the mechanisms responsible for recovery or loss of tungsten. A phenomenological model, even if relatively simple, would better serve this purpose. The overload model is derived as follows.

Overload can be represented by a relatively simple model. We first consider that for all four overloads, cumulative losses before the onset of overloading are negligible, which means that the Knelson is in capable of capturing all three tungsten size classes irrespective of gangue type (even with coarse magnetite, cumulative losses converge to zero at a small feed mass).

However, captured tungsten is increasingly lost after the onset of overloading. It is reasonable to assume that the losses can be explained by erosion of the concentrate bed by the feed to which it is exposed. It is also reasonable to postulate that the tungsten captured before the onset of overloading is not subjected to erosion.

A model can therefore be derived if we assume that the rate at which tungsten of a specific size is lost is proportional to the mass of tungsten recovered, subject to erosion, and also to the mass of feed flowing over the concentrate bed, which is the scouring medium.

The terms used for the derivation are defined as:

W: mass of tungsten recovered in concentrate (g)

W_f: mass fed to the Knelson Concentrator (g)

W_c: mass of tungsten collected in the bowl at which overload begins (g)

W_o: mass of feed corresponding to W_c (g)

G_f: feed grade (fractional)

R: cumulative recovery (fractional)

K: erosion rate constant (g^{-1})

We define W_c as the tungsten mass already collected in the Knelson concentrate at the beginning of overloading. As long as the mass of tungsten recovered, W, is less than W_c, there is no overload, and no tungsten loss, thus:

$$W = G_f \cdot W_f \tag{5-3}$$

The fractional recovery is equal to

$$R = 100\% \tag{5-4}$$

During the overload phase, we assume that all the tungsten still reports to the concentrate bed, but can be eroded by the material flowing past the bed. The mass eroded (dW) is proportional to the mass of tungsten recovered in excess of W_c and the mass of feed flowing over the concentrate bed. With the above assumptions, we obtain the following mass balance:

$$dW = G_f \cdot dW_f - K \cdot (W - W_c) \cdot dW_f \tag{5-5}$$

K (in g^{-1}) is an erosion rate constant. As Equation 5-5 applies from the onset of overload (i.e. $W = W_c$, and $W_f = W_o$), it can be integrated with the following limits:

$$\int_{W_c}^{W} \frac{dW}{G_f - K \cdot (W - W_c)} = \int_{W_o}^{W_f} dW_f \tag{5-6}$$

$$W_o = \frac{W_c}{G_f} \qquad 5\text{-}7$$

The above integration is trivial. The solution can be re-arranged as,

$$W = W_c + \frac{G_f}{K} \cdot [1 - e^{-K(W_f - W_o)}] \qquad 5\text{-}8$$

therefore, cumulative recovery (the tungsten recovered in concentrate over the tungsten fed to the Knelson), is equal to

$$R = \frac{W_c + \frac{G_f}{K} \cdot [1 - e^{-K(W_f - W_o)}]}{G_f \cdot W_f} \qquad 5\text{-}9$$

In equations 5-8 and 5-9, the exponential term is equal to G_f/K at steady state, which is the mass of tungsten in excess of W_c for which the capture rate, $G_f dW_f$, is equal to the erosion rate. This steady state is reached at 95% after a mass $W_o + 3/K$ has been fed to the Knelson Concentrator. Note that W_o is a function of the feed grade, G_f (i.e. Equation 5-7).

This model is similar to one that has been proposed for the Falcon Concentrator (Laplante et al, 1994), the major difference being that the rate of capture for the Falcon Concentrator was assumed to be proportional to the number of capture sites. The erosion rate constant was also found to be extremely sensitive to the amount of magnetite in the feed (which was varied from 0 to 20%), and as a result, overloading of the Falcon was far more severe than for the Knelson Concentrator.

5.5.2 Size-by-Size Data and Fit of the Model

The model was fitted to the -25, 25-38 and +38 μm size classes of the four tests. For each cumulative recovery curve, the two parameters of Equation 5-9 were estimated using the non-linear minimization function of the software Quatro.Pro 4.0. The lack-of-fit of the model (the sum of the squared residuals) was minimized.

$$\sum_{i=1}^{10} (R_i^{caculated} - R_i^{measured}) \tag{5-10}$$

Table 5-7 gives the parameters of the model for the four gangue types. The onset of overloading is also represented by the mass of the feed at which it takes place, i.e. W_o.

TABLE 5-7 Model Parameters for the Four Gangue Type

Gangue	Size (μm)	W_o (g)	W_c (g)	K (g^{-1})
Coarse Magnetite	38-75	160	3.08	6.71E-04
	25-38	135	3.07	6.91E-04
	8-25	26	0.15	7.79E-04
Coarse Silica	38-75	2013	42.83	3.28E-04
	25-38	1984	42.23	1.04E-03
	8-25	1860	8.21	3.85E-03
Fine Magnetite	38-75	2786	59.28	1.64E-04
	25-38	1952	44.13	1.20E-04
	8-25	1178	4.76	2.38E-04
Fine Silica	38-75	316	7.04	2.82E-06
	25-38	737	17.88	3.16E-06
	8-25	485	2.66	9.14E-06

Coarse magnetite yields almost immediate overload (after 26 to 160 g feed), with erosion rate constants that are virtually independent of particle size (6.7-7.8 x 10^{-4} g^{-1}). For coarse silica, overload takes place more slowly (W_o = 1860 g to 2013 g), with erosion rate constants that are very size dependent (K for the -25 μm fraction, 0.0039 g^{-1}, is more than tenfold its value for the 38-75 μm fraction, 0.00033 g^{-1}).

For fine magnetite, the onset of bed erosion takes place earlier than for coarse silica, W_o = 1178 g to 2786 g), but the erosion rate constants are extremely low, 0.00016 to 0.00024 g^{-1}. This shows that fine magnetite can reach the concentrate bed more easily than coarse silica (i.e. by percolation), but its erosion potential (which is dependent on particle mass) is much more limited. For fine silica, the erosion rate constants are so low ($K = 2.82$ to 9.14×10^{-6}) that the description of bed erosion is merely an academic exercise. Total cumulative losses at the end of the test are less then 0.5% for +25 μm tungsten and only about 1% for -25 μm tungsten.

Figure 5-11 to 5-14 give the size by size cumulative recoveries, as measured and fitted to Equation 5-9.

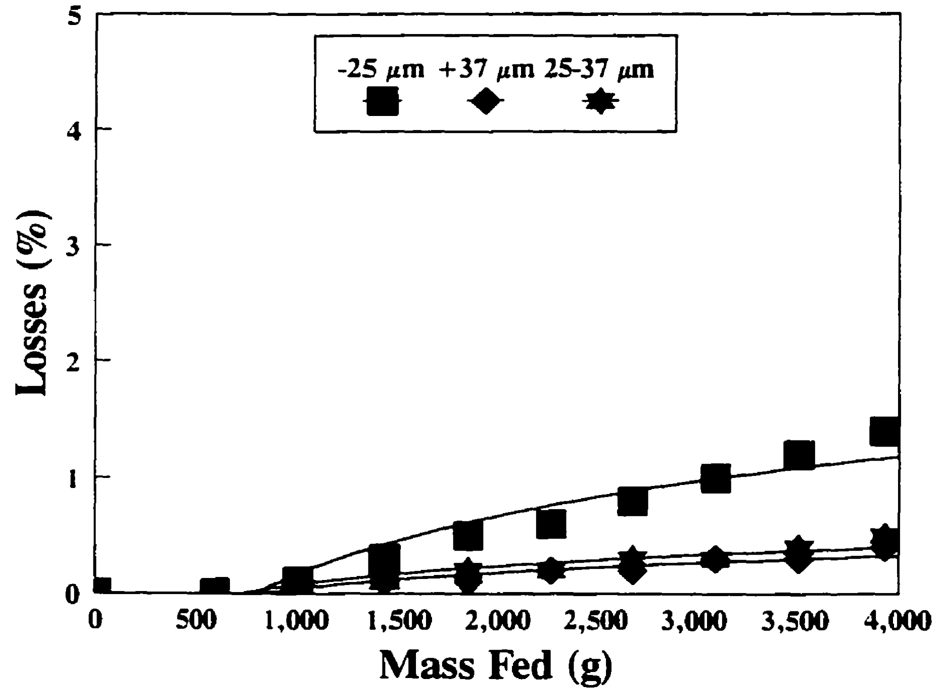

FIGURE 5-11 Overload with Fine Silica Gangue (Lines: fit of Equation 5-9)

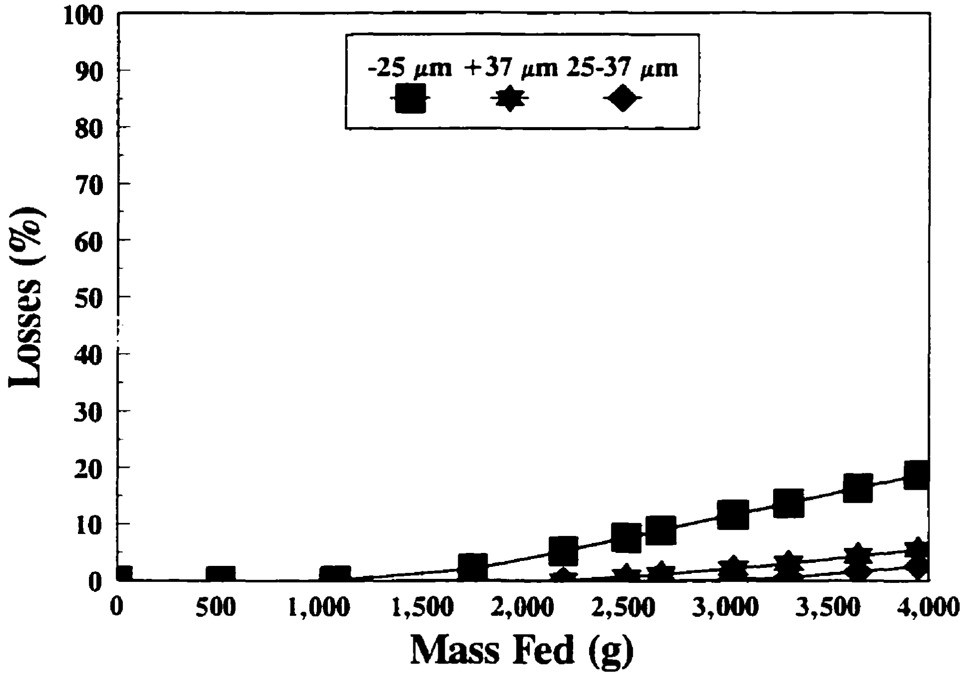

FIGURE 5-12 Overload with Fine Magnetite Gangue

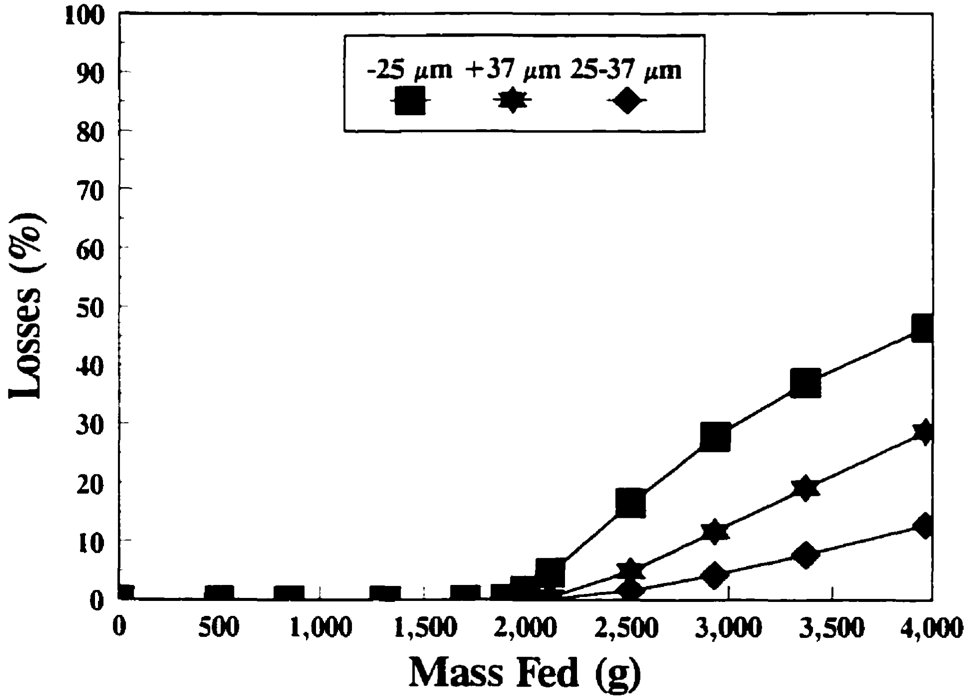

FIGURE 5-13 Overload with Coarse Silica Gangue

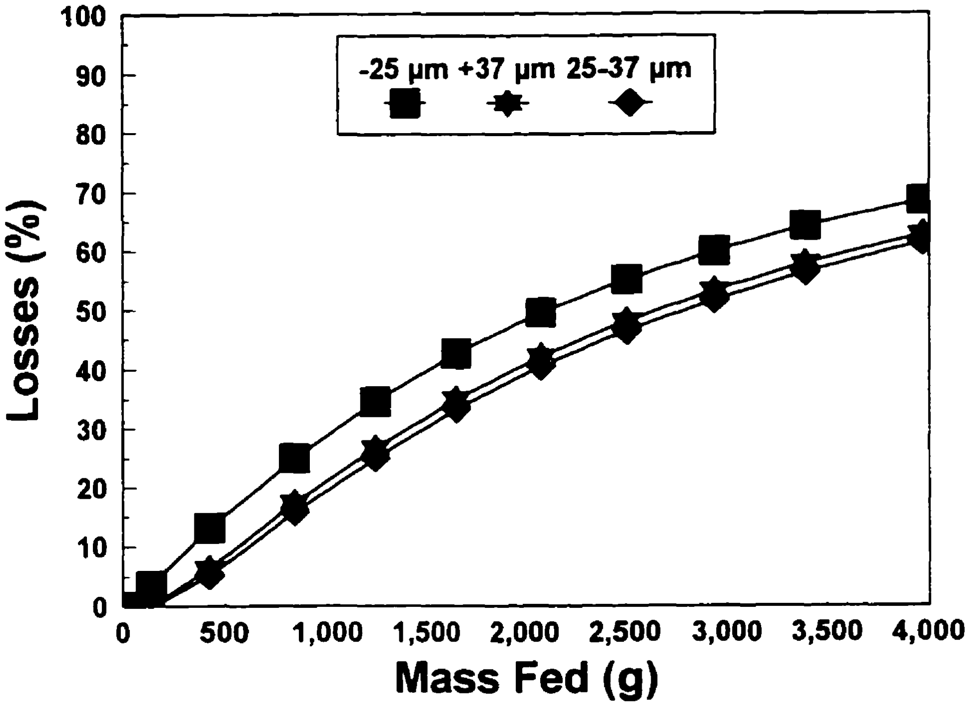

FIGURE 5-14 Overload with Coarse Magnetite Gangue

The fine silica, Figure 5-11, had such low losses (<2%) that overloading did not really take place, even for the -25 µm (note the different vertical scale). There is an apparent difference between the trend of the experimental data (which appears linear) and the model fit (which is parabolic), this would be due to experimental errors. Results show that fine silica could not displace even the finest tungsten.

Figure 5-12 shows that the fine magnetite gangue had more significant losses, especially for the -25 µm fraction. The onset of overloading began after 1000 g of feed for the -25 µm fraction, but only after 2000 g of feed for the two coarser size classes. Results show that fine magnetite can displace the -25 µm tungsten.

For the coarse silica (Figure 5-13), the onset of overloading began at around 2000 g of feed, and depended on the tungsten particle size. Coarse silica can displace tungsten in all size classes, but to very different levels.

For the coarse magnetite, (Figure 5-14), overloading began almost immediately (there was a slight lag for the two coarsest size classes), and was very severe for all size classes. Coarse magnetite can replace all tungsten particles easily, to the extent that there was very little difference between tungsten recovery for the various size classes. The onset of concentrate overload depended very little on the particle size of tungsten, but the extent of the overload did.

5.6 Conclusions

- The use of synthetic tracers to mimic the behaviour of minerals has been practised for many years. In the present contribution, it is suggested that the use of tungsten to mimic gold for gravity studies is a practically effective application of this approach.

- The study has demonstrated that the capture of fine (minus 75 μm) spherical and near-spherical particles with of the density of gold was achieved very effectively in the presence of the four gangue types tested, including coarse magnetite. However, overload of the bed, characterized by erosion of the captured particles, limited the overall recovery.

- For coarse magnetite, overload took place almost at the very beginning of the cycle, and all tungsten particles (up to 75 μm) were severely eroded. For coarse silica, the onset of overload required the growth of a significant concentrate bed and erosion was very particle size dependent. Fine magnetite gangue triggered its overload sooner than coarse silica, but with much less serious consequences. The above results can be fitted to a model of two parameters, the first linked to the onset of bed erosion, and the second to its extent. They also suggest that Knelson performance can be improved with appropriate sizing of its feed.

CHAPTER 6 THE DISTRIBUTION OF CONCENTRATE IN THE KNELSON CONCENTRATOR RINGS

Unlike other gravity separators, e.g. shaking tables and spirals, the separation processes taking place in the Knelson Concentrator are not easily observed. To understand them requires indirect means. In this chapter, the focus will be on one such technique, an in-situ study of the material recovered in the rings.

6.1 Description of the Separable Bowl

A separable Knelson bowl as shown in Figure 6-1 was specially created. It is a conventional bowl split into two halves which can be easily joined, sealed with silicon, and further tightened by two wire rings. After a curing period of 24 hours, it is ready to use as a conventional bowl. The main inside dimensions of the bowl are shown in Table 6-1.

TABLE 6-1 Inside Dimensions of the Separable Bowl

Ring No*	D_1 (cm)	D_2 (cm)	D_3 (cm)	A (cm^2)	S (cm)	V (cm^3)
5	7.5	6.2	5.0	0.88	1.95	17.2
4	6.8	5.6	4.4	0.86	1.76	15.1
3	6.2	5.0	3.8	0.75	1.57	11.8
2	5.6	4.4	3.2	0.72	1.38	9.9
1	5.0	3.8	2.6	0.71	1.19	8.4
Average	6.2	5.0	3.8	0.78	1.57	12.5

* from the bottom to the top

D_1: diameter of the bottom of a riffle

D_2: diameter of the central line of a riffle

D_3: diameter of the inner rim of a riffle

A: average cross-sectional area of a ring, which is almost the same for each of the five different rings

S: length of the central line of a ring

V: volume of a ring

Note: the slope angle of the bowl is about 15°; there are 150 fluidization water holes.

6.2 Experimental Methodology

A total of four tests was performed. For each, the feed consisted of 1900 g of -425 μm silica or magnetite, mixed with 100 g of tungsten (the same size distribution as that used in Chapter 5, yielding a tungsten grade of 5%). A feed of top size intermediate between the coarse and fine feeds of Chapter 5 was chosen to minimize the percolation of fine tungsten particles into the pressurized water jacket (a phenomenon observed with the fine feed, which would make ring-by-ring data analysis difficult) and erosion problems (a phenomenon observed with the coarse magnetite). The average diameter of the fluidization water holes in the bowl is around 0.3 mm, and it was verified that a top particle of 425 μm could prevent tungsten particles from percolating into the pressurized water jacket. The size distribution of the gangue minerals is shown in Table 6-2.

FIGURE 6-1 Separable Knelson Concentrator Bowl

TABLE 6-2 Size Distribution of the Gangue Minerals for Split Bowl Tests

Size (μm)	300-425	212-300	150-212	106-150	75+105	53-75	38-53	25-38	-25	Total
Mass (%)	10.0	20.8	24.7	18.4	12.7	7.2	4.9	0.9	0.5	100.0

The Knelson Concentrator was operated at a fluidization water flowrate of 2.9 L.min^{-1} for the silica feed and 4.4 L.min^{-1} for the magnetite feed, which are intermediate between the optimum conditions determined for coarse and fine gangue in Chapter 5.

To recover concentrate in its original position at end of a test, a procedure was developed by trial and error (inadequate procedures resulted in part of the concentrate sloughing to the bottom of the bowl at the end of the test). The final procedure was as follows: once all material was fed and no more solids were discharged in the tails, the fluidization water was turned off and the bottom valve of the water jacket was opened to drain part of water in the jacket; the Knelson Concentrator was spun for an additional five minutes to achieve additional drainage. The whole bowl was then removed and put into a freezer. Only once the riffle content was completely frozen was the bowl taken out and separated into two halves. The frozen concentrate could then be scooped out ring by ring and/or cut into pieces, depending on the information needed.

The analytical procedure used was that of Chapter 5; it was applied on the contents of the various rings, as well as various sections of specific rings. Because there was such a clear difference in the content of a ring of concentrate (see Figures 6-11 and 6-12), some rings of the frozen concentrate were cut into three sections, i.e. inner, middle and outer, as shown in Figure 6-2. Each section was then analyzed separately. The transition between the three parts was chosen to minimize mass in the middle section, whilst keeping the content of the outer and inner sections as homogenous as possible. Hence the middle section is essentially a transition zone between the outer and inner ones, and is the one whose content is most dependent on the actual choice of the cut-off between the three sections.

Several photographs were taken to illustrate the distribution of tungsten in the whole concentrate or individual rings. Three tests with silica gangue and one test with magnetite were performed.

Test One

This test used a silica gangue and a fluidization water flowrate of 2.9 $L.min^{-1}$. The concentrate was analyzed ring by ring.

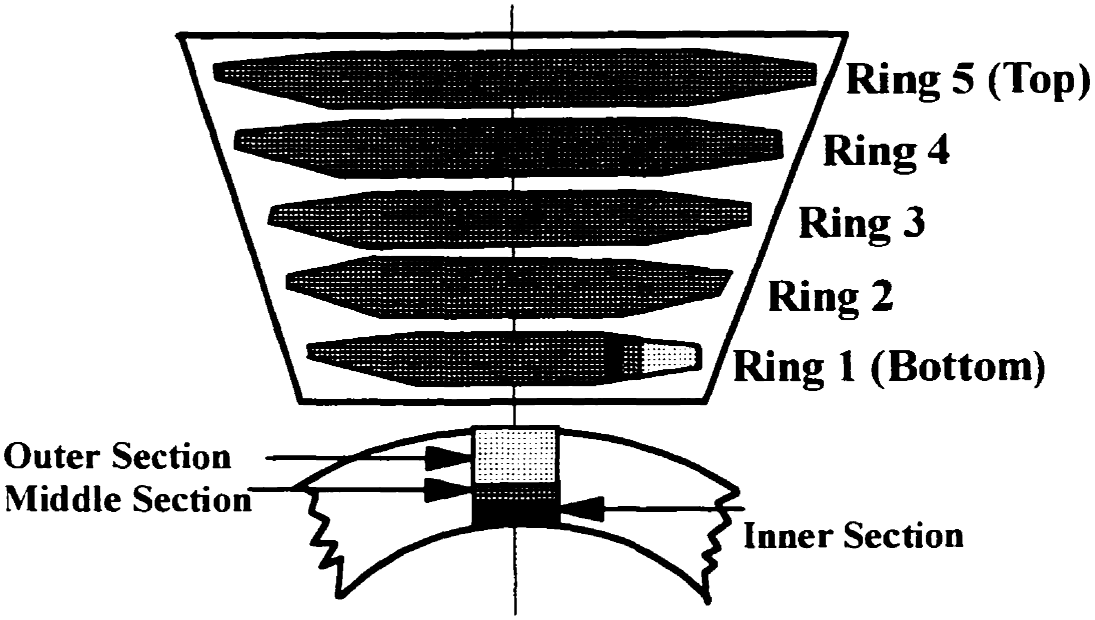

FIGURE 6-2 Schematic Diagram of the Concentrate Split

Test Two

Test 1 showed that most of the tungsten reported to the inner section of each ring. The purpose of this second test was to analyze the radial distribution of tungsten. The products of test 1 were combined and fed again to the Knelson under the same operating conditions. The frozen concentrate was also analyzed ring by ring. For the fourth ring, the concentrate was cut into inner, middle and outer sections and analyzed separately.

Test Three

The analysis of the results of ring four of test 2 showed significant differences in the distributions of concentrate size and tungsten recovered in the three sections. The purpose of test 3 was to explore if all the five rings had the same density as that of ring four in test 2, using the same material and operating conditions as tests 1 and 2. All five ring concentrates were separated into three sections, and the five inner sections combined and analyzed. The middle and outer sections received the same treatment.

Test Four

This test used a magnetite gangue and a fluidization water flowrate of 4.4 L per minute; the five ring concentrates were analyzed individually. To monitor the progression of tungsten losses to the tails, the feed was split into three 80 g and seven 250 g samples. Ten tail samples corresponding to the ten feed samples were collected individually. The first four tail samples were screened and the size fractions analyzed in order to focus on the early stages of the concentrate bed build-up.

6.3 Results

6.3.1 Test 1

This test yielded a tungsten recovery of 91% with a grade of 57.2% W, which is slightly lower than that (98.5%) obtained half-way through the coarse silica gangue test reported in Chapter 5. The slight drop in recovery may have been the result of small leaks between the two halves of the bowl at the top of the fifth riffle, which eroded part of its the concentrate (that closest to the cut). Table 6-3 shows the overall results. Mass, tungsten and grade ring-by-ring distributions are shown in Figure 6-3.

The riffle volume increases linearly from rings 1 to 5 (as dictated by geometry), but the mass only did so from rings 1 to 4, after which there was a sharp drop in weight from 44 to 31 g in ring 5 (Table 6-3). The drop could be linked to the erosion of the concentrate in the fifth ring. This erosion firstly arose locally where the bowl was split. Secondly, the transition in tail flow from nearly vertical inside the bowl to a horizontal motion at the edge of the fifth ring caused some erosion all around the ring. The mass of silica recovered actually increased from 16.6 g in ring 4 to 17.5 g in ring 5. The corresponding mass of tungsten recovered, however, dropped dramatically, from 27.6 g to 13.5 g, in part because of erosion, but also because there was no more tungsten to recover, as the test was stopped just before the onset of overloading. Concentrate grade was similar for the first four rings, but dropped sharply for the fifth, as a result of the bed erosion and lack of additional tungsten to recover.

TABLE 6-3 Overall Results of Test 1

Ring Number	Mass (g)	Tungsten		Silica (g)
		Grade (%)	Recovery (%)	
5	30.95	43.5	13.5	17.50
4	44.22	62.4	27.6	16.61
3	35.15	58.9	20.7	14.45
2	26.90	57.3	15.4	11.50
1	21.91	62.9	13.8	8.16
Total	159.13	57.2	91.0	68.18
Recovery by Size (%)				
+25 μm	91.4			
-25 μm	84.3			

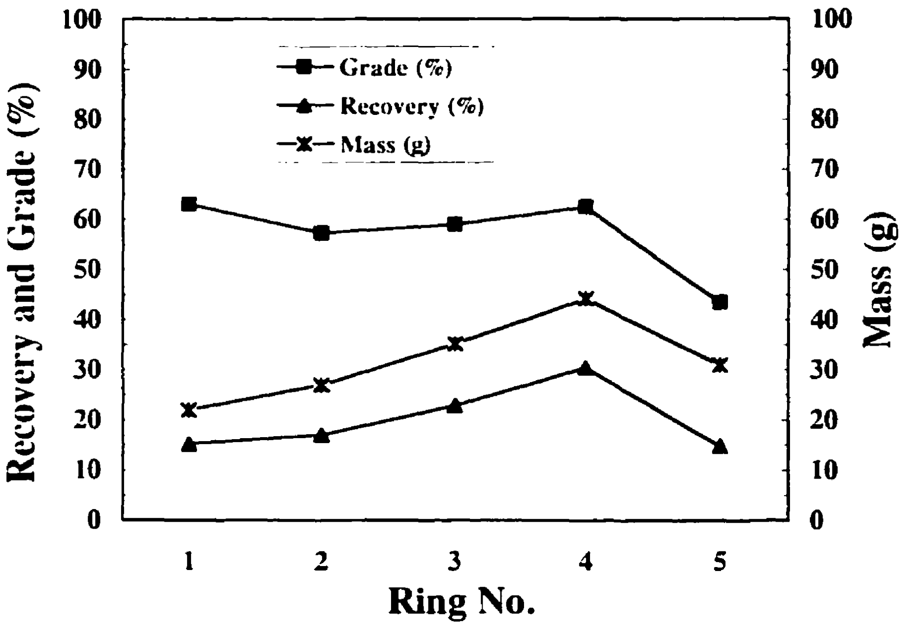

FIGURE 6-3 Test 1: Ring-by-Ring Mass, Recovery and Grade (Feed: -425 μm Silica)

Test 1 yielded a tungsten recovery of 91.4% for the +25 μm and 84.3% for the -25 μm fraction (Table 6-3). The distribution of the different size classes of tungsten in the five rings is shown in Figure 6-4. Coarser tungsten particles (38-75 μm) were the most abundant in ring 1 and least abundant in ring 5, the opposite being true for the -25 μm fraction, which showed very little recovery in ring 1. This is in good agreement with the findings of Chapter 5 for a coarse silica gangue, which showed that erosion of tungsten from the concentrate bed was very size dependent, being highest for the -25 μm fraction. Thus, -25 μm tungsten recovered in ring 1 would have a high probability of erosion; much would be recovered in downstream rings -- i.e. in the rings above, since the slurry flow is upward. Another factor, whose importance cannot be assessed at this point, is that -25 μm tungsten, which has a lower terminal settling velocity, is likely to percolate at a lower rate than coarser tungsten.

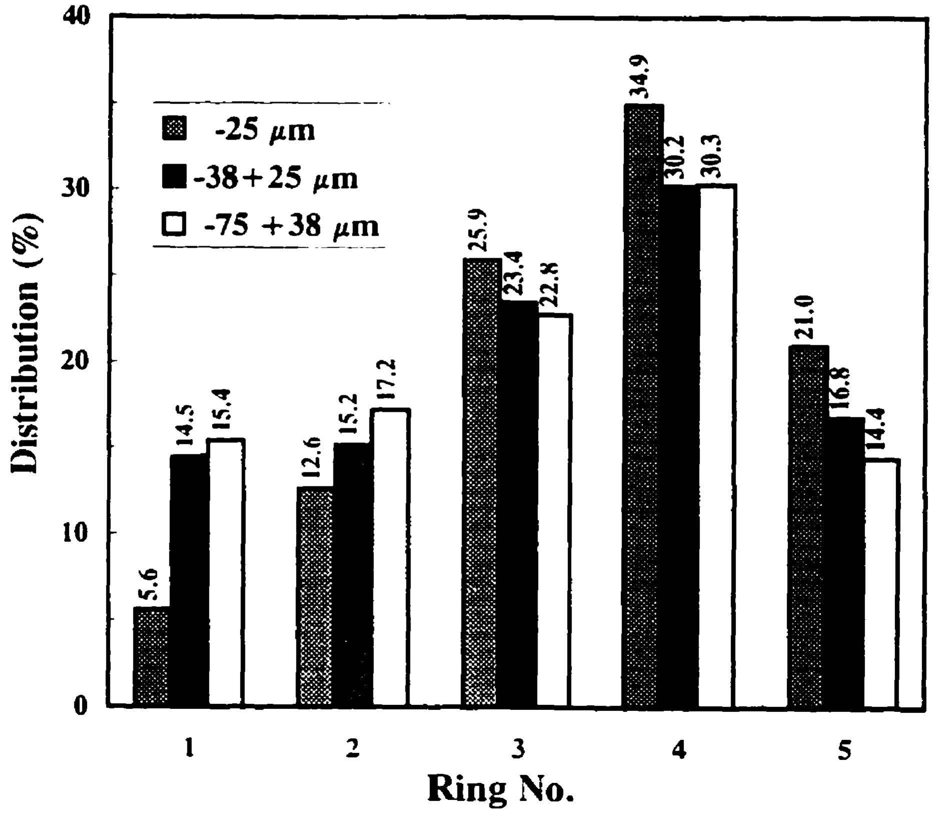

FIGURE 6-4 Tungsten Size Distribution in Concentrate (Feed: -425 μm Silica)

6.3.2 Test 2

The overall results are shown in Table 6-4; the total mass recovered in the concentrate being very close to that of test 1, 163.37 g versus 159.13 g. Recovery was 87%, 4% lower than for test 1; this could, in part, be due to the re-use of the products of test 1 as feed of test 2[1]. This test shows the same significant drop in the recovery of ring 5; variations from ring 1 to 4 show smaller and less definite trends. Similarly, test 2 yields a tungsten recovery 88.2% for the +25 μm fraction, and a lower recovery, 52.8%, for the -25 μm fraction. Figure 6-5 shows how the tungsten was distributed in the three sections of ring four; Table 6-5 shows the same data, but size-by-size. The size distribution of the three sections of ring four is shown in Figure 6-6.

TABLE 6-4 Overall Results of Test 2

Ring Number	Mass (g)	Tungsten		Silica (g)
		Grade (%)	Recovery (%)	
5	30.99	42.8	13.3	17.65
4	41.39	59.2	24.5	16.87
3	38.47	56.7	21.8	16.65
2	32.79	55.6	18.2	14.57
1	20.03	44.5	8.9	11.12
Total	163.67	53.0	86.7	76.63

Recovery by Size (%)	
+25 μm	88.2
-25 μm	52.8

---

[1] As recovery is based on the mass of tungsten in the feed of test 1, any tungsten lost to manipulations will report as losses to test 2.

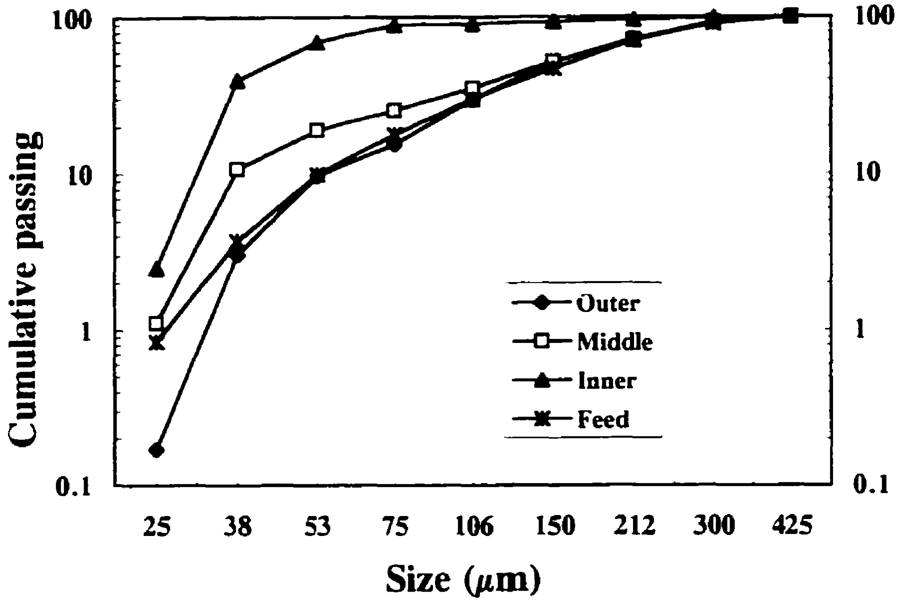

FIGURE 6-5 Concentrate Size Distribution of the Three Sections of Ring Four (Test 2)

TABLE 6-5 Content of the Three Sections of Ring Four (Test 2)

Size (μm)	Mass (g)	Inner Section		Middle Section		Outer Section	
		Mass (g)	W (g)	Mass (g)	W (g)	Mass (g)	W (g)
300-425	1.40	0.35		0.39		0.66	
212-300	3.69	0.72		1.13		1.84	
150-212	3.64	0.73		1.02		1.89	
106-150	3.51	0.61		0.89		2.01	
75-105	2.37	0.57		0.52		1.28	
53-75	6.08	5.24	5.14	0.33	0.198	0.51	0.0171
38-53	9.17	8.12	7.96	0.44	0.115	0.61	0.0409
25-38	10.79	10.02	9.82	0.51	0.455	0.26	0.0858
-25	0.75	0.67	0.65	0.06	0.034	0.02	0.0028
Total	41.40	27.03	23.57	5.29	0.802	9.08	0.1466

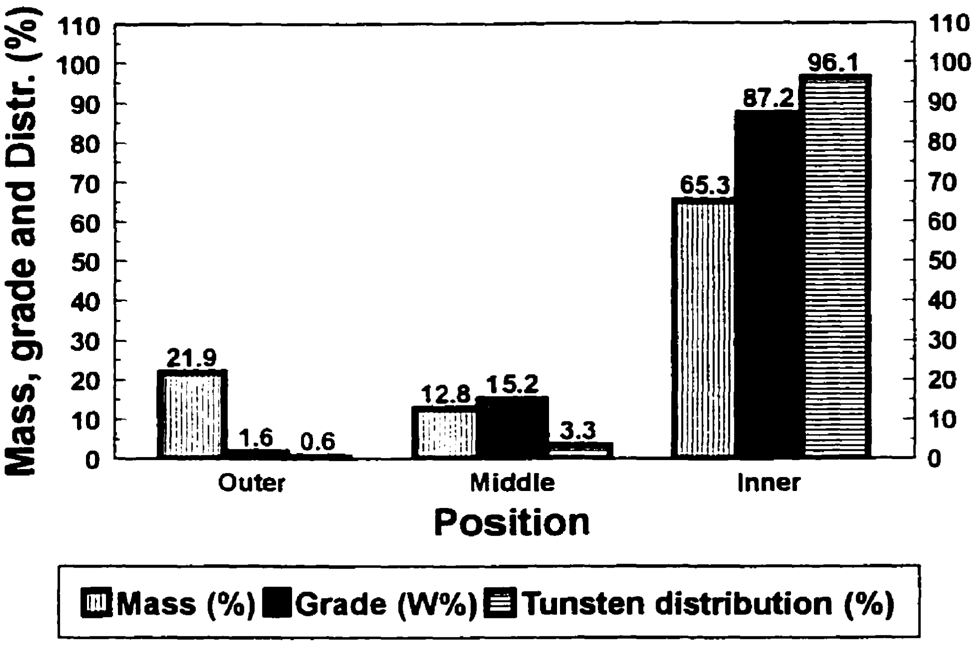

FIGURE 6-6 Mass, Grade and Tungsten Distribution in the Three Sections of Ring Four (Test 2)

Tungsten was found predominantly in the inner section (that exposed to the flowing slurry), where 65% of the mass and 96% of the tungsten in the concentrate reported, at a grade of 87% W. The outer section contained 22% of the mass, but only 0.6% of the tungsten, at a grade of 1.6% W, which is much lower than that of feed, 5% W. The middle section showed a transition between the barrenness of the outer section and the high grade of the inner one.

Table 6-5 and Figure 6-5 show that the size distribution in the outer section was much coarser than that of inner section, because most tungsten (minus 75 μm) was recovered in the inner section while coarser silica particles were recovered in the outer.

6.3.3 Test 3

The overall results of test 3 are summarized in Table 6-6; grade variations along the radial direction ring by ring are shown in Table 6-7. Figure 6-7 shows the size distribution of three sections for the whole concentrate, while Figure 6-8 shows the mass, grade and tungsten distribution in three sections of the concentrate.

Table 6-6 shows that test 3 yielded a recovery of 86.6% at a grade of 49.2% W, which are close to those of test 2. The significant difference of tungsten grade between the inner and outer sections for the five rings of the concentrate was reproduced, 84.8% in the inner section to 0.7% in the outer section (Table 6-7).

TABLE 6-6 Overall Results of Test 3

Ring Number	Mass (g)	Tungsten		Silica (g)
		Grade (%)	Recovery (%)	
5	34.26	44.1	17.3	19.16
4	36.12	49.7	20.6	18.17
3	32.13	51.9	19.1	15.47
2	28.26	50.6	16.4	13.95
1	22.72	50.7	13.2	11.19
Total	153.49	49.2	86.6	77.94

Recovery by Section (%)		
Inner Section	Middle Section	Outer Section
84.7	1.6	0.4

TABLE 6-7 Grade Variation (% W) along the Radial Direction, Ring by Ring

Ring No.	Inner Part	Middle part	Outer Part
5	82.1	6.3	0.5
4	86.6	7.7	0.4
3	85.4	6.7	0.3
2	86.0	10.3	0.4
1	84.3	9.7	1.9
Average	84.8	8.1	0.7

The size distribution of the three sections also reproduced the results of test 2, as the trends of Figure 6-7 were very similar to those of Figure 6-5 (test 2). The size distribution of the outer section was much coarser than that of the inner one, the finest on account of its high tungsten content. The size distribution of the middle section was similar to that of feed.

Figure 6-8 shows the mass, grade and tungsten distribution in the three sections for the whole concentrate. Again, the columns are very similar to those of test 2 (Figure 6-6). The overall size distributions differ markedly, and the tungsten mainly reported to the inner section, 98% contained in 57% of the weight. The outer section, 99.3% silica, was much coarser than the feed, or even the silica fraction of the feed. This would be expected from the results of the pure silica tests, which showed that fluidization water alone could reject fine silica, even when the riffles are not packed. The middle section had a distribution similar to that of the feed, but little weight should be given to this observation, as the middle part is a transition area, whose content is dependent on the cut-off between the three parts.

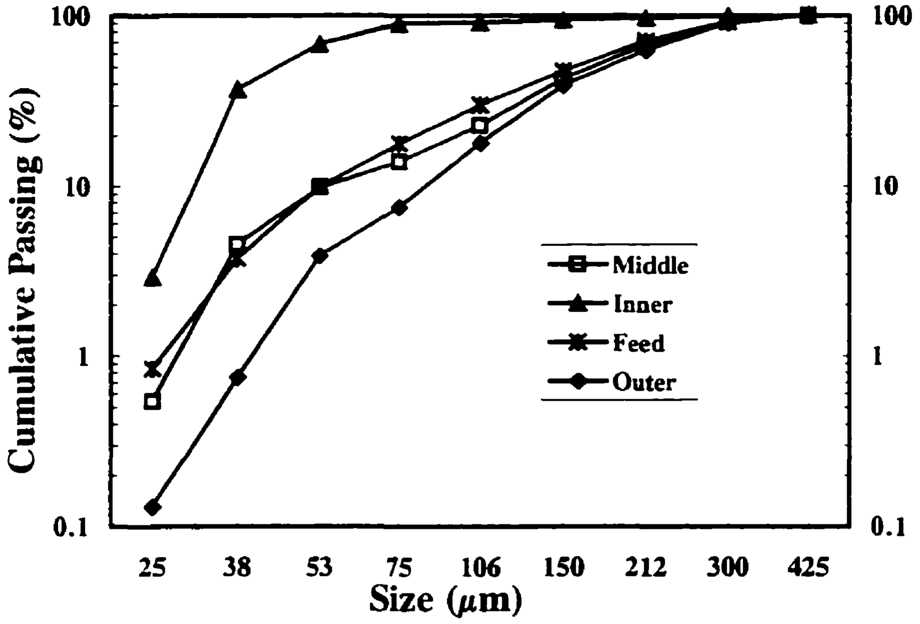

FIGURE 6-7 Size Distribution in the Three Sections of the Concentrate (Test 3, all five rings combined)

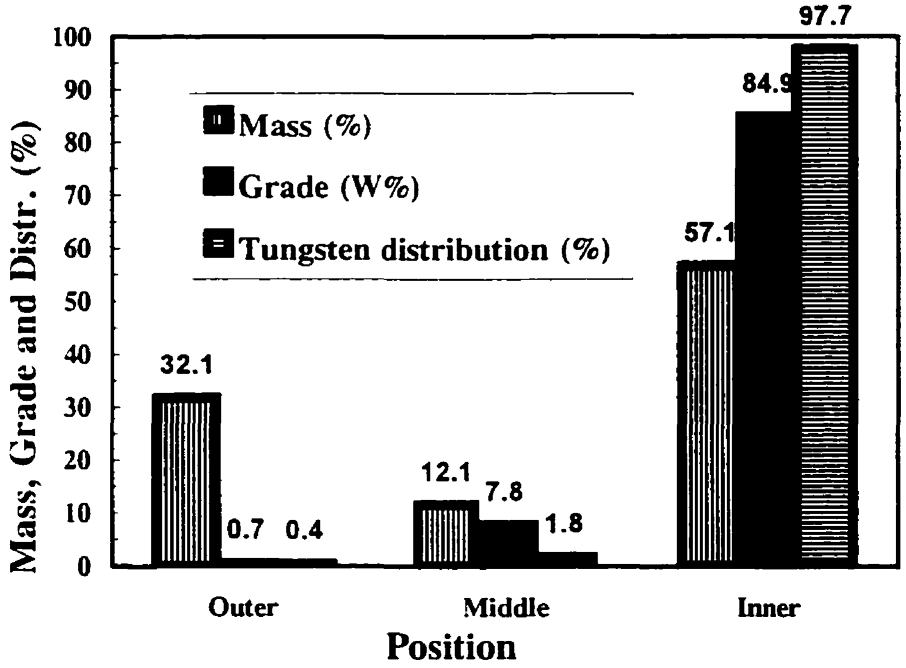

FIGURE 6-8 Mass, Grade and Tungsten Distribution in the Three Sections of the Concentrate (Test 3, all five rings combined)

6.3.4 Test 4

The overall results of test 4 are summarized in Table 6-8. Figure 6-9 shows how recovery and grade varied from rings 1 to 5, and Figure 6-10 shows the size analysis of the four tail samples. Table 6-8 shows that the total tungsten recovery for the -425 μm magnetite gangue was 47.4%, which is in between the recoveries of fine (94.4%) and coarse (31.2%) magnetite gangue (Chapter 5).

TABLE 6-8 Overall Results of Test 4

Ring Number	Mass (g)	Tungsten		Magnetite (g)
		Grade (%)	Recovery (%)	
5	47.35	20.3	9.6	37.76
4	42.60	21.3	9.0	33.52
3	40.15	24.8	10.0	30.20
2	35.86	25.5	9.2	26.24
1	30.56	31.4	9.6	20.98
Total	196.55	24.1	47.4	47.40
Recovery by Size (%)				
+25 μm	48.1			
-25 μm	30.5			

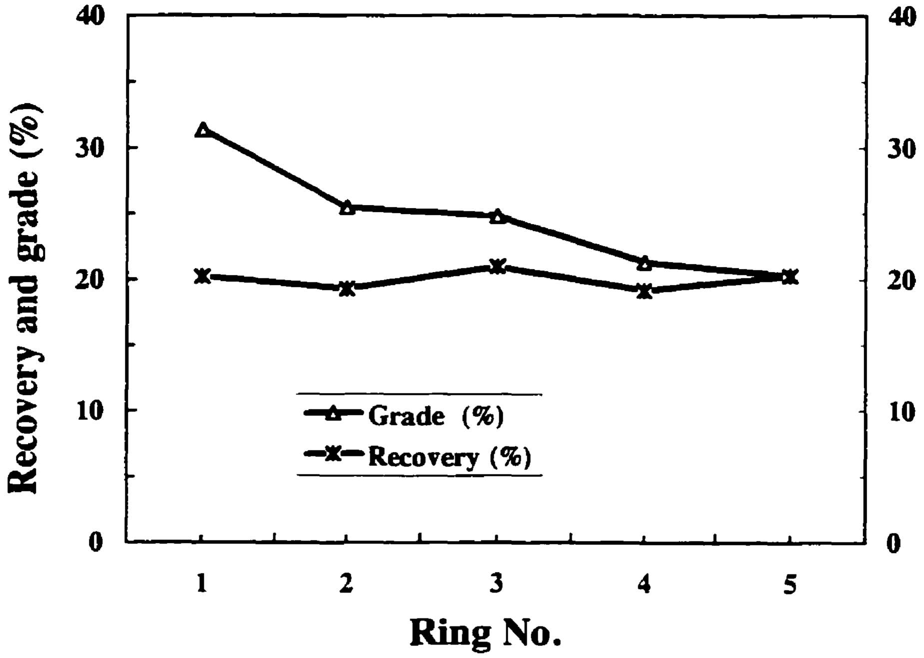

FIGURE 6-9 Recovery and Grade vs Ring No (Test 4)

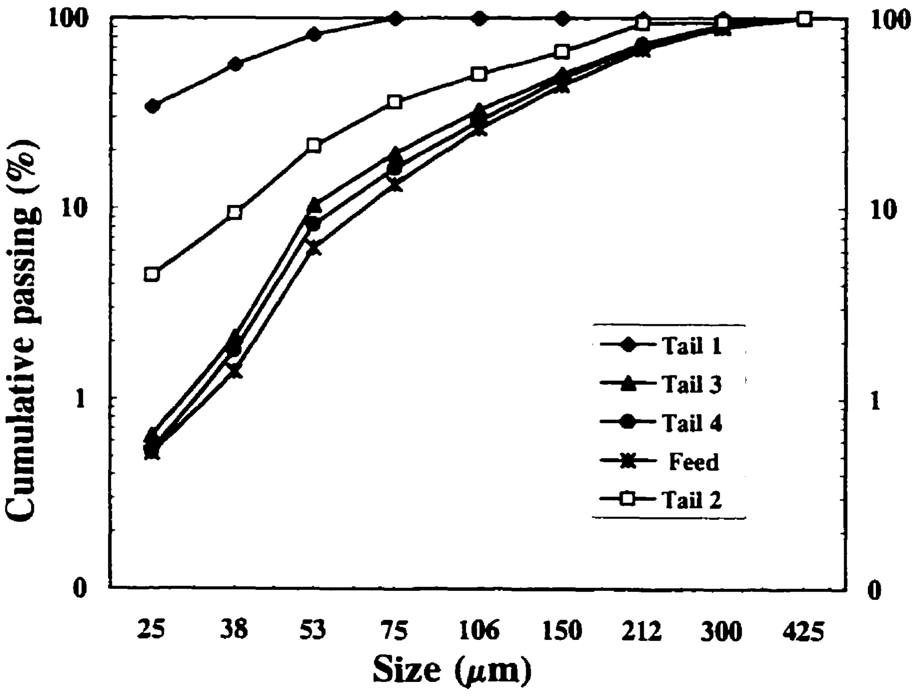

FIGURE 6-10 Size Analysis of First Four Tails (Test 4)

By comparing the results of tests 1 and 4, it can be seen that, unlike the silica feed of similar size distribution, the tungsten recovery for the magnetite feed was evenly distributed between the five rings (Figure 6-9). As concentrate mass increased progressively from rings 1 to 5, grade dropped, from slightly above 30% down to 20%. Recovery did not drop in ring 5 because there was appreciable tungsten still to be recovered (rings 1 to 4 recovered only 38% of the tungsten). The importance of bed erosion was demonstrated in the previous chapter. This suggests that at least part of the tungsten captured in ring 5 had previously been captured in rings 1 to 4, only to be later eroded away. Another possible source of recovery was the tungsten that had not yet trickled to the concentrate bed of rings 1 to 4. Clearly, further research work will be needed to assess the relative importance of each contributing factor.

Figure 6-10 shows the substantial differences of the size distributions of the four consecutive tails samples during build-up of the concentrate bed. The first tail was the finest, then coarseness increased to approach the size distribution of the feed. The amount of the mass fed for the first three tail samples was about 240 g, which was the approximate mass of magnetite needed to build-up the concentrate bed of a laboratory Φ 7.5 cm Knelson. The results demonstrate that during the concentrate bed build-up, fine particles were first rejected to the tails, whereas relatively coarser particles were recovered deep into the rings. After the concentrate bed build-up was complete, very little additional mass was recovered, and the tails size distribution approached that of the feed (tails 4 in Figure 10).

6.3.5 Photographic Evidence of the Concentrate Distribution

The following photographs were taken from frozen concentrates obtained from different feeds and operating conditions. Figures 6-11 and 6-12 show a half bowl of the concentrate obtained from -425 μm silica and magnetite gangues, respectively.

FIGURE 6-11 A Half Bowl of the Concentrate with -425 μm Silica Gangue

FIGURE 6-12 A Half Bowl of the Concentrate with -425 μm Magnetite

Figure 6-11 shows that tungsten (tungsten: grey, silica: white) predominantly reported to the inner section in the Knelson bowl, which is about one-fifth of the total depth of a ring, whereas the remaining four-fifths were virtually all silica. The fifth ring contained less tungsten, either because most of the tungsten had already been recovered in the first four rings, or became part of the tungsten near the bowl rim was eroded away to the tails.

Figure 6-12 shows a similar situation for the magnetite gangue: most of the tungsten (tungsten: brown, magnetite: black) was located in the inner section. However, unlike silica, the whole surface of the concentrate is not covered by tungsten, and appreciable magnetite can be seen. Interestingly, the ridges of the riffles show a higher tungsten coverage than the riffles themselves.

Figure 6-13 shows a bottom view of a piece of the concentrate obtained from -425 μm silica gangue at the optimal fluidization water flowrate of 2.6 L.min^{-1}. A similar picture taken from the concentrate with magnetite gangue is shown in Figure 6-14.

Tungsten reported mostly to the inner rings. However, there is still an obvious difference between silica and magnetite gangues (Figures 6-13 and 6-14). For the magnetite gangue, parts of the tungsten layer were covered with a thin magnetite layer or coating (e.g. Figure 6-14, bottom right). This suggests bed erosion, as the magnetite obviously percolated to the tungsten bed. Its presence there may or may not be permanent i.e. it could itself be eroded again if further material is fed to the Knelson. It certainly demonstrates the intimate interaction between magnetite particles and the concentrate bed, and even hints at a possible application for the Knelson, in its existing or a modified version, for the recovery of heavy minerals of density considerably less than that of gold.

Figure 6-15 shows two pieces of the concentrate obtained from the same material

FIGURE 6-13 A Bottom view of a Piece of the Concentrate with -425 μm Silica Gangue (Fluidization Water Flowrate: 2.6 L.min^{-1})

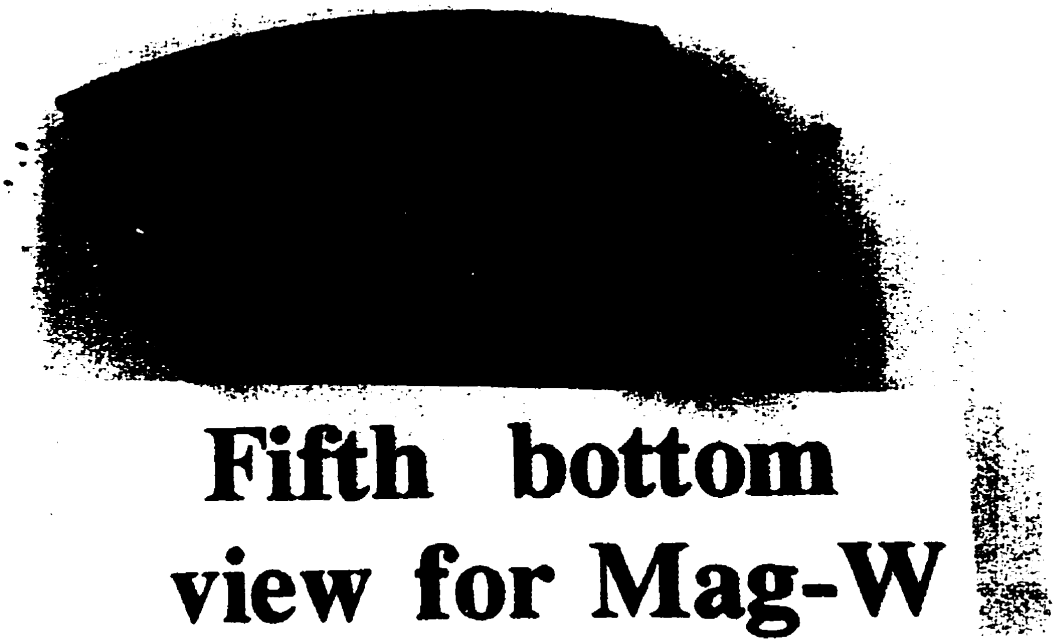

FIGURE 6-14 A Bottom View of a Piece of the Concentrate Obtained from -425 μm Magnetite Gangue

as that of Figure 6-13, but at a higher fluidization water flowrate. Although most of the tungsten reported to the inner section, part also penetrated deep into the ring, along the fluidization water channels. However, these channels were only observed when operating well above the optimum fluidization water flowrate for the conventional bowl design.

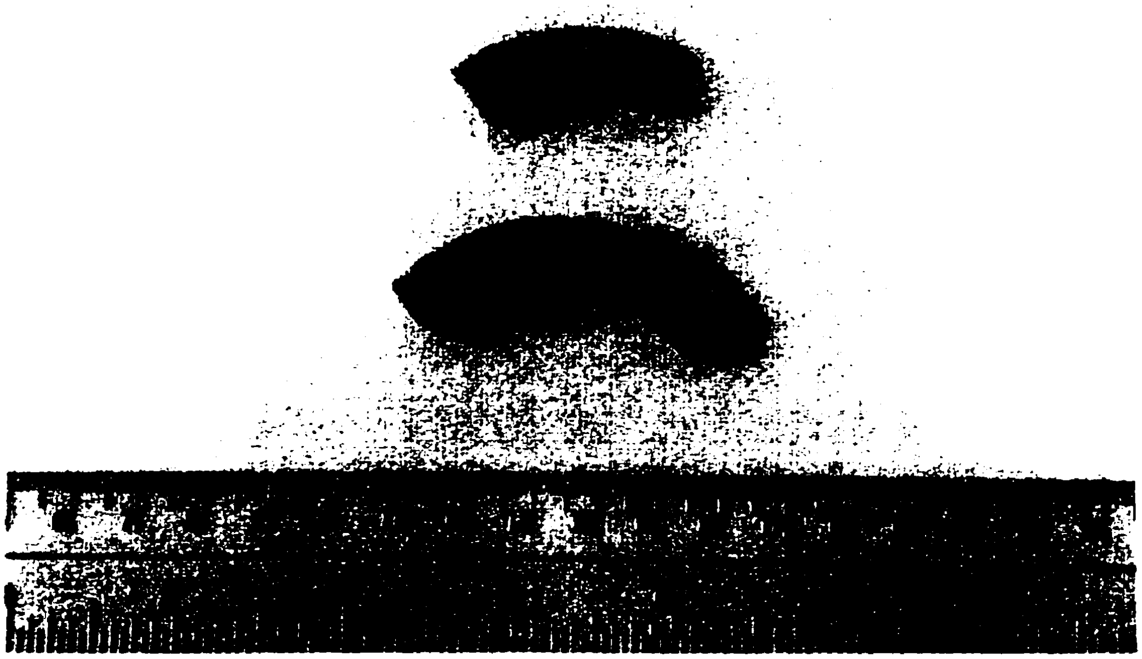

FIGURE 6-15 Two Pieces of the Concentrate with -425 μm Silica Gangue (Fluidization Water Flowrate: 4.9 L.min^{-1})

6.4 Discussion

6.4.1 Possible Separation Mechanisms of the Knelson Concentrator

The results of this and the previous chapter suggest the following sequence of events during the recovery cycle of the Knelson Concentrator.

6.4.1.1 At the Beginning of a Test, the Rings Are Completely Fluidized

At the beginning of the loading cycle, and up to a relatively small feed mass (100 to 200 g for the 7.5 cm unit, depending on gangue density), solid will gradually build up from the outer to the inner ring. Only fine light particles of very low terminal velocity are rejected by the fluidization water. Coarse particles report preferentially to the outer ring, because of their higher terminal velocity. This explains why the outer ring had a tungsten content well below that of the feed in tests 2 and 3 (similar results are also apparent in tests 1 and 4), of size distribution coarser than the feed (Figures 6-5 and 6-7).

6.4.1.2 As Soon as the Concentrate Bed Builds-up, It Is only Partially Fluidized

In this case, water can penetrate the void spaces between particles, and partially fluidizes the bed (predominantly along the paths of fluidization water streams). As a result, there is little or no mass transfer between the material subsequently recovered and the solids already in the outer ring, even fine dense particles, cannot penetrate the bed. Thus, the outer rings retain their coarse size and low grade of heavies.

6.4.1.3 The Selective Recovery Begins Once the Initial Concentrate Bed Formed

The main forces acting on a particle inside the Knelson Concentrator bowl are the centrifugal force and axial drag force, as shown in Figure 6-16. The terminal settling velocity of a particle is determined by its size and specific density when the rotation is kept constant. If the particles have the same size, the terminal settling velocity of a gold or tungsten particle is much higher than that of silica or magnetite (Chapter 4), and it should, therefore, be readily captured in the concentrate bed; if the size of silica particles is much larger than that of tungsten or gold, the terminal settling velocity of silica particles will be higher than that of tungsten and gold. However, the terminal settling velocity alone cannot explain why the riffles are not only occupied by coarse gangue particles, even though their terminal velocities are much higher that those of fine gold particles (or tungsten in this case). For instance, the terminal settling velocity of a 260 μm silica particle is greater than that of a 15 μm tungsten particle (Table 4-3), but the tungsten in this size range can still be recovered. Therefore, other concentration mechanisms must account for the selective recovery of the fine, high density particles.

Fifty-six years ago, Gaudin described consolidation trickling to explain the concentration process of jigging (Gaudin, 1939). The coarse particles are bridging against each other and incapable of movement, although the fine particles are still free to move. Aside from any velocity that may be imparted to these small particles by the moving fluid, they are bound to settle under the influence of gravity in the passages between the coarse particles. The phenomenon is most pictorially described as consolidation trickling. This may be regarded as representing a condition under which sedimentation of fine particles continues while coarse particles are "bound and gagged." Of course, the fine particles do not settle as rapidly during consolidation trickling as during suspension, but if consolidation trickling can be made to last long enough, the effect can be most important. Consolidation trickling seems to be a general phenomenon not limited to jigging.

Whereas consolidation trickling is normally associated with a short phase of the jigging cycle (just before full collapse of the bed), percolation can be sustained over long time periods if a bed of coarser particles can be dilated, in the Knelson case by the combined action of fluidizing water and a shear-induced dispersive force (i.e. the Bagnold effect, Bagnold, 1954; Holtham, 1992; Kelly and Spottiswood, 1982; Sun, 1982). Percolation is always related to powder material. It can be described as the drainage of one powder phase through another. Normally, a particle smaller than the principal bed material will be prevented from falling by the underlying particles. However, these underlying particles are shuffled with respect to each other due to the strain applied across the failure zone. Eventually, the movement of the large particles will yield a space where a smaller one may drop (Bridgwater et al, 1983).

In the Knelson Concentrator, under the influence of the centrifugal force, fine tungsten or gold particles move outward along the passages between coarse particles. These effects help heavy particles with further concentration in the concentrate bed.

In the separation zone, due to the accumulation of tungsten or gold particles, the density of the suspension will progressively be increasing, and a hollow truncated cone-like heavy suspension from the bottom to the top will progressively be formed. The specific density of this truncated cone could be high enough (e.g. if the volume fraction of tungsten reaches 9%, the density of the suspension will be 2.65) to reject most of the silica but not the magnetite. Hence, from the frozen concentrate, an almost pure tungsten layer can be seen on the surface of the concentrate for the process of silica-tungsten, whereas both tungsten and coarse magnetite can be observed for processing a magnetite-tungsten mixture. The proposed concentrating process in the Knelson Concentrator is illustrated in Figure 6-16.

6.4.2 Practical Implications

The findings of this and the previous chapter can be applied to the upgrading of primary gravity concentrates. The focus here will be on the production of a smeltable grade material from table tails.

Liberated gold present in table tails is found mostly in the fine size range. The presence of coarse dense particles (e.g. sulphides, mimicked here with magnetite) has been proven to be very deleterious to tungsten recovery. Since most of the gold that must be recovered is fine, a primary processing step should be screening to remove the coarse particles. Results of Chapter 5 suggest that a cut-size of 150-300 μm would be appropriate. Feeding the undersize would ensure that concentrate bed erosion problems are minimized. Results of this chapter not only confirm this finding, but explain why coarse dense gangue yields immediate erosion of the concentrate bed (i.e. overload):

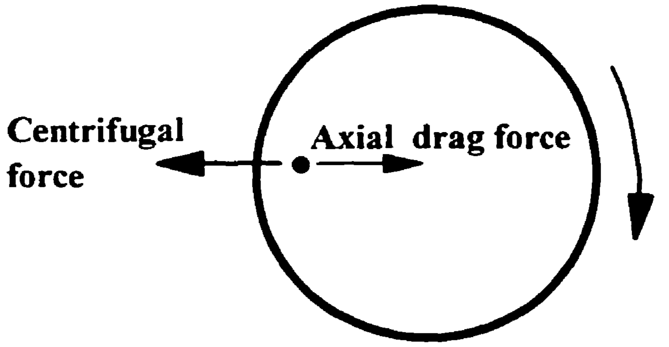

A. Forces acting on a particle

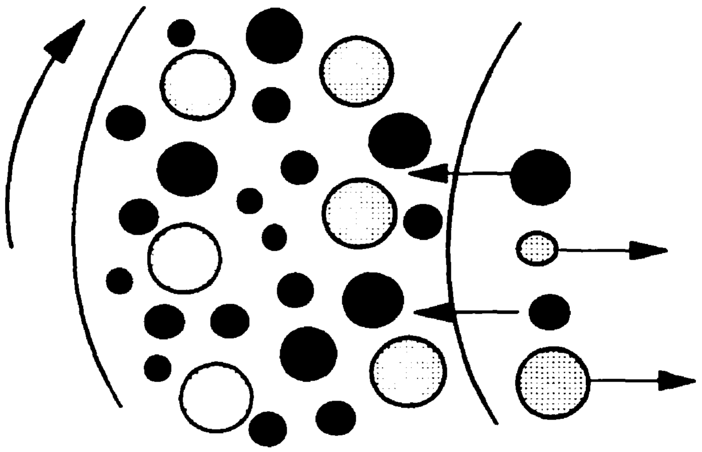

B. Heavy suspension effect

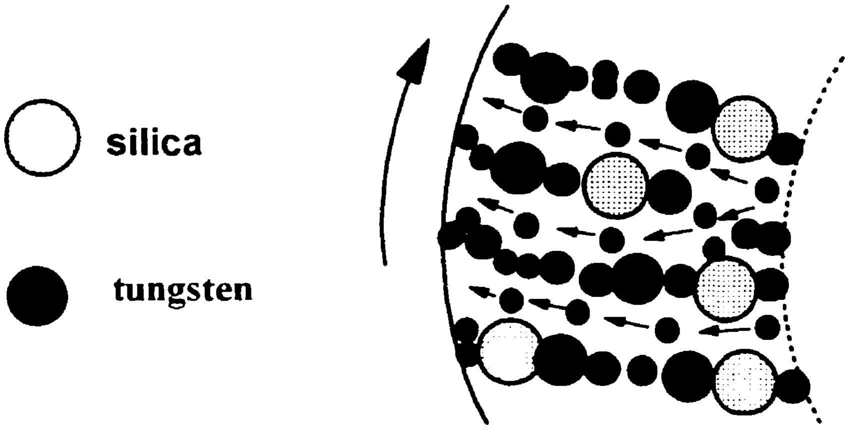

C. Percolation or consolidated trickling

FIGURE 6-16 Forces Acting on a Particle and the Possible Concentration Processes when fed a coarse dense gangue, the unfluidized ring volume extends past the locus of concentrate that is eroded by the flowing slurry. As a result, there is virtually no concentrate volume which is protected from erosion.

The above "size preparation" achieves improved recovery, but may still yield a low concentrate grade. This second problem can be minimized if one considers that most material recovered non-selectively is captured in the outer rings at the beginning of the recovery cycle. A material easily separated from the concentrate in the inner rings should therefore be pre-fed to the Knelson, to fill the outer rings, e.g. magnetite and calcite. At the end of the recovery cycle, the full concentrate could be processed (physically or chemically) and the inner ring high grade portion isolated. This approach is tested in chapters 7 and 8.

CHAPTER 7 KNELSON BOWLS WITH DIFFERENT CONFIGURATIONS

7.1 Objectives

The conventional Knelson Concentrator bowl with the standard design has proved very effective in recovering gold (Laplante, 1994; Hope et al, 1995; Poulter et al, 1995). However, the question arises as to whether the present bowl is the optimum, and which approaches may be explored to improve its design. With the help of Knelson Concentrators Inc., three modified bowls were tested, a cleaner bowl, a 'shaven' bowl, and a bowl with a different distribution of superficial fluidization water flowrate, designated bowl#1, bowl#2, and bowl#3, respectively. The primary objective of these tests was to determine the effect of various design parameters on performance.

7.2 Bowl#1

7.2.1 Features of the Bowl

Bowl#1 is a 7.5 cm diameter laboratory Knelson Concentrator bowl with the same geometrical dimensions as the conventional one used previously. The only difference is that about half of each riffle, 6 mm in depth, is filled with a porous nylon filter, as shown in Figure 7-1. The intention is to distribute the fluidization water more evenly in each ring. This design was expected to yield a second benefit. As the outer halves of the riffles are mainly occupied by the filter, the concentrate mass is lower than that obtained by a conventional bowl. As a result, higher grade concentrates should be obtained.

7.2.2 Methodology

Test feeds contained 950 g of coarse silica and 50 g of tungsten, which had the same size distributions as those used in Chapter 5. The feed rate was kept at 250 g.min^{-1} in all the tests. First, three tests were carried out at different fluidization water flowrates in order to determine its optimum range and yield data comparable to that of section 5.4.2. Concentrates were screened and tungsten recovered from each size class with the MLS.

In Chapter 6, most material recovered non-selectively was captured in the outer rings of the Knelson bowl at the beginning of the recovery cycle. This suggested a special test design, that is, a material which is easily separated from the bulk concentrate, would first be pre-fed to the Knelson to build up the concentrate bed. The normal test would then follow. At the end of the test, this material would be separated from the bulk concentrate to significantly upgrade the remainder. Test 4 followed this design: at the beginning of the test, 200 g magnetite was first pre-fed to the Knelson as a filler, followed by the normal feed. The test was carried out at a fluidization water flowrate of 3.2 L.min^{-1} (which yielded the highest recovery of the first three tests) and a feed rate of 250 g.min^{-1}. The size distribution of the magnetite is shown in Table 7-1. A distribution rather than monosized fraction was used, to produce fluidization water distribution patterns similar to those of typical concentrates. The top size, 425 μm, was chosen to eliminate concentrate trickling into the pressurized water jacket. The bottom size, 75 μm, is coarser than that of tungsten, to facilitate concentrate analysis. The concentrate obtained was dried, and the magnetite in the concentrate was removed with a hand magnet. The non-magnetic fraction was processed as for the other tests.

TABLE 7-1 Size Distribution of Magnetite as a Filler

Size (μm)	300-425	212-300	150-212	106-212	75-106	Total
Mass (g)	40	40	40	40	40	200
Mass (%)	20	20	20	20	20	100

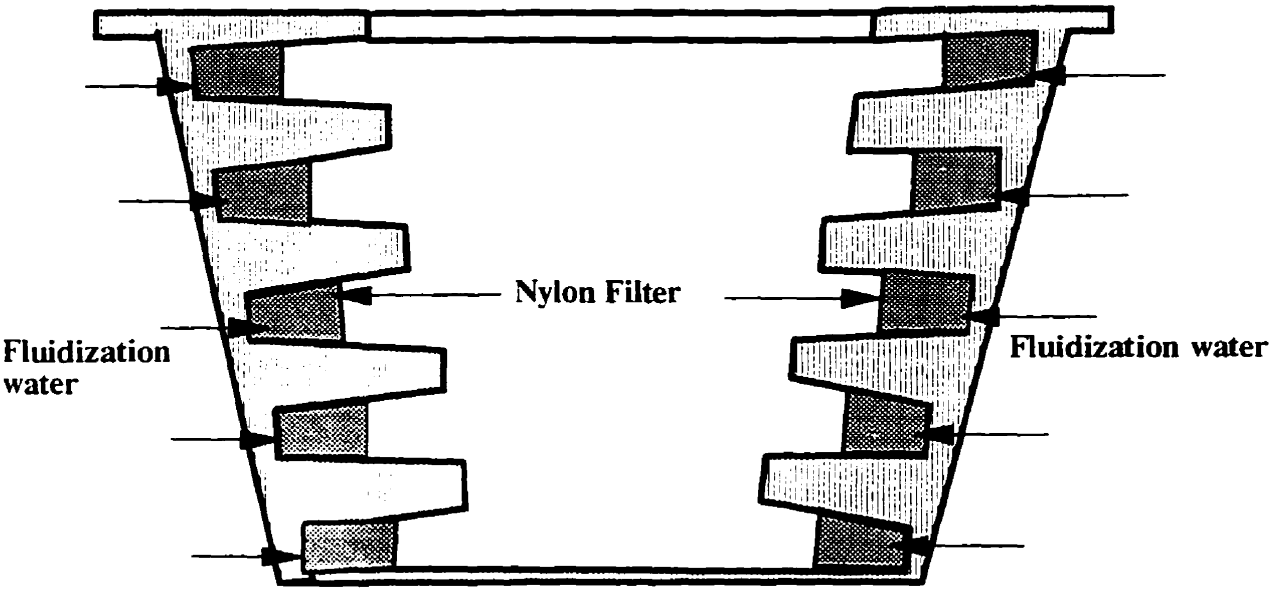

FIGURE 7-1 Schematic Diagram of Bowl#1

7.2.3 Test Results

The performance of bowl#1 at different fluidization water flowrates is compared to that of the conventional bowl in Table 7-2 and Figure 7-2. The optimum fluidization water flowrate for bowl#1 was still around 3.2 L.min^{-1}, as for the conventional bowl. The mass of concentrate dropped to 54-58% of that obtained with the conventional bowl. Bowl#1 clearly yielded a better performance--i.e. a much higher concentrate grade at a slightly higher recovery. The results of test four (with 200 g magnetite pre-fed) are plotted in Figure 7-3[1].

TABLE 7-2 Comparing Bowl#1 to the Conventional Bowl

Test No	Water (L.min^{-1})	Bowl #1			Conventional Bowl			Difference		
		Grade (%)	Mass (g)	Recovery (%)	Grade (%)	Mass (g)	Recovery (%)	Grade (%)	Mass (g)	Recovery (%)
Test 1	2.3	65.9	70.6	93.1	34.2	121.4	83.1	+32	-51	+10
Test 2	3.2	68.5	67.6	95.4	39.8	115.9	92.2	+29	-48	+3
Test 3	4.8	73.5	61.9	90.9	38.0	114.1	86.8	+36	-52	+4

7.2.4 Discussion

These results are consistent with the information generated in Chapter 6, where it was shown that the heavy phase, tungsten, was predominantly located in the inner ring sections. In the current tests, it is highly probable that the tungsten was also located mainly in the inner section of the concentrate (though the bowl could not be separated for observation). The increased recovery, which was not expected, suggests that the channelling of fluidization water could be detrimental to Knelson performance. This may assist in the design of future Knelson bowls.

The magnetite pre-feed increased concentrate grade significantly, from 68.5% to 91.1%, at the cost of a modest drop in recovery, from 95.4 to 89.7%. This increase was the result of a drop in concentrate mass of 18.4 g.

---

[1] The mass shown in this figure is the mass of the concentrate after magnetic separation. The mass of the bulk concentrate was 78.6 g, and 29.4 g of magnetite was removed.

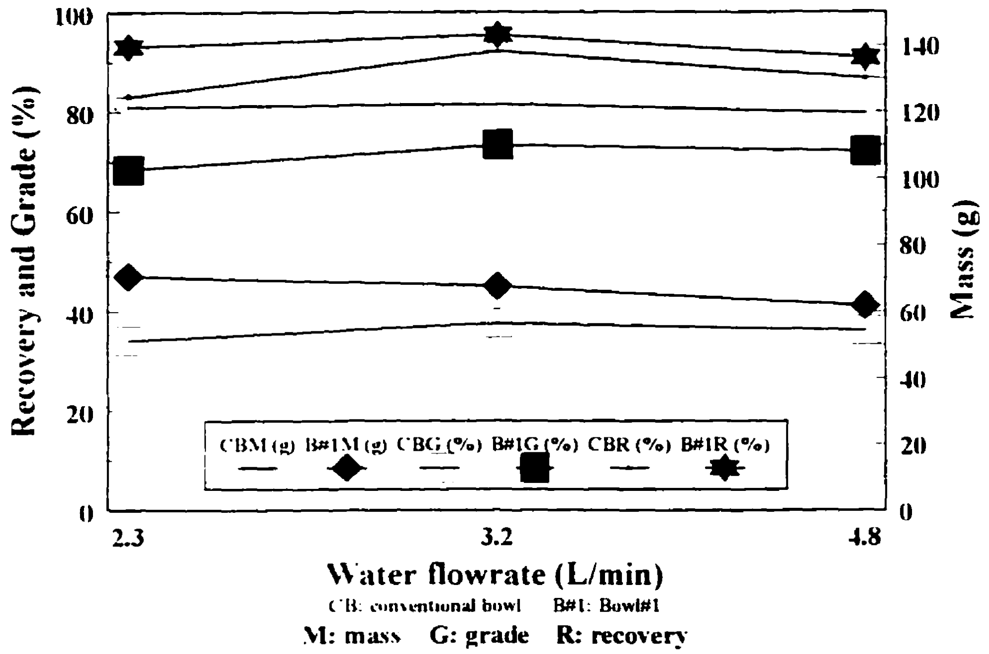

FIGURE 7-2 Concentrate Grade. Mass and Tungsten Recovery as a Function of Fluidization Water Flowrate for Bowl#1 and the Conventional Bowl (feed: 950 g silica; 50 g tungsten)

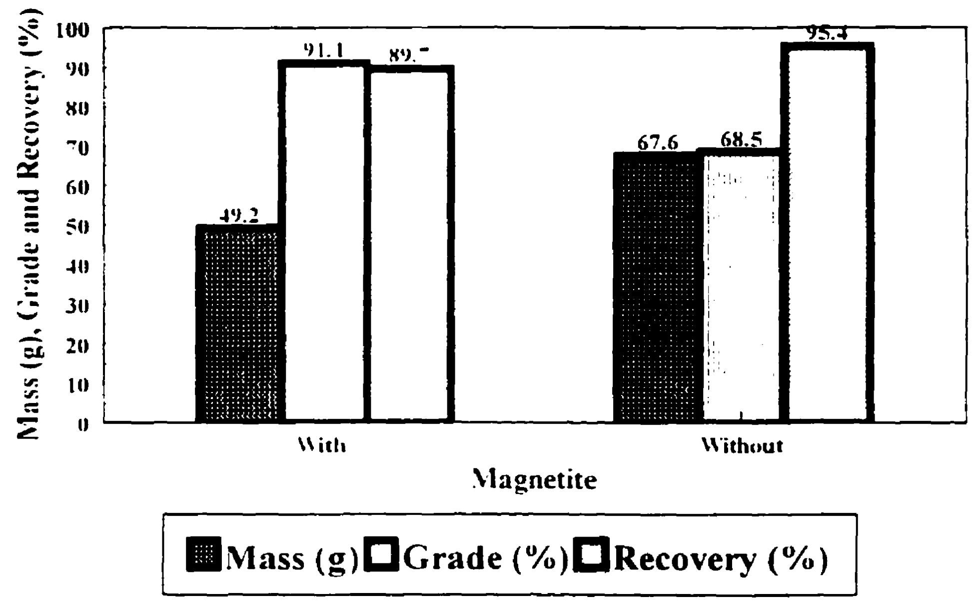

FIGURE 7-3 The Effect of Magnetite Pre-feed on Bowl#1 Performance

7.3 Bowl#2

7.3.1 Description of the Bowl

The results obtained above and in Chapter 6 have shown that during separation, heavy materials, such as gold and tungsten, will be predominantly located in the inner section of the riffles. This raised the question as to whether it was necessary to make the riffles as deep as in the conventional design. If the riffles are slightly shallowed by shaving their rims, what would be the resultant effect on performance? For this purpose, after some preliminary tests for a conventional bowl were done (presented in 7.3.2), 2 mm were shaven off the riffles from top to bottom. This bowl was identified as bowl#2.

7.3.2 Testwork

Before shaving the riffles, three tests using 950 g coarse silica and 50 g tungsten (the same size distributions as used for bowl#1) were carried out at a feed rate of 250 $g.min^{-1}$ and different fluidization water flowrates. The results show that the optimum fluidization water flowrate was still 3.2 $L.min^{-1}$, with a recovery of 98.7% and a grade of 36.1%. The average tungsten grade of the -75 μm fraction of the concentrate was as high as 91.2%, which would make it difficult to analyze size-by-size grade variation if grade was further increased with bowl#2. Therefore, a magnetite gangue of intermediate size distribution (-425 μm, as in section 6.2) was chosen as gangue for bowl#2 tests.

Two duplicate tests using 950 g of magnetite of intermediate size distribution and 50 g tungsten were carried out at a fluidization water flowrate of 4.4 $L.min^{-1}$ and a feed rate of 300 $g.min^{-1}$. After the ribs of the riffles of the bowl were shaven by 2 mm, another pair of duplicate tests were completed at the same operating conditions. Concentrates were screened and processed with the MLS, using the standard procedure.

7.3.3 Results and Discussion

The recoveries and grades for medium size magnetite-tungsten feeds before and after shaving 2 mm from the riffles are shown in Figure 7-4 (the average of two tests in both cases). Concentrate grade was increased by about 2%, but recovery decreased by about 8%. The results imply that even though heavy particles do not penetrate very deeply into the riffles during the separation, the space in the riffles is still necessary for fluidization water distribution.

It is not certain that bowl#2 is worse than the conventional one, as the shallower riffles may require a different (probably lower) optimal fluidization water flowrate. Although additional tests are needed to prove this point, this bowl definitely shows less potential than bowl#1.

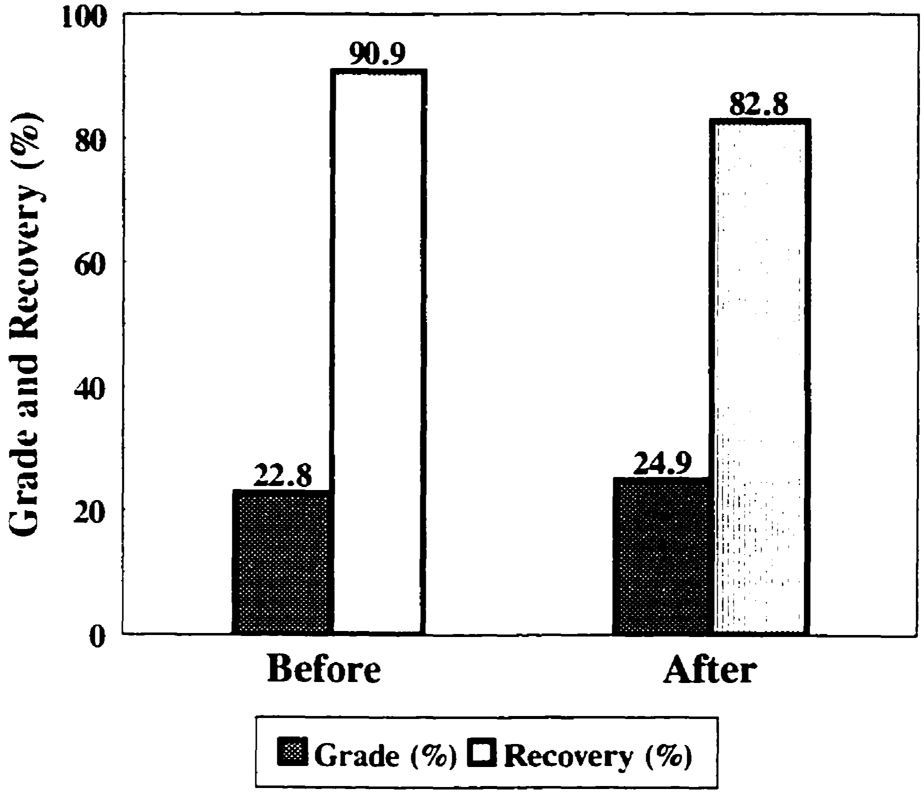

FIGURE 7-4 Knelson Performance before and after Shaving 2 mm of the Riffle Ribs

7.4 Bowl#3

7.4.1 Description of the Bowl

The bowl is identical to the conventional one except for its distribution of fluidization water flow. The difference was obtained by varying the number of holes in each ring (the total number was not changed) as shown in Table 7-3. The objective of the tests was to see if this could affect Knelson Concentrator performance, especially concentrate overload. The modification was in part prompted by an observation of B. Knelson that fluidization flowrate in the lower rings of the new 48" (122 cm) Knelson Concentrator was too low (Knelson, 1966).

TABLE 7-3 Hole Distribution for Both the Conventional Bowl and Bowl#3

Ring No.	Conventional Bowl		Bowl#3	
	Number of Hole	Distribution (%)	Number of Hole	Distribution (%)
5	42	28	34	22.7
4	36	24	32	21.3
3	30	20	20	20.0
2	24	16	29	18.7
1	18	12	26	17.3
Total	150	100	150	100.0

7.4.2 Testwork

Test 1

A mixture of 3800 g coarse silica and 200 g tungsten was fed to the Knelson at a fluidization water flowrate of 3.2 L.min^{-1} and a feed rate of 250 g.min^{-1}. Ten tail samples were collected and analyzed with the MLS to measure the progression of overloading. The methodology was similar to that of Chapter 5.

Test 2

A mixture of 3800 g coarse magnetite and 200 g tungsten was fed to the Knelson at a fluidization water flowrate of 5.3 L.min^{-1} and a feed rate of 300 g.min^{-1}. Ten tail samples were collected and analyzed.

Test 3

The bowl was split into two halves. A mixture of 1900 g of -425 μm silica (intermediate particle size) and 100 g of tungsten was fed to the Knelson at a fluidization water flowrate of 2.9 L.min^{-1} and a feed rate of 250 g.min^{-1}. The concentrate was then partially dewatered and frozen in a freezer. The methodology was similar to that described in Chapter 6.

7.4.3 Results and Discussion

Figure 7-5 shows that with coarse silica gangue, both grade and recovery were very high, 74.5% and 99.1%, respectively. These values are close to those obtained with the conventional bowl for fine silica, 75.8% and 99.4%, no overload was observed. These results are clearly better than those obtained with the conventional bowl for coarse silica (grade: 62.5%; recovery: 76.8%).

For coarse magnetite, Figure 7-6 shows a situation which was quite different from that of silica. Both grade and recovery were very close to those obtained with the conventional bowl for coarse magnetite. In this test, severe overload occurred, as with the conventional bowl, which can be rationalized as follows. The coarse magnetite gangue is such an aggressive gangue (with respect to bed erosion) that the modified bowl performs as poorly as the conventional one, as the increased fluidization of the first ring blows the fine tungsten out. Silica is a relatively benign gangue, which requires lower fluidization water flowrate, at which fine tungsten can still be recovered effectively. The optimum bowl configuration, therefore, is likely to be application specific.

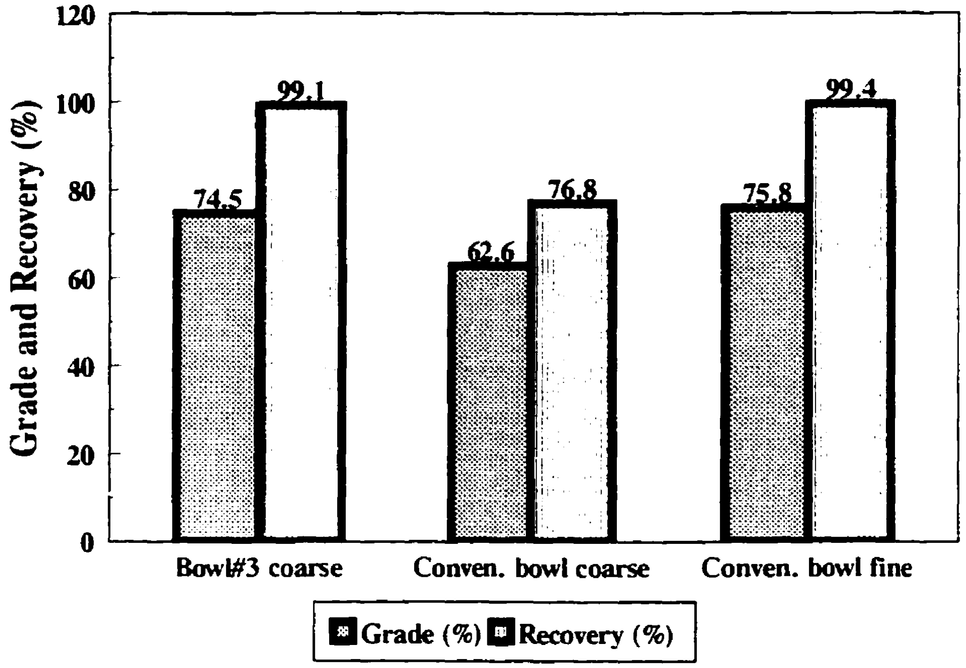

FIGURE 7-5 Overload of Bowl#3 Compared to the Conventional Bowl (Test 1)

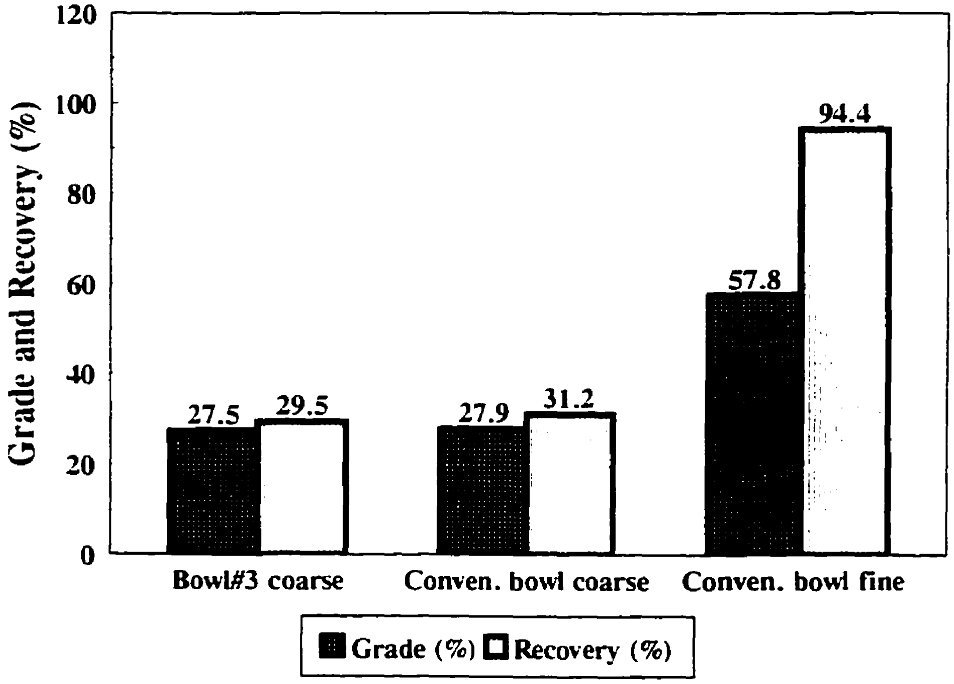

FIGURE 7-6 Overload of Bowl#3 Compared to the Conventional Bowl (Test 2)

Cumulative losses as a function of the mass of feed are shown in Figure 7-7, for the coarse silica and magnetite, with the conventional bowl and bowl#3. For coarse silica with bowl#3, no overload occurred, while with the conventional bowl it started half way through the test. For coarse magnetite, the increments of tail grade were approximately at the same level for both bowls, and overload was severe.

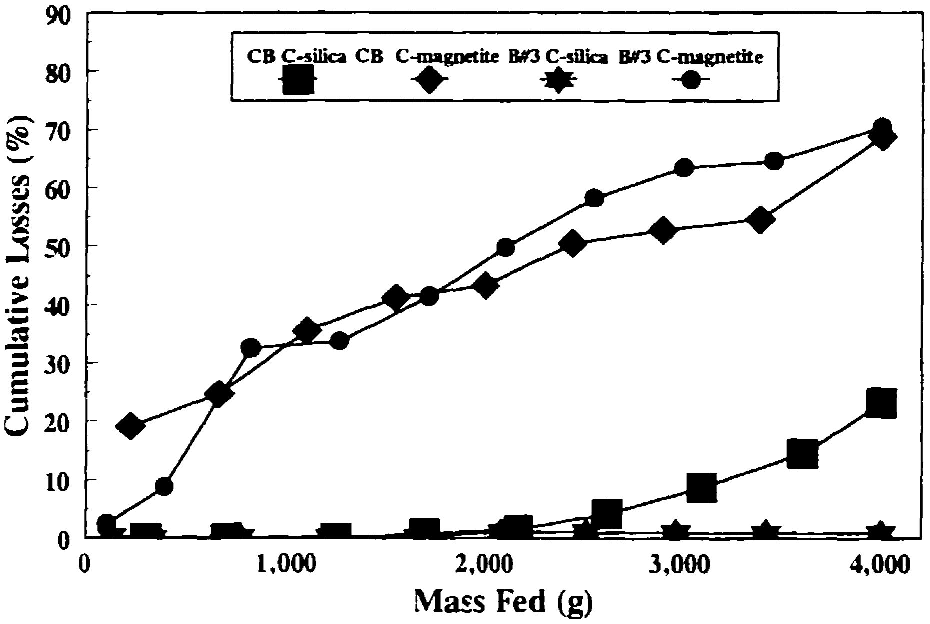

CB: Conventional bowl C: Coarse B#3: bowl#3

FIGURE 7-7 Overload Tests of Bowl#3 Compared to Conventional Bowl

Table 7-4 shows size distributions of the concentrates of tests 1 and 2, with the two types of gangue, coarse silica and magnetite. For the magnetite gangue, coarser particles percolated into concentrate bed easily. This is confirmed by the coarse size distribution of the concentrate, 37% +300 μm, compared to 11% for the silica gangue which eroded smaller tungsten particles from the concentrate bed and rejected them to the tails. For the silica gangue, the coarsest particles could not penetrate the bed as easily, and produced much less bed erosion. The high tungsten recovery, in fact, cannot be maintained indefinitely, as it eventually results in bed build-up into the flowing slurry and the onset of bed erosion. However, for test 1, this clearly did not take place.

Figure 7-8 shows the two halves of bowl#3 with the concentrate for test 3. The appearance is similar to that obtained with the conventional bowl (Figure 6-11), in which a layer of tungsten covered the surface of the rings and riffles on the inner side. Closer examination of the different rings, however, reveals that the lower rings contained more tungsten than the upper rings; the fifth ring contained the least.

TABLE 7-4 Concentrate Size Distributions of Silica and Magnetite Gangue

Size (μm)	Coarse Silica	Coarse Magnetite
+850	2.9	9.8
600-850	2.5	9.2
425-600	2.2	7.6
300-425	3.0	10.4
212-300	2.4	9.0
150-212	4.0	9.9
105-150	2.9	7.2
75-106	2.6	5.2
53-75	17.1	9.5
38-53	30.7	12.4
25-38	24.4	8.0
-25	5.3	1.7
Total	100.0	100.0

Figures 7-9 and 7-10 detail these differences. Figure 7-9 shows that in the first ring (bottom ring) tungsten almost completely occupied the whole space, with very little silica in the outer section. This explains the high grade of this ring, 74.3% tungsten. The whole ring was completely fluidized during separation, so that the tungsten could penetrate almost everywhere. Figure 7-10 shows that, in the fourth ring, the tungsten was located mainly in the inner section, with some tungsten scattered along the fluidization water paths, which means that there was better fluidization than for the conventional bowl.

The above results indicate that in bowl#3 tungsten was preferentially recovered in the lower rings, in a higher active volume (virtually the full ring). The losses of tungsten to the tails were reduced because there was no, or only slight, overload in the upper rings.

The grade and tungsten distributions in the various concentrate rings of test 3 are shown in Figure 7-11. They are significantly different from those of the conventional bowl. For bowl#3, the grade and distribution decreased with increasing ring number. Both the highest grade and tungsten distribution were in ring 1, 74.2% and 29.4%.

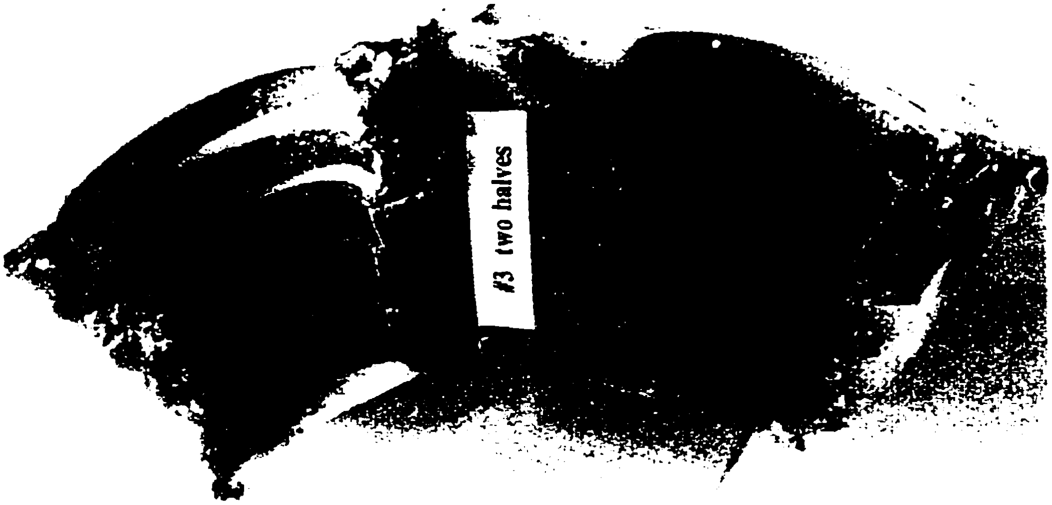

FIGURE 7-8 Two Halves of Bowl#3 with the Concentrate (Test 3)

FIGURE 7-9 A Piece of the Concentrate in First Ring with Bowl#3 (Test 3)

FIGURE 7-10 A Piece of the Concentrate in Fourth Ring with Bowl#3 (Test 3)

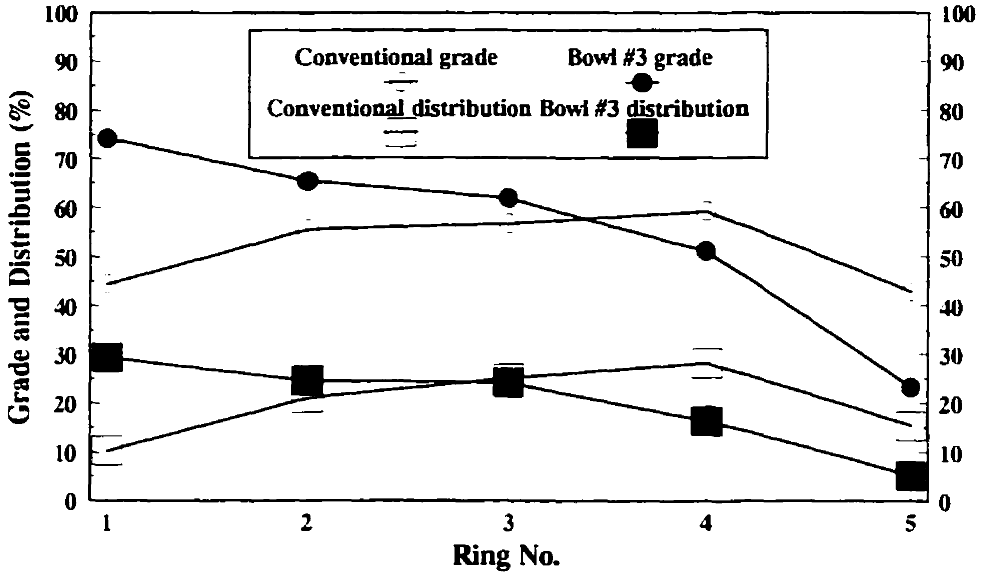

FIGURE 7-11 Grade and Tungsten Distribution in the Various Rings (Feed: 1900 g of -425 μm silica and 100 g tungsten)

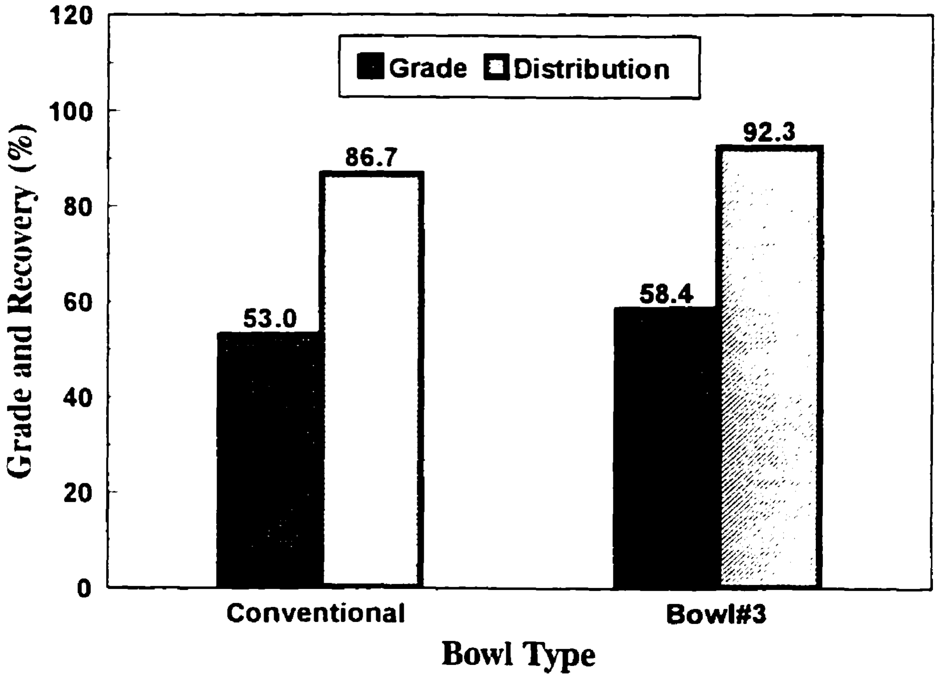

FIGURE 7-12 Grade and Recovery of Bowl#3 and the Conventional Bowl (Feed: 1900 g of -425 μm silica and 100 g tungsten)

respectively, even though the ring possessed the smallest volume, 13.5%. For the conventional bowl, the grade and distribution increased as the ring number increased until ring 4. Both the highest grade and distribution were in ring 4, 59.2% and 28.3%, respectively. For both bowls, the grade and tungsten distribution of ring 3 were very similar, which is in agreement with their fluidization water hole distribution (Table 7-3), one fifth of the total. The total tungsten distribution in rings 4 and 5 for the conventional bowl was 44%, while it was only 22% for bowl#3.

For the separable bowl tests, the mass of the concentrates for the conventional bowl and bowl#3 were 164 g and 158 g, respectively. However, more tungsten was recovered by bowl#3, and both higher grade and recovery were achieved, which can be seen from Figure 7-12. The grade and recovery were 5.4% and 5.7% higher, respectively.

7.4.4 Superficial Fluidization Water Velocity

Superficial fluidization water velocity, a concept used frequently in column flotation (Finch and Dobby, 1990) is now introduced. It is defined as the volumetric flowrate of water divided by the cross section area of a ring[2], that is:

$$J_w = \frac{Q_w}{A_r} \qquad \text{7-1}$$

where,

J_w: superficial fluidization water velocity, cm.s^{-1}

Q_w: volumetric flowrate of fluidization water, cm^{3}s^{-1}

A_r: section area of a ring or a series rings, cm^2

For the Knelson Concentrator at constant fluidization water flowrate, the

---

[2] For column flotation, the cross-section of the column is used.

superficial velocity of specific rings will be different if the same total number of holes is distributed differently. To simplify, it is assumed here that each hole has an identical diameter and water flows irrespective of its location[3]. The distribution of holes and corresponding superficial velocity of fluidization water for both the conventional bowl and bowl#3 are shown in Figure 7-13. Compared to the conventional bowl, the lower rings of bowl#3 contain more holes, the upper rings fewer. Although the total volumetric water flowrate is the same for both bowls, superficial velocity increases with ring number for the conventional bowl, whereas it decreases for bowl#3.

This last series of tests indicates that distribution of superficial fluidization water velocity can have a significant influence on the metallurgical performance of the Knelson Concentrator. The improvement of superficial velocity distribution in bowl#3 maximized the capture of tungsten in the lower rings. Therefore, even though there was overload in the lower rings, there remained the possibility of the tungsten being recovered in the upper ones, where overload did not occur, or only occurred slightly. As a result, both higher grade and recovery were achieved.

The two bowls (the conventional bowl and bowl#3) yielded a dramatically different profile of superficial velocity vs. ring number. In Chapter 5, it was determined that the optimum flowrate (hence superficial velocity) decreased with decreasing tungsten particle size. Hence, if the upper rings are aimed at scavenging, fine tungsten (i.e. gold in a normal application), using a profile of decreasing velocity with increasing ring number is the appropriate strategy. This needs to be confirmed by further testing.

---

[3] In fact, the centrifugal force increases with increasing ring diameter from bottom to top, and therefore, the resistance to the fluidization water would increase. Additionally, there is also a difference in the hydrostatic pressure between rings. Both would slightly reduce the water flow per hole from rings 1 to 5.

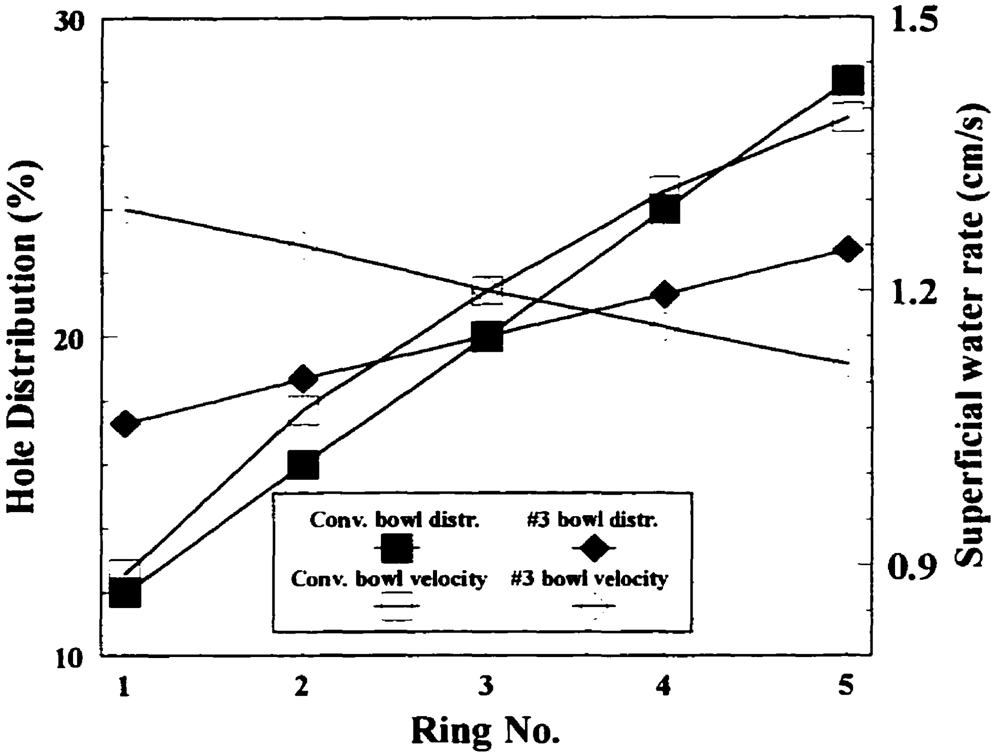

FIGURE 7-13 Fluidization Water Hole Distribution and Superficial Velocity for the Conventional Bowl and Bowl#3 (Total flowrate: 2.8 L.min^{-1})

7.5 Conclusions

Of the three bowls tested, two showed significant improvements over the conventional bowl (for some or all of the feeds tested). It is interesting to note that in all three cases (even for bowl#2), the difference in response was linked in part to the distribution of fluidization water. What was clearly revealed was the importance of its appropriate distribution, be it between the various rings or even within each ring.

Thus, bowl#1 could yield a superior recovery, presumably because the nylon filter distributed fluidization water more effectively. The poor recovery with bowl#2 could be the result of precisely the opposite effect. Bowl#3 can be advantageous because it uses more fluidization water in the first ring where the faster percolating coarser tungsten (or gold) is preferentially recovered, and less in the upper rings where finer tungsten recovery should be favoured.

CHAPTER 8 UPGRADING OF GOLD TABLE TAILS

8.1 Introduction

Since shaking tables operates at only one 'g', their use as cleaners for concentrates of the Knelson Concentrator not surprisingly yields significant losses. This suggests that table tails should be recycled to the primary Knelson Concentrator, but this may just lead to the building of a circulating load of fine gold, as gold scavenged with the Knelson Concentrator could well be lost again on the table. Scavenging with a small-scale Knelson Concentrator (7.5 cm or 3") is the preferred route and ideally should yield a concentrate of smeltable grade.

For the purposes of determining how much gold can be recovered from table tails using a Knelson Concentrator, and assessing if high grade concentrates can be obtained at acceptable recovery, five gold table tail samples from different Canadian gold mills that funded the present work were systematically tested; two additional samples (Aurbel, MSV) were also tested, albeit to limited extent, to broaden the data base (Table 8-1).

As shown in Table 8-1, for nearly all the table tails whose feeds were concentrates of Knelson Concentrators, the gold contents were in the range of 1000 g - 3500 $g.t^{-1}$. Two table tails, Resources MSV Inc. and Snip Operations, had lower gold grades; at Snip, this was because the table feed was a low grade jig concentrate.

TABLE 8-1 A Summary of Gold Table Tails Processed

Name of Mine	Grade ($g.t^{-1}$)	Table feed produced by	Location
Lucien Béliveau	1070	Knelson	Val d'Or, Québec
Meston Resources	3350	Knelson	Chibougamau, Québec
Hemlo Golden Giant Mine	2730	Knelson	Marathon, Ontario
Snip Operations	150	Jig	British Columbia
Les Mines Casa Berardi	1220	Knelson	La Sarre, Québec
Les Resources Aurbel Inc.	1650	Knelson	Val d'Or, Québec
Resources MSV Inc.	80	Knelson	Chibougamau, Québec

The results of chapters 5 - 7 with synthetic feeds suggest that simple processing with a Knelson Concentrator, even at optimum fluidization water flowrate, is not the only approach possible. Increased recovery can be achieved by either diluting a high density (typically sulphides) with a low density material (silica sand), or by removing the coarser feed to reduce gangue particle size. Both are particularly appropriate for table tails, which have a high density, and whose free gold content lies largely in the fine size classes. The dilution approach would be impractical in a plant, and is designed more specifically to achieve an optimum measure of the gravity recoverable gold content at the laboratory scale. Removing the coarse fraction, on the other hand, is perfectly feasible at plant scale, as a small, inexpensive screen could easily provide the required capacity.

Chapter 6 provides an approach to maximize concentrate grade. Since the outer section of each riffle is occupied mainly by the gangue minerals, its content dilutes the concentrate. Pre-feeding a material which can be separated magnetically from the active concentrate zone at the end of the test is the proposed approach. Therefore, direct processing of table tails, as well as of the three alternative routes, was tested on the various table tails samples shown in Table 8-1.

8.2 Lucien Béliveau

8.2.1 Description of the Mill

The Lucien Béliveau mill was part of Cambior's Val d'Or division, located 25 km east of Val d'Or, Québec. Ore was treated from Béliveau & Chimo at a rate of 1100 $t.d^{-1}$ for the former and 700 $t.d^{-1}$ for the latter (Bissonnette and Ladouceur, 1991). The mill produced doré bar from the gravity circuit, and a flotation concentrate shipped to the Yvan Vézina mill for cyanidation. Now the Lucien Béliveau ore body was mined out, the mill was shut down, dismantled, and moved to the Chimo mine site. The grinding-gravity circuit of the mill is illustrated in Figure 8-1.

The SAG mill, 6 metres in diameter and 3 metres in length, was operated in closed circuit with two 52 cm primary cyclones. One cyclone underflow (CUF) flowed to a ball mill (BM), and the second returned to the SAG mill. The overflow of both cyclones was fed to the flotation circuit. The ball mill discharge was fed to a flash flotation cell, whose concentrate, at the time of sampling, was processed with a 76 cm Knelson Concentrator. The Knelson concentrate was pumped to a bin then fed to a Deister table whose concentrate was smelted. The middling of the table was recycled and its tails returned to the grinding circuit. The Knelson Concentrator tails were dewatered by cycloning, and added to a thickener prior to filtration. Both secondary cyclone and thickener overflows were recycled to the SAG mill as process water.

8.2.2 Ore Characteristics

Béliveau Ore

Quartz and tourmaline veins with inclusions of pyrite and native gold make up the Béliveau gold deposit. The mean grade of the ore was about 2.25 $g.t^{-1}$ Au. Microscopic examination revealed that 70% of the gold was greater than 100 μm, 20% finer than 100 μm but could be liberated, and the remaining 10% was associated with pyrite. The content of pyrite was 1-2%. Optimum gold liberation was obtained at the fineness of 70% passing 75 μm (Bissonnette and Ladouceur, 1991).

Chimo Ore

The mean grade was about 4.5 g.t^{-1} Au; 48% of the gold is greater than 100 μm, 37% finer than 100 μm, and the remaining 19% finely associated with arsenopyrite. The contents of pyrite and arsenopyrite were about 1% to 2%, respectively. The graphite content is 1-2%. The optimum liberation of gold is 75% passing 75 μm.

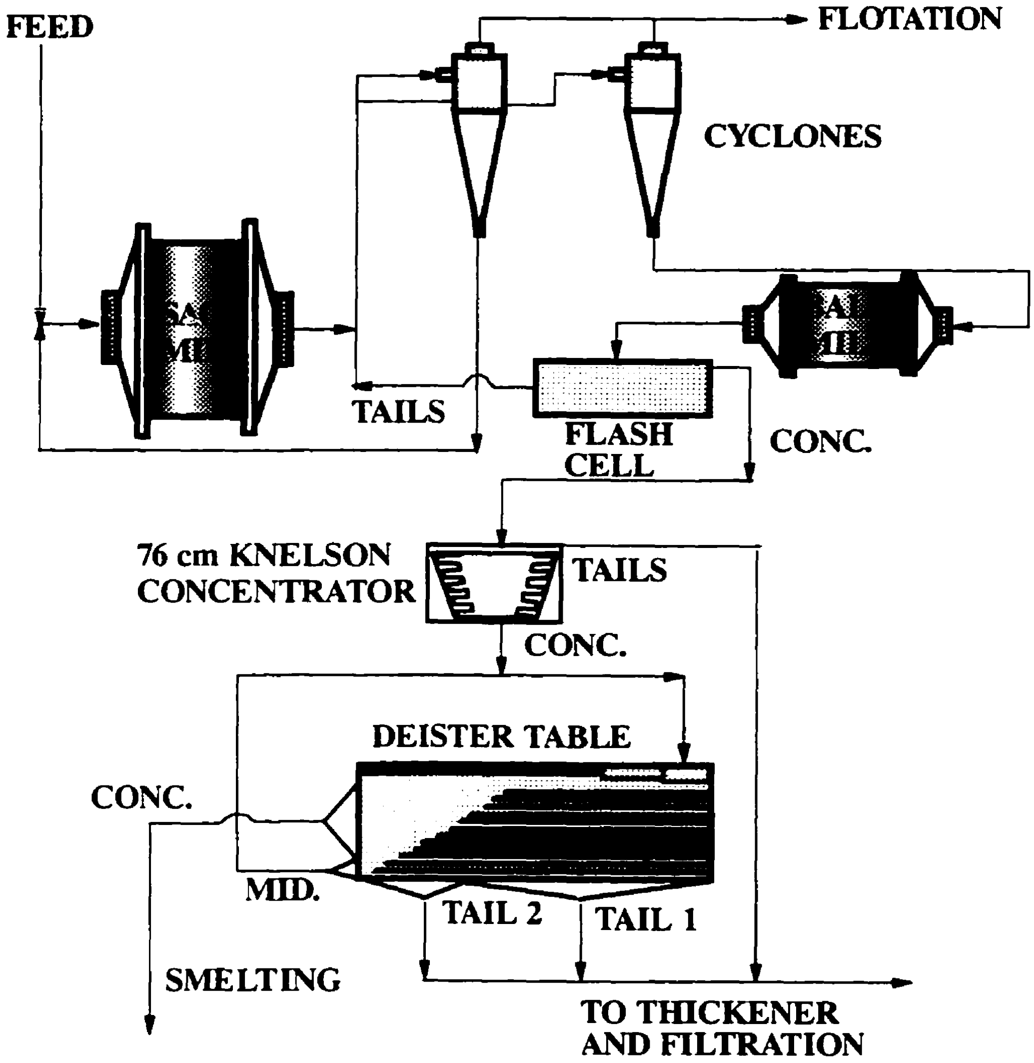

FIGURE 8-1 Grinding-gravity Circuits of the Lucien Béliveau Mill (as of 1992)

8.2.3 Laboratory Testwork

Sample Description

Table tails 1 and 2 were sampled separately on March 2, 1992, from two flows of table tails in the mill, as shown in Figure 8-1. The sampling time for each was measured (the weight split vs. total tails was 50.4% : 49.6%). Total tails were obtained by combining tails 1 and 2 according to the measured weight split.

The Knelson Concentrator and Falcon Concentrator Tests

Tests 1 and 2: The first two tests, with the Knelson Concentrator, were aimed at determining the amount and distribution of gravity recoverable gold which was lost by the shaking table in the two tail samples. For this purpose, the samples were diluted with 212 μm (70 mesh) silica (4:1) in order to maximize gold recovery. The rationale for this dilution was to bring the gangue density from about 5 g.cm^{-3} for the table tails down to 3 g.cm^{-3}, where gold recovery would be maximum for the Knelson Concentrator (Laplante et al, 1995).

Test 3: This test was performed with the total tails (appropriate weight split of tails 1 and 2), without dilution, to provide comparative results for both tests 1 and 2 (with silica dilution) and test 4 (total tails with the Falcon Concentrator).

Test 4: This test was performed with the total tails, without silica dilution, with a B6 Falcon Concentrator. The objective was to compare the performance of the Knelson Concentrator with that of another centrifugal concentrator specially designed for gold recovery.

Test Procedure

Knelson Concentrator Tests

The samples were split by either a Jones Riffles or a rotating splitter. The representative sample was fed to a Φ 7.5 cm laboratory Knelson Concentrator at a feed rate about 300 g.min^{-1} and a fluidization water pressure of 27 kPa (4 psi). For each test, a representative sample of the tails was cut and the full concentrate was recovered.

The Knelson Concentrator tail sample was first wet-screened at 25 μm and then dry screened on a Rotap for 20 minutes. The +106 μm fractions were pulverised in a Siebtechnic pulveriser.

The total concentrate of the Knelson Concentrator was only dry screened since it was virtually slime-free. All size fractions were submitted to the Lucien Béliveau mill for fire-assaying.

Falcon Concentrator Test

The Falcon Concentrator Model B6 can be used with one of three bowls with angles of 8°, 10°, and 14°, as shown in Figure 8-2. It has a rotation speed of 1950 rpm, yielding a centrifugal intensity of 340 'g'. The feed is introduced near the base of the bowl via a downcomer where it impacts on a rubber impeller rotating with the bowl.

The centrifugal force generated by the rotation of the bowl forces the material to settle out to the wall of the bowl. The light material flows upwards and out of the bowl into a collection launder to be tails. The heavy material remains in the bowl and is eventually removed by the flushing water once an operating cycle is complete (Buonvino, 1993).

For this test, a 14° bowl was used. The material was fed to the Falcon at a pulp density of 8% solids for the rougher and 5% for the cleaner stages and at a flowrate of 28 L.min^{-1} for the rougher and 19 L.min^{-1} for the cleaner stages. The rougher concentrate was subjected to two cleaning stages. Eventually, a concentrate, tail A (the tail of the second cleaner), tail B (the tail of the first cleaner), and tail C (the rougher tail) were obtained. The concentrate and three tails were processed in a manner similar to that for the Knelson Concentrator samples.

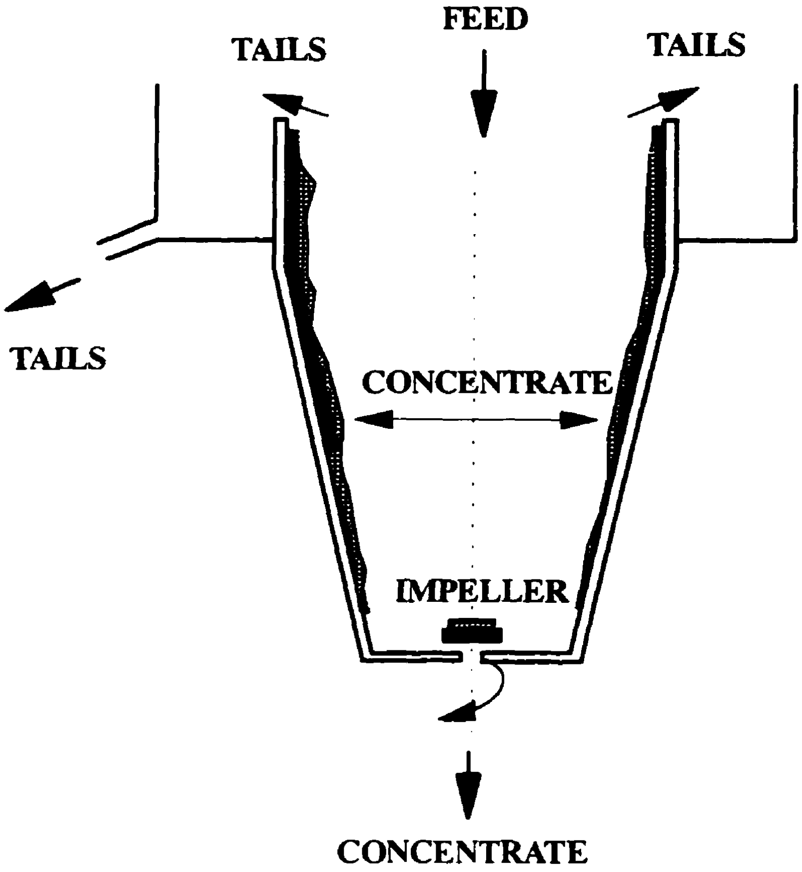

FIGURE 8-2 Schematic Diagram of a B6 Falcon Concentrator

8.2.4 Test Results

A summary of the test results is shown in Table 8-2. Detailed results are shown in Appendix 8-1. Gold recovery and grade as a function of particle size for tests 1 to 4 are given in Figures 8-3 to 8-6, respectively.

8.2.5 Discussion

Gold Distribution in the Table Tails

For tail 1 diluted with silica, the gold content of the -25 μm fraction was 11,307 g.t^{-1} (Appendix 8-1), which is 62 times higher than the overall grade; even though this fraction was only 0.9% of the total mass, it contained 56.9% of the total gold. The -37 μm fraction contained 75% of the total gold in only 3.2% of the total weight. This implies that much of the fine gold recovered by the 76 cm Knelson Concentrator was lost again during the table treatment.

TABLE 8-2 A Summary of the Test Results for L. Béliveau Table Tails

Product	Mass (%)	Gold (g.t^{-1})	Recovery (%)
Test 1 Knelson test for table tails 1 diluted with 70 mesh silica (4:1)			
Concentrate	2.10	7183	82.62
Tail	97.90	32	17.38
Total	100.00	182	100.00
Test 2 Knelson test for table tails 2 diluted with 70 mesh silica (4:1)			
Concentrate	1.96	12916	81.09
Tail	98.04	60	18.91
Total	100.00	312	100.00
Test 3 Knelson test for the total table tails			
Concentrate	7.09	12335	81.53
Tails	92.91	213	18.47
Total	100.00	1073	100.00
Test 4 Falcon test for the total table tails			
Concentrate	9.20	4153	33.42
Tails-A	4.24	688	2.55
Tails-B	2.64	636	1.47
Tails-C	83.92	852	62.56
Total	100.00	1143	100.00

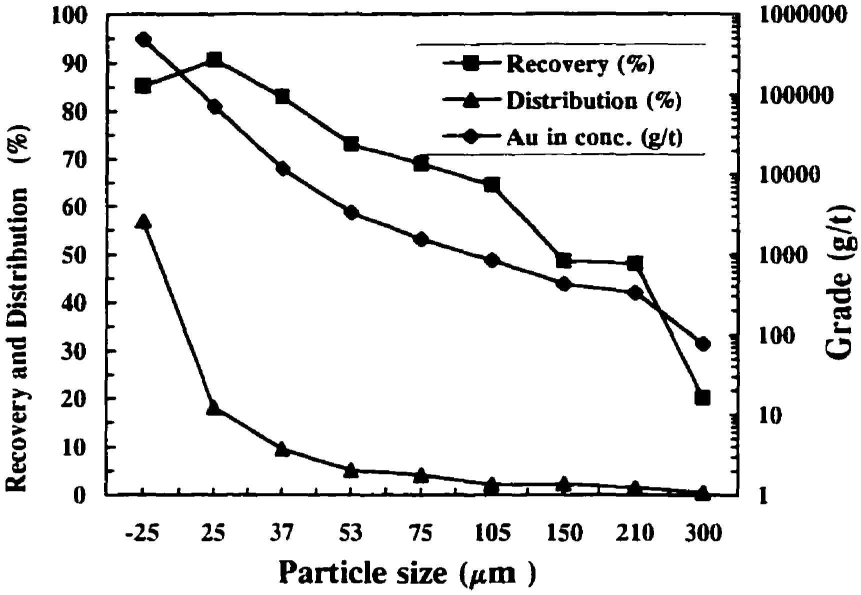

FIGURE 8-3 Results of the Knelson Concentrator - Feed: Lucien Béliveau Table Tail 1 Diluted with Silica (4:1)

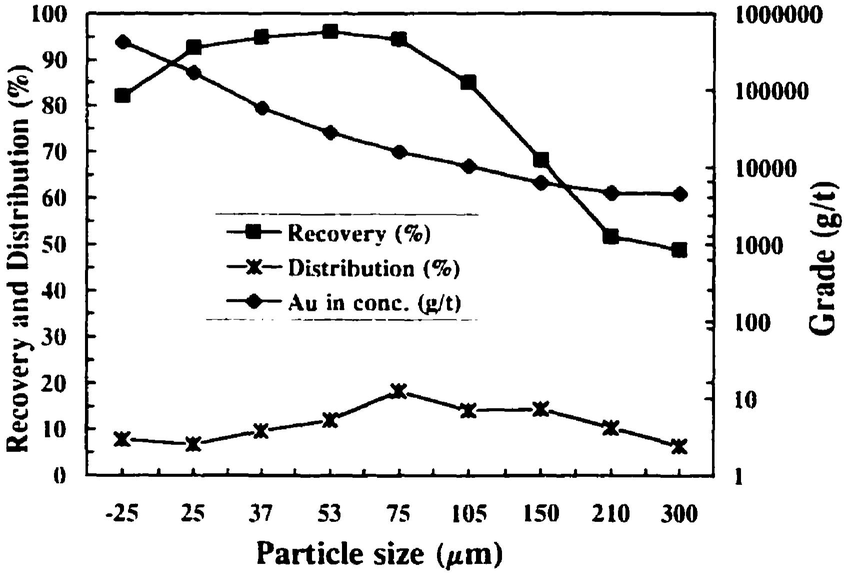

FIGURE 8-4 Results of the Knelson Concentrator - Feed: Lucien Béliveau Table Tail 2 Diluted with Silica (4:1)

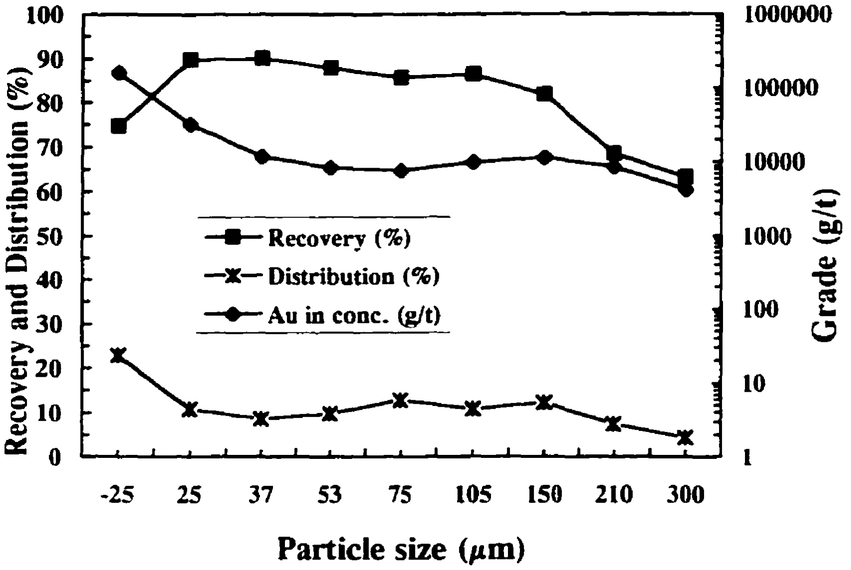

FIGURE 8-5 Results of the Knelson Concentrator - Feed: Lucien Béliveau Total Table Tails (undiluted)

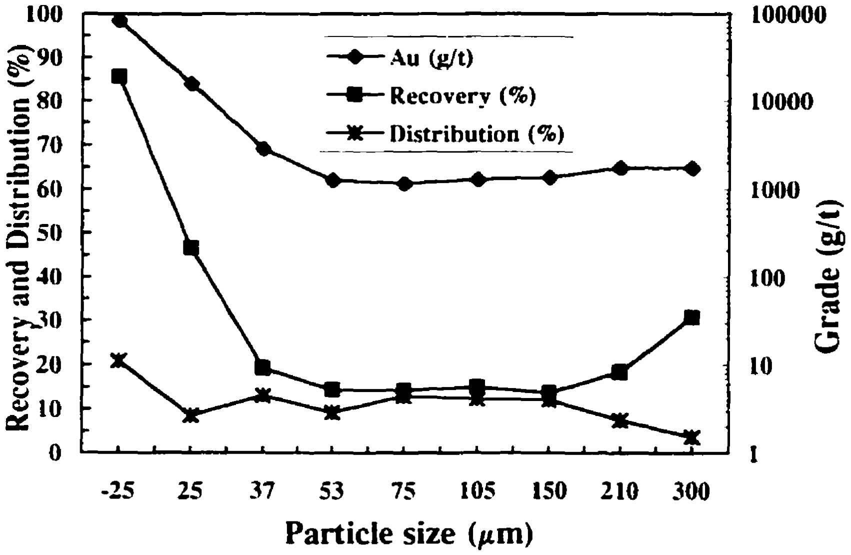

FIGURE 8-6 Results of the Falcon Concentrator - Feed: Lucien Béliveau Total Table Tails (undiluted)

For tail 2 diluted with silica, the gold content of -25 μm was 6503 $g.t^{-1}$ (Appendix 8-1), which was about 21 times higher than the overall grade; below 105 μm the gold distribution percent was higher than the mass percent of the same fraction. However, gold in the -25 μm fraction accounted for only 7.9 % of the total, which was much lower than for tails 1 (56.9%). This is reasonable because gold fines are mostly washed away as soon as they are fed on the table, opposite to the feeding box, where the tail 1 sample was collected.

Knelson and Falcon Performance

The recoveries of the Knelson Concentrator for tests 1 to 3 were virtually identical, 82.6%, 81.1%, and 81.5%, respectively (Table 8-1). This implies that the Knelson Concentrator was a very effective scavenger and that silica dilution, at least for this table tail, had little impact.

Figure 8-3 details the results of test 1. It is clear that gold was distributed predominantly in the fine classes, this gold being mostly liberated. In fact, recovery increased with decreasing particle size, which was exactly the trend expected if recovery is closely correlated with liberation. Figure 8-4 shows that although the overall metallurgical performance of test 2 was similar to that of test 1, size-by-size it was quite different. Gold distribution was not in the finer, but in the intermediate size classes, 53-300 μm. Maximum gold recovery was over a wider range, 25 to 105 μm, above which it decreased, presumably because of incomplete liberation. Concentrate grade was similar to that of test 1 in the fine size range, but did not decrease as rapidly with increasing particle size (because more coarse gold was recovered); as a result, overall grade was higher, 12,920 $g.t^{-1}$ vs. 7,180 $g.t^{-1}$.

Figure 8-5 shows the performance of the Knelson Concentrator when processing the combined tails. As expected, the curves are very much a weighted average of those of Figures 8-3 and 8-4. Concentrate grade did not decrease so dramatically with increasing particle size, because no 212 μm (70 mesh) silica was used to dilute the feed sample, and as a result much less of the concentrate was in the coarse size classes. The distribution of the gold was bimodal, with the distinct peak at 25 μm from the fine gold in tails 1, and the more diffused peak of tails 2 in the 53-105 μm range. Gold recovery was similar to that of tests 1 and 2, except for minus 25 μm where it was lower, 75% vs. 85% (test 1) and 82% (test 2). The recovery of the 25-37 μm fraction was also slightly lower, but by only 2%, which is explained by the absence of silica dilution. It can be concluded that in this case silica dilution has an impact on recovery, albeit a small one.

Figure 8-6 shows a rather unusual pattern for gold recovery with the Falcon. The recovery and concentrate grade curves are saddle-shaped, which is quite different from those obtained with the Knelson Concentrator. Similar results were obtained and explained by Buonvino (1993). The concentrate grade and recovery of the Falcon Concentrator were only 4150 $g.t^{-1}$ and 33.4%, much lower than that of the Knelson Concentrator. The difference in concentrate grade could have been higher, as the grade of the Knelson Concentrator can easily be increased at almost equivalent recovery by processing more mass. Although a single test at sub-optimal conditions may not yield the best results, the work of Buonvino (1993) suggests that the operating conditions of test 4 were not far from optimum and that the performance of the Falcon Concentrator is relatively insensitive to operating conditions (except for the total mass fed). Recent B6 Falcon Concentrator work (Laplante and Nickoletopoulos, 1996) with synthetic feeds has shown that the presence of a medium density phase (in this case sulphides) significantly decreased the recovery of the high density phase (in this case gold). The mechanism most likely responsible for this decrease in recovery is erosion of the concentrate bed by the medium density phase. As the Knelson Concentrator clearly outperformed the Falcon Concentrator, the latter was not used in further testwork.

Possible Reasons for Gold Losses into Table Tails

It is possible, from these results, to suggest how gold losses may occur during table operation. As soon as the table feed contacts the table surface, a significant fraction of the feed, mostly slimes, reports to the tails (tails 1). This results in losses that are mostly fine gold that never settled on the table surface, either because it was washed away, or because it floated on the surface owing to the residual flotation reagent coating.

Gold losses also come from unliberated gold, especially in the coarse size, but they are less important. For tails 2, the size distribution was clearly coarser, with only 9.6% of the mass below 75 μm. The size distribution of gold was also coarser. Free gold particles spanned a wider size distribution. However, there is an indication that much more of the gold that was lost in the intermediate sizes was well liberated, especially between 25 and 150 μm. This gold was probably rejected because of the mechanical limitations of the Deister table.

8.3 Meston Resources

8.3.1 Concise Description of the Mill

The Chibougamau mill of Meston Resources is located on Merrill Island, about 500 km north of Montréal, Québec, and has processed ores from copper-gold deposits since 1955 (Coté et al. 1978). In the early seventies, flotation concentrates assayed 23-26% Cu with 75-82% gold recovery. The recovery of gold was not emphasized because of its low price. After that, gold price increased significantly and remained high. Therefore, in order to maximize the value of the flotation concentrates, the copper grade was lowered to 17-19% Cu, with a corresponding increase in gold recovery to high eighties. A gravity circuit was retrofitted to the grinding circuit in the fall of 1984 to recover coarse gold ahead of flotation, as a result, gold recovery increased further to 87-90% (Laplante et al. 1986).

The sulphides in the mine are mostly pyrite, pyrrhotite and chalcopyrite, with traces of sphalerite and galena. The host matrix contains chlorite, quartz and carbonates (calcite, siderite and ankerite) (Hawkins, 1960), and head grade of gold is 6-14 $g.t^{-1}$.

The flowsheet of the grinding/gravity circuit is shown in Figure 8-7. After three stages of crushing, the fine ore is fed to an open circuit of a rod mill (3.4 x 4.40 m) at 122 $t.h^{-1}$, then two ball mills (3.1 m x 3.7 m) in parallel and closed circuit with two 76 cm cyclones. Ball and rod mill discharges are directed to sluices. The concentrate of the sluices is screened at 1.7 mm (10 mesh), and the undersize fed to one of two 76 cm (30") Knelson Concentrators operating with a loading cycle of 90 minutes (the other is on stand-by). Continuous operation is maintained by diverting the feed to the stand-by unit before concentrate removal. The Knelson concentrate is pumped to a high security gold room, where, the roughing concentrate is first screened at 1.7 mm to remove metallic wires, and is then upgraded in a 30 cm Knelson Concentrator. Its rougher tail is processed again with the same unit, and the rougher and scavenger concentrates combined and fed to a 213 x 102 cm home-made shaking table. A magnet over the table removes magnetic materials, such as magnetite and tramp iron. The table yields a final concentrate containing about 50% Au which is acid cleaned prior to direct smelting. Table and the Knelson Concentrator tails are column-cyanided, the cyanidation residue being washed and returned to the grinding circuit. The tails of the sluice and the Knelson Concentrator are pumped to cyclones, the overflow going to copper flotation.

8.3.2 Laboratory Testwork

Sample Preparation

On August 12, 1992, the table tails were sampled. A single sample was dried and split into twelve parts using a rotary splitter.

The Knelson Concentrator Tests

Four tests were carried out in a similar procedure to that as presented in 8.2.3.

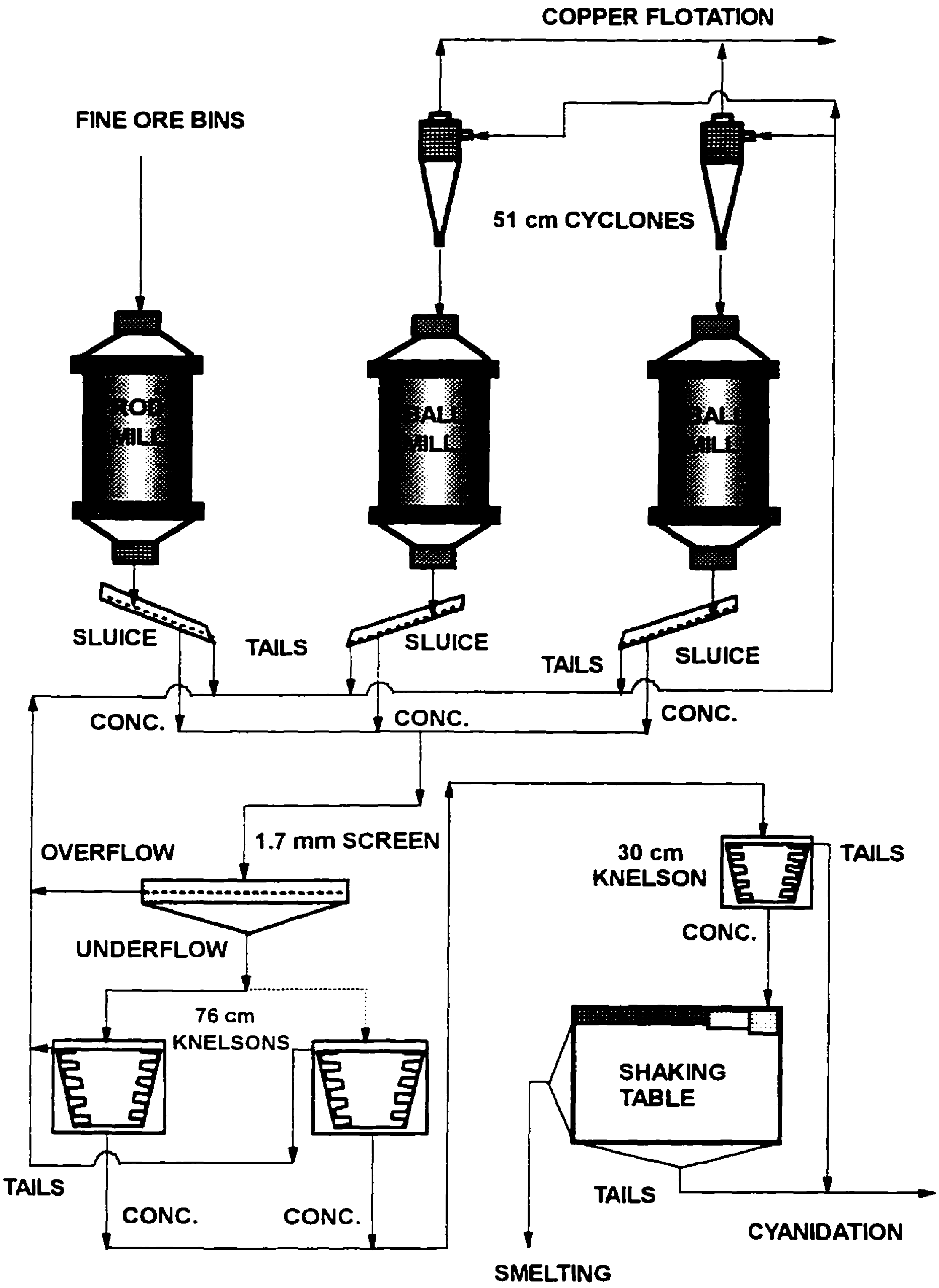

FIGURE 8-7 Grinding and Gravity Circuit of Meston Resources

Test 1: A sub-sample, 5.14 kg in weight, was fed undiluted to the laboratory Knelson Concentrator, at a fluidization water pressure of 27 kPa (4 psi), and a feed rate of 250 g per minute.

Test 2: Another sub-sample of the original tails, 2.49 kg in weight, was diluted with 212 μm silica (3:1) and fed to the Knelson Concentrator at the same operating conditions as for Test 1.

Test 3: The results of Test 1 showed that material > 150 μm had 72.5% of the weight, but only 14.8% of the gold (Appendix 8-2). This is an ideal situation for oversize removal, and hence, the original table tails were first screened at 150 μm (100 mesh). The undersize of 2.6 kg was fed to the Knelson Concentrator at a fluidization water flowrate of 4.1 $L.min^{-1}$, corresponding to 23 kPa (3.4 psi). The Knelson Concentrator tails were recovered sequentially in eight subsamples, to determine the variation of performance with time.

Test 4: The "magnetic" test designed to achieve a higher concentrate grade was tested with 2.3 kg of -150 μm material. The operating conditions of the Knelson Concentrator were the same as for Test 3, but a 200 g, 75-425 μm, magnetite sample was first fed to the Knelson Concentrator. The magnetite was equally divided in each of the following Tyler classes, 75-106, 106-150, 150-212 and 300-425 μm.

8.3.3 Test Results

The main results of the four tests are summarized in Table 8-3; details are given in Appendix 8-2. Test results for the original table tails, the table tails diluted with -212 μm silica and the -150 μm table tails are shown in Figure 8-8, 8-9, and 8-10, respectively, and are compared in Figure 8-11. Figure 8-12 compares size-by-size recovery for the entire tails and -150 μm table tails. Figures 8-13 and 8-14 show Scanning Electronic Microscope (SEM) photographs of gold particle in the Knelson

Concentrator tails.

TABLE 8-3 Results of the Knelson Concentrator Tests for Meston Resources

Test 1 Original table tails				
Product	Mass (%)	Grade (g.t^{-1})	Recovery (%)	
Concentrate	2.97	51584	45.6	
Tail	97.03	1880	54.4	
Total	100.00	3355	100.0	
Test 2 Table tails diluted with -212 μm silica (3:1)				
Product	Mass (%)	Grade (g.t^{-1})	Recovery (%)	
Concentrate	1.48	37760	60.9	
Tail	98.52	364	36.1	
Total	100.00	917	100.0	
Test 3 -150 μm table tails				
Product	Mass (%)	Grade (g.t^{-1})	Recovery (%)#	Recovery (%)*
Concentrate	4.58	194813	63.4	54.5
Tails	95.42	5405	36.6	30.7
Total	100.00	14088	100.0	85.2
Test 4 -150 μm table tails with 200 g magnetite pre-feed				
Product	Mass (%)	Grade (g.t^{-1})	Recovery (%)#	Recovery (%)*
Concentrate	1.00	604188	49.1	41.1
Tails	99.00	6605	50.9	44.1
Total	100.00	12581	100.0	85.2

* Recovery was calculated on the basis of 100% in the total table tails, as for the other tails (except for the Snip Operation, from which the exact gold distribution of the original table tails was not available).

\# Recovery was calculated on the basis of 100% in the -150 μm table tails.

8.3.4 Discussion

Gold Distribution in the Table Tails

Compared to the table tails of Lucien Béliveau, the size distribution of gold in the Meston table tails was much finer (Figures 8-5 and Figure 8-8); the tails themselves, however, were much coarser. For example, in the -150 μm fraction, the Lucien Béliveau table tails contained 65% of the gold and 63% of the mass (Appendix 8-1): the Meston table tails, in the same size range, contained 85% of the gold, but only 27.5% of the weight (Appendix 8-2).

The grade of Meston table tails was the highest, 3340 g.t^{-1}, of the seven samples tested. The grade of -150 μm was 10,600 g.t^{-1}, which was 17 times higher than that of the +150 μm fraction, 608 g.t^{-1} (Appendix 8-2). The finer gold and coarser gangue explain the lower recovery with the Knelson Concentrator for the Meston table tails, 45.6% vs. 81.5% for Lucien Béliveau.

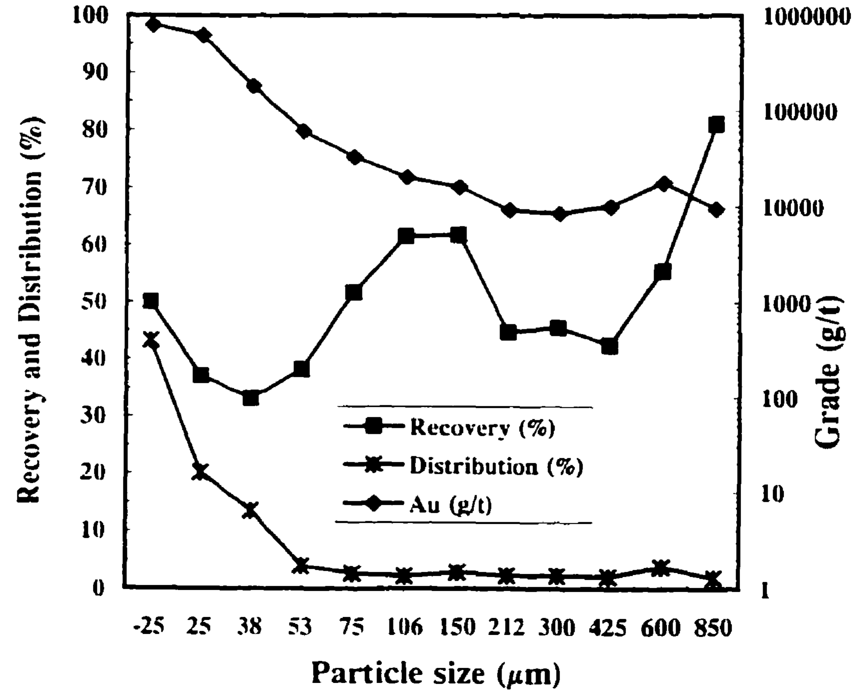

FIGURE 8-8 Results of the Knelson Concentrator for Meston Original Table Tails

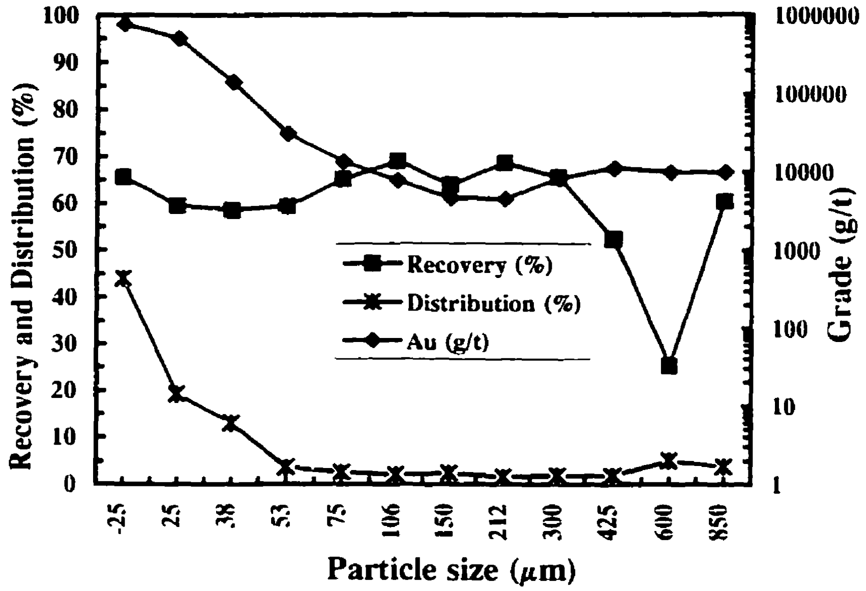

FIGURE 8-9 Size-by-Size Performance of Test 2 (Feed: Meston table tails diluted by -212 μm silica 3:1)

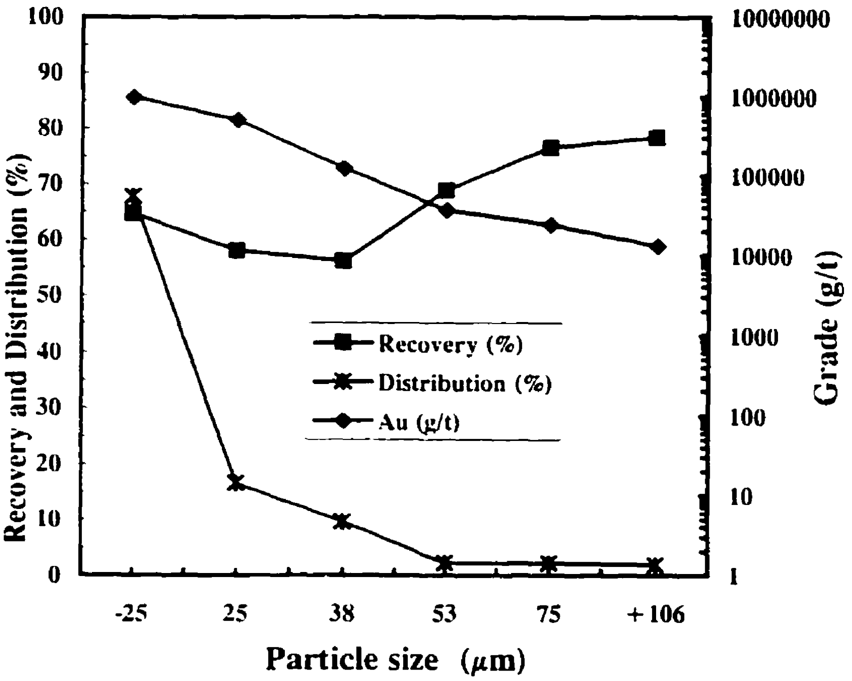

FIGURE 8-10 Size-by-Size Performance of Test 3 (Feed: Meston -150 μm table tails)

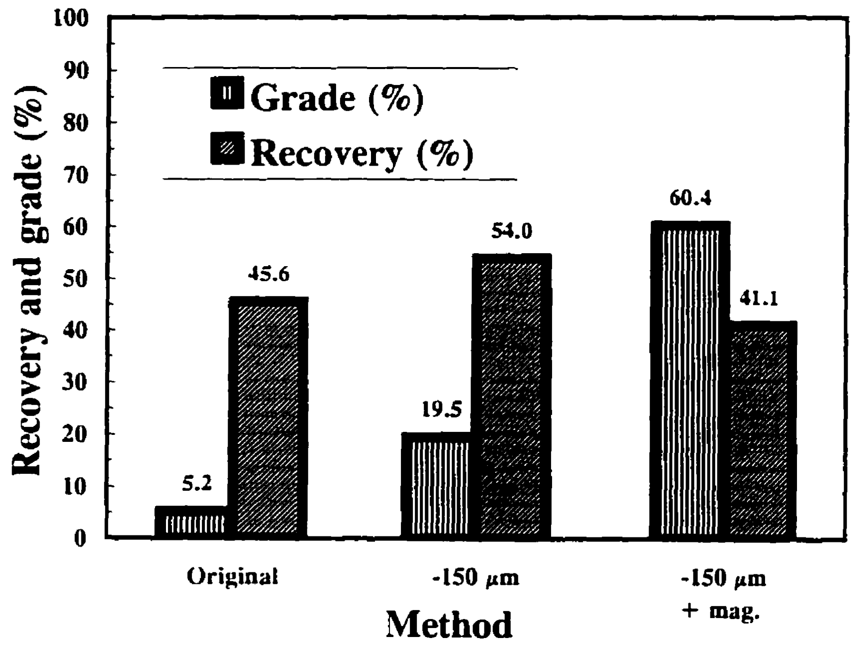

FIGURE 8-11 Comparing Tests 1, 3 and 4 (Feed: Meston table tails)

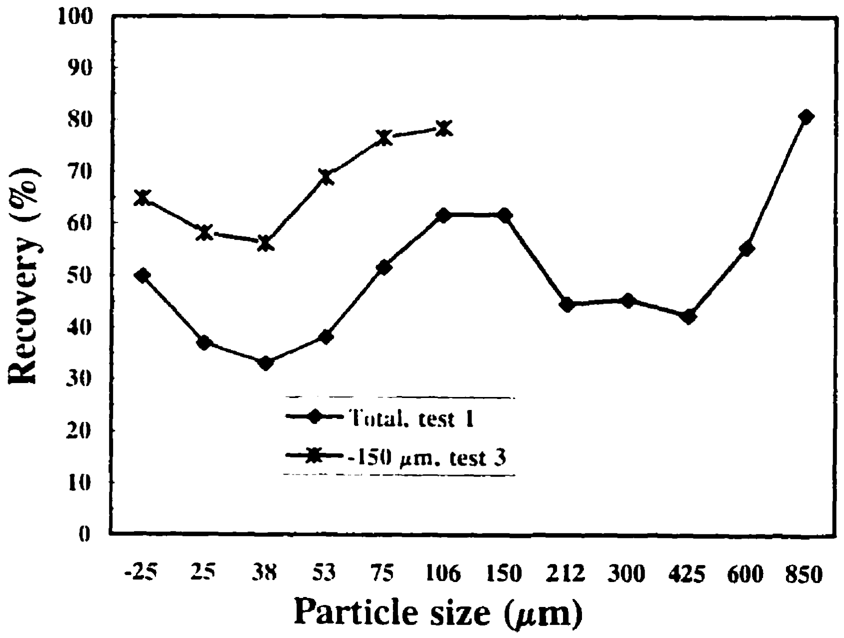

FIGURE 8-12 Size-by-Size Recoveries of Tests 1 and 3 (Feed: Meston table tails)

FIGURE 8-13 SEM Back-Scattered Image of +106 μm Knelson Tails for Processing Meston Table Tails (1: locked gold; 2: arsenopyrite; 3: silica)

FIGURE 8-14 SEM Back-Scattered Image of 38-53 μm Knelson Tails for Meston Table Tails Processing (1: gold; 2: gold with small inclusion; 3: arsenopyrite; 4: pyrite; 5: silica)

The Performance of the Knelson Concentrator

Silica dilution increased gold recovery significantly, to 60.9%. The lower concentrate grade, 37.760 $g.t^{-1}$, stemmed from the lower gold grade of the feed. Increased feed mass would have corrected this problem with only a modest drop in recovery.

Size-by-size recovery showed the same tendency for tests 1 and 2 (Figure 8-12). In the size range of 25 to 300 μm, the shape of the recovery curve was similar to that of the Béliveau table tails. In the very coarse size, +850 μm, recovery went up sharply, which implies that most of the coarse gold in the table tails was liberated.

The Impact of Classification on Knelson Performance

When only 27.5% of the total mass (-150 μm fraction) was treated, gold recovery increased to 54% of the entire table tails with a concentrate grade of 19.5% Au. Test recovery (referring to the feed of the test) was even higher, 63.4%. This can be explained by the absence of competition between coarse gangue and fine gold particles, which resulted in a lower erosion rate of the concentrate bed.

Size-by-size recoveries for both the coarse and fine materials are shown in Figure 8-12. The curve of -150 μm is almost parallel to that of the entire material, at about 20% higher.

The results obtained indicate that although the Knelson Concentrator can treat materials with a wide size range, say -6 mm down to 25 μm, it still obeys one of the general rules of gravity separation, that is, the narrower the feed size range being processed, the better the performance. Decreased interaction between coarser, light and fine, heavy particles is the key.

Gold in the Knelson Concentrator Tails

Cursory SEM scanning of a +106 μm Knelson Concentrator tails sample (from test 1) could not find free gold particles. Figure 8-13 shows a typical sighting, a small gold particle which is locked with asenopyrite and silica. For the 37-53 μm fraction, free gold particles were much more easily found. Figure 8-14 (from test 1) shows two such particles, one of them totally free, the other with a very small silica fragment.

Figure 3-1 shows a SEM photograph of the -25 μm fraction of the Knelson tails (from test 1). The number of free gold particles is high, and in fact, the gold is almost completely liberated. Although the Knelson Concentrator is a very efficient unit, part of the free gold, especially in the -25 μm fraction, will still escape to the tails.

Using Magnetite to Increase Concentrate Grade

As expected, a significant increase in gold grade was achieved when 200 grams of magnetite was pre-fed to the Knelson Concentrator. The grade of the non-magnetic fraction of the concentrate, 60.4%, is high enough for direct smelting. It was 3 times higher than that achieved when treating the -150 μm tails, and 12 times higher when treating the entire tails.

The total recovery was 4% lower than when treating the entire table tails and 13% lower than when treating the -150 μm material; this might have been partially caused by the coarse size range of the magnetite, much coarser than that of the actual table tails processed. This is supported by an analysis of size-by-size recovery, which identifies a recovery drop of about 15% below 53 μm (Appendix 8-2). This problem is not serious, as the Knelson Concentrator would probably be operated without magnetite as a scavenger, and with pre-feeding of magnetite as a cleaner, once enough gold had been scavenged. The cleaner tail would likely be returned to the next scavenging step.

Magnetite plays a role in forming the basic concentrate bed in the Knelson

Concentrator riffles. Most of the magnetite that is pre-fed and recovered will not be swept away by the subsequent real feed, but will stay in the riffles to prevent packing with barren, non magnetic material that cannot be removed so readily from the gold.

8.4 Hemlo Golden Giant Mine

8.4.1 Concise Description of the Mill

The Golden Giant Mine, of Hemlo Gold Mines Inc., is located in 35 km east of Marathon, Ontario. As of December 31, 1993, the total proven and probable reserves were 11,789,000 tonnes with an average grade of 11.44 g.t^{-1} (Giancola et al, 1995). The mill processes 3000 t.d^{-1} of ore at an average grade of 13 g.t^{-1} Au.

The ore is processed using conventional crushing-ball milling-cyanidation and CIP. After one stage of primary crushing underground, the ore is crushed from 150 mm to 12 mm in two stages with cone crushers. Fine ore is fed to grinding circuits to produce a fineness of 89% passing 75 μm. Gold recovery averages 96.5%.

The circulating load of gold in the primary cyclone underflow has been as high as 6000%; gold nuggets as large as 184 g have been found in the crushing plant: the largest gold flake found in pump boxes was 2.5 cm in diameter; free gold has been found in leach tailings (Giancola et al, 1995). These facts led to the installation of a gravity circuit with a jig in the grinding circuits in 1992. Later, following successful laboratory and pilot testing in the grinding circuit, a Knelson Concentrator along with a shaking table was installed. The current principal flowsheet is shown Figure 8-15 (Honan and Luinstra, 1996).

In the gravity circuit, a bleed of one out of four primary cyclone underflows is fed to a 1.7 mm screen, the other three being fed to the secondary ball mill. The undersize of the screen reports to a 76 cm CD Knelson Concentrator, and the oversize of the screen and the tails of the Knelson Concentrator are recycled to the primary cyclones. The Knelson Concentrator produces a concentrate at a grade of 2-5% gold from a feed containing 50-200 $g.t^{-1}$ of gold. The Knelson concentrate is further upgraded on a Gemini shaking table to achieve an average gold grade of 75%, as shown in Figure 8-15 (Honan and Luinstra, 1996).

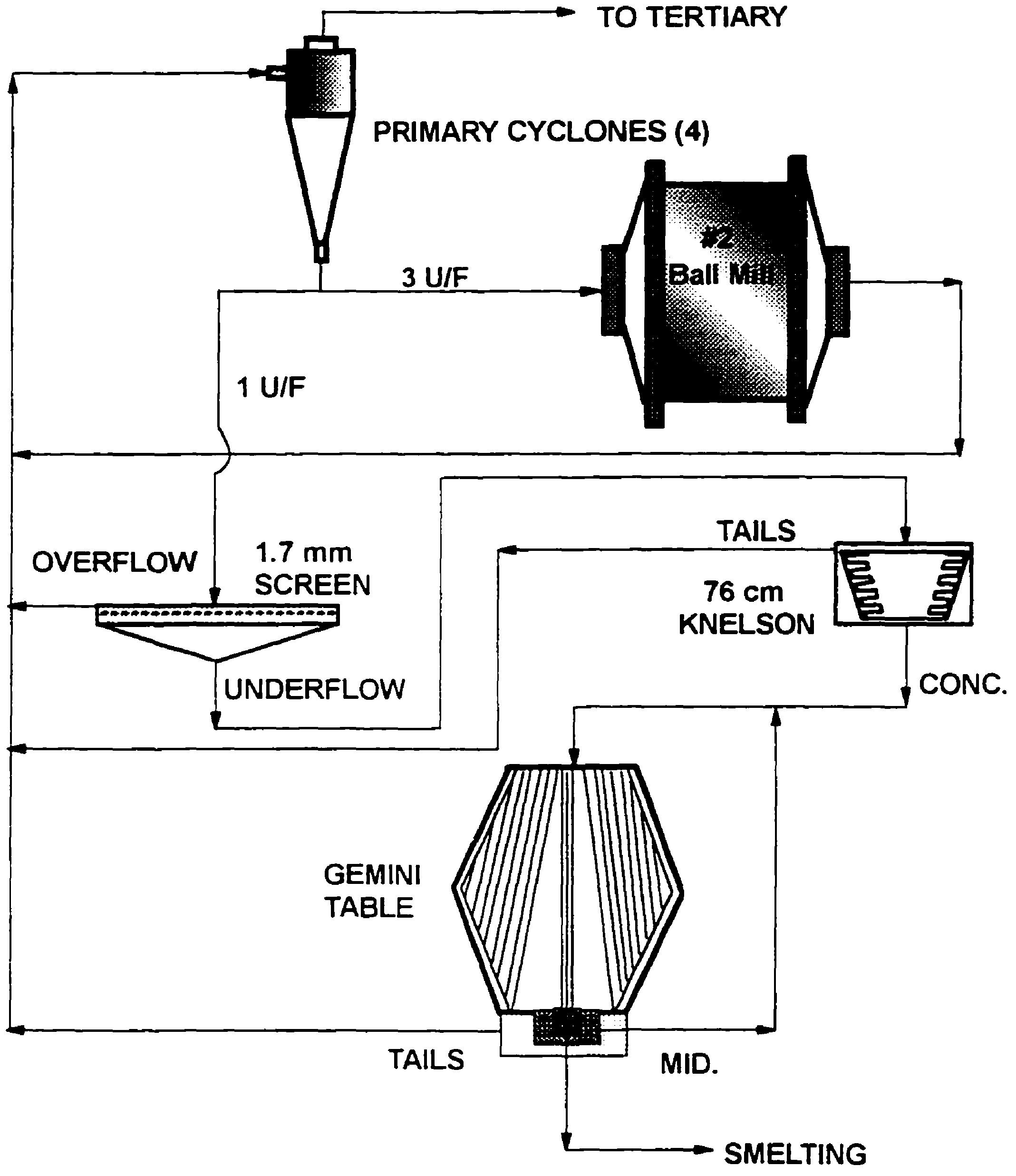

FIGURE 8-15 The Hemlo Gravity Circuit Flowsheet

8.4.2 Laboratory Testwork

In May 1994, a 19 kg sample of Hemlo table tails was received at McGill. It was first dried and screened at 2.4 mm (8 mesh). The oversize was broken and then combined with the undersize, and the total sample split into 12 sub-samples with a rotary splitter. Three Knelson Concentrator tests were completed.

Test 1: A 4 kg sub-sample of the original table tail was fed to the laboratory Knelson Concentrator at a 5.6 $L.min^{-1}$ fluidization water flowrate.

Test 2: A second 4 kg sub-sample was screened at 212 μm (70 mesh). Magnetite and tramp iron were manually removed from the -212 μm fraction using a hand magnet. The sample was then fed to the Knelson Concentrator at a 4.6 $L.min^{-1}$ fluidization water flowrate. The tails were collected into eleven separate pails to measure the progressive increase in gold losses as the test progressed.

Test 3: A third 4 kg sample was screened at 212 μm, and the -212 μm fraction processed. The operating conditions of the Knelson Concentrator were similar to test 2, but a 200 g magnetite sample was pre-fed. The tails were collected into eleven separate pails to measure the progressive increase in gold losses as the test progressed. The preparation of magnetite and its separation from the bulk concentrate were the same as that described in 8.2.2.

8.4.3 Test Results

The results are summarized in Table 8-4 and Figure 8-18; details are given in Appendix 8-3. Results of tests 1 and 2 are shown in Figures 8-16 and 8-17, respectively. Tail grade as a function of feed mass for the two tests of -212 μm material (with and without magnetite pre-feed) is given in Figure 8-19.

TABLE 8-4 Results of the Knelson Concentrator Tests for Hemlo Gold Mines

Test 1 Original table tails

Product	Mass (%)	Grade (g.t^{-1})	Recovery (%)
Concentrate	3.20	35431	41.5
Tails	96.80	1654	58.5
Total	100.00	2735	100.0

Test 2 -212 μm fraction

Product	Mass (%)	Grade (g.t^{-1})	Recovery (%)#	Recovery (%)*
Concentrate	3.67	98727	91.8	70.8
Tails	96.33	334	8.2	6.3
Total	100.00	3943	100.0	77.1

Test 3 -212 μm fraction with magnetite pre-feed

Product	Mass (%)	Grade (g.t^{-1})	Recovery (%)#	Recovery (%)*
Concentrate	0.41	625354	70.5	54.1
Tails	99.59	1058	29.5	23.0
Total	100.00	3618	100.0	77.1

* *Recovery was calculated on the basis of 100% in the total table tails, as for the other tails*

\# *Recovery was calculated on the basis of 100% in the -212 μm table tails.*

8.4.4 Discussion

Size Distribution and Knelson Performance

The grade of the Hemlo table tail sample received was 2740 g.t^{-1}. The size-by-size gold distribution was close to normal (Figure 8-16), with a mean around 150 μm (100 mesh), and 53% of its gold content between 106 and 300 μm (Figure 8-16 and Appendix 8-3). It was quite different from that of Lucien Béliveau, which was nearly equi-probable, and Meston, in which the gold was found mainly in the finer sizes.

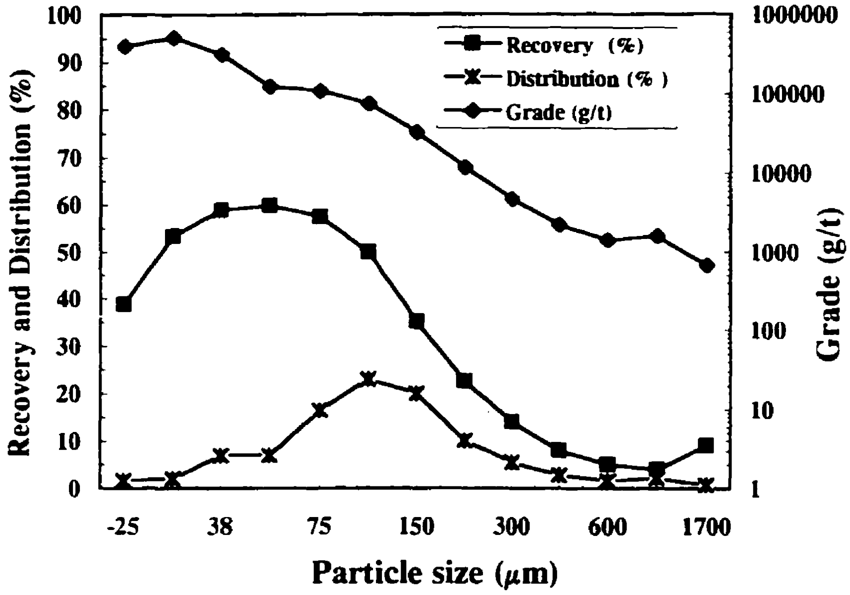

FIGURE 8-16 Size-by-Size Performance of Test 1 (Feed: Hemlo gold table tails)

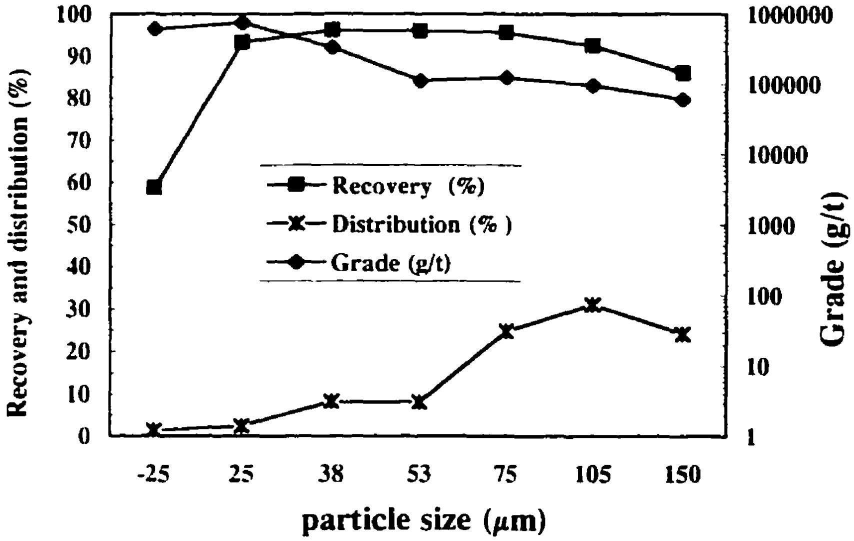

FIGURE 8-17 Size-by-Size Performance of Test 2 (Feed: Hemlo -212 μm table tails)

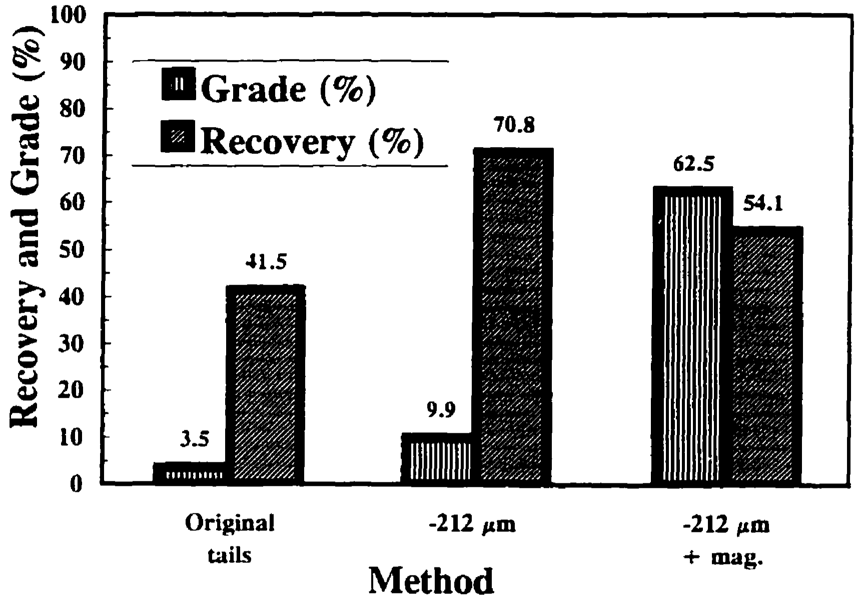

FIGURE 8-18 Comparing the Three Hemlo Gold Tests

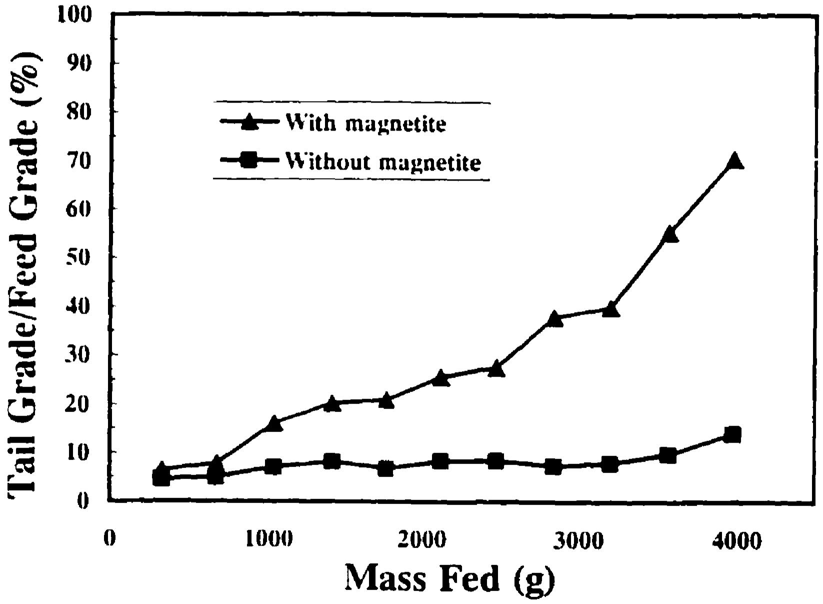

FIGURE 8-19 Evolution of Gold Losses in Tests 2 and 3 (Feed: Hemlo Gold -212 μm table tail, with and without magnetite pre-feed)

For the original table tails (Figure 8-17 and Appendix 8-3), a recovery of 41.5% with a grade of 3.54% Au was obtained, compared to the recovery of 45.6% Au for Meston. Recovery and grade for the two table tails were similar, perhaps because they had the same size ranges, 0-1.7 mm, while the size distribution of the Lucien Béliveau table tails, originally a flash flotation concentrate, was much finer, 0-425 μm.

For the -212 μm material, a very high recovery, 91.8%, with a grade of 9.87% Au, was achieved. Figure 8-17 explains this high recovery: gold was distributed mainly in the size range of 25 to 150 μm, which is the size range where the Knelson performs best.

Pre-feeding Magnetite and the Evolution of Tail Grade Throughout the Test

When 200 g of magnetite was pre-fed to the Knelson Concentrator, a recovery of 54.1% with a grade of 62.5% Au was obtained (on the basis of 100% in the total table tails). As for Meston, this grade is high enough for direct smelting. It was 18 times that obtained when processing the total table tails and 6 times that obtained when processing the -212 μm fraction without a magnetite pre-feed. The recovery was 13% higher than that of processing the total table tails, even though there was a substantial drop in recovery compared with test 2.

The total recovery for Meston table tails with the magnetite pre-fed was 4% lower than when processing the total table tails. It can be attributed to the fact that for Meston, -150 μm material was processed; for Hemlo, -212 μm material was processed, but for both, the same size distribution of magnetite, -425 μm, was used. On the other hand, the gold at Meston was much finer. It was more easily eroded, therefore, more severe overload occurred.

Figure 8-19 shows interesting data about the evolution of the Knelson Concentrator tail grade throughout the test. For the -150 μm material without magnetite, the cumulative tails grade increased very slowly, and no severe overload occurred, much as for the synthetic feed with fine magnetite (Figure 5-9).

For the -150 μm table tails with magnetite pre-feed, the situation was quite different, as the incremental tails grade went up quickly, from 6% for the first tail sample to 71% for the last. The severity of the overload is in between that of the coarse silica-tungsten and coarse magnetite-tungsten systems. This again suggests that tests with a finer magnetite pre-feed should be carried out.

After separating magnetite from the bulk concentrate, the grade of the non-magnetic concentrate increased from 6.5% to 62.5% Au, at the cost of only 0.3% recovery (i.e. gold entrapped in the magnetite concentrate, Appendix 8-3). The use of the Knelson Concentrator with magnetite pre-feed as a final cleaner to upgrade gold gravity concentrates, therefore, is very promising.

8.5 Snip Operation

8.5.1 Concise Description of the Mill

The Snip Operation is located on the Iskut River, about 40 km upstream of its confluence with the Stikine, and about 80 km east of the town of Wrangell, Alaska, 110 km from Stewart, B.C. The mine was operated by Cominco Metals Ltd. on behalf of a joint venture between Cominco and Prime Resources Inc. (Carter, 1992).

It is an underground mine, but the direction of the mining is upward from 180 m above sea level to the upper reaches of the ore body inside Johnny Mountain. In this rugged area dominated by the Coast Mountains and covered with dense evergreen forest, roads are almost nonexistent.

The ore body contains distinct ore types: streaky quartz ore, crackle quartz ore, and massive sulphide veins containing mostly pyrite and pyrrhotite (Carter, 1992).

Mining reserves at start-up totalled 936,000 tonnes grading 28.5 $g.t^{-1}$ of gold, and production began in January 1991 (Morrison, 1992). The concentrator was purchased from a defunct Northwest Territories mine. Cominco added a large gravity table, and installed jaw and cone crushers, and a ball mill. Overcrafts and air freighters transport the concentrates and bullion to market.

Mining and milling are at 450 tonnes per day with a head grade of about 30 $g.t^{-1}$. Ore entering the mill is crushed to -7.5 cm (3 inch) in a jaw crusher, followed by secondary crushing to 9.5 mm in a shorthead cone crusher. The ore is then ground in an Allis Chalmers ball mill. The ball mill discharge is fed to a double hutch Yuba-Richards jig, whose concentrate is continuously fed to a No.6 Deister table. The table operates 24 hours per day to produce a concentrate grading 45-55% Au, which is accumulated for smelting in an on-site, oil-fired, Wabbi type furnace. Table tailings return to the mill circuit, and jig tailings are directed to classification. Cyclone overflow is fed to a single-stage flotation circuit, which produces a gold-bearing bulk sulphide concentrate, which is filtered and bagged for sale. Gold recovery averages 91%, of which 25-35% is obtained as bullion from the gravity circuit, and the rest as sulphide concentrate. A simplified flowsheet of the grinding and gravity circuit is shown in Figure 8-20.

8.5.2 Laboratory Testwork

On September 12, 1994, a 32.5 kg Snip table tail sample was received at McGill. The total sample was screened at 212 μm, yielding 19.3 kg of -212 μm fraction. A coarse table tail sample was obtained by combining 10 kg of the +212 μm fraction with 2 kg of the -212 μm fraction (to minimize the mass of -212 μm used); the balance of the -212 μm was halved.

Test 1: The coarse tail sample was processed with a 7.5 cm Knelson Concentrator at a feed rate of 450 $g.min^{-1}$ and a fluidization water flow rate of 5.8 $L.min^{-1}$. The concentrate and a single tails sample were collected.

Test 2: Eight kilos of the -212 μm tail was fed to the 7.5 cm Knelson Concentrator at a fluidization water flowrate of 4.5 L.min^{-1} and a feed rate of 350 g.min^{-1}. One concentrate and twelve consecutive tails samples were collected.

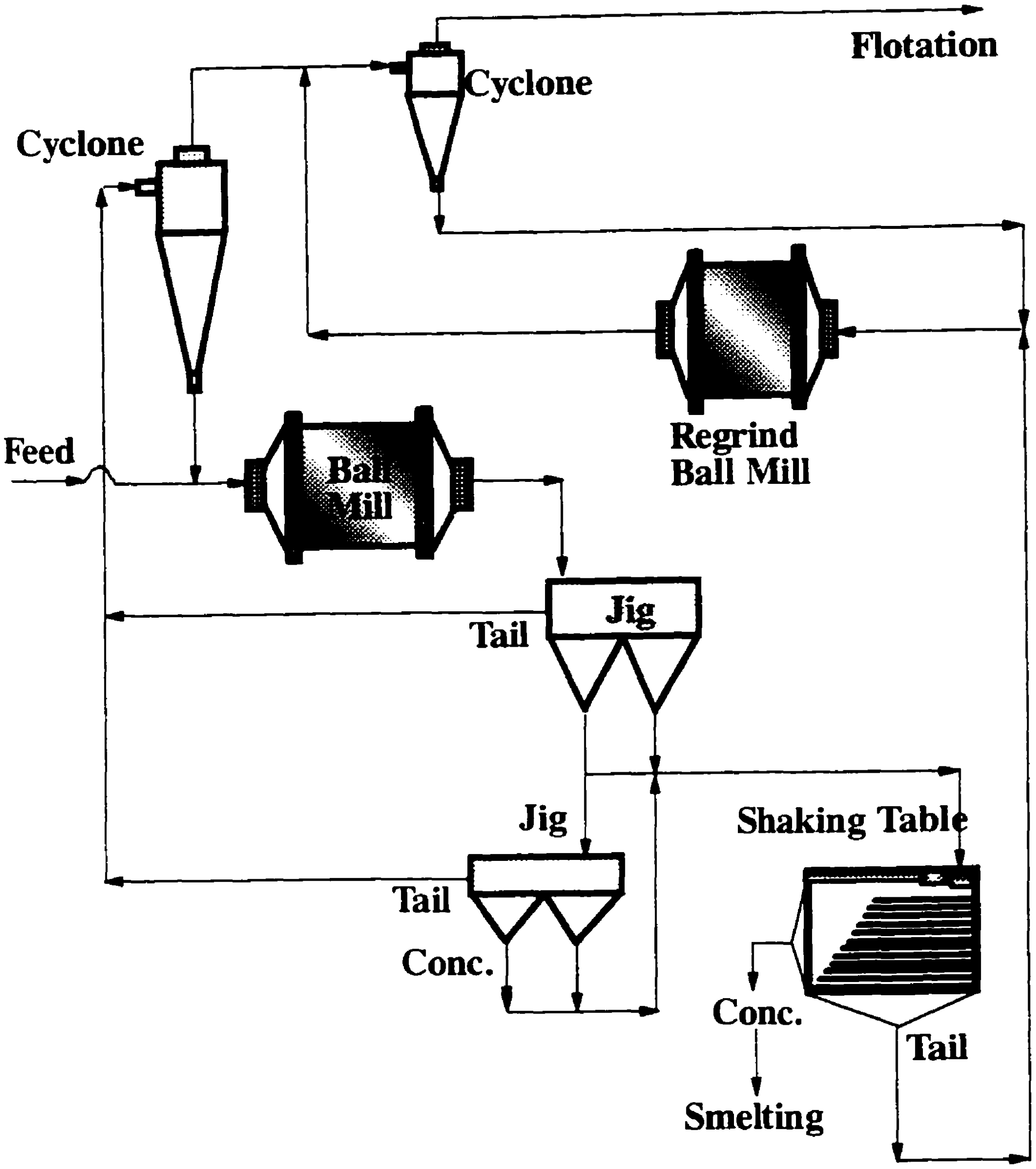

FIGURE 8-20 Simplified Diagram of the Snip Grinding/Gravity Circuits

Test 3: A 200 g sample of magnetite (the same size distribution as used in section 8.3 and 8.4) was pre-fed to a 7.5 cm Knelson Concentrator. An eight kilo sample of the -212 μm tail was then fed at a fluidization water flowrate of 4.5 L.min^{-1} and a feed rate of 350 g.min^{-1}. One concentrate and twelve consecutive tails samples were collected.

8.5.3 Test Results

A summary of the test results is shown in Table 8-5; further details are given in Appendix 8-4. Size-by-size results of tests 1 and 2 are shown in Figures 8-21 and 8-22, respectively. Figure 8-23 shows the evolution of the tails grade as tests 2 and 3 progressed. A comparison of the results obtained by the different treatments is given in Figure 8-24.

8.5.4 Discussion

Gold Distribution

Unlike most other gold mills, where Knelson concentrates are fed to a shaking table, the Snip shaking table feed comes from a jig concentrate. As a result, the total grade of the table tails, about 150 g.t^{-1}, is much lower than those of other mills.

As shown in Figures 8-21 and 8-22, most of the gold was in the intermediate size range, 25- 425 μm. In the finer size range, gold grade did not go up sharply, even for the -25 μm fraction (Appendix 8-4). This is because fine gold is poorly recovered by jigs (Laplante et al, 1994).

The Knelson Concentrator Performance

For the coarse tail (Appendix 8-4 and Figure 8-21), a total recovery of 24.9% with a grade of 2480 g.t^{-1} (an enrichment ratio of 27.6) was obtained. About 50% of the gold was in the 212-600 μm fraction, where recovery was only 1 to 5%. The low recovery can be attributed to the very poor liberation of gold in these size ranges.

Recovery did go up slightly above 600 μm, where very little gold was found. In the intermediate size range (25-106 μm), the recovery of the Knelson Concentrator increased to the 50-80% range. Recovery dropped again below 25 μm, an inevitable result when a very coarse material is processed (Figure 8-21).

TABLE 8-5 Results of the Knelson Concentrator Tests for Snip Operation

<table>
<tr><td colspan="5"><i>Test 1 Coarse material (83.3% +212 μm) **</i></td></tr>
<tr><td>Product</td><td>Mass (%)</td><td>Gold (g.t$^{-1)}$</td><td>Recovery (%)*</td><td>Recovery (%)#</td></tr>
<tr><td>Concentrate</td><td>0.91</td><td>2483</td><td>24.9</td><td>7.21</td></tr>
<tr><td>Tail</td><td>99.09</td><td>69</td><td>75.1</td><td>21.73</td></tr>
<tr><td>Total</td><td>100.00</td><td>91</td><td>100.0</td><td>28.94</td></tr>
<tr><td colspan="5"><i>Test 2 -212 μm material</i></td></tr>
<tr><td>Product</td><td>Mass (%)</td><td>Grade (g.t^{-1})</td><td>Recovery (%)*</td><td>Recovery (%)#</td></tr>
<tr><td>Concentrate</td><td>1.72</td><td>8145</td><td>68.4</td><td>55.83</td></tr>
<tr><td>Tail</td><td>98.28</td><td>66</td><td>31.6</td><td>25.79</td></tr>
<tr><td>Total</td><td>100.00</td><td>205</td><td>100.0</td><td>81.62</td></tr>
<tr><td colspan="5"><i>Test 3 -212 μm material with magnetite pre-feed</i></td></tr>
<tr><td>Product</td><td>Mass (%)</td><td>Grade (g.t^{-1})]</td><td>Recovery (%)*</td><td>Recovery (%)#</td></tr>
<tr><td>Concentrate</td><td>0.20</td><td>61295</td><td>60.5</td><td>49.38</td></tr>
<tr><td>Tail</td><td>99.80</td><td>83</td><td>39.6</td><td>32.24</td></tr>
<tr><td>Total</td><td>100.00</td><td>205</td><td>100.00</td><td>81.62</td></tr>
</table>

** and # Recovery based on the feed and the total table tails, respectively.*

*** The weight percent of +212 μm of the original table tails was 40.4%.*

For the -212 μm tail fraction, a recovery of 68.4% with a total grade of 8150 g.t^{-1} was obtained (Figure 8-22, Appendix 8-4). The recovery (to the size range processed) was 43.5%, higher than that of processing coarse material. In the intermediate size range, the size-by-size recovery showed similar trends as for the coarse material, but at a higher level. The recovery of the -25 μm fraction was 32% higher, as would be expected with the finer feed.

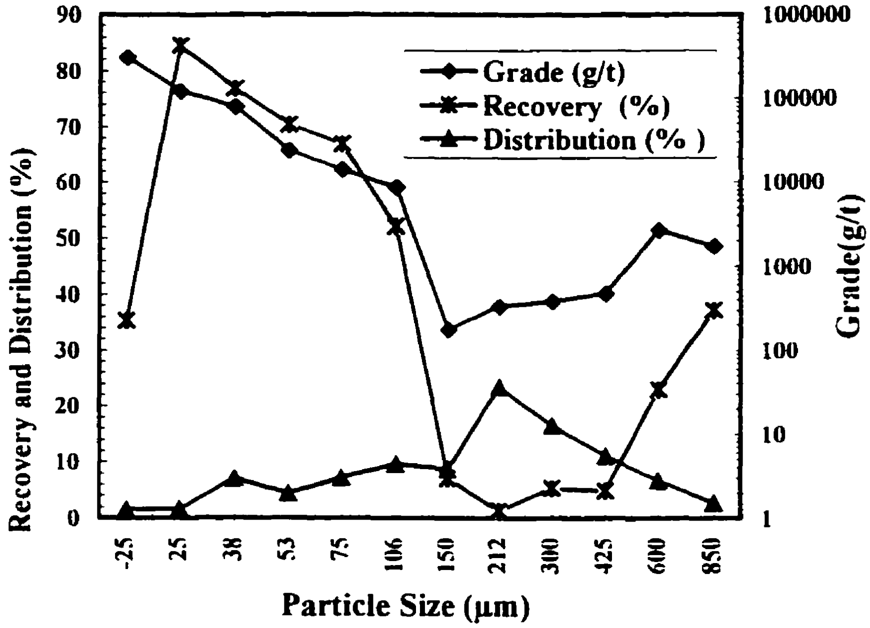

FIGURE 8-21 Size-by-Size of the Snip Test 1 (Feed: coarse table tails)

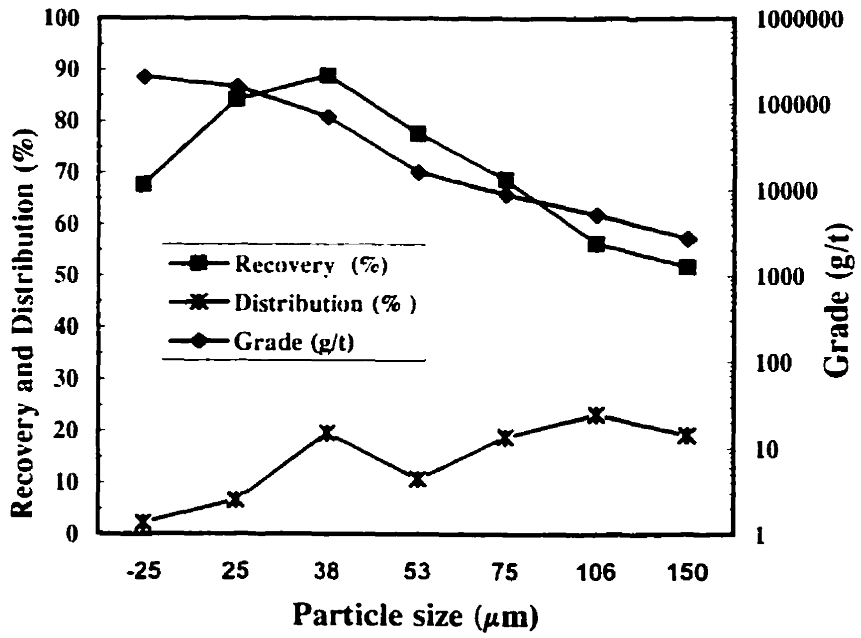

FIGURE 8-22 Size-by-Size of the Snip Test 2 (Feed: -212 µm table tails)

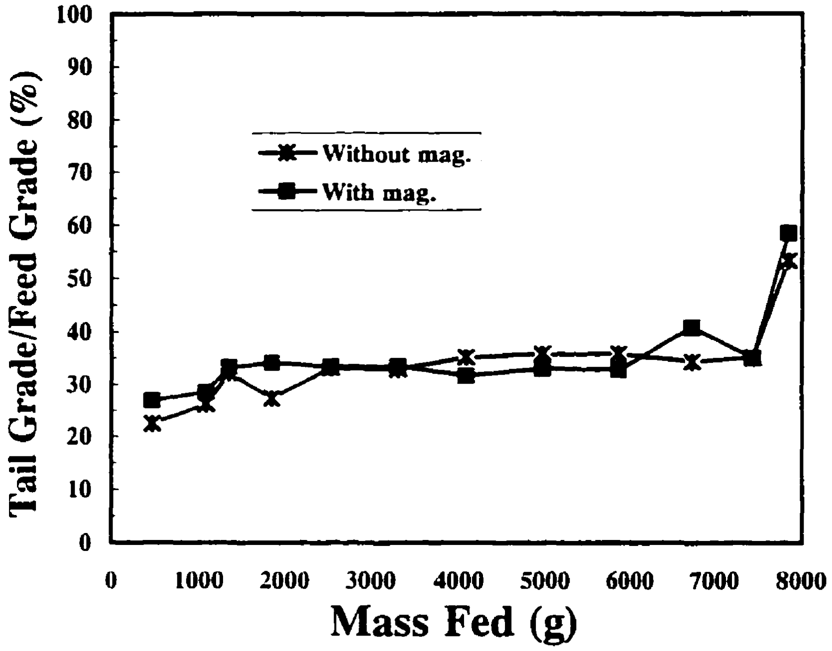

FIGURE 8-23 Evolution of the Tailings Grade for the Snip Tests 2 and 3 (Feeds: -212 µm table tails, with and without magnetite pre-feed)

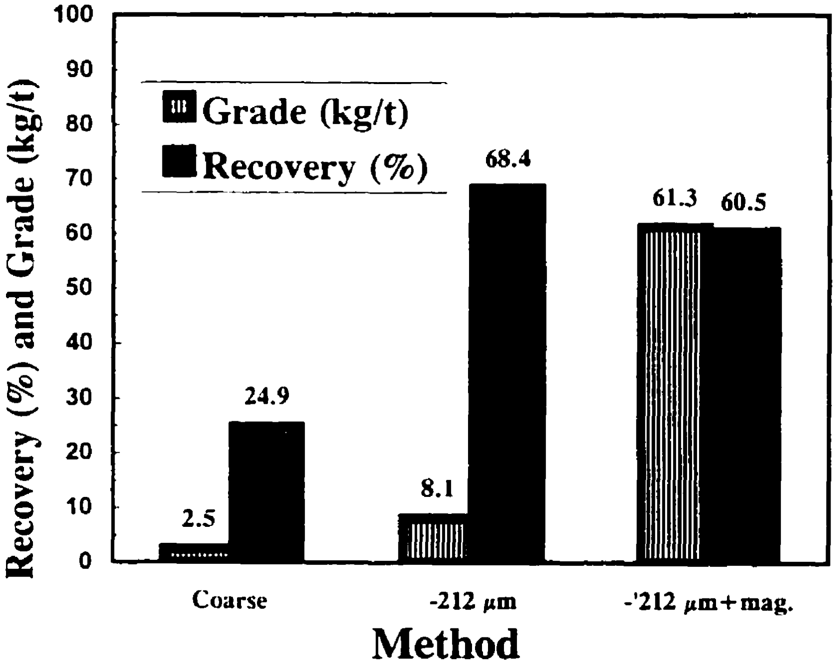

FIGURE 8-24 Comparing the Three Snip Tests

Evolution of the Knelson Tail Grade with Feed Mass

Figure 8-23 shows the gold losses as a function of feed mass for tests 2 and 3. For both tests, the tail grade increases slowly with increasing feed mass. However, unlike the previous table tail samples, the magnetite pre-feed had little impact on recovery, as it did not result in severe overload (cf. Figure 8-19). This can attributed to the low feed grade, 204 $g.t^{-1}$ - 17 times lower than that of Hemlo Gold Mines. As a result, the magnetite pre-feed yielded a recovery of 60.5% with a grade of 6.13% (Figure 8-24). Again, the relatively low grade of the table tails explains the relatively low concentrate grade, which was nevertheless, 673 times higher than that of the table tails grade, 25 times higher than that obtained with the coarse material, and 7.5 times higher than that obtained with the -212 μm material without magnetite pre-feed.

8.6 Les Mines Casa Berardi

8.6.1 Concise Description of the Mill

Les Mines Casa Berardi is located near La Sarre, Québec. It is a joint venture owned by TVX Gold Inc (60%) and Golden Knight Resources (40%), and operated by TVX Gold Inc. The mines, Casa Berardi East and West, were put into operation in September 1987, and as of May 1994, the remaining life was seven years. The mill design capacity is 2000 tonnes per day, but it is normally operated at 1800 tonnes per day (Giancola et al. 1995). The average head grades of the East and West mines are 14 $g.t^{-1}$ and 6.2 $g.t^{-1}$, respectively.

The run-of-mine ore is fed to a jaw crusher, whose product becomes the grinding circuit feed. The ore is then fed to a SAG mill, whose discharge is fed to two cyclone stages, the overflow of the first feeding the second. Both cyclone underflows are fed to a ball mill, although a bleed of the primary cyclone underflow, about 30 $t.h^{-1}$, is screened at 1.7 mm and fed to a 76 cm CD Knelson Concentrator, whose concentrate feeds a shaking table producing a smelting grade concentrate. The table middlings are recycled to the table feed, and tails pumped back to the grinding circuit. The ball mill discharge and the tails of the Knelson Concentrator are returned to the primary cyclone pump sump. The secondary cyclone overflow is thickened prior to cyanidation in a CIL circuit. A simplified flowsheet of the grinding/gravity circuit is shown in Figure 8-25.

8.6.2 Laboratory Testwork

In January 1995, three pails of table tails were received at McGill. The sample was first mixed and fed to a rotary splitter to produce twelve sub-samples. Some of the sub-samples were then classified at 212 μm. Four Knelson Concentrator tests were performed.

Test 1: Five kilos of the unclassified table tail sample was fed to the Knelson at a fluidization water flowrate of 5.6 L.min^{-1} and a feed rate of 350 g.min^{-1}. The full tail and concentrate were collected.

Test 2: The results of test 1 showed that 94% of the total gold was in the -212 μm size range with 55% of the total mass and 84% of the total gold was in the -150 μm size range with only 37% of the total mass; therefore, two tests were specially designed. For test 2, five kilos of the -212 μm table tails sample were fed to the Knelson at a fluidization water flowrate of 4.6 L.min^{-1} and a feed rate of 300 g.min^{-1}. The full concentrate and fourteen consecutive tail samples were collected.

Test 3: Three kilos of -150 μm table tails were fed to the Knelson Concentrator at 4.1 L.min^{-1} fluidization water flowrate and 300 g.min^{-1} of feed rate. The full concentrate and eleven consecutive tail samples were collected.

Test 4: Five kilos of -212 μm table tails were fed to the Knelson Concentrator at a fluidization water flowrate of 4.5 L.min^{-1} and with 200 g of magnetite pre-feed. The full concentrate and fourteen consecutive tail samples were collected. For the purpose of producing visual evidence of the impact of magnetite, the separable bowl was used.

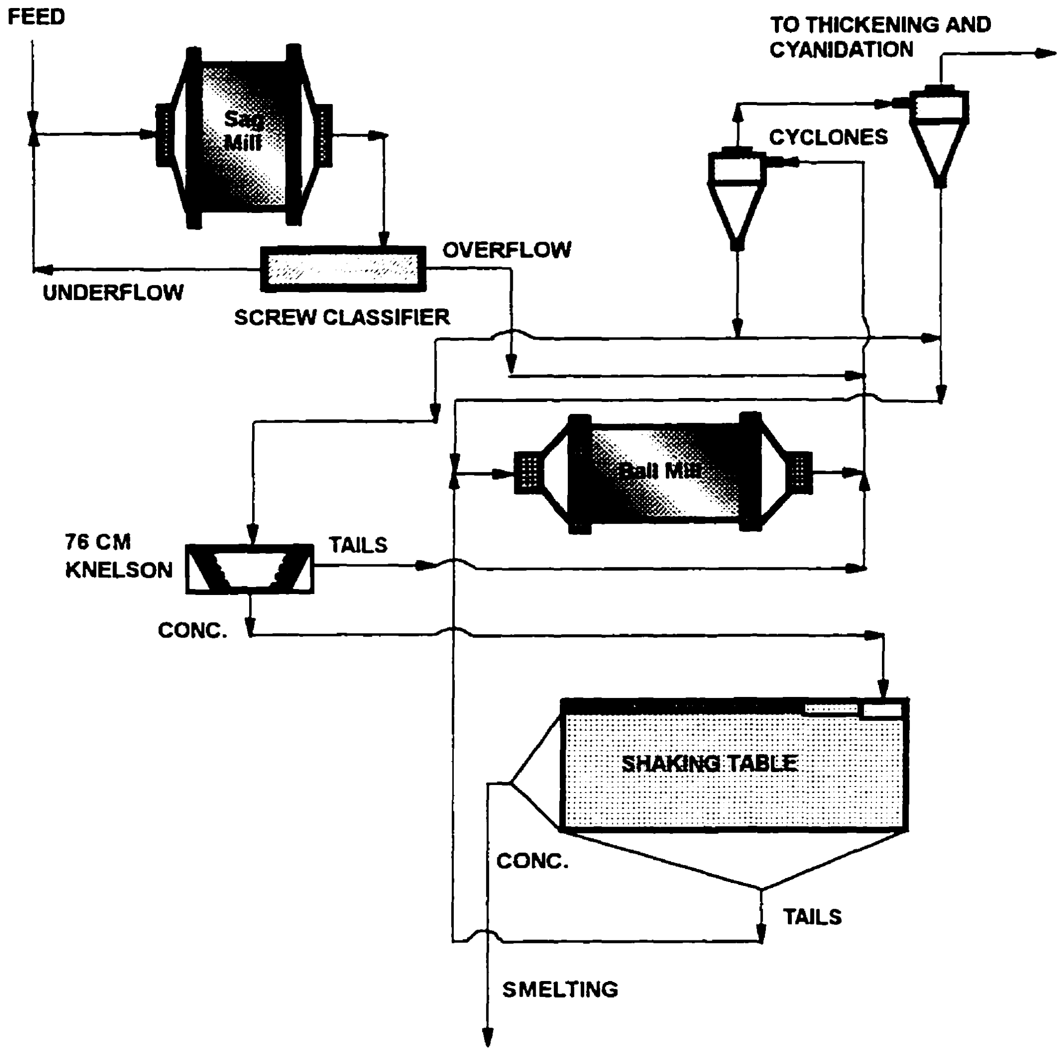

FIGURE 8-25 Simplified Grinding/Gravity Circuit of Casa Berardi

8.6.3 Test Results

A summary of the test results is shown in Table 8-6; details are found in Appendix 8-5. Size-by-size results of tests 1 to 3 are shown in Figures 8-26 to 8-28. Gold losses as a function of the mass fed for tests 2 and 4 are given in Figure 9-29. The four tests are compared in Figure 8-30. A series of photographs showing where gold reported in the riffles is given in Figures 8-31 to 8-34.

TABLE 8-6 Results of Knelson Concentrator Tests for Les Mines Casa Berardi

Test 1 Original table tails

Product	Mass (%)	Gold (g.t^{-1})	Recovery (%)
Concentrate	2.87	20966	49.4
Tail	97.13	636	50.6
Total	100.00	1220	100.0

Test 2 -212 μm table tails

Product	Mass (%)	Grade (g.t^{-1})	Recovery (%)#	Recovery (%)*
Concentrate	2.63	63185	81.6	77.0
Tail	97.37	384	18.4	17.4
Total	100.00	2035	100.0	94.4

Test 3 -150 table tails

Product	Mass (%)	Grade (g.t^{-1})	Recovery (%)#	Recovery (%)*
Concentrate	3.84	50313	74.3	62.7
Tail	96.16	693	25.7	21.6
Total	100.00	2597	100.0	84.3

Test 4 -212 μm table tails with magnetite pre-feed

Product	Mass (%)	Grade (g.t^{-1})	Recovery (%)#	Recovery (%)*
Concentrate	0.29	454220	67.3	63.5
Tail	99.71	657	32.7	30.9
Total	100.00	1973	100.0	94.4

* *Recovery was calculated on the basis of 100% in the total table tails.*

\# *Recovery was calculated on the basis of 100% of the Knelson Concentrator feed.*

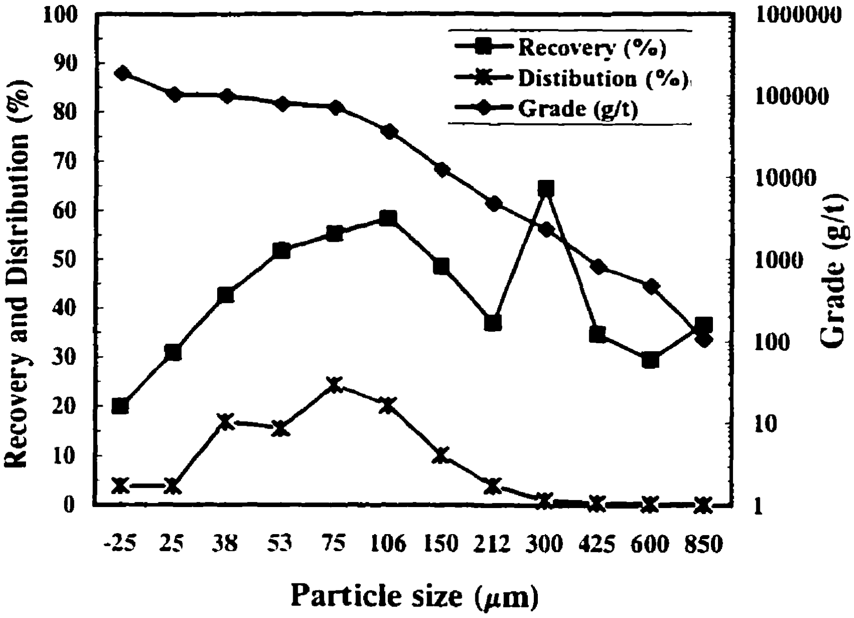

FIGURE 8-26 Size-by-Size Performance of the Casa Berardi Test 1 (Feed: total table tails)

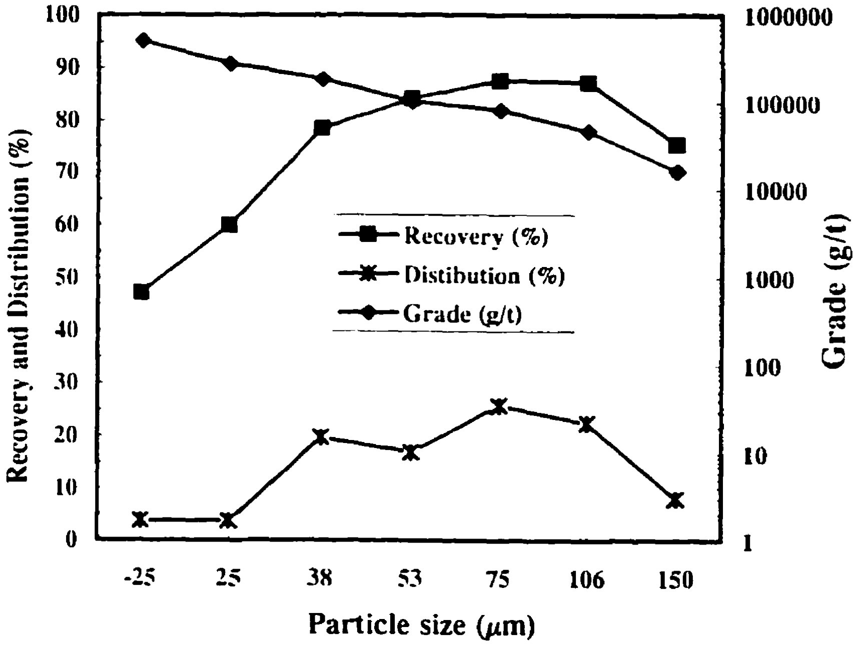

FIGURE 8-27 Size-by-Size Performance of the Casa Berardi Test 2 (Feed: -212 μm table tails)

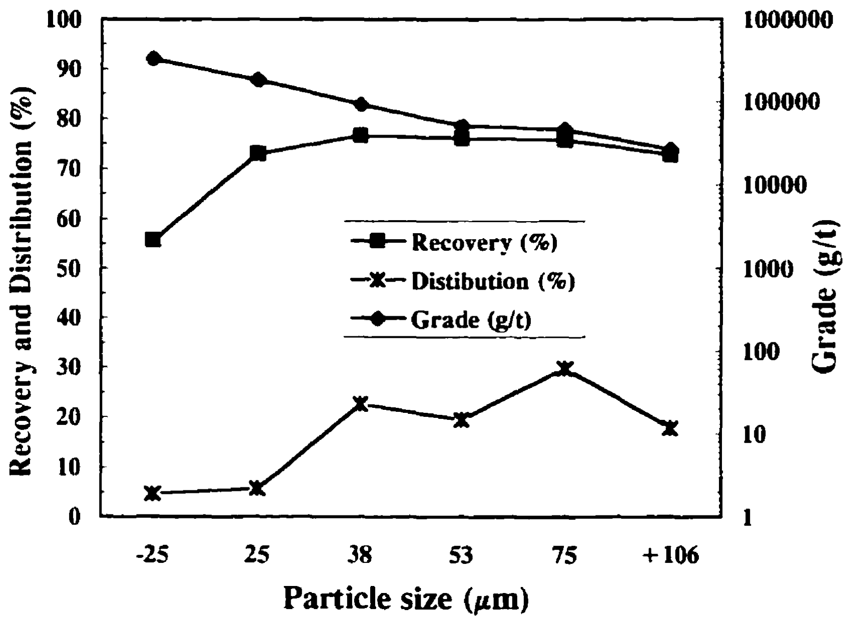

FIGURE 8-28 Size-by-Size Performance of Casa Berardi Test 3 (Feed: -150 μm table tails)

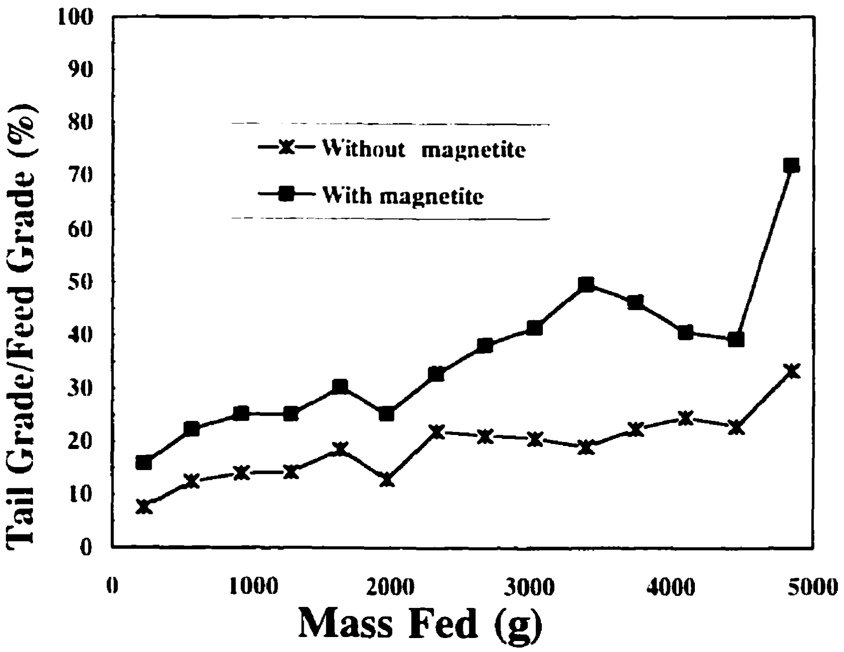

FIGURE 8-29 Evolution of the Tail Grade for Casa Berardi Tests 2 and 4 (Feed: -212 μm table tails)

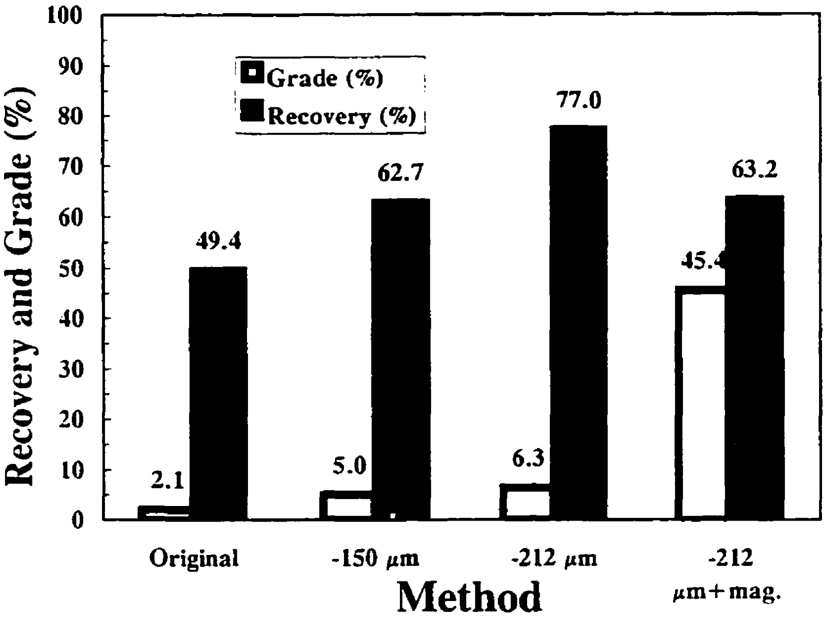

FIGURE 8-30 Comparing the Results of the Four Casa Berardi Tests

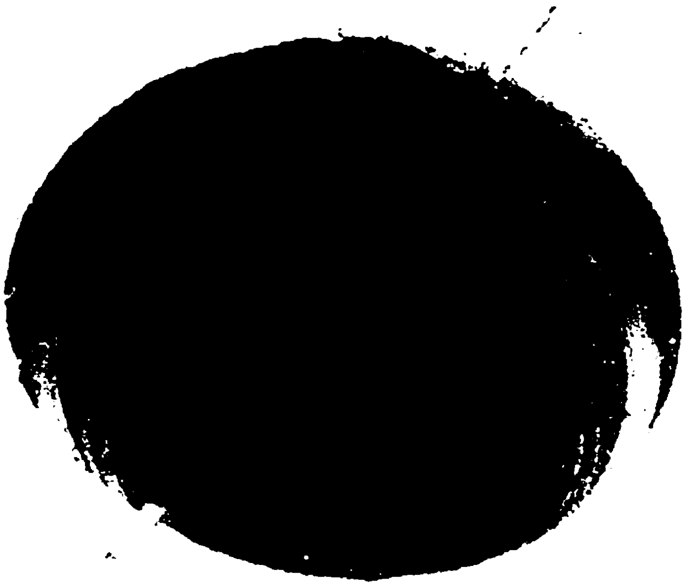

FIGURE 8-31 Frozen Concentrate of Casa Berardi Test 4 Prior to Separation

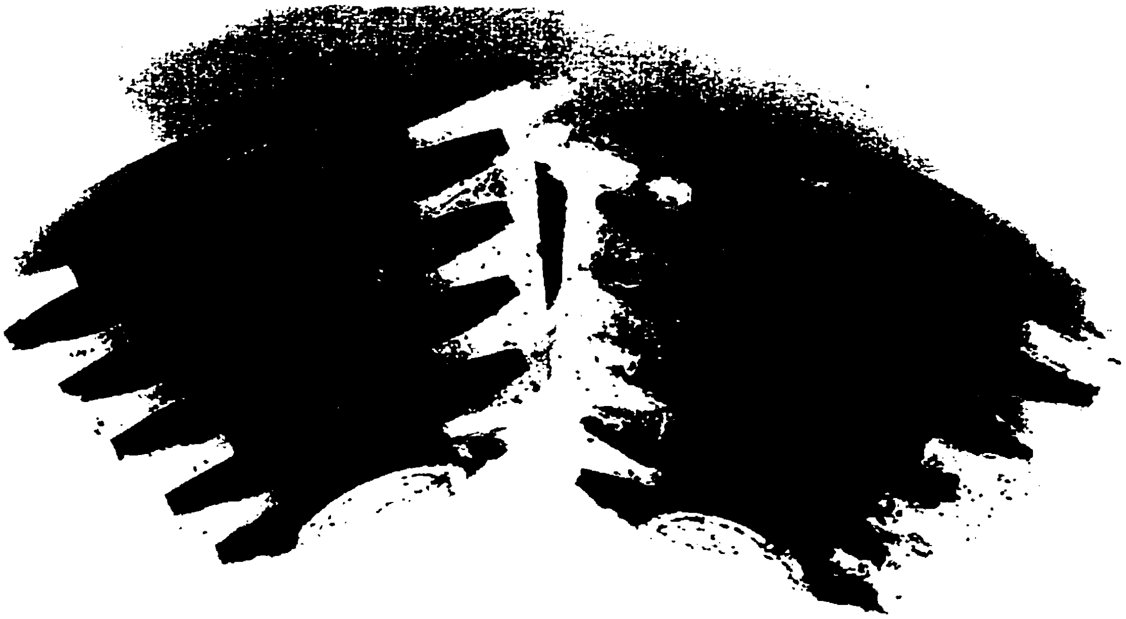

FIGURE 8-32 Frozen Concentrate of Casa Berardi Test 4 after Separation of the Two Halves

FIGURE 8-33 Close-up of Part of the Concentrate of a Ring (Casa Berardi Test 4)

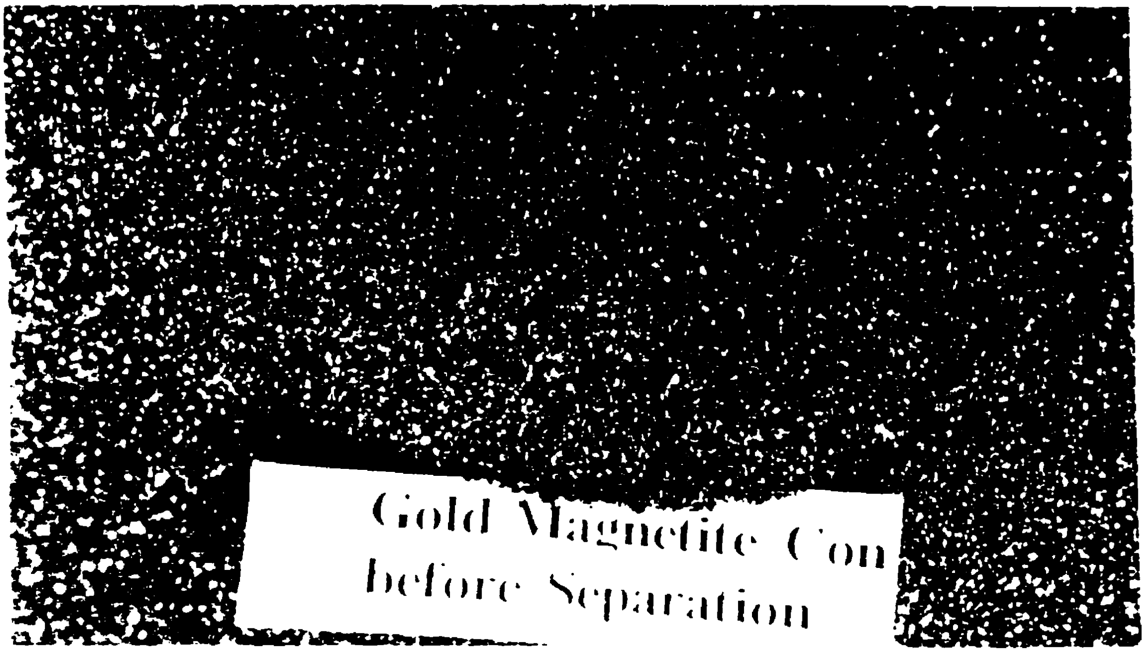

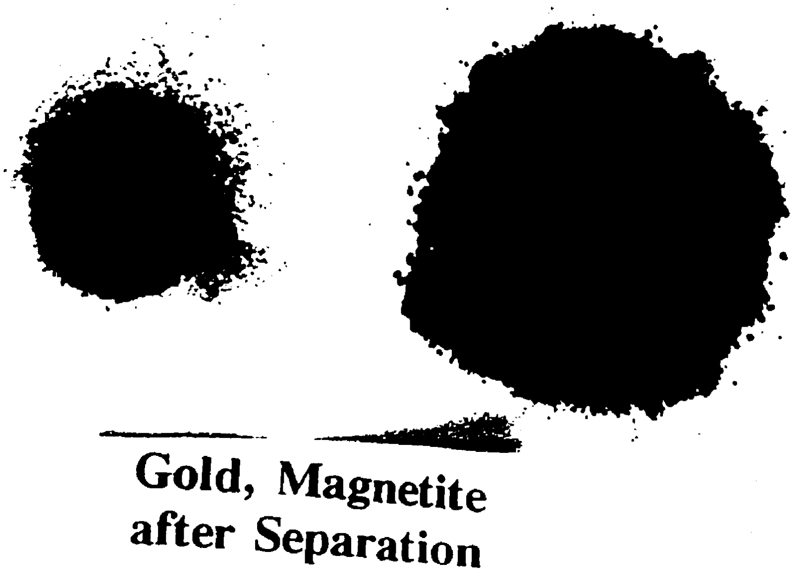

FIGURE 8-34 and 8-35 Total Concentrate of Casa Berardi Test 4 before and after Magnetic Separation

8.6.4 Discussion

Gold Distribution

In the Casa Berardi table tails, 94.4% of the gold was finer than 212 μm, in 55% of the mass; 84.3% of the gold was finer than 150 μm, in only 37% of the mass; 86.8% of the total gold was in the size range of 38-212 μm (Appendix 8-5). Therefore, it could be expected that removal of the oversize would be highly beneficial to further processing.

The Knelson Concentrator Performance

For the processing of the original table tails, a recovery of 49.4% was obtained with a grade of 2.10% Au. The results are similar to those of table tail samples from other mills, such as 41.5% for Hemlo and 45.6% for Meston Resources.

Recovery as a function of particle size follows generally observed Knelson performance, with the highest fraction recoveries in the intermediate size range, 38 to 212 μm. The peak at 300-425 μm cannot be considered statistically significant (it can be the result of one or very few gold flakes), because of the very low amount of gold involved. Woodcock has analyzed the Casa Berardi gravity recoverable gold content, and found very little above 212 μm (Woodcock, 1994).

When processing the -212 μm fraction (test 2), a total recovery of 77.0% (on the basis of 100% in total table tails) with a grade of 6.3% Au was obtained. Although only 55% of the total mass was processed, the recovery obtained was 27.6% higher than when processing the total tails, with a gold grade three times higher (Figure 8-30).

For the processing of -150 μm material (test 3), a total recovery of 62.7% was achieved with a grade of 5.0% Au. Only 37.2% of the total mass was processed, but the recovery obtained (on the basis of 100% in total table tails) was 13.3% higher than when processing the total table tails, with a concentrate grade 2.4 times higher (Figure 8-30).

However, compared to that of processing -212 μm fraction, the recovery was 14% lower. This is because the fraction of 150-212 μm contained 10% of the total gold that is easily recovered by the Knelson Concentrator.

Further Upgrading with Magnetite

For the -212 μm table tails with magnetite pre-fed, after separation the non-magnetic concentrate graded 45.4% Au, 22 times that of processing the entire tails, with a recovery 13.8% higher. The magnetite fraction assayed 273 $g.t^{-1}$ Au, at a cost of recovery of only 0.4%. This confirms the effectiveness of the magnetite pre-feed once again.

Observations of the Gold Concentrate Configuration

In Chapter 6, the distribution of tungsten in Knelson concentrates was measured and depicted using a separable bowl and synthetic ores. Figures 8-31 to 8-33 depict how, with an actual gold sample and the same separable bowl, similar results are achieved. Figure 8-31 shows the whole Knelson bowl with the concentrate of test 4. Gold accumulated on the surface, at a particularly high grade in the first ring of the bowl. Figure 8-32 shows the two halves the bowl; almost no gold particles can be found below the surface layer of gold.

Figure 8-33 shows a close view of a piece of frozen concentrate scooped out of a ring and confirms that gold particles reported almost only on the inner section of the riffle in a thin layer of high purity. Figures 8-34 and 8-35 show the bulk concentrate before and after magnetic separation. Even before separation, gold particles could be identified. After separation, the gold-enriched product showed a very high gold content, in a much lower mass than that of the magnetite product. This set of photographs makes it easy to understand why concentrate grade can be greatly increased with the magnetite pre-feed.

8.7 Les Resources Aurbel Inc.

8.7.1 Laboratory Testwork

Aurbel, a division of Les Resources Aurbel Inc., is located in Val d'Or, Québec. On May 4, 1994, a 33.2 kg sample of Aurbel table tails was received at McGill. Only two tests were performed, as Aubel did not fund the present work.

Test 1: A 5.4 kg sub-sample of the total tails was fed to the Knelson Concentrator at a feed rate of 370 $g.min^{-1}$ and a fluidization water flowrate of 6 $L.min^{-1}$. The complete tail and concentrate were collected.

Test 2: A 4 kg sub-sample of -212 μm tails was treated, after a 200 g magnetite pre-feed, at a feed rate of 370 $g.min^{-1}$ and a fluidization water flowrate of 4.4 $L.min^{-1}$. One concentrate and eleven tail samples were sequentially collected.

TABLE 8-7 Results of the Knelson Tests for the Aurbel Table Tail Sample

<table>
<tr><td colspan="5">*Test 1 Original table tails*</td></tr>
<tr><td>Product</td><td>Mass (%)</td><td>Grade ($g.t^{-1}$)</td><td colspan="2">Recovery (%)</td></tr>
<tr><td>Concentrate</td><td>3.44</td><td>22309</td><td colspan="2">46.4</td></tr>
<tr><td>Tail</td><td>96.56</td><td>919</td><td colspan="2">53.6</td></tr>
<tr><td>Total</td><td>100.00</td><td>1665</td><td colspan="2">100.0</td></tr>
<tr><td colspan="5">*Test 2 -212 μm table tails with magnetite pre-feed*</td></tr>
<tr><td>Product</td><td>Mass (%)</td><td>Grade ($g.t^{-1}$)</td><td>Recovery (%)#</td><td>Recovery (%)*</td></tr>
<tr><td>Concentrate</td><td>0.85</td><td>189754</td><td>51.8</td><td>28.0</td></tr>
<tr><td>Tail</td><td>99.15</td><td>1553</td><td>48.2</td><td>26.3</td></tr>
<tr><td>Total</td><td>100.00</td><td>3153</td><td>100.0</td><td>54.3</td></tr>
</table>

* *Recovery was calculated on the basis of 100% in the total table tails.*

\# *Recovery was calculated on the basis of 100% of the Knelson Concentrator feed.*

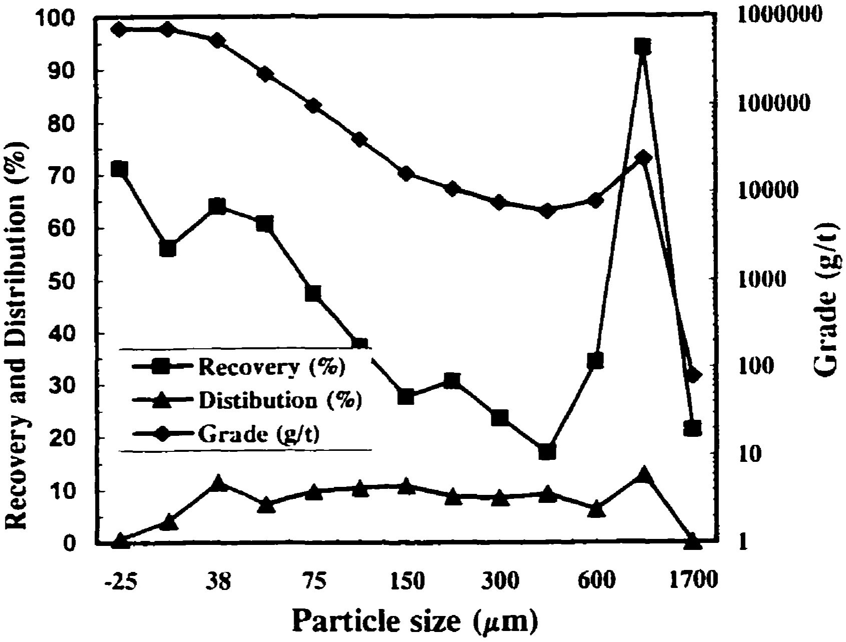

FIGURE 8- 36 Size-by-Size Performance of the Aurbel Test 1 (Feed: total table tails)

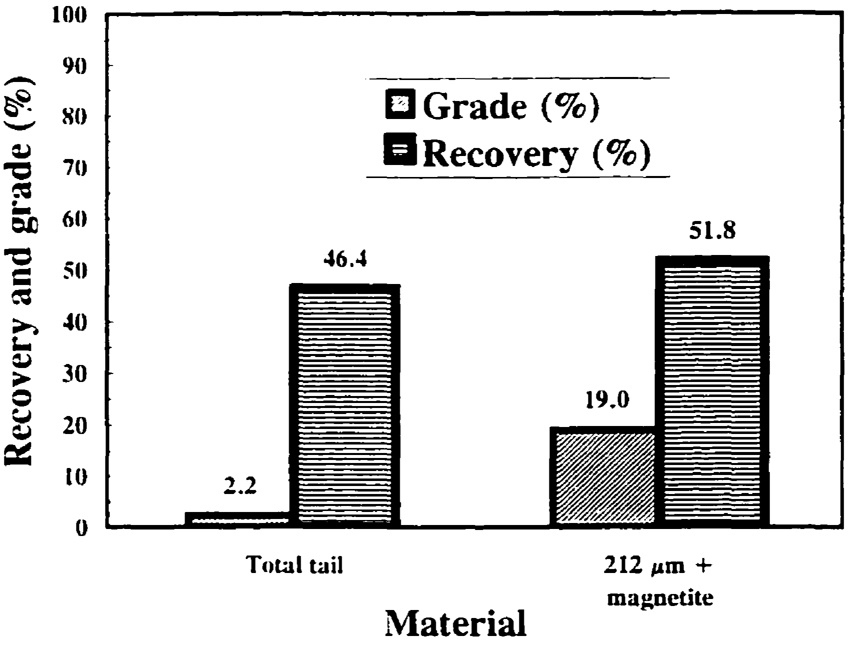

FIGURE 8-37 Comparing the Results of the Aurbel Tests 1 and 2

8.7.2 Test Results

A summary of the test results is shown in Table 8-7; details are given in Appendix 8-6. Size-by-size performance of test 1 is shown in Figure 8-36. Results of the two tests are compared in Figure 8-37.

8.7.3 Discussion

Compared to the other table tails, both the solids and gold size distributions of the Aurbel table tails were coarser (see Appendix 6). Gold was finer than the table tail, as 63% of the gold was finer than 300 μm, compared to 40% of the table tails. From a feed grade of 1655 g.t^{-1}, the first test yielded a recovery of 46.4% at a grade of 2.23% Au. By processing the -212 μm table tails with 200 g magnetite pre-feed, both recovery and grade were improved, to 51.8% and 3.74% Au, respectively. Since the -212 μm fraction only contained 54.3% of the total gold, the recovery (referring to the entire table tails) was only 28%. After magnetic separation, the final concentrate assayed 19.0% Au; only 0.7% of the gold reported to the magnetic fraction (it would be recycled to the next pre-feed run in normal plant practice).

8.8 Resources MSV Inc.

8.8.1 Laboratory Testwork

On April 6, 1994, 1600 g of table tails, 430 g of table feed and 86 g of table middling were received at McGill University. Since the samples mass were limited, only one test, with the table tails sample, was performed. The full table tails sample was fed to the Knelson Concentrator at a fluidization water flowrate of 5.2 L.min^{-1} and a feed rate of 350 g.min^{-1}.

8.8.2 Test Results and Discussion

The main results are summarized in Table 8-8; details are shown in Appendix 8-7. The recovery, grade and gold distribution as a function of particle size are shown in Figure 8-38.

TABLE 8-8 Results of the Knelson Concentrator Test for MSV

The original table tails			
Product	Mass (%)	Gold (g.t^{-1})	Recovery (%)
Concentrate	7.01	933	79.7
Tail	92.99	18	20.3
Total	100.00	82	100.0

Compared to the other table tails, MSV table tails had the coarsest size distribution and the lowest grade, only 82 g.t^{-1}. Below 300 μm, 83.4% of the gold reported in only 30.5% of the tail mass. Gold losses in the table tails were mainly fines. The test yielded a high recovery, 79.7%, which can attributed to almost complete gold liberation in a relatively narrow size range.

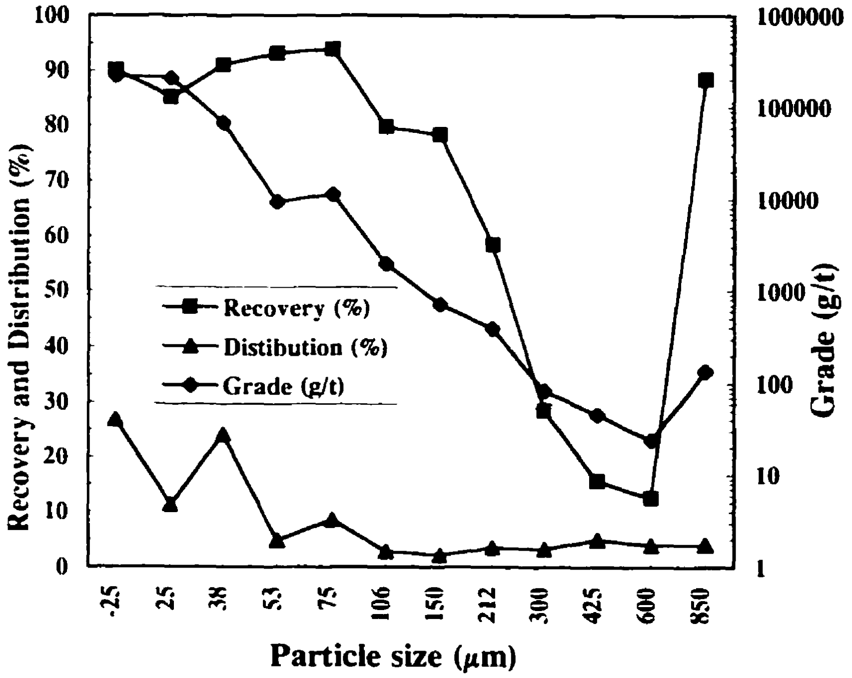

FIGURE 8-38 Recovery, Grade and Distribution for MSV

8.9 Discussion

Tables 8-9 and 8-10 summarize the table tails data. Only Lucien Béliveau is a relatively fine feed; of the others, Snip is the finest, Aurbel and MSV are the coarsest. Gold has a highly variable distribution: Aurbel is the coarsest, with a F_{80} of 405 μm, and virtually no -25 μm gold; Meston has the most -25 μm gold, 43%, and, the smallest F_{80}, 51 μm. The performance of the laboratory Knelson Concentrator is loosely correlated with the feed data: processing the total table tails yielded the highest recovery with the finest feed, Lucien Béliveau; other tests yielded very similar results, recoveries of 34 to 46%, except for MSV (whose test results, because of the small mass used, are subject to caution).

TABLE 8-9 Properties of the Table Tails Processed

Mine Name	Grade (g.t^{-1})	Ore, F_{80} (μm)	Au, F_{80} (μm)	Au%, -25 μm
Béliveau	1070	113	119	23.0
Meston	3355	425	51	43.1
Hemlo	2735	274	160	1.7
Snip	150	228	145	3.1
Casa Berardi	1220	350	100	3.8
Aurbel	1665	565	405	0.6
MSV	82	565	156	26.7

When removing the oversize, recovery increased in all cases, even when calculated on the basis of the total table tails. Recovery based on the material fed to the Knelson varied between 63 and 92%, with not apparent correlation with the size distribution of gold (either its F_{80} or the %-25 μm).

The performance of the laboratory Knelson is a function of too many variables, such as mineralogy or prior processing, to be readily predicted from relatively simple size data. For example, if primary recovery is aimed at recovering only highly gravity recoverable gold, and table operation is very selective, the amount of GRG in the table tails will be high, as will the performance of the laboratory Knelson when processing the table tails; such seems to be the case at Hemlo, as the primary recovery unit is a rather overloaded 76 cm Knelson CD, and table operation is producing a high grade concentrate, typically 80% Au (Honan and Luinstra, 1996). To some extent, this is also the case at Casa Berardi. Both Hemlo and Casa Berardi have little -25 μm gold in their table tails, an indication that very fine gold is not recovered well by the primary Knelson[1]. For Snip, much of the coarse gold is unliberated, as it is associated with coarse pyrite recovered by the jig. Removing the coarse fraction (+212 μm) more than doubles Knelson performance.

TABLE 8-10 Recovery (%) of the Table Tails Tests

Name of Mine	Total Table Tails	-212 or -150 μm without Magnetite		-212 or -150 μm with Magnetite	
		To Feed	To Total	To Feed#	To Total#
Béliveau	81.5	-	-	-	-
Meston	45.6	63.4	54.5**	41.1**	49.1
Hemlo	41.5	91.8*	70.8	70.5*	54.1
Snip	33.8	68.4*	55.8	60.5*	49.4
Casa Berardi	49.4	81.6* 74.3**	77.0 62.7	67.3* -	63.5 -
Aurbel	46.4	-	-	51.8*	28.0
MSV	79.7	-	-	-	-

* -212 μm; ** -150 μm. # To Feed: recovery based on the Knelson feed; To Total: recovery based on the original total table tails.

Of interest are the tests where the progression of Laboratory Knelson

---

[1] At Casa Berardi, the feed to the primary Knelson is coarse, -1.7 mm, and contains significant concentrations of arsenopyrite, two factors that would favour the recovery of highly gravity recoverable gold.

Concentrator overload was monitored, which can be compared both to the synthetic feed data and the overload model. Two types of tests were performed, with and without magnetite pre-feed. Figures 8-39 and 8-40 compare the progression of overload, represented by the ratio of incremental tails grade to that of the feed, to the magnetite and coarse silica tests (fine silica did not produce any overload).

The -212 μm feeds of most tests have a similar size distribution to that of the fine magnetite tests. Without magnetite pre-feed, gold recovery should therefore approach that of tungsten with the fine magnetite gangue, in that tail grade should not increase significantly with increasing feed mass, as the relatively low grade of gold should minimize overload. Yet, Figure 8-39 shows quite a different response: initial tailing grade is not negligible, and increases slightly as each test progresses. That the initial tailing grade is not null is not surprising: some of the gold of the table tails is not gravity recoverable, because of incomplete liberation or inappropriate particle size and shape. This fraction is very small for Casa Berardi and Hemlo, as the Knelson Concentrators used recover mostly GRG, but it is significant for Snip, whose primary concentrate is produced by a jig. The increase in tails grade appears to take place at the very beginning of the test, as for the coarse magnetite gangue, rather than after a finite mass of concentrate has been recovered, as for the coarse silica and fine magnetite feed. The rate of increase is lowest for the low grade Snip sample, and highest for the Casa Berardi sample, whose feed grade, at 2035 g.t^{-1}, is slightly lower than Hemlo's, 3943 g.t^{-1}.

Figure 8-40 shows a different behaviour when magnetite is first fed to the Knelson. All tests exhibit an increase in tail grade as more mass was fed. The increase is least for Snip, and indeed is almost negligible. That of Meston is very significant, as it is similar to that of tungsten with coarse magnetite gangue. Hemlo and Casa Berardi display intermediate behaviours. None of the tests shows an "induction time" before the onset of overloading. All tests show an initial loss (no-zero tails grade), whose magnitude is similar to that of the tests without magnetite pre-feed.

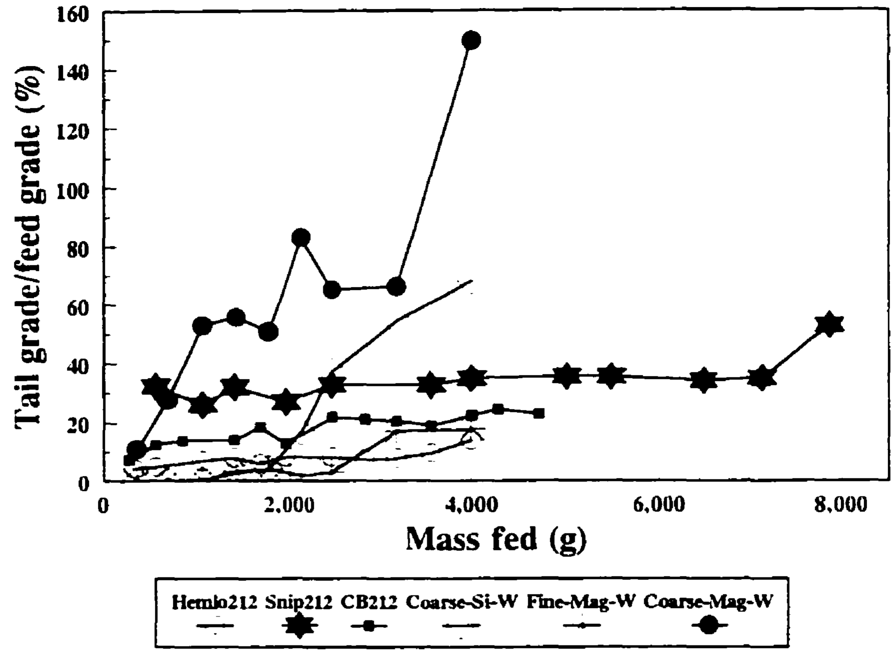

FIGURE 8-39 Evolution of Gold Losses without Magnetite Pre-Feed

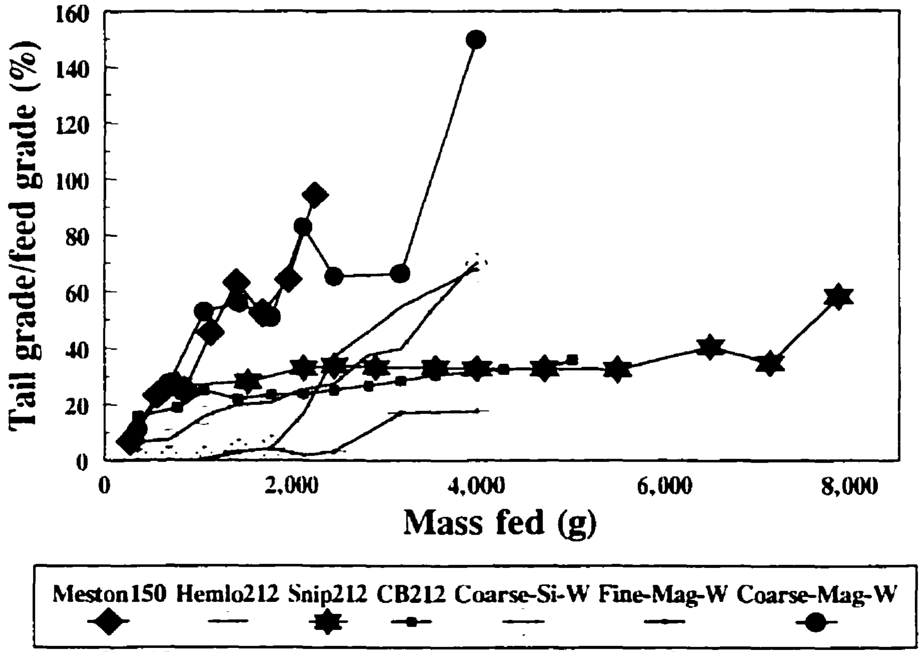

150: -150 μm, 212: -212 μm; Mag: magnetite; Si: silica, CB: Casa Berardi

FIGURE 8-40 Evolution of Gold Losses with Magnetite Pre-Feed

To continue data analysis, the data of Figures 8-39 and 8-40 must be treated statistically to filter out significant noise. An expedient approach will be to fit cumulative (rather than incremental) recovery to the overload model, with the addition of a correction factor, R_o, that accounts for the initial losses to the Knelson tails. R_o is the Knelson recovery at the beginning of the recovery cycle. This can be presented as,

$$R = R_o \frac{W_c + \frac{G_f}{K} \cdot [1 - e^{-K(W_f - W_o)}]}{(G_f \cdot W_f)} \tag{8-1}$$

The parameters of Equations 5-9 (for the synthetic feeds) and 8-1 (for table tails) were estimated using the QUATTRO.PRO 4.0 function OPTIMIZE with a quasi-Newton search, forward differentiating of derivatives, and tangent estimates of the variables, to minimize the sum of the squared residuals (fitted - measured recovery).

TABLE 8-11 Parameters of Equations 5-9 (Synthetic Feeds) and 8-1 (Table Tails Feeds)

Feed	W_o (g)	K (g^{-1})	R_o (fractional)
Coarse silica	1487	4.96E-04	-
Fine magnetite	1011	6.69E-05	-
Coarse magnetite	0	6.26E-04	-
Casa Berardi (no mag)	0	5.21E-05	0.915
Hemlo (no mag)	0	1.78E-05	0.956
Snip (no mag)	4336	1.31E-04	0.699
Casa Berardi (mag)	0	5.58E-05	0.844
Hemlo (mag)	257	1.61E-04	0.939
Meston* (mag)	169	5.93E-04	0.941
Snip (mag)	256	2.74E-05	0.732

* only table tails test at -150 μm, all others at -212 μm

no mag: without magnetite pre-feed; mag: with magnetite pre-feed

Equation 8-1 is similar to Equation 5-9 with the addition of the R_o term to account for the initial gold losses. Figures 8-41, 8-42 and 8-43 show that the initial model can fit the synthetic ore data well, as can the modified model for the table tails processing data, with and without magnetite pre-feed. The parameters of the two models are given in Table 8-11.

The data of Table 8-11 confirms the absence of induction time (or feed mass) before the onset of overload for the table tails data. The only exception, the Snip tails with no magnetite pre-feed, is numerically ill-conditioned, as the recovery curve is almost horizontal. The data can also be fitted with a null W_0, at a very small increase in the sum of squares; the R_o term then assumes a value of 0.716, much closer to what was measured with magnetite pre-feed, 0.732; the erosion rate constant then takes a value of 2.20E-05 g^{-1}, which is also much closer to that measured with magnetite pre-feed, 2.74E-05 g^{-1}. Other test results are much better conditioned numerically, and the non-linear least-square fit yielded consistent results - i.e. independent of initial estimates.

The data of Table 8-11 also confirm that initial recoveries are very high for table tails originating from Knelson concentrates (Meston, Casa Berardi, Hemlo), and are only slightly lower with magnetite pre-feed: the largest difference is 0.07, or 7%, for Casa Berardi, and the smallest is 0.02 for Hemlo.

The erosion rate constants are of particular interest. First, magnetite pre-feed had little impact on the erosion rate constant, which is what one would expect, since the medium which is responsible for concentrate bed erosion is the same for the two types of test (the only major difference, for Snip, is numerically insignificant - see the above discussion). Second, the value of the erosion rate constant varies significantly, from 2.74E-05 g^{-1} for Snip (with magnetite pre-feed) up to 5.93E-04 g^{-1} for Meston. Figure 8-44 suggests that there is a correlation between the head grade and K (for the four tests with magnetite pre-feed). The relationship is not simply proportional, as the head grades

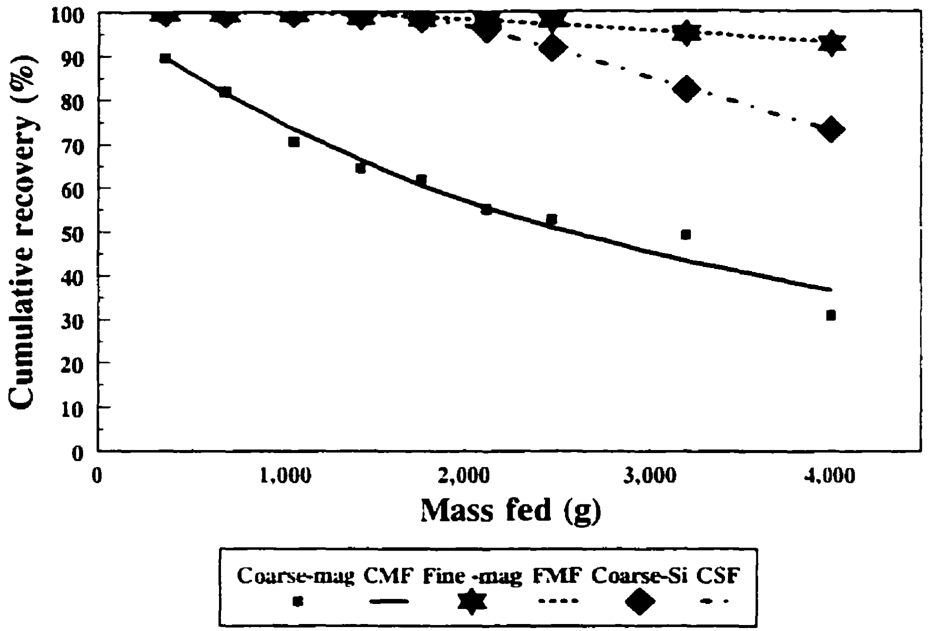

CMF: Coarse Magnetite Fit; FMF: Fine Magnetite Fit; CSF: Coarse Silica Fit

FIGURE 8-41 Fit of the Synthetic Ores to Equation 5-9 (parameters in Table 8-11)

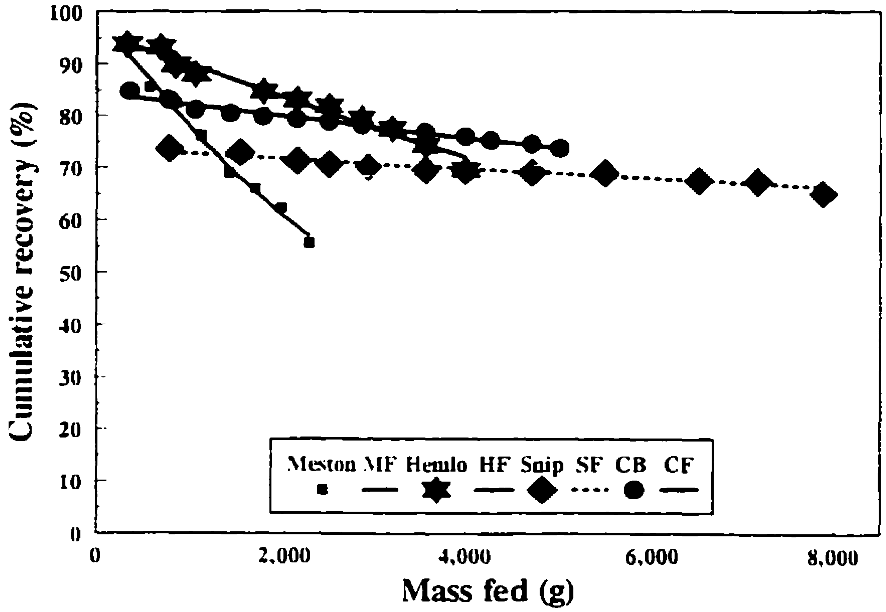

MF: Meston Fit; HF: Hemlo Fit; SF: Snip Fit; CB: Casa Berardi; CF: Casa Berardi

FIGURE 8-42 Fit of the Table Tails Processing Data with Magnetite Pre-Feed to Equation 8-1 (Parameter in Table 8-1)

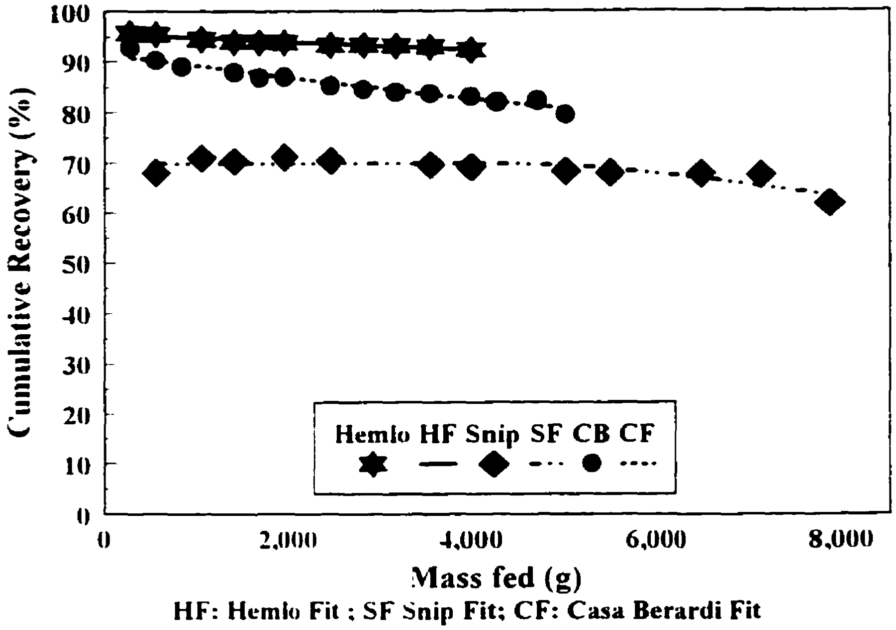

FIGURE 8-43 Fit of the Table Tails Processing Data without Magnetite Pre-Feed to Equation 8-1 (Parameters in Table 8-11)

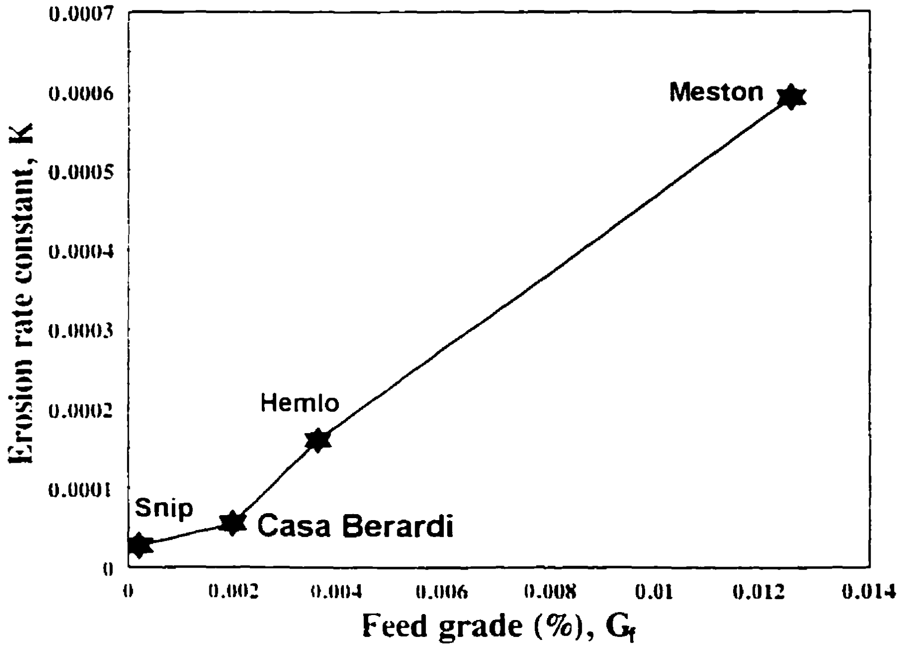

FIGURE 8-44 K as a function of G_f

vary by a factor of 61, much more than the rate constant, a factor of 22. it could be postulated that as the mass of gold recovered builds up, it extends further into the slurry, and is more exposed to erosion. The differences are significant: the Meston test recovered 15 grams of gold, and the Snip test only 1 gram. The range for the K values is consistent with those estimated with synthetic feeds, with Meston's close to that of coarse silica gangue (the two highest values of K), and Snip's slightly lower than that of fine magnetite. The synthetic feeds had shown that the erosion rate constant was a function of both tungsten and gangue particle size. With table tails feeds, results are even more difficult to analyze, as particle shape, liberation and density (all gold particles contain some silver) can affect the rate constant. It is not surprising that the Meston tails yielded the highest value of K, as they contain the highest proportion of -25 μm gold, in electrum with a 20% silver content (hence with a specific gravity of 17, compared to 19 for pure gold).

8.10 Summary

The test results of the Knelson Concentrator of seven actual gold table tails have demonstrated the following key points:

1. Table tails contain significant amounts of gravity recoverable gold, essentially free gold that can be recovered with a laboratory Knelson Concentrator. Most of this gold is fine, typically 77 to 94% -212 μm.

2. A very effective means of recovering this fine gold is to remove the lower grade +212 μm fraction by screening, and to feed the -212 μm fraction to a Knelson Concentrator.

3 A very high grade concentrate can be produced using a magnetite pre-feed which is removed magnetically from the bulk concentrate at the end of the test. The procedure results in some very small losses because of concentrate bed overload,

and should only be performed to produce a concentrate with a very high gold content.

4 The table tails data fit a slightly modified version of the overload model: initial recovery must be corrected for non gravity recoverable gold, and the onset of overload occurs very early in the recovery cycle for almost all ores tested. The erosion rate constant is highly variable, and has a function of gold content.

The above conclusions can be applied to plant practice, with minimum scale-up considerations, since a 30 cm Knelson Concentrator would probably be used. Already, the practice of directing table tails to a Knelson Concentrator has been implemented at Agnico-Eagle's La Ronde Division with success. Typically, 5% of the 20% gravity production is scavenged using a 30 cm Knelson Concentrator treating the tails of the two full size Gemeni tables. At Lucien Béliveau, the recycling of the table tails to the 76 cm Knelson Concentrator resulted in a significant increase in gravity recovery. In both cases, the potential for additional recovery and high grade concentrate has yet to be tapped, as the optimum scavenging procedure (oversize removal and magnetite pre-feed) is not followed.

Maybe more importantly, this testwork validates some of the results obtained with the synthetic ores, and partially confirms the legitimacy of using tungsten to mimic gold in gravity testing, in this case for the Knelson Concentrator. The tungsten/silica or magnetite mixtures yielded much "clearer" results, that lent themselves to modelling. Gold ores have a more complex behaviour, and the generally flaky particles can be eroded more easily, especially when feed grade is high. This sets limits to the applicability of synthetic feeds, whose findings should be validated and adjusted by additional work on gold samples. Differences between the responses of tungsten and gold provide very useful insight into the effect of gold's particle shape, as was the case here.

It is expected if the table feed (rougher concentrate of the Knelson Concentrator) was fed to a cleaner Knelson Concentrator with a magnetite pre-feed, better results would be achieved than with a shaking table. This may not prove to be more practical than the use of a shaking table to produce the smeltable grade concentrate with the addition of a Knelson Concentrator as a scavenger, but it is an avenue worth considering that would first require experimental validation. The main drawback of by-passing the table may well be of primary concentrate that the very high head grade will result in a high erosion rate constant, should the trend of Figure 8-44 hold.

CHAPTER 9 CONCLUSIONS

9.1 Overall Conclusions

- A new method for the study of the basic behaviour of minerals and separation mechanisms in the Knelson Concentrator, using synthetic ores and bowls with different features was established. The use of metallic tungsten to mimic gold has proved particularly effective. Particles with both spherical and irregular shapes, and with different sizes, have been used.

- Overloading a Knelson Concentrator has been systematically investigated using four types of gangue. For coarse magnetite, overload took place almost at the very beginning of the recovery cycle; at the end, the concentrate bed was severely eroded. For coarse silica, the onset of overload required the growth of a sizeable concentrate bed, before significant bed erosion (which was very particle size dependent) occurred. Fine magnetite gangue actually triggered its overload sooner than coarse silica, but with much less severe consequences. For the fine silica gangue, no overload was measured. A two-parameter model for overload was derived, which fits the experimental data well.

- A slightly modified version of the overloading model was used to fit data derived from the processing of table tails samples. Model fit was good; unlike synthetic feeds, overload was triggered very early in the recovery cycle and its rate constant higher than for tynthetic feeds, and dependent on feed grade.

- Overload is the result of physical contact (i.e. collisions) between gangue being fed to the unit and tungsten (or gold) particles already recovered. It is therefore linked to particle mass, i.e. gangue density and particle size, as well as tungsten (or gold) particle size. The study of overload is of significance to gold recovery practice with Knelson Concentrators. How soon in the loading cycle overload takes place, and how severe it is, depend heavily on the nature of the gangue type, and will dictate how frequently a Knelson should be stopped to recover its concentrate. Although this should be investigated for each individual gold gravity circuit, evidence suggests that problems are much more likely to occur with high density gangue, and can be controlled with careful sizing of the Knelson feed.

- In the Knelson Concentrator, particle behaviour and separation mechanisms may be described as follows:

    - The concentrate rings are completely fluidized only at very beginning of the recovery cycle.

    - As soon as a material bed builds up in each ring, there is almost no mass exchange between the fresh feed and the solids recovered in the outer section of the rings, since the material in the rings is practically unfluidized.

    - Separation takes place at the surface of the rings, where the concentrate bed is completely fluidized by the tangential fluidization water flow and the Bagnold shearing effect provided by the slurry flow.

    - In the separation zone, whether a particle is collected at the surface of a ring or rejected to the tails mainly depends on competing forces: centrifuge, drag and fluidization water flow pressure, which causes vigorous collisions between particles. At the same time, consolidation trickling (or the percolation effect) of heavy particles and the high density of the separation zone accelerate the enrichment process, especially for fine, heavy particles.

  - Material recovered at the surface of the concentrate bed can be subsequently eroded away.

- As most material in the outer section of each concentrate ring is recovered unselectively, a "filler", such as magnetite, can be pre-fed to the Knelson to initially build up the concentrate bed. This could be followed by the normal recovery cycle. Magnetite would then be recovered magnetically from the concentrate, yielding a substantially upgraded non-magnetic concentrate. This technique has been demonstrated on a large number of samples of table tails (tails of the cleaning step which normally follows primary gravity recovery)

- Bowl#1 (the cleaner bowl, whose riffles were approximately half-filled with a porous nylon filter) was superior to the conventional bowl both in recovery and grade based on laboratory-scale tests. The effect of the texture-filled rings was similar to that of the filler pre-feed. However, this filter would very likely scale up and rapidly become obstructed in plant operation (a problem already encountered with the conventional bowl).

- The results obtained with bowl#2 (a conventional bowl with 2 mm shaven off the riffles) indicate that even though most of the heavy particles do not penetrate deeply into the rings, the outer section of the rings is still necessary for effective fluidization water distribution.

- The results of bowl#3 (with a different distribution of fluidization water injection holes) show the significant impact of superficial fluidization water velocity on the performance of the Knelson Concentrator. Bowl#3 was designed with nearly even superficial fluidization water velocity ring-by-ring. Unlike the conventional bowl, much better fluidization of the concentrate bed in the lower rings (especially the bottom one) can be achieved in this case; as a result, overload can be postponed or minimized.

- The results obtained with synthetic ores were confirmed with actual gold table tails. For any gold table tails, removing the +150 or +212 μm fraction to process only the undersize will increase both recovery and concentrate grade. If a filler is first fed to the Knelson Concentrator, the gold grade can be considerably increased (up to the smeltable grade). For example, a concentrate containing 625 $kg.t^{-1}$ Au was obtained from Hemlo -212 μm gold table tails assaying 3.6 $kg.t^{-1}$ Au, an enrichment ratio of 174, at a recovery of 70.5%.

9.2 Claims for Original Research

- An effective new methodology, based on the use of tungsten as a substitute for gold and separable bowls to characterize the distribution of concentrate in-situ, has been derived and used to study the separation mechanisms of the Knelson Concentrator.

- Using different types of gangue, overload of the Knelson Concentrator has been systematically investigated for the first time and described with a two-parameter phenomenological model. These results are of significant practical importance for the operation of Knelson Concentrators in gold mills.

- Using the separable bowls, the concentrate configuration and distribution along both longitudinal and horizontal axes inside the Knelson Concentrator bowls was measured for the first time, and has led to a better understanding of the separation mechanisms in the Knelson Concentrator, which should result in improvement of its design and performance.

- Feed pre-sizing resulted in a significant improvement both in concentrate grade and recovery. Feeding a "filler", such as magnetite, prior to processing gold ores or concentrates, resulted in significantly higher concentrate grade, which makes it possible to consider the use of the Knelson Concentrator as a cleaner to produce smelting-grade concentrates.

- Three Knelson bowls with different configurations were tested, two of them for the first time. The importance of adequate fluidization water distribution was demonstrated. For low density gangue, Knelson performance could be significantly increased by judiciously choosing the most appropriate bowl geometry. For high density gangues, severe erosion problems tend to mask the effect of fluidization water distribution.

9.3 Suggestions for Future Work

- In this research, overload tests were carried out based on both coarse and fine magnetite and silica. Overload with the materials having densities between 2.7 to 5.0 and different size ranges should be studied[1].

- The centrifugal force is one of the main forces acting on a particle during separation in a Knelson Concentrator. All tests in this research were carried out with a Knelson of 60 'g'. It is suggested that a variable speed unit be tested for gangues of different size distributions and densities. Of particular interest is the problem of recovering gold from higher density gangues, and whether or not this problem can be alleviated at higher rotation velocities.

- Superficial fluidization water velocity was found to be a most important operating parameter for the Knelson performance when the bowl rotation speed is kept

---

[1] This work has been initiated by Wei (1995), under the supervision of the candidate.

constant. It is suggested that more modified bowls be designed and tested in order to find optimum fluidization water distributions for gangues of different densities and size distributions.

- It was found in this research that the use of magnetite as a filler led to a significant increase of concentrate grade, but with some drop of recovery. The effect of the size distribution of magnetite on the gold grade and recovery should be studied. Feed pre-sizing and the use of a suitable size range of magnetite as a filler should be tested commercially, and this testwork carefully documented[2].
- It is suggested that chlorination and/or thiocyanate leaching be conducted on high grade gold gravity concentrates. This might yield a complete technology of upgrading gold gravity concentrates; i.e. the Knelson Concentrator being a cleaner to produce high grade concentrates, followed by chlorination or thiocyanate leaching. As a result, pure gold and silver would be obtained, and the expensive, environmentally costly technology of smelting and traditional refining could be by-passed.

---

[2] As a result of the present work, part of the scavenging procedure has been applied at the Lucien Béliveau, Chimo, MSV and Agnico Eagle La Ronde Division mills. Significant increases in gold recovery have been informally reported, but not documented.

REFERENCES

1 Adamson, R.J., Gold Metallurgy in South Africa, printed by Cape & Transval Printers Ltd, Cape Town, 1972, 452 p.

2 Anderson, M.N., Canadian Gold Today...and Tomorrow? Engineering and Mining Journal, Vol. 190, No. 2, February 1989, C1-C23.

3 Ayat, M.G. and J.W. Leonard, Novel tracing technique for the coal preparation industry, Minerals and Metallurgical Processing, Vol. 4, No. 1, February 1987, pp. 43-45.

4 Bagnold, R.A., Experiments on a gravity-free dispersion of large solid spheres in a Newtonian fluid under shear, Proceedings of the Royal Society of London, Vol. 225, 99. pp. 49-63, 1954.

5 Banisi, S., A.R. Laplante and J. Marois, The behaviour of Gold in Hemolo Mines Ltd Grinding Circuit, CIM Bulletin, November-December 1991, Vol. 84, No. 955, pp. 72-78.

6 Barin, I., H. Barth and A. Yaman, Electrochemical investigation of the kinetics of gold cementation by zinc from cyanide solutions, Erzmetall, V.33, No.7/8, 1980, pp. 399-403.

7 Bath, M.D., A.J. Duncan and E.R. Rudolph, Some factors influencing gold

recovery by gravity concentration, Journal of the South African Institute of Mining and Metallurgy, June 1973, Vol. 73, No. 11, pp. 363-384.

8 Belardi, G., N. Sheau, P. Plescia and F. Veglio, Recent developments in gravity treatment of chromite fines, Minerals and Metallurgical Processing, Vol. 12, No. 3, August 1995, pp. 161-165.

9 Beniuk, V.G. and C.A. Vadeikis, J.N. Enraght-Moony, Centrifugal jigging of gravity concentrate and tailing at Renison Limited, Minerals Engineering, Vol.7, No. 5/6, 1994, PP. 577-589.

10 Bhappu, R.B., D.H. Reynolds, R.J. Roman and D.A.Schwab, Hydrometallurgical recovery of molybdenum from the Questa Mines, New Mexico, Bur. Mines Miner. Resour. Cir., 81, 1, 1965.

11 Bissonnette, B. and G. Ladouceur, L'usine de la mine Lucien C. Béliveau, Canadian Mineral Processors Regional Conference, Rouyn-Noranda, January 1991.

12 Blenkinsop, T.G., Small-scale gold mining in Zimbabwe, Agid News No. 61/62, February/May 1990, pp. 11-12.

13 Blowers, M., Handbook of Small Scale Gold Mining for Papua New Guinea, Second Edition Pacific Resource Publications, Christchurch, 1992, 260 p.

14 Bodsworth, C., The Extraction and Refining of Metals, CRC Press, Amsterdam, New York, 1994, 605 p.

15 Bourke P., Flash flotation in the gold industry, Randol Gold Forum Perth'95

March 14-17, 1995, Perth, Western Australia, pp. 61-71.

16 Boyle, R.W., The Geochemistry of Gold and its Deposits, Geological Survey of Canada Bulletin No. 280, published by the Ministry of Supply and Services, Canada.

17 Boyle, R.W., Gold: History and Genesis of Deposits, Van Nostrand Reinfold, New York, 1987, 676 p.

18 Bridgwater, J., H.H. Cook and J.A. Drahun, Strain induced percolation, Powtch'83: Particle Technologies, I. CHEM. E. SYMPOSIUM SERIES NO. 69, Pergamon Press, 1983, pp. 171-187.

19 Bridgwater, J. and N.D. Ingram, Rate of spontaneous inter-particle percolation, Trans. Instn. Chem. Engrs, Vol. 49, 1971, pp 163-169.

20 Bridgwater, J., N.W. Sharpe and D.C. Stocker, Particle mixing by percolation, Trans. Instn. Chem. Engrs, Vol. 47, 1969, pp. T114-119.

21 Broadhurst, J.L. and J.G.H du Preez, A thermodynamic study of the dissolution of gold in an acidic aqueous thiocyanate medium using iron (III) sulphate as an oxidant, Hydrometallurgy, 32 (1993), pp. 317-344.

22 Buonvino, M., A study of the Falcon Concentrator, Master of Engineering thesis, McGill University, 1993, 195 p.

23 Burt, R.O., Gravity Concentration Technology, Elsevier Science publishers B.V., Amsterdam; New York, 1984, 605 p.

24 Burt, R.O., G. Korinek, S.R. Young, and C. Deveau, Ultrafine Tantalum Recovery Strategies, Minerals Engineering, Vol. 8, No. 8, 1995, pp. 859-870.

25 Campbell, S.D.G. and P.E.J. Pitfield, Training small-scale miners in Zimbabwe, Agid News, No.66, May 1991, pp. 15-18.

26 Carter, R. A., Snip's first year is a success, Engineering and Mining Journal, Vol. 193, No. 6, June 1992, pp. 29-31.

27 Chan, B.S.K. and R.H. Mozley, G.J.C. Childs, Extended trials with the high tonnage Multi-Gravity-Separator, Minerals Engineering, Vol. 4, No. 3/4, pp. 489-496, 1991.

28 Cho, E.H., Leaching studies of chalcopyrite and sphalerite with hypochlorous acid, Metallurgical Transactions, Vol. 18 B, No. 2, June 1987, pp. 315-323.

29 Cloutt, B., Gravity Concentration at W.M.C.'s S_T I_{VES} Gold Mines, Randol Gold Forum Perth'95 Proceedings, Australia, March 1995.

30 Coté, J., Y. Strasser and A. Cauchon, Cambpell Chibougamau, Mining Practice in Canada, CIM special Vol.16, 1978, pp. 91-93.

31 Coulson, J.M., J.F. Richardson, J.R. Backhurst and J.H. Harker, Chemical Engineering, Vol. 2, Fourth Edition, Particle Technology and Separation Processes, Pergamon Press, Oxford, New York. 1991, 968 p.

32 Cox, H. and A.K. Schellinger, An ion exchange approach to molybdic oxide, Engineering and Mining Journal, Vol. 159, No. 10, October 1958, pp.101-103.

33 Cramer, S.W., The legal battle for small-scale mining in the Philippines, Agid News, 61/62, May 1990, pp. 13-15.

34 Dadgar, A., Refractory concentrate gold leaching: cyanide vs. bromine, Journal of Metals, Vol. 41, No. 12, December 1989, pp. 37-41.

35 Dadgar, A., B.M. Sanders, J.A. Mckeown and R.H. Sergent, Leaching and recovery of gold from black sand concentrate and electrochemical regeneration of bromine, Advances in Gold and Silver Processing, Proceedings of the Symposium at GOLDTech 4, Reno, Nevada, September 10-12, 1990, edited by M.C. Fuerstenau, J.L. Hendrix, published by Society for Mining, Metallurgy, and Exploration, Inc., Littleton, Colorado, 1990, 291 p., pp. 75-89.

36 Darnton, B., Steve Lloyd and Mary Anne Antonioli, Gravity concentration: research, design and circuit performance at Montana Tunnels, Randol Gold Forum Vancouver '92, March 25-27, 1992, the Westin Bayshore, Vancouver, B.C. pp. 137-143.

37 Darnton, B., Steve Lloyd and Mary Anne Antonioli, Gravity circuit improvements at the Montana Tunnels Mine, KNELSON CONCENTRATOR Technical Papers and Performance Reports 1995, edited by Knelson Concentrators.

38 Davidson, R.A., G.A. Brown and C.G. Schmolt, The intensive cyanidation of gold-plant gravity concentrates, Journal of the South African Institute of Mining and Metallurgy, Vol. 78, No. 6, January 1978, pp. 146-165.

39 Davis, A. and T. Tran, Gold dissolution in iodide electrolytes, Hydrometallurgy, 26, 1991, pp. 163-167.

40 Davis, J.J., C.J. Wood and G.J. Lyman, The use of density tracers for the determination of dense medium cyclone partition characteristics, Coal Preparation, 1985 (2), pp. 107-125.

41 Davis, A., T. Tran and D.R. Young, Solution chemistry of iodide leaching of gold, Hydrometallurgy, 32 (1993), pp. 143-159.

42 Deschenes, G., Literature survey on the recovery of gold from thiourea solutions and the comparison with cyanidation, CIM Bulletin, Vol. 70, No. 895, 1986, pp. 76-83.

43 DeVries, F.W. and J.B. Hiskey, Environment Impact of Lixiviants: A Overview that Includes Noncyanide Chemistry, Randol Gold Forum Vancouver '92, March 25-27, 1992, the Westin Bayshore, Vancouver, B.C. pp. 89-92a.

44 Dewhirst, R.F., S.P. Moult and J.A. Coetzee, Intensive cyanidation for the recovery of coarse gold, Journal of the South African Institute of Mining and Metallurgy Vol. 84, No. 6, 1984, pp. 159-163.

45 Eissler, M., The Metallurgy of Gold, Fifth Edition, London: Crosby Lockwood and Son, New York: D. Van Nostrand Company, 1900, 638 p, pp. 345-447.

46 Fan, X., Retrospect and prospect of gravity separation, Metallic Ore Dressing Abroad, 7/8, 1991, pp. 21-26.

47 Farinha, P.A., M.J.N. Correia and J.R. Carvalho, Technical note: Leaching of gold from a Portuguese concentrate with thiourea, Minerals Engineering, Vol. 5, No. 8, 1992, pp. 953-959.

48 Finch, J.A. and G.S. Dobby, Column Flotation, Pergamon Press, Oxford, 1990, 180 p.

49 Finkelestein, N.P. and R.D. Hancock, A New approach to the chemistry of gold, Gold Bulletin, 7 (3), July 1974. P.72.

50 Finkelstein, N.P.,R.M. Hoare, G.S. James, D.D. Howat, J.J.E. van Zyl, H.J. Bovey, D.D. Marsden and W.D. Dougles, An aqueous chlorination process for the treatment of Merrill slimes and gravity concentrates from gold ores, Part I, Part II and part III, Journal of the South African Institute of Mining and Metallurgy, Vol. 67, No. 5, December 1966, pp. 196-245.

51 Forssberg, E. and T. Nordquist, Pilot plant trials of new gravity equipment, SME-MMP, 1986, pp. 86-89.

52 Franzidis, J.P., M.C. Harris and C.T. O'Connor, Review of column flotation practice on South Africa mines, Proceedings of an International Conference on Column Flotation, June 2-6, 1991, Vol. 2, pp. 479-509.

53 Furey, J.T., Rougher column flotation of gold tellurides, Proceedings-22nd Annual Meetings of the Canadian Mineral Processors, January 16-18, 1990, Ottawa, Ontario, pp. 242-256.

54 Galvin, K.P., S.K. Nicol and A.G. Waters, Selective ion flotation of gold, Colloids and Surface, 64 (1992), pp. 21-23.

55 Gasparrini, C., Gold and Other Precious Metals, Springer-Verlag, 1993, pp. 98-102.

56 Gaudin, A.M. Principles of Mineral Dressing, McGraw-Hill Book Company, 1939, New York, 554 p.

57 Giancola, D., J. Wan, T. Yap, and M. Syed, Canadian Mines Handbook, 1994-1995, Published by Doug Donnelly.

58 Glembotskii, V.A., V.I. Klassen and I.N. Plaksin, Flotation, New York, Primary Sources, 1963, 620 p.

59 Groves, R.D. and P.B. Smith, Reactions of copper minerals with chlorine in an aqueous system, Rep. Invest. 7801, U.S. Bureau of Mines, Arlington, VA, 1973.

60 Guay, D.W. How Carli treats gold ores by double oxidation, World Mining, Vol. 33, No.3, March 1980, pp. 47-49.

61 Guay, W.J. and D.G. Peterson, Recovery of gold from carbonaceous ores at Carlin, Nevada, AIME Transactions, Vol. 254, March 1973, pp. 102-104.

62 Guest, R.N. and R.C. Dunne, An evaluation of gravity separators by use of synthetic ore, Journal of the South African Institute of Mining and Metallurgy, Vol. 85e, No. 6 June 1985, pp. 187-195.

63 Gupta, C.K. and T.K. Mukherjee, Hydrometallurgy in Extraction Processes, Vol. II, CRC Press, Boca Raton, Ann Arbor, Boston, 1990.

64 Habashi, F., One hundred years of cyanidation, CIM Bulletin, Vol. 80, No. 905, 1987, pp. 108-114.

65 Harris, G.B., The refining of gold and precious metals, presented at Refining and

Recycling of Precious Metals-- A Technology Update, Professional Development Seminar, Department of Mining and Metallurgical Engineering, McGill University, Montreal, April 29-May 1, 1991.

66 Harris, G.B., Private correspondence, February 1995.

67 Hart, S.D. and G.J. Hill, Gravity separation development at Boddington Gold Mine, Randol Gold Forum Perth'95, March 14-17, 1995, Perth, Western Australia, pp. 53-59.

68 Hawkins, W.M., A spectrochemical study of rocks associated with the sulphide ore deposits of the Chibougamau district, Québec, McGill University Ph.D. thesis, 1960, 156.

69 Henrie, T.A. and R.E. Lindstrom, Mercury recovery by electroxidation, Encyclopedia of Chemical Technology, Supplementary Volume, seconde edition, Stander, A., Eds., John Wiley & Sons, New York, 1971, 1007 p, p. 541.

70 Heslop, R.B. and P.L. Robinson, Inorganic Chemistry, Amsterdam, New York, Elsevier publishing Company, 1960, 555 p, p. 486.

71 Holtham, P.N., Particle transport in gravity concentrators and the Bagnold effect, Minerals Engineering, Vol. 5, No. 2, pp. 205-221, 1992.

72 Honaker, R.Q., B.C. Paul, D. Wang and M. Hunag, Application of centrifugal washing for fine-coal cleaning, Minerals and Metallurgical Processing, Vol. 12, No. 2, May 1995, pp. 80-84.

73 Honan, S.G. and W.F. Luinstra, Gravity gold concentration at Hemlo Gold

Mines Inc. Golden Giant Mine, Proceedings-28th Annual Meetings of the Canadian Mineral Processors, January 23-25, 1996, Ottawa, Ontario.

74 Hope, G.H., J. McMullen and D. Green, Process advances at Lac Minerals Ltd.-Est Malartic division, Knelson Concentrator Technical Papers and Performance Reports 1995, Edited by KNELSON CONCENTRATORS.

75 Hu, J. and Q. Gong, Substitute sulphate for sulphite during extraction of gold by thiosulphate solution, RANDOL CAIRNS '91, PP. 333-336.

76. Huang, L., A.R. Laplante and G.B. Harris, "Upgrading of gold gravity concentrates", Proceedings of Thirty-second Annual Conference of Metallurgists, Quebec City, August 28 to September 2, 1993.

77 Hubli, R.C., T.K. Mukherjeea and C.K. Gupta, On the aqueous chlorination of copper-nickel sulphide concentrate, Proc. Indo. U.S. Workshop Udaipur, India. December 14-17, 1981.

78 Huyhua, J .C. and I.H. Gundiler, Kinetics of leaching gold and silver in acidic thiourea solutions, Hydrometallurgical Reactor Design and Kinetics, Edited by Bautista, R.G. et al, 1984, pp. 247-264.

79 Jackman, I. and S. Williams, The role of flotation in the recovery of gold, Proceedings -27th Annual Meetings of the Canadian Mineral Processors, January 17-19, 1995, Ottawa, Ontario, pp. 426-436.

80 Jackson, K.J. and J.D.H. Strickland, The dissolution of sulphide ores in acid chlorine solution; A study of the more common sulphide minerals, Transactions of the Metallurgical Society of AIME, Vol. 212, June 1958, pp. 373-379.

81 Jacobson, R. and J. Murphy, The feature of solution and in-situ leaching, SME-AIME Conference, Denver, CO, February 1987.

82 Jing, T. and J. Chen, The study of technology and mechanism for the gold extraction of copper-bearing gold ore (Ph.D. thesis), Beijing, China, 1990.

83 Jolles, Z.E., Bromine and Its Compounds, Academic Press, New York, 1966. 980 p.

84 Kelly, E.G. and D.J. Spottiswood, Introduction to Mineral Processing, John Wiley & Sons, 1982, New York, 491 p.

85 Knelson, B., Centrifugal concentration and separation of precious metals, Second International Conference on Gold Mining, Vancouver, Canada, November 1988.

86 Knelson, B., The Knelson concentrator metamorphosis from crude beginning to sophisticated world wide acceptance, Minerals Engineering, Vol. 5. No. 10-12, 1992, pp. 1091-1097.

87 Knelson, B., Private communication, 1996.

88 Knelson, B. and R. Jones, A new generation of Knelson concentrators, a totally secure system goes on line, Minerals Engineering, Vol.7, No. 2-3, 1994, pp. 201-207.

89 Kok, S.K., Gold concentration by flotation, Journal of the South African Institute of Mining and Metallurgy, Vol. 76, Special issue, October 1975, pp. 139-141.

90 Kuhn, A.T., Electrochemical recovery of metals from dilute solutions, Chemistry

and Industry. July 1978, No. 13, PP. 447-453.

91 Laplante, A.R., Private correspondence, 1995.

92 Laplante, A.R., Mineralogy and metallurgical performance of Various gold-copper ores of the Chibougamau area, Quebec, Proceedings of the International Symposium on Gold Metallurgy, edited by R.S. Salter, D.M. Wyslouzll and G.W. McDonald, Pergamon Press, 1987, Vol. 1., pp. 141-156.

93 Laplante, A.R., A comparative study of two centrifugal concentrators, Randol Gold Forum Beaver Creek '93 September 7-9, 1993, Hyatt Beaver Creek Resort, Vail Valley, Colorado, pp. 113-123.

94 Laplante, A.R, M. Buonvino, A. Veltmeyer, J. Robitaille and G. Naud, A study of the Falcon concentrator, Canadian Metallurgical Quarterly, Vol. 33, No. 4, pp. 279-288, 1994.

95 Laplante, A.R., L. Liu and A. Cauchon, Gold gravity recovery at the mill of Les Mines Camchib Inc., Chibougamau, Québec, International symposium of gold recovery, Salt Lake City, February 1990.

96 Laplante, A.R., A. Putz, L. Huang and F. Vincent, Practical considerations in the operations of gold gravity circuits, Proceedings--26th Annual Meeting of the Canadian Mineral Processors, Ottawa, January 1994.

97 Laplante, A.R. and N. Nickoletopoulos, Validation of a Falcon model with a synthetic ore, Canadian Metallurgical Quarterly, 1996 (in print).

98 Laplante, A.R. Y. Shu, The use of a laboratory centrifugal separator to study

gravity recovery in industrial circuits, Proceedings--24th Annual Meeting of the Canadian Mineral Processors, Ottawa, January 1992.

99 Laplante, A.R. Y. Shu and J. Marios, Experimental characterization of a centrifugal separator, accepted in the Canadian Metallurgical Quarterly, 1996. Vol. 35, No. 1, pp. 23-29.

100 Laplante, A.R., A. Wibisono and A. Cauchon, Development of a flowsheet for the S-3 ore, CMP Reginal Meeting., Chibougamau, September 1986, pp. 155-192.

101 Li, X., J. Ke, X. Meng and B. Li, Chlorine leaching of gold-bearing sulphide concentrate and its calcine, Hydrometallurgy, 29 (1992), pp. 205-215.

102 Lindeman, D. And R.M. Nendick, A comparison of South African and North American practices in the extraction metallurgy of gold, Proceedings--24th Annual Meeting of the Canadian Mineral Processors, Ottawa, January 1992, 16 pages.

103 Lins, F.F., M.M. Veiga, J.A. Stewart, A. Papalia and R. Papalia, Performance of new centrifuge (Falcon) in concentrating a gold ore from Texada Island, B.C., Canada, Minerals Engineering, Vol. 5., No. 10-12, 1992, pp. 1113-1121.

104 Lins, F.F. and R. Adamian, The influence of some physical variables on gold flotation, Minerals Engineering, Vol. 6, No. 3, 1993, pp. 267-277.

105 Lloyd, P.J.D., The flotation of gold, uranium, and pyrite from Witwatersrand ores, Journal of the South African Institute of Mining and Metallurgy, Vol. 81, No. 2, February 1981, pp. 41-47.

106 Louis, H., A handbook of gold milling, London and New York, Macmillan and Co., 1894, 504 p.

107 Loveday, B.K. and J.F. Forbes, Some considerations in the use of gravity concentration for the recovery of gold, Journal of the South African Institute of Mining and Metallurgy, May 1992, pp. 121-124.

108 Lui, L., An investigation of gold recovery in the grinding and gravity circuits at Les Mines Camchib Inc. Master of Engineering thesis, 1989, McGill University, 180 p.

109 Lu, Y., Theory and practice of the centrifugal injection film separation for ultra-fines, Nonferrous Metals, Quarterly, No. 4, 1990, pp. 25-31.

110 Marsden, J. and I. House, I. The Chemistry of Gold Extraction, Ellis Horwood, New York, 597, 1992.

111 Masliyan, J. and J. Bridgwater, Particle percolation: a numerical study, Trans. Instn. Chem. Engrs., Vol. 52, 1974, pp. 31-42.

112 McAlister, S., Case study in the use of the Falcon gravity concentrator, Proceedings--24th Annual Meeting of the Canadian Mineral Processors, Ottawa, January 1992, 20 pages.

113 McCulloch, W.E., Flash flotation for improved gold recovery at Freeport Indonesia, Minerals and Metallurgical Processing, August 1990, pp. 144-148.

114 McGuinness, M., Improving the Tri-Flo Performance of TANCO's Heavy Media Circuit, Technical Report, McGill University, Montreal, October 1994, 32 pp.

115 McGuiness, M. and D. Anonychuk, Recovery of fine gold and tantalum particles using the Falcon concentrator. Research Project, Course 306-410B, McGill University, Department of Mining and Metallurgical Engineering, 1994.

116 McQuiston, F.W. and R.S. Shoemaker, Gold and Silver Cyanidation Plant Practice, SEM-AIME, New York. 1975.

117 Mellor, J.W. A Comprehensive Treatise on Inorganic and Theoretical Chemistry, Vol. 2, London and New York, Longmans, Green and Co., 1922, 894 p.

118 Metals & Minerals Annual Review, 1994.

119 Meza S, L. A., W. Hartmann and Carlos A. Escobar, Recovery of placer gold using the Knelson Concentrator, Knelson Concentrator Technical Papers and Performance Reports 1995, Edited by KNELSON CONCENTRATORS.

120 Michaelis, H.V., Alternative leaching reagents, Engineering and Mining Journal, Vol. 188, No. 6, June 1987, pp. 42-47.

121 Morrison, T.A. (Mine Superintendent), Cominco Metals Ltd/Prime Resources Group Inc., Presented at a Minerals North 1992, Terrace, B.C.

122 Muir, D.A., D.C. Gale, A.J. Parker and D.E. Giles, Leaching of the McArthur River zinc-lead sulphide concentrate in aqueous chloride and chlorine systems, Proc. Australians. Inst. Min. Metll., September 23, 259, 1976.

123 Neisser, W.E., Problems associated with the use of mercury by small-scale gold miners in developing countries, Master of Engineering thesis, McGill University, 1993, 104 p.

124 O'Connor, C.T. and R.C. Dunne, The flotation of gold bearing ores-A review, Mineral Engineering, Vol. 7, No. 7, 1994, pp. 839-849.

125 O'Connor, C.T. and R.C. Dunne, The practice of pyrite flotation in South Africa and Australia, Minerals Engineering, Vol. 4, No. 7-11, 1991, pp. 1057-1069.

126 Ounpuu, M., Gravity concentration of gold from base metal flotation mill, Proceedings--24th Annual Meeting of the Canadian Mineral processors, Ottawa, January 1992, 22 pages.

127 Pachejieff, B., S. Gaidarjiev and D. Lazarov, Technical note: Opportunities for fine gold recovery from a copper flotation circuit using a Knelson Concentrator, Minerals Engineering, Vol. 7, N0. 2-3, 1994, pp. 405-409.

128 Pang, S., S. Chang and Y. Xi, An investigation of the extraction of gold and silver by ammonium thiocyanate, Gold, Vol. 13, No. 9, 1992, pp. 33-37 (Chinese Text).

129 Pesic, B. and H. Sergent, The rotating disc study of gold dissolution with bromine, EPD Congress'91, Edited by Gaskell, D.R., 1991, pp. 613-636.

130 Piret, N.L.D. Muller and B. Shoukry, Gold gravity concentrate treatment by upgraded intensive cyanidation as an economic and ecological alterative to amalgamation, RAMDOL CAIRNS, 1991, pp. 289-298.

131 Poulter, S., C. Fitzmaurice and G.Steward, The Knelson Concentrator: Application and Operation at Rosebery, KNELSON CONCENTRATOR Technical Papers and Performance Reports 1995, edited by Knelson Concentrators.

132 Prasad, M.S. R. Mensah-Biney and R.S. Pizarro, Modern trends in gold processing - Review, Minerals Engineering, Vol. 4, No. 12, 1991, pp. 1257-1277.

133 Preisler, W.P. and L. Berger, Oxidation-reduction potentials of thiol-dithio system: thiourea-formamidine disulphide, The J. of the Am. Chem. Soc., Vol. 69, February 1947, pp. 322-325.

134 Pryor, E.J., Mineral Processing, Third Edition, Elsevier Publishing Co Ltd, Amsterdam, New York, 1965, 844 p, pp. 736-763.

135 Puddephatt, R.J., The Chemistry of Gold, Elsevier Scientific Pub. Co., Amsterdam, New York, 1978, 274 p.

136 Putnam, G.L., Chlorine as a solvent in gold hydrometallurgy, Engineering and Mining Journal, Vol. 145, No. 3, March 1944, pp. 70-73.

137 Putz, A. An investigation of the gravity recovery of gold, Master of Engineering thesis, McGill University, 1994, 230 p.

138 Putz A., A.R. Laplante and G. Ladouceur, Evaluation of gravity circuit in Canadian gold operation, Randol Gold Forum, Beaver Creek, September 1993, pp. 145-149.

139 Qi, P.H. and J.B. Hiskey, Dissolution kinetics of gold in iodine solutions, Hydrometallurgy, 19 (1988), pp. 361-375.

140 Raudsepp, R. and R. Allgood, Thiourea leaching of gold in a continuous pilot plant, Proceedings of the international symposium on gold metallurgy, Edited by

Salter R.S. et al, pp. 87-93, 1987.

141 Roberson, J.A. and C.T. Crowe, Engineering Fluid Mechanics, third edition, Boston, Houghton Mifflin Company, 1985, 712 p.

142 Roorda, H.J. and P.E. Queneau, Recovery of nickel and cobalt from limonites by aqueous chlorination in sea water, Institution of Mining and Metallurgy Transactions, Section C, Mineral Processing & Extractive Metallurgy, Vol. 82, No. 799, 1973, C 79-87.

143 Rose, T., The Metallurgy of Gold, C. Griffin and Company, Limited, third edition, London, 1898, 528 p.

144 Sax, N.I., Dangerous properties of industrial material, fourth edition, New York, Toronto, Van Nostrand Reinhold Co., 1975, 1258 p.

145 Scheisner, B.J., D.C. Thompson, G.A. Smyres and R.E. Lindstrom, Chlorine -oxygen leaching of complex sulphide concentrates, TMS paper Selection, A77-36, 1977.

146 Scheiner, B.J., G.A. Smyres and R.E. Lindstorm, Lead-zinc extraction from flotation concentrates by chlorine-oxygen leaching, in Society of Mining Engineering Preprint No.75-B-314, SME Fall Meeting, AIME, Salt Lake City, 1975.

147 Scheiner, B.J., R.E. Lindstorma and T.A. Henrie, Processing refractory carbonaceous ores for gold recovery, Journal of Metals, Vol. 23, No. 3, March 1971, pp. 37-40.

148 Scheiner, B.J., R.E. Lindstorm, D.E. Shranks and T.A. Henrie, Tech. Prog. Rep. 26 . Electrolytic oxidation of cinnabar ores for mercury recovery, U.S. Bureau of Mines, Arimgton, VA, 1970.

149 Sergent, R.H. and A. Dadgar, Advancements in bromine chemistry for use in large-scale gold extraction, RANDOL FORUM SQUAW VALLEY 90, PP. 225-228.

150 Seymour, D. and G. Ramadorai, Rapid oxidation of refractory gold-bearing ores by intense "flash chlorination" at Newmount Gold Company, Precious Metals '89, Edited by M.C. Jha and S.D. Hill, The Minerals, Metals & Materials Society, 1988, Proceedings, pp.165-178.

151 Sherman, M.I. and J.D.H. Strickland, Dissolution of lead sulphide ores in acid chlorine solutions, Journal of Metals, Vol. 9, No. 6, June 1957, pp. 795-800.

152 Shukla, P.P., T.K. Mukherjee, C.K. Gupta, R.A. Nagle, K.S. Koppikar and T.K.S. Murthy, Chlorination leaching of nickel-copper sulphide concentrate, Institution of Mining and Metallurgy Transactions, Section C, Mineral Processing & Extractive Metallurgy, Vol. 88, June 1979, C 133-135.

153 Snoeyink, V. L. and D. Jenkins, Water Chemistry, John Wiley & Sons. Inc., New York, 1980, 463 pp.

154 Sorensen, J., Carbon-in-leach circuit to up silver-gold recovery in Equity, Canadian Mining Journal, Vol. 105, No. 11, 1984, pp. 22-25.

155 Stassen, F.J.N., Conditioning in the gold flotation, uranium oxide, and pyrite, Journal of the South African Institute of Mining and Metallurgy, Vol. 91, No. 5,

May 1991, pp. 169-174.

156 Stockes, G.G., Mathematical and Physical Papers, Trans. Cambridge Phil. Soc., 9, Part II, 51ff, (1851).

157 Subramanian, K.N., Commercialization of a column flotation circuit for gold sulphide ore, Column Flotation '88, Proceedings of a International Symposium on Column Flotation, 1988, pp. 13-18.

158 Sun, J., Metallurgy of Gold and Silver, Metallurgy Press, 1986, 449 p (Chinese Text).

159 Sun, Y., Gravity Separation, Metallurgy Press, Beijing, 1982, 310 p (Chinese Text).

160 Swaminathan, C., P. Pyke and R.F. Johnston, Reagent trends in the gold extraction industry, Minerals Engineering, Vol. 6, No. 1, 1993, pp. 1-16.

161 Taggart, A.F., Handbook of Mineral Dressing, John Willey & Sons Inc., 1945, New York, 1915 p, pp. 1410-1424.

162 Thomas, B.K. and D.J. Fray, Leaching of oxide zinc materials with chlorine and chlorine hydrate, Metallurgical Transactions, 12 B (June), 281, 1981.

163 Traore, A., P. Conil, R. Houot and M. Save, An Evaluation of the Mozley MGS for Fine Particle Gravity Separation, Minerals Engineering, Vol. 8, No. 7, 1995, pp. 767-778.

164 Turner, J.F., Gravity concentration, past, present and future, Minerals

Engineering, Vol.4., No. 3/4, 1991, pp. 213-223.

165 Vincent, F., Comparing Knelson and jig performance, Master of Engineering Thesis, McGill University, 1996.

166 Wang, W. and G.W. Poling, Methods for recovering fine placer gold, CIM Bulletin, Vol. 76, No. 860, December 1983, pp. 47-56.

167 Warren, I. H., A. Ismay and J. King, Metallurgical Society CAM, Annual Volume, Pergamon Press, Canada 1978, II.

168 Warren, I. H. and D.M. Monseuy, Factors influencing the selective leaching of molybdenum with sodium hypochlorite from copper molybdenum sulphide minerals, Hydrometallurgy, Vol.10, No. 3, June 1983, pp. 343-357.

169 Wei, K., Study of Overloading in the Knelson Concentrator, Research Report McGill University, 1995, 40 p.

170 Weiss, N.L., SME Mineral Processing Handbook, New York, Society of Mining Engineers of the American Institute of Mining, Metallurgical and Petroleum Engineers, Inc. 1985, pp. 18-21.

171 Wells, J. and C. Patel, Contemporary practices in gravity recovery installations in the Canadian gold mining industry, Minerals Engineering, Vol. 4, No. 3/4, 1991, pp. 399-409.

172 Wills, B.A., Mineral Processing Technology, Fourth Edition, Oxford, New York, Beijing, Pergamon Press, 1992, 785 p.

173 Woodcock, F.C, Use of a Knelson unit to quantify gravity recoverable gold in a ore sample, Master of Engineering Thesis, McGill University, September 1994, 124 p.

174 Wyslouzil, H.E., Evaluation of the Kelsey Centrifugal Jig at Rio Kemptville Tin, Proceedings--22nd Annual Meeting of the Canadian Mineral Processors, Ottawa, January, 1990, pp. 461-470.

175 Yannopoulos, J.C., The Extractive Metallurgy of Gold, Van Nostrand Reinhold, New York, 1991, 279 p, pp. 73-75.

176 Yen, W. T., R.A. Pindred and M.P. Lam, Hypochlorite leaching of gold ore, Advances in Gold and Silver Processing, Proceedings of the Symposium at GOLDTech 4, Reno, Nevada, September 10-12, 1990, edited by M.C. Fuerstenau, J.L. Hendrix, published by Society for Mining, Metallurgy, and Exploration, Inc., Littleton, Colorado, 1990, 291 p. pp. 67-73.

177 Zadra, J.B., A process for the recovery of gold from activated carbon by leaching and electrolysis, Bureau of Mines Report of Investigations 4672, 1950, 47 p.

178 Zipperrian, P., S. Raghavan, Gold and silver extraction by ammoniacal thiosulphate leaching from a rhyolite ore, Hydrometallurgy, 19 (1988), pp. 361-375.

APPENDIX 1-1 A Review of Gold Chlorination

Table of Contents

1 Introduction A2

2 Chlorine Chemistry A2

3 Gold Chlorination and Precipitation A5

- 3.1 Chlorination A5
- 3.2 Precipitation A7

4 Chlorination Chemistry of Some Sulphides A8

- 4.1 Pyrite and Pyrrhotite A8
- 4.2 Copper Sulphides A9
- 4.3 Lead and Zinc Sulphides A9
- 4.4 Nickel-Copper Sulphides A10
- 4.5 Nickel-Zinc Oxides A12
- 4.6 Hypochlorite Leaching of Molybdenite A13
- 4.7 Hypochlorite Leaching of Mercury Ore A14
- 4.8 Hypochlorous Acid Leaching A15

5 Methodology and Technology A15

- 5.1 Earlier Chlorination Processes A15
  - 5.1.1 The Plattner Process A15
  - 5.1.2 Improved Plattner Processes A15
- 5.2 Recent Processes A20
  - 5.2.1 Merrill Slimes A20
  - 5.2.2 Gold Gravity Concentrates A20
  - 5.2.3 Carbonaceous Refractory Ores A21
  - 5.2.4 Hypochlorite Leaching of Gold Ores A21
  - 5.2.5 Gold-bearing Sulphide Concentrate and Its Calcine A22

6 Conclusions A22

1 INTRODUCTION

Gold extraction by chlorination was originally invented by Plattner in 1848 (Louis, 1894). About 110 years ago, gold ores were broadly treated by roasting and subsequent leaching with aqueous solutions of chlorine, followed by gold precipitation and melting. Gold recoveries were in the range of 90-98% and chlorine consumptions were 0.68-2.3 kg per tonne of ore. Since cheaper cyanide was first successfully introduced to the gold industry in 1887, the chlorination process has almost completely been replaced by cyanidation (Putnam, 1944). In addition to gold, aqueous chlorination has also been extensively investigated for the extraction of a variety of sulphide minerals and their concentrates, such as copper, lead, zinc, nickel etc.

Even though chlorination is no longer used for the leaching of primary gold ores, it is successfully applied for the pretreatment of some carbonaceous refractory ores. There are also quite a few published papers pertaining to the treatment of gold gravity concentrates, Merrill slimes, and even original gold ores. Gold chlorination has the advantages of fast leaching rate and the ability to attack carbon and organic materials. If the selectivity of leaching gold from gold concentrates containing sulphides can be achieved, gold chlorination-precipitation might be a promising approach for treating high-grade gold gravity concentrates.

2 CHLORINE CHEMISTRY

Chlorine is widely used in water and waste treatment both as an oxidizing agent and disinfectant. At room temperature and atmospheric pressure, Cl_2 is a pale-green gas, which can be compressed to a yellow-green liquid. Both gaseous and liquid chlorine react with water to become hydrated, and below 9.4°C, liquid chlorine forms a solid hydrate, $Cl_2.8H_2O$ (Snoeyink and Jenkins, 1980).

Chlorine gas is soluble in water. At ambient temperature and pressure, its solubility is 2.26 L per litre of water (corresponding to 7.05 g.L^{-1} Cl_2), compared with 8.2 mg.L^{-1} for oxygen (Gupta, 1990; Yannopoulos, 1991). In water it forms hydrochloric acid and hypochlorous acid (Marsden and House, 1992). $Cl_{2\,(aq)}$ reacts with water, with one atom being oxidized to Cl (+I) and the other being reduced to (-I). The HCl formed is completely dissociated under usual dilute aqueous solutions (Snoeyink and Jenkins, 1980).

$$Cl_{2\,(g)} \leftrightarrows Cl_{2\,(aq)} \qquad K_h = 6.2 \times 10^{-2} \qquad (A1\text{-}1)$$

$$Cl_{2\,(aq)} + H_2O \leftrightarrows HOCl + H^+ + Cl^- \qquad K_h = 4 \times 10^{-4} \qquad (A1\text{-}2)$$

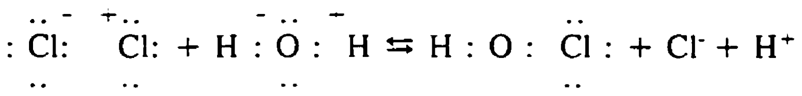

$$:\overset{\cdot\cdot\,-}{\underset{\cdot\cdot}{Cl}}: \quad \overset{+\,\cdot\cdot}{\underset{\cdot\cdot}{Cl}}: + H:\overset{-\,\cdot\cdot}{\underset{\cdot\cdot}{O}}: \overset{-}{H} \leftrightarrows H:O:\overset{\cdot\cdot}{\underset{\cdot\cdot}{Cl}}: + Cl^- + H^+ \qquad (A1\text{-}3)$$

Hypochlorous acid is a weak acid.

$$HOCl \leftrightarrows H^+ + OCl^- \qquad pK_a = 7.5 \qquad (A1\text{-}4)$$

The Eh-pH diagram of aqueous chlorine is shown in Figure A1-1.

At 25°C, from (A1-4) it can be deduced that at pH 7.5 the activities of [HOCl] and [OCl^-] are equal. Below pH 7.5, HOCl predominates, while above pH 7.5, OCl^- is the predominant species. It was reported that the disinfecting ability of HOCl is about 80-100 times higher than that of OCl^-. The distribution of various chlorine species as a function of pH is shown in Figure A1-2.

Figure A1-2 shows that under typical natural water conditions, HOCl and OCl^- are the major chlorine species, $Cl_{2\,(aq)}$ being unimportant above pH 2. In the pH range of natural waters (pH 6-9), the relative amounts of HOCl and OCl^- are very sensitive to pH.

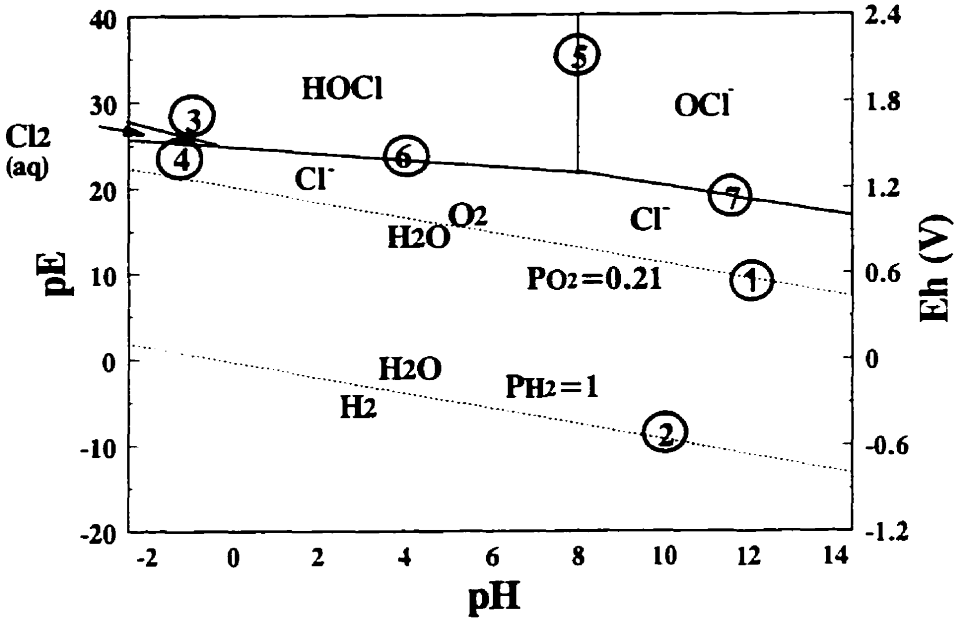

FIGURE A1-1 The Eh-pH Diagram for Aqueous Chlorine, 25 °C, $C_{T,Cl} = 1 \times 10^{-4}$ M (after Snoeyink and Jenkins, 1980)

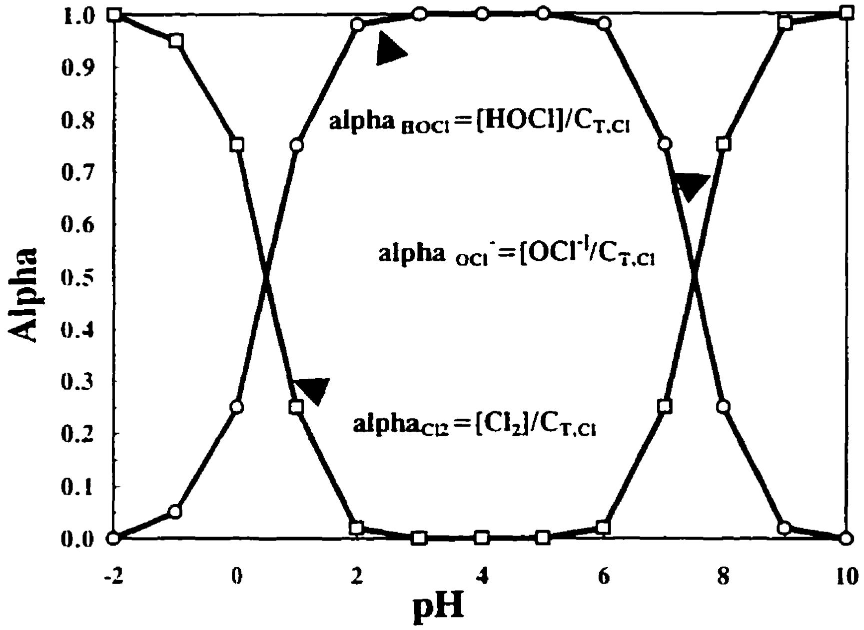

FIGURE A1-2 Distribution Diagram for Chlorine Species at 25 °C. $[Cl^-] = 10^{-3}$ M, $C_{T,CL} = [Cl_2] + [HOCl] + [OCl^-]$ (after Snoeyink and Jenkins, 1980)

From Eq. (A1-2), two half reactions can be written (Marsden and House, 1992):

$$2HOCl + 2H^+ + 2e \leftrightarrows Cl_2 + H_2O \qquad E^\circ = +1.64\ V \qquad (A1\text{-}5)$$

$$Cl_2\,(aq) + 2e \leftrightarrows 2Cl^- \qquad E^\circ = +1.358\ V \qquad (A1\text{-}6)$$

From A1-5 and A1-6, it can be seen that both HOCl and Cl_2 (aq) are strong oxidizing agents. Also, the strong oxidizing hypochlorite species can be generated by adding inorganic hypochlorite salts to a solution, for example:

$$NaOCl \leftrightarrows Na^+ + OCl^- \qquad (A1\text{-}7)$$

$$Ca(OCl)_2 \leftrightarrows Ca^{2+} + 2OCl^- \qquad (A1\text{-}8)$$

The hypochlorite species further reacts with water to form hypochlorous acid with a corresponding increase in pH.

$$OCl^- + H_2O \leftrightarrows HOCl + OH^- \qquad (A1\text{-}9)$$

3 GOLD CHLORINATION AND PRECIPITATION

3.1 Chlorination

Gold dissolves in aqueous chloride solution to form both the gold (I) and gold (III) chloride complexes (Marsden and House, 1992).

$$AuCl_2^- + e \leftrightarrows Au + 2Cl^- \qquad E^\circ = 1.113\ V \qquad (A1\text{-}10)$$

$$AuCl_4^- + 3e \leftrightarrows Au + 4Cl^- \qquad E^\circ = 0.994\ V \qquad (A1\text{-}11)$$

$$2Au + 3Cl_2 + 2Cl^- \leftrightarrows 2AuCl_4^- \qquad (A1\text{-}12)$$

The mass transport of chloride ions to the gold surface is the rate-determining step. Chloride ions transport rates are maximized by high chlorine-chloride concentration and increased temperature. It was reported that in cyanide solution the dissolution rate of gold leaf was 0.008 $g.m^{-2}.s^{-1}$, compared with 0.3 $g.m^{-2}.s^{-1}$ in chloride solution, i.e. 37.5 times higher (Putnam, 1944). This can be attributed to the differences in solubility since the solubility of chlorine in water is much higher than that of oxygen (861 times higher). An Eh-pH diagram of $Au\text{-}H_2O\text{-}Cl^-$ system is shown in Figure A1-3.

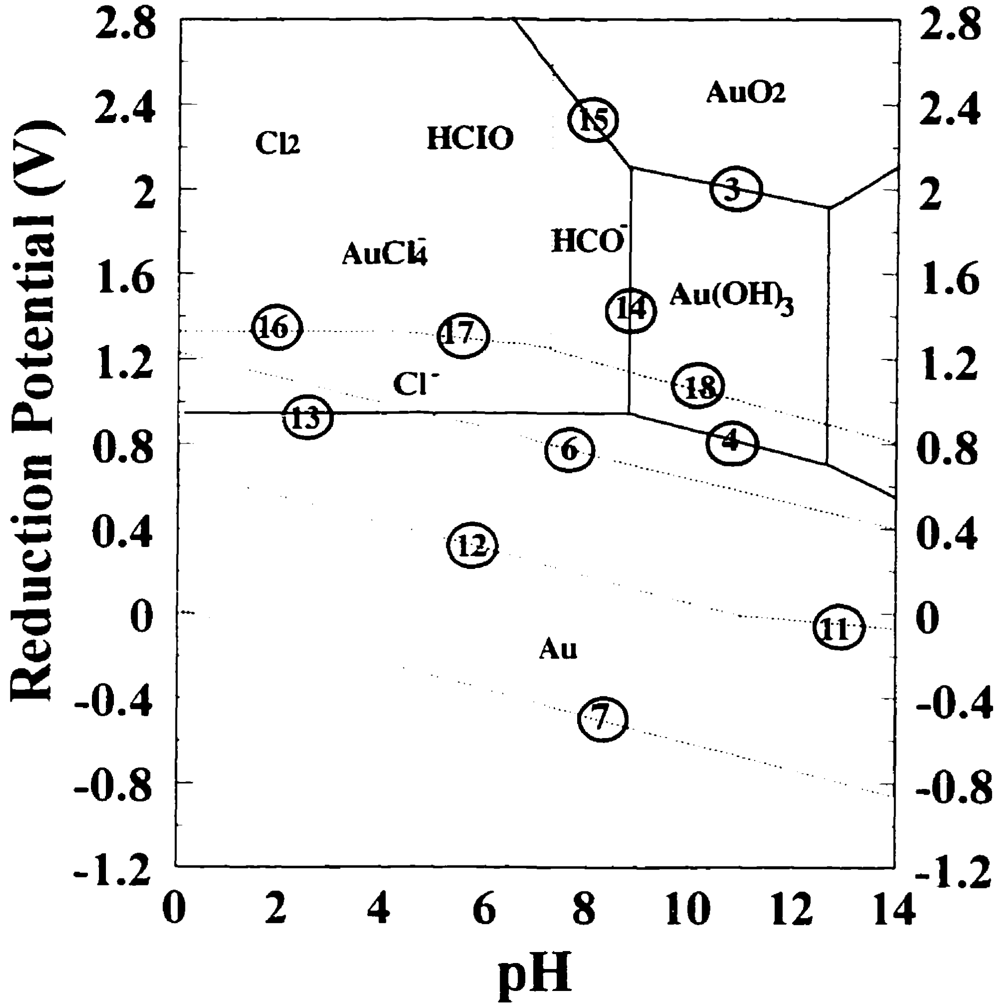

FIGURE A1-3 Eh-pH Diagram for the System of $Au\text{-}H_2O\text{-}Cl^-$ at 25 °C. $[Au(III)] = 10^{-2}$ M, $[Cl^-] = 2$ M, $P_{Cl_2} = 0.1$ atm, $[HClO] = [ClO^-] = 6 \times 10^{-3}$ M, $P_{O_2} = P_{H_2} = 1$atm (After Adamson, 1972).

Since the leaching media of chlorination is highly corrosive, special materials such as stainless steels and rubber-lined equipment are required, and any leakage of gaseous chlorine must be avoided. If the process is carried out at a pH of 2.0 to 2.5, the chlorine gas adsorption rate is maximized, but the solution becomes increasingly difficult to handle because of the very low pH.

3.2 Precipitation

Gold (I) sulphide can be formed by reaction of $Au(CN_2)^-$ with H_2S. It is a black-brown powder which is only very slightly soluble in water ($K_{sp}=[Au^+]^2\ [S^{2-}]=4 \times 10^{-69}$, at 25°C) (Puddephatt, 1978).

Gold (III) sulphide can be prepared by reaction of H_2S with Au_2Cl_6 in anhydrous ether at low temperature. Attempts to prepare it in aqueous solution lead to reduction to metallic gold. The black powder decomposes to the elements on being heated to 200 °C (Puddephatt, 1978).

The most common precipitants of gold are sodium sulphite ($Na_2SO_3.7H_2O$), sulphur dioxide (SO_2), and ferrous sulphate ($FeSO_4.7H_2O$). Among them, sulphur dioxide is more economical and more convenient to use on a large scale. According to the tests done in South Africa, in the precipitation stage, the reaction always proceeded smoothly and with high recoveries. The addition of a precipitant first led to the discharge of the golden-yellow color of the solution, followed by the precipitation of gold. The fine precipitates soon coagulated to coarser ones which were easily separated from the suspension by filtration (Finkelestein, 1966).

The possible reactions for gold precipitation with SO_2 are (Harris, 1995; Finkelstein et al, 1974):

$2AuCl_4^- + 3SO_2 + 6H_2O \rightarrow 2Au + 6HCl + 3H_2SO_4 + 2Cl^-$ (A1-13)

$2AuCl_4^- + 3SO_2 + 6H_2O + 2H^+ \rightarrow 2Au + 8HCl + 3H_2SO_4$ (A1-14)

4 CHLORINATION CHEMISTRY OF SULPHIDES

All sulphides commonly associated with gold will be readily oxidized by aqueous chlorine, especially pyrite, arsenopyrite, pyrrhotite. Both silver and lead will form insoluble chlorides in chlorine-chloride solutions. Less copper will be dissolved in the chlorine media than in cyanide, therefore, there is a potential attraction for the treatment of some copper-gold ores by chlorination (Marsden and House, 1992).

4.1 Pyrite and Pyrrhotite

The reaction of pyrite at pH 3-5 in aqueous chlorine solution (the pH range of operation of carbonaceous ores) is (Marsden and House, 1992):

$2FeS_2 + 15HOCl + 7H_2O = 2Fe(OH)_3 + 23H^+ + 4SO_4^{2-} + 15Cl^-$ (A1-15)

Pyrite reacts with chlorine gas (Li, 1992):

$FeS_2 + 7Cl_2 + 8H_2O \rightleftharpoons FeCl_2 + 12Cl^- + 2SO_4^{2-} + 16H^+$ (A1-16)

It has been found that small spheroidal pyrite (0.5-2 μm) particles with well developed pore structures were much more rapidly oxidized than large euhedral, non-porous particles. An ore containing 1% sulphur as pyrite will consume 82 kg chlorine per ton of ore if the pyrite is completed oxidized. If the same amount of sulphur is present as pyrrhotite, over 100 kg.t^{-1} is required. For the higher sulphur gold concentrate, pre-aeration (82°C, sodium carbonate 25 kg.t^{-1}, vigorously aerated and agitated) or roasting (800°C) may be needed.

4.2 Copper Sulphides

Sulphide copper minerals, chalcopyrite, chalcocite, bornite, covellite, are readily dissolved in an acidic chlorine solution at an ambient temperature, as shown in the following equations (Gupta, 1990; Jackson, 1958; Groves, 1973).

$$\mathrm{Cus} + 4\mathrm{Cl_2} + 4\mathrm{H_2O} \rightarrow \mathrm{Cu^{2+}} + \mathrm{SO_4^{2-}} + 8\mathrm{H^+} + 8\mathrm{Cl^-} \tag{A-17}$$

$$\mathrm{CuFeS_2} + 8.5\mathrm{Cl_2} + 8\mathrm{H_2O} \rightarrow \mathrm{Cu^{2+}} + \mathrm{Fe^{3+}} + 2\mathrm{SO_4^{-2}} + 16\mathrm{H^+} + 17\mathrm{Cl^-} \tag{A-18}$$

$$\mathrm{Cu_2S} + 5\mathrm{Cl_2} + 4\mathrm{H_2O} \rightarrow 2\mathrm{Cu^{2+}} + \mathrm{SO_4^{2-}} + 8\mathrm{H^+} + 10\mathrm{Cl^-} \tag{A-19}$$

$$\mathrm{Cu_5FeS_4} + 18.5\mathrm{Cl_2} + 16\mathrm{H_2O} \rightarrow 5\mathrm{Cu^{2+}} + \mathrm{Fe^{3+}} + 4\mathrm{SO_4^{2-}} + 32\mathrm{H^+} + 37\mathrm{Cl^-} \tag{A1-20}$$

$$\mathrm{FeS_2} + 7.5\mathrm{Cl_2} + 8\mathrm{H_2O} \rightarrow \mathrm{Fe^{3+}} + 2\mathrm{SO_4^{2-}} + 16\mathrm{H^+} + 15\mathrm{Cl^-} \tag{A1-21}$$

Leaching of covellite and chalcopyrite produces elemental sulphur as the intermediate product, and as the leaching progresses to completion, the sulphur is oxidized to sulphate. For chalcocite, in addition to sulphur, covellite might be an intermediate product. The chlorine required is about 3-10 kg for 1 kg of copper for the minerals.

4.3 Lead and Zinc Sulphides

Sherman and Strickcland reported first that the rate of reaction of chlorine with galena in an aqueous solution was first order, and both sulphate and elemental sulphur could be formed (Sherman et al, 1957). At the temperatures higher than 45°C, the reaction rate is controlled by transport, but at room temperature, it is by both transport and chemically controlled (Gupta, 1990; Sherman et al, 1957).

Muir et al studied the chlorination of the sample containing 31.5% Zn, 10.5% Pb, 10.5% Fe, and found that copper chloride might catalyze the extraction of zinc according to the following reactions (Muir et al, 1976):

$$\mathrm{ZnS} + 2\mathrm{CuCl_2} \rightarrow \mathrm{ZnCl_2} + 2\mathrm{CuCl} + \mathrm{S} \tag{A1-22}$$

$$2\mathrm{CuCl} + \mathrm{Cl_2} \rightarrow 2\mathrm{CuCl_2} \tag{A1-23}$$

Chlorine-oxygen: Chlorine-oxygen leaching consists of two steps. First, the sample is treated with aqueous chlorine in a sealed reactor, followed by oxygenation under moderate overpressure, which ensures favourable metal extraction without excess chlorine consumption (Scheiner et al, 1975, 1977). Lead-zinc flotation complex sulphide concentrates and lead smelter matte were leached by Scheiner et al. It was suggested that during chlorination, metal chloride, metal sulphate, and HCl were formed. The following reactions might occur in the presence of O_2.

$$MS + 2HCl + \tfrac{1}{2}O_2 \rightarrow MCl_2 + S + H_2O \qquad (A1\text{-}24)$$

$$2Fe_2^{+} + \tfrac{1}{2}O_2 + 2H_2O \rightarrow Fe_2O_3 + 4H^{+} \qquad (A1\text{-}25)$$

$$Pb^{2+} + SO_4^{-2} \rightarrow PbSO_4 \qquad (A1\text{-}26)$$

The test was conducted in a 10 L capacity teflon-lined reactor at 90-105°C at a pulp density of 50%. Leaching with 0.462 kg of Cl_2 per kg of the concentrate for 1 hour followed by oxygenation at 115°C for 3 hours resulted in 99.9% Zn, 98.2% Cu, 97.3% Pb, and 0.1% K extractions. The addition of calcium chloride (180 $g.kg^{-1}$) was found to be essential to reject 97.5% of the sulfate from the pregnant solution.

$$CaCl_2 + MSO_4 \rightarrow CaSO_4 + MCl_2 \qquad (A1\text{-}27)$$

By precipitation with zinc dust, trace metals of Cu, Cd, and Ag can be recovered. Zinc was next recovered through the solution evaporation to dryness. Lead was the last metal to be extracted as lead chloride through brine leaching and crystallization.

4.4 Nickel-Copper Sulphides

Shukla et al reported the leaching of nickel-copper complex concentrate (Shukla et al. 1979; Gupta, 1990). The different minerals in the concentrate were chalcopyrite, pyrite, pentlandite, millerite, bravoite, violerite, analyzing 9% Cu, 6% Ni, and 20% Fe. It was possible to recover 98% Ni by Cl_2 leaching at pH 2, ambient pressure, and 28%

pulp density. Due to the exothermic nature of the leaching reactions, the slurry attained 60°C without any external heating. However, the process lacked selectivity as the leach liquor was highly contaminated with iron.

As a remedial measure, the concentrate was roasted in air at 450°C prior to chlorine leaching. The roasting treatment converted 96% of the copper and 35% of the nickel to their sulphate forms. A major portion of the iron sulphides was oxidized to Fe_2O_3, which was inert in the subsequent chlorine leaching. The recoveries of copper and nickel were almost the same as those without roasting, but the chlorine consumption was much lower since it was only needed to oxidize the non-roasted copper and nickel sulphides. The nickel-copper bearing solution was subjected to solvent extraction with LIX 64N to yield separate copper and nickel sulphate.

An alterative of this process, without the pre-roasting step, was reported by Hubli et al (1981). A similar nickel-copper concentrate was subjected to aqueous chlorination in the presence of oxygen. The chlorination was carried out in a glass-lined reactor for about 1 hour and then continued for about 6 hours with oxygenation at 110°C and 0.38 mPa pressure. 90% of the stoichiometric chlorine required to form dichlorides of copper and nickel resulted in 97% Ni, 70% Cu and 7% Fe extractions. When leaching was conducted in the presence of 5.2 g $CaCl_2$ per 100 g of the concentrate, the recovery of copper increased to 95% and iron extraction decreased to 1%.

The Falconbridge Chlorine Leach Process for the recovery of nickel from converter matte is the most recent example of large scale aqueous chlorination (Gupta et al, 1990). The matte contains 35-40% Ni, 30-35% Cu, 22-24% S, 2-3% Fe, and 0.9-1.0% Co. The process essentially consists of the selective dissolution of nickel by controlling the redox potential of the slurry with chlorine in a series of leach-cementation tanks. Most of the copper remains in the residue as CuS. The nickel-bearing solution is subsequently purified with respect to iron and arsenic by precipitation before subjecting it to electrolysis to produce various nickel products. The chlorine gas produced during electrolysis is recycled to the chlorine leaching tanks. The main chemical reactions taking place in the leach tank were suggested as:

$$2Cu^{+} + Cl_2 \rightarrow 2Cu^{2+} + 2Cl^{-} \quad (A1\text{-}28)$$

$$Ni_3S_2 + 2Cu^{2+} \rightarrow 2NiS + Ni^{2+} + 2Cu^{+} \quad (A1\text{-}29)$$

$$NiS + 2Cu^{2+} \rightarrow Ni^{2+} + 2Cu^{+} + S^{o} \quad (A1\text{-}30)$$

$$Cu_2S + S^{o} \rightarrow 2CuS \quad (A1\text{-}31)$$

The reactions above indicate that the dissolution of nickel sulphide takes place due to its reaction with cupric ions which are generated by the oxidization of cuprous ions with aqueous chlorine. It implies that the dissolution of nickel and copper from the matte depends on the redox potential (Cu^{2+}/Cu^{+}) of the solution. For example, at 275 mV, only 2% Cu and 70% nickel dissolved, but at 375 mv, about 65% Cu and 90% Ni dissolved.

4.5 Nickel-Zinc Oxides

Nickeliferous limonitic ore, analyzing 0.8% Ni, 34% Fe, and 0.05% Co, was first reduction roasted at 750°C. Nickel oxide was reduced to particulate nickel metal and Fe_2O_3 reduced to FeO. The reduced ore was next leached in chlorine at 80°C and pH 2-3. Since there was substantially no free acid present, dissolution of FeO and other undesirable metals was minimized. It could be carried out advantageously in sea water instead of fresh water (Gupta, 1990; Roorda and Queneau, 1973).

Thomas and Fray (1981) studied aqueous chlorination to recover zinc from low grade oxide ores, residue, and zinc ferrite. The dissolution of zinc likely takes place according to the following equations:

$$ZnO + Cl_2(aq) \rightarrow ZnCl_2 + \tfrac{1}{2}O_2 \quad (A1\text{-}32)$$

$$ZnFe_2O_4 + Cl_2\,(aq) \rightarrow ZnCl_2 + Fe_2O_3 + ½O_2 \qquad (A1\text{-}33)$$

In comparison to H_2SO_4, the dissolution of iron was much lower. The novel feature of the study is that leaching was conducted at temperatures as low as 4°C, which is advantageous since below 9°C and at 1 atm pressure, chlorine forms solid chlorine hydrate.

$$Cl\,(g) + nH_2O \rightarrow Cl_2nH_2O\,(s) \qquad (A1\text{-}34)$$

where n=6-8. This provides a very convenient way to transport and to store it.

4.6 Hypochlorite Leaching of Molybdenite

Hypochlorite is considered as the strongest oxidizing reagent among the various chloride-based lixiviants. It can attack a stable sulphide mineral like molybdenite under ambient conditions. A hypochlorite solution generated in situ by the electrolysis of brine solution can also be used for the treatment of mercury, gold, and silver ores (Gupta et al, 1990).

Low grade molybdenite concentrates, often associated with rhenium, are recovered as by-products from porphyric ores. It is difficult to upgrade by flotation without losing too much recovery. Cox et al (1958) first demonstrated such concentrates could be leached with hypochlorite. A 3% hypochlorite solution could dissolve 100% of the sulphide in 30 minutes at room temperature. The reaction is assumed as:

$$7NaClO + MoS_2 + 4e \rightarrow MoO_4^{2-} + S_2O_3^{2-} + 7NaCl \qquad (A1\text{-}35)$$

The leach liquor was subjected to an ion exchange process to prepare a pure molybdenum solution before precipitating molybdic acid through neutralization of the solution with HNO_3.

$$Na_2MoO_4 + 2HNO_3 \rightarrow MoO_3 + 2NaNO_3 + H_2O \qquad (A1\text{-}36)$$

Bhappu et al (1965) found that the reaction did not follow Equation A1-35 when hypochlorite was present in excess. It was postulated that some intermediate sulphur-bearing species such as $S_2O_3^{2-}$ or S^o were likely to be oxidized into SO_4^{2-}.

$$MoS + 9OCl^- + 6OH^- \rightarrow MoO_4^{2-} + 2SO_4^{2-} + 9Cl^- + 3H_2O \qquad (A1\text{-}37)$$

Warren et al (1978, 1983) investigated hypochlorite leaching of rougher concentrates containing a small amount of molybdenum (0.3%) and a large amount of copper (12%). The efficient extraction of molybdenum was achieved at pH 9 with the addition of sodium carbonate. In the presence of carbonate ions, the extraction was improved, which was attributed to the formation of a $CuCO_3$ aqueous complex in weakly acidic solutions. The highest recovery (~98%) could be achieved in the pH range 9-10 because it did not favour the formation of copper molybdate. At the same time, CO_3^{2-} could remove Ca^{2+} from the solution to prevent from the formation of insoluble calcium molybdate.

4.7 Hypochlorite Leaching of Mercury Ore

Pilot plant tests on hypochlorite leaching of different cinnabar ores containing 0.381-1.9 kg.t^{-1} has been reported (Scheiner et al, 1970; Henrie et al, 1971; Gupta, 1990). The ground ores (90-96% <- 250 μm) were leached with hypochlorite in an electrolytic cell, followed by the cementation of Hg by zinc dust. The resultant Zn-Hg amalgam, analyzing 40% Hg, was distilled at 500-600°C to recover pure mercury. Hypochlorite solution oxidized the cinnabar to the sulphate, then further hydrolysed to the basic sulfate.

$$HgS + 4OCl^- \rightarrow HgSO_4 + 4Cl^- \qquad (A1\text{-}38)$$

$$3HgSO_4 + 2H_2O \rightarrow HgSO_4.2HgO + 2H_2SO_4 \qquad (A1\text{-}39)$$

These mercury compounds have limited solubilities in neutral solutions, but they dissolve in sodium chloride electrolyte solution and form a soluble tetrachloro mercury complex.

4.8 Hypochlorous Acid Leaching

Hypochlorous acid can dissolve metals such as Cu, Ni, Zn etc. without bringing the associated iron into the solution. Hypochlorous acid leaching of two different sulphide minerals has been investigated at the laboratory scale (Cho, 1987). Pure chalcopyrite and 89% pure sphalerite were ground to 90-250 μm. More than 90% extraction of Cu and Zn was achieved in 1 hour using 0.3 M hypochlorous acid at ambient temperature. The consumption of the acid varied from 3.1 to 4.4 mole per mole of sphalerite. The following reactions were suggested for the leaching of sphalerite.

$$3ZnS + 6HClO \rightarrow 3Zn^{2+} + 2S + 2SO_4^{2-} + 2H^+ + 6Cl^{+-} + 2H_2O \qquad (A1\text{-}40)$$

$$ZnS + 4HClO \rightarrow Zn^{2+} + SO_4^{2-} + 4Cl^- + 4H^+ \qquad (A1\text{-}41)$$

5 METHODOLOGY AND TECHNOLOGY

5.1 Earlier Chlorination Processes

5.1.1 The Plattner Process

The process of gold extraction by chlorination adopted by Plattner (around 1860) can be described as follows (Eissler, 1900):

a) The auriferous concentrates having been perfectly oxidized were moistened with water and put into a wooden vat, coated with tar and rosin and having a false bottom.

b) Chlorine gas, generated by decomposing salt and of manganese peroxide with sulphuric acid, was introduced between the false and true bottoms for 15-58 hours. Then, the gas was shut off and the vat allowed to stand for a few hours. Fresh water was then added to wash the soluble gold trichloride until a test showed that there was no trace of gold.

c) A prepared solution of iron sulphate was next carefully added to this drawn-off solution, and the gold deposited as a black or brownish precipitate. The precipitate was filtered, washed, melted and cast into almost pure gold ingots.

For the concentrates with some types of pyrite, roasting was needed. All metals, except gold, had to be converted into their oxides. In the presence of lead, roasting had to be carried out carefully, starting with a very low temperature. The chlorine gas had to be free from hydrochloric acid, which dissolved the oxides and caused the formation of hydrogen sulphide, which precipitated the dissolved gold.

From the generator the gas was forced through clear water, by which the hydrochloric acid was absorbed. If the roasting was perfect, the metallic gold was dissolved in the chlorinated water and extracted. However, if there remained a small quantity of unreacted sulphides or arsenosulphides, it was preferable to use chlorine gas, the extraction was performed in the following way as shown in Figure A1-4.

In Figure A1-4, "C" is a glass cylinder with a neck "b". At the base was a layer of small clean quartz fragments, then a layer of fine quartz sand, which formed a filter. The roasted, moistened ore was placed over the sand as loosely as possible. The cylinder had a cover of wood or indiarubber, in which a glass pipe "c" was fixed, and dipped into another cylinder containing rolled, stiff blotting paper or pieces of blotting paper, or shavings of wood moistened with alcohol. For treating 20 ounces of roasted sulphides, the glass vessel "A" was charged with 1 ounce of pulverized manganese peroxide, 4 ounces of hydrochloric acid, and 1 ounce of sulphuric acid, mixed with 1 ounce of water. The bottle "B" contained water.

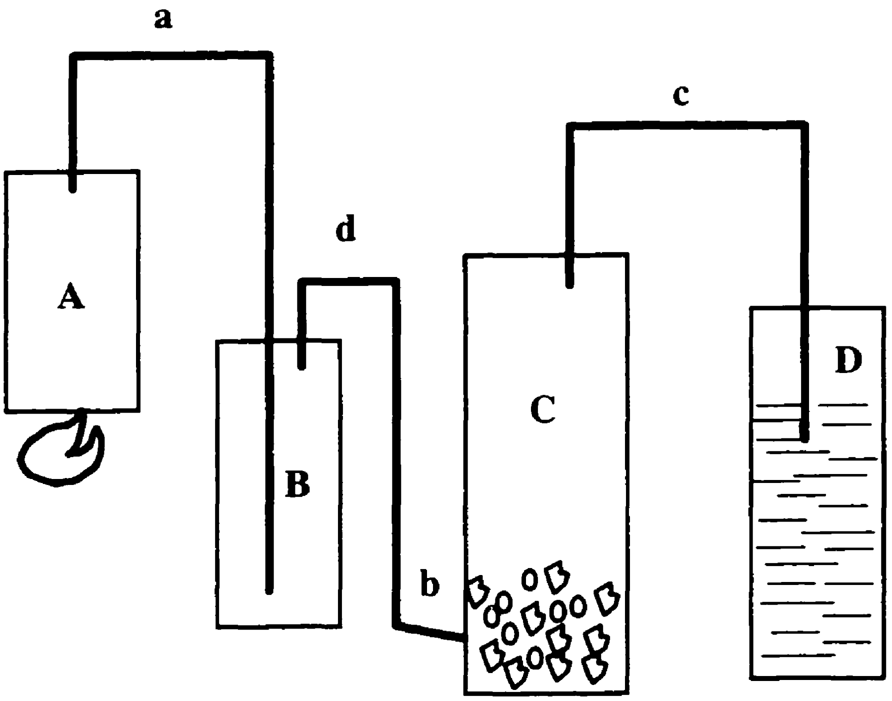

FIGURE A1-4 Chlorination Test Apparatus (after Eissler, 1900)

The presence of lead, zinc, antimony and copper sulphides did not interfere with chlorination as long as roasting was taken to completion. If the roasting was not properly finished, the undecomposed sulphides and sulphates consumed a great deal of chlorine, and the chlorides of lead and antimony formed were carried into the precipitating vat. Both were precipitated as a white powder (as chlorides) by dilution with the washing water. The lead would be precipitated by sulphuric acid prior to gold precipitation, lasting for two hours, and this was especially required if there was a great deal of lead in the ore and roasting was performed with salt.

After the lead precipitate was deposited on the bottom, the clear solution above was transferred to another vat to precipitate gold with iron sulphate. Fine gold particles contained 40-50% silver resisted chlorination, unless in the finest state of pulverisation, as the silver formed an impermeable coating of silver chloride, which could only be removed by a chlorinated solution of salt, which dissolved the chlorides of both silver and gold. The formation of silver chloride prevented complete chlorination of gold.

The presence of lime and talc made the chlorination of roasted ores very difficult, but the addition of salt during roasting solved this problem. When salt was used in roasting, according to Plattner, gold first formed auric chloride ($AuCl_3$) far below red heat. At 200°C, it lost a part of its chlorine, and at 240°C, changed into a sub-chloride (AuCl), which was not soluble in the cold water. At red heat, it was converted into metallic gold.

Iron sulphate was the precipitant usually employed, but hydrogen sulphide was also used. When some drops of the solution of iron sulphate were put into a gold solution, a dark brown powder (metallic gold) settled down. Sulphur dioxide (sulphurous acid) is an excellent precipitant for gold, which precipitated in the metallic state in the form of a dark powder. Copper sulphide was another precipitant used. It was converted into sulphate, which dissolved, while gold was deposited in the metallic state. Iron sulphide and lead sulphide were also used as precipitant. The reactions with these three sulphides are similar to H_2S (Eissler, 1900).

$$3CuS + 2AuCl_3 = Au_2S_3 + 3CuCl_2 \qquad (A1\text{-}42)$$

$$3FeS + 2AuCl_3 = Au_2S_3 + 3FeCl_2 \qquad (A1\text{-}43)$$

$$3PbS + 2AuCl_3 = Au_2S_3 + 3PbCl_2 \qquad (A1\text{-}44)$$

If salt was added to the roasting charge in the presence of copper or zinc, most of copper and zinc were converted into soluble chlorides. Copper sulphide or zinc sulphide produced by precipitation was mixed with the precipitated gold. In this case, precipitation with sulphides was more favourable.

5.1.2 Improved Plattner Processes

Several improved chlorination methods were developed after the Plattner process appeared. The principal ones are briefly presented as follows (Eissler, 1900):

The Mears Process

The roasted ore was moistened with a small quantity of water, then charged into an iron lead-lined barrel which revolved, and into which gas was forced. By this means the ore was kept constantly stirred and tumbled.

In California, a good deal of the gold in sulphides made the gold so highly alloyed with silver that was not easily dissolved by chlorine. It was almost impossible to dissolve this alloy, even in aqua regia, unless the coating formed on the gold particles was constantly removed by rubbing. Part of the silver became chloride which coated the gold particles and retarded further action of the chlorine. However, there was no difficulty in treating such material in a revolving barrel, because mechanical attrition rubbed off the silver chloride coating.

An the Deloro Mine, the ores were gold-bearing arsenopyrite containing 42% arsenic. The roasted concentrates were chlorinated by the Mears process. In the precipitation stage, the lime contained in the ore gave rise to unexpected difficulties. The usual precipitant, ferrous sulphate, was found to form a voluminous precipitate of principally calcium sulphate along with the gold. In order to avoid this, sulphuric acid was added to remove the lime, but this proved to be too tedious. Eventually, the chloride liquor was allowed to filter slowly through a mass of charcoal. The charcoal containing the gold was burned in a open pan to recover the gold bullion.

The Von Pateras and Roesner Process

Based on the solubility of silver chloride in a concentrated salt solution, this process was adapted for the processing gold, silver, and copper ores. Copper chloride and gold chloride are soluble in water, whereas silver chloride is not. If a concentrated salt solution is not used, silver chloride would remain behind in the residue. To solve this problem, chlorine was passed through a salt solution to saturation to dissolve gold, silver and copper simultaneously.

Auriferous silver ores were submitted to chloridizing roasting, then they were charged into vats and washed with the cold solution of salt saturated with chlorine. The washed waters were drawn off into the precipitating tanks and diluted with clear water, which produced a white precipitate of silver chloride. After 12 hours, the fluid above was drawn off into the gold-precipitating tanks, where the gold was precipitated by a solution of iron sulphate. When all the gold had settled, the fluid was drawn off into the third copper-precipitating tank, where the copper was precipitated with scrap iron.

5.2 Recent Processes

5.2.1 Merrill Slimes (*Also see section 3.1, Chapter 3*)

After Merrill slimes are chlorinated, the slurry is filtered to separate insoluble AgCl and $PbCl_2$ precipitates. Na_2SO_3 (or sulphur dioxide) is added to the filtrate to precipitate gold. The solution is then filtered to recover the gold precipitate, which is melted to obtain gold bullion with a fineness of 995 (Finkelstein, 1966).

5.2.2 Gold Gravity Concentrates (Also see 3.1, Chapter 3)

Laboratory and pilot results obtained by the Anglo American Research Laboratory showed that the wet chlorination process could recover gold with 999.5 parts per thousand gold fineness from gravity concentrates (Finkelstein et al, 1966).

A (907 kg (2000 lbs) gold gravity concentrate sample (6% Au, 60% sulphide, 29% tramp metal) was first roasted in a rotary kiln at 800°C. The roasted concentrate was leached with the addition of 500 lbs (226.8 kg) concentrated hydrochloric acid, 2000 lbs (907 kg) water, and 250 lbs (113.4 kg) chlorine gas. Then, the chlorinated slurry was filtered. Gold was precipitated from the filtrate with the addition of 30 lbs (13.6 kg) sulphur dioxide. Finally, the gold precipitant was melted to produce gold bullion with a fineness of 999. Gold recovery was 99% with a silver recovery of 90% (Finkelstein, 1966).

5.2.3 Carbonaceous Refractory Ores

The main purpose of chlorination is to oxidize the carbonaceous material and humic acid as well as to decompose pyrite so that the entrained gold becomes amenable to cyanidation.

At Carlin, a so-called "double oxidation" was developed. In order to oxidize pyrite and thus reduce the consumption of gaseous chlorine, a slurry at 40-50% solids, at an optimum temperature (82°C) and with an addition of 25 $kg.t^{-1}$ of sodium carbonate was agitated and aerated for 12 hours. Air (oxygen) and soda reacted with pyrite to form soluble sulphates and iron oxides, and thus the consumption of gaseous chlorine was significantly reduced even without roasting of the ore. Two commercial operations that use chlorination are Carlin and Jerritt Canyon (Nevada, USA). Gold dissolution of 85%-90% is obtained by chlorination. The chlorinated slurry is subsequently neutralized to pH 10-11 for cyanidation (Scheiner et al, 1971; Guay et al, 1973; Guay, 1980).

5.2.4 Hypochlorite Leaching of Gold Ores

The authors used three kinds of gold samples: an artificial gold precipitate with 99.5% gold; a free milling ore containing 9.5 $g.t^{-1}$ Au, and a refractory ore sample containing 10.5 $g.t^{-1}$ Au, 38.1% Fe as well as 41.2% S. By using NaOCl, NaCl and HCl, 90-95% gold extractions were obtained. For the refractory ore, pressure oxidation in an autoclave at 210°C was required with the additions of 10 $kg.t^{-1}$ $Ca(OCl)_2$, 3% HCl, and 2 $kg.t^{-1}$ NaCl (Yen et al. 1990).

5.2.5 Gold-bearing Sulphide Concentrate and Its Calcine

The concentrate treated contained 50 g.t^{-1} Au, 24 g.t^{-1} Ag, 29% Fe_2O_3 and 20% S. For the concentrate, using gaseous chlorine and HCl, leaching was conducted at 90°C for 6 hours, and 98.9% gold extraction was obtained; for the calcine of the concentrate, a 97.9% gold recovery was obtained under the same operating conditions, but at 20°C. Results show again that in hot solutions, pyrite is much more easily oxidized, and thus the consumption of chlorine is reduced (Li, 1992).

6 CONCLUSIONS

- Over 100 years ago, chlorination followed by precipitation was the principal technology for extracting gold from both free milling ores and sulphide ores. Since the cheaper and simpler method of cyanidation was first introduced to the gold industry in 1887, widespread chlorination has disappeared.

- Gold chlorination has recently again been studied at the laboratory and pilot plant scale because of its advantages of very fast leaching rates, attacking carbon and other organic materials in refractory gold ores, and reduced environmental problems.

- Compared with cyanidation, less copper is dissolved in the chlorine medium, and therefore, it is beneficial to treat some copper-gold ores by chlorination. Based on the solubility of silver chloride in concentrated salt solutions, the chlorination of gold-silver ores can be conducted in a saturated salt solution, and then the pregnant solution diluted to precipitate silver.

- It has been shown that many of sulphides commonly associated with gold are readily oxidized by aqueous chlorine. In order to maximize extraction of gold and reduce the consumption of chlorine, roasting prior to chlorination is generally needed for the treatment of sulphide gold ores or gravity gold concentrates (the main gangue minerals are always sulphides).

- In hot solutions (80-90°C) with the addition of sodium carbonate and vigorous agitation, sulphides, such as pyrite, are much more easily and quickly oxidized. Oxygen and soda react with pyrite to form soluble sulphate and iron oxides, and therefore, chlorine consumption can be significantly reduced even without prior roasting.

- There would be merit in conducting test work to see if the chlorination-precipitation is a feasible method for the further upgrading of gold gravity concentrates. For example, gold gravity concentrates with high sulphur contents can be subjected to such treatments with or without roasting, elevating temperature and with vigorous agitation in the presence of sodium carbonate. Hypochlorous acid can selectively leach Cu, Zn, Ni without bringing the associated iron into solution. Whether it has similar selectivity for gold gravity concentrates might also be worth exploring.

APPENDIX 4-1 Settling Distance as a Function of Time

Initial acceleration is size independent (Kelly and Spottiswood, 1982), therefore, at very beginning of a settling period, denser particles will travel fast than all the less dense ones. After this short period, settling velocity will be size dependent, as a result, coarser light particles will catch and overpass finer denser particles.

Assuming all the particles are spheres and settle in a centrifugal field at the same centrifugal acceleration, 60 'g'. Since their Reynolds' Numbers are high (Table A4-1), Newton equation can be used. The settling distance as a function of settling time can be approximately calculated according to the following equations:

$$R = \frac{d v_r \rho}{\mu} \qquad \text{A4-1}$$

$$S = A\ V_o \ln \frac{2 + e^{\frac{t}{A}} + e^{-\frac{t}{A}}}{4} \qquad \text{A4-2}$$

$$V_o = \sqrt{\frac{2(\delta - \rho)\ 60g\ V_{ol}}{\pi \rho\ r^2\ Q}} \qquad \text{A4-3}$$

$$A = \frac{k'}{2\ V_o} \qquad \text{A4-4}$$

$$k' = \frac{\delta\ V_o^2}{(\delta - \rho) 60g} \qquad \text{A4-5}$$

where

d: diameter of a particle, cm^{-1}

v_r: velocity at radial distance r, $cm.s^{-1}$

μ: the viscosity of the fluid medium, 0.01 $g.cm^{-1}.s^{-1}$ for water at 20°C

V_o: terminal settling velocity, $cm.s^{-1}$

S: settling distance, cm

t: settling time, second

V_{ol}: the volume of spherical particle, cm^3

Q: Coefficient of resistance, 0.4 for spherical particle

Reynolds' Numbers and settling distance as a function of settling time for tungsten, silica and magnetite particles settling in a 60 'g' centrifugal field are illustrated in Tables A4-1, A4-2 and A4-3, respectively.

TABLE A4-1 Settling Velocities and Reynolds' Numbers

Time (s)	$R_{Si1000\ \mu m}$	$V_{Si1000\ \mu m}$	$R_{Mag300\ \mu m}$	$V_{Mag300\ \mu m}$	$R_{W50\ \mu m}$	$V_{W50\ \mu m}$	$R_{W15\ \mu m}$	$V_{W15\ \mu m}$
0	0	0	0	0	0	0	0	0
0.0001	36.6	3.66	14.1	4.71	2.8	5.58	0.8	5.57
0.0006	218.8	21.88	83.8	27.93	16.4	32.80	4.7	31.34
0.0011	396.5	39.05	149.7	49.91	28.7	57.42	7.5	50.19
0.0016	566.4	56.64	209.4	69.81	39.0	78.06	9.2	61.54
0.0021	725.8	72.58	261.4	87.13	47.1	94.28	10.1	67.59
0.0026	872.7	87.27	305.1	101.70	53.2	106.41	10.6	70.61
0.0031	1005.7	100.57	340.8	113.59	57.6	115.14	10.8	72.07
0.0036	1124.5	112.45	369.2	123.07	60.6	121.25	10.9	72.76
0.0041	1229.1	122.91	391.5	130.49	62.7	125.44	11.0	73.09
0.0046	1320.2	132.02	408.6	136.21	64.1	128.28	11.0	73.24
0.0051	1398.6	139.86	421.7	140.57	65.1	130.19	11.0	73.31
0.0056	1465.5	146.55	431.6	143.85	65.7	131.46	11.0	73.34
0.0061	1522.2	152.22	439.0	146.32	66.2	132.31	11.0	73.36
0.0066	1570.0	157.00	444.5	148.16	66.4	132.87	11.0	73.37
0.0071	1610.0	161.00	448.6	149.53	66.6	133.24	11.0	73.37
0.0076	1643.3	164.333	451.6	150.55	66.7	133.49	11.0	73.37
0.0081	1670.9	167.09	453.9	151.30	66.8	133.65	11.0	73.37
0.0086	1693.8	169.38	455.6	151.86	66.9	133.75	11.0	73.37
0.0091	1712.7	171.27	456.8	152.26	66.9	133.82	11.0	73.37
0.0096	1728.3	172.83	457.7	152.57	66.9	133.87	11.0	73.37
0.0101	1741.1	174.11	458.4	152.79	67.0	133.90	11.0	73.37
0.0106	1751.6	175.16	458.9	152.95	67.0	133.92	11.0	73.37
0.0111	1760.2	176.02	459.2	153.07	67.0	133.94	11.0	73.37
0.0116	1767.3	176.73	459.5	153.16	67.0	133.94	11.0	73.37
0.0121	1773.1	177.31	459.7	153.23	67.0	133.95	11.0	73.37
0.0126	1777.8	177.78	459.8	153.28	67.0	133.95	11.0	73.37
0.0131	1781.7	178.17	459.9	153.31	67.0	133.96	11.0	73.37
0.0136	1784.8	178.48	460.0	153.34	67.0	133.96	11.0	73.37
0.0141	1787.4	178.74	460.1	153.36	67.0	133.96	11.0	73.37
0.0146	1789.5	178.95	460.1	153.37	67.0	133.96	11.0	73.37
0.0151	1791.3	179.13	460.1	153.38	67.0	133.96	11.0	73.37
0.0156	1792.7	179.27	460.2	153.39	67.0	133.96	11.0	73.37

TABLE A4-2 Settling Distance (cm) vs Settling Time for a Relatively Long Period

Time	Silica (μm)			Magnetite (μm)			Tungsten (μm)	
(second)	100	300	1000	100	300	1000	15	50
0	0	0	0	0	0	0	0	0
0.0001	0.000183	0.000183	0.000183	0.000235	0.000235	0.000235	0.000279	0.000279
0.0006	0.006437	0.006541	0.006579	0.008334	0.008427	0.008460	0.009713	0.009941
0.0011	0.020525	0.021576	0.021985	0.026993	0.027957	0.028321	0.030428	0.032639
0.0016	0.040383	0.044369	0.046093	0.054147	0.057984	0.059547	0.058632	0.066687
0.0021	0.063957	0.073709	0.078443	0.087474	0.097328	0.101721	0.091080	0.109949
0.0026	0.089730	0.108308	0.118456	0.124966	0.144645	0.154302	0.125718	0.160275
0.0031	0.116737	0.146966	0.165470	0.165124	0.198567	0.216658	0.161431	0.215781
0.0036	0.144416	0.188662	0.218780	0.206934	0.257820	0.288084	0.197656	0.274964
0.0041	0.172453	0.232579	0.277672	0.249745	0.321283	0.367838	0.234125	0.336697
0.0046	0.200681	0.278091	0.341452	0.293157	0.388015	0.455161	0.270707	0.400167
0.0051	0.229010	0.324736	0.409464	0.336925	0.457252	0.549300	0.307343	0.464810
0.0056	0.257392	0.372179	0.481104	0.380904	0.528389	0.649529	0.344004	0.530238
0.0061	0.285801	0.420178	0.555829	0.425008	0.606955	0.755159	0.380677	0.596188
0.0066	0.314225	0.468566	0.633162	0.469184	0.674591	0.865548	0.417355	0.662485
0.0071	0.314657	0.517222	0.712682	0.513404	0.749025	0.980105	0.454036	0.729012
0.0076	0.371093	0.566066	0.794029	0.557650	0.824050	1.098295	0.490717	0.795690
0.0081	0.399531	0.615038	0.876898	0.601910	0.899574	1.219639	0.527400	0.862469
0.0086	0.427970	0.664100	0.961026	0.646179	0.979302	1.343709	0.564083	0.929314
0.0091	0.456410	0.713223	1.046197	0.690453	1.051329	1.470129	0.600765	0.996203
0.0096	0.484850	0.762388	1.132226	0.734730	1.125733	1.598567	0.637448	1.063121
0.0101	0.513290	0.811583	1.218963	0.776009	1.203867	1.728735	0.674131	1.130058
0.0106	0.541730	0.860799	1.306281	0.823289	1.280297	1.860384	0.710814	1.197007
0.0111	0.570170	0.910028	1.394076	0.867570	1.356798	1.893297	0.747497	1.263964
0.0116	0.598610	0.959266	1.482261	0.911851	1.433351	2.127287	0.784180	1.330927
0.0121	0.627051	1.008512	1.570767	0.956132	1.509942	2.262194	0.820863	1.397894
0.0126	0.655491	1.057762	1.659534	1.000413	1.586561	2.397882	0.857545	1.464863
0.0131	0.683931	1.107015	1.748516	1.044695	1.663201	2.534233	0.894228	1.531833
0.0136	0.712372	1.156270	1.837683	1.088976	1.739856	2.671147	0.930911	1.598805
0.0141	0.740812	1.205527	1.926973	1.133258	1.816523	2.808539	0.967594	1.665777
0.0146	0.769252	1.254784	2.012389	1.177539	1.893198	2.946335	1.007277	1.732750
0.0151	0.797693	1.304043	2.105902	1.221821	1.969879	3.084475	1.040960	1.799722
0.0156	0.826133	1.353302	2.195492	1.266102	2.046564	3.222906	1.077643	1.866696

TABLE A4-3 Settling Distance (cm) vs Settling Time for a Relatively Short Period

Time (second)	Silica (μm)			Magnetite (μm)			Tungsten (μm)	
	100	300	1000	100	300	1000	15	50
0	0	0	0	0	0	0	0	0
0.00010	0.000183	0.000183	0.000183	0.000235	0.000235	0.000235	0.000279	0.000279
0.00015	0.000412	0.000412	0.000412	0.000529	0.000529	0.000530	0.000626	0.000627
0.00020	0.000731	0.000732	0.000733	0.000940	0.000941	0.000941	0.001112	0.001115
0.00025	0.001140	0.001143	0.001145	0.001467	0.001470	0.001471	0.001733	0.001741
0.00030	0.001639	0.001645	0.001648	0.002110	0.002116	0.002118	0.002489	0.002504
0.00035	0.002226	0.002238	0.002242	0.002867	0.002878	0.002882	0.003378	0.003406
0.00040	0.002899	0.002921	0.002928	0.003738	0.003757	0.003763	0.004379	0.004443
0.00045	0.003659	0.003693	0.003705	0.004722	0.004752	0.004762	0.005534	0.005617
0.00050	0.004503	0.004554	0.004572	0.005817	0.005862	0.005878	0.006813	0.006925
0.00055	0.005430	0.005504	0.005530	0.007021	0.007087	0.007110	0.008204	0.008367
0.00060	0.006437	0.006541	0.006579	0.008333	0.008427	0.008460	0.009713	0.009941
0.00065	0.007524	0.007666	0.007718	0.009753	0.009880	0.009926	0.011336	0.011646
0.00070	0.008688	0.008877	0.008947	0.011277	0.011447	0.011508	0.013070	0.013481
0.00075	0.009928	0.010174	0.010265	0.012904	0.013125	0.013206	0.014910	0.015445
0.00080	0.011240	0.011556	0.011674	0.014632	0.014916	0.015020	0.016852	0.017535
0.00085	0.012624	0.013022	0.013171	0.016458	0.016818	0.016949	0.018892	0.019750
0.00090	0.014076	0.014571	0.014757	0.018381	0.018829	0.018994	0.021027	0.022088
0.00095	0.015595	0.016201	0.016432	0.020398	0.020950	0.021154	0.023252	0.024548
0.00100	0.017178	0.017913	0.018195	0.022507	0.023179	0.023429	0.025563	0.027128
0.00105	0.018823	0.019705	0.020046	0.024707	0.055515	0.025818	0.027956	0.029826
0.00110	0.020529	0.021576	0.021985	0.026993	0.027957	0.028321	0.030428	0.032639
0.00115	0.022291	0.023524	0.024010	0.029365	0.030505	0.030938	0.032973	0.035566
0.00120	0.024109	0.025550	0.026123	0.031820	0.033157	0.033669	0.035589	0.038606
0.00125	0.025980	0.027650	0.028322	0.034355	0.035912	0.036512	0.038272	0.041754
0.00130	0.027902	0.029826	0.030606	0.036967	0.038768	0.039468	0.041018	0.045011
0.00135	0.029873	0.032074	0.032977	0.039656	0.041726	0.042537	0.043823	0.048373
0.00140	0.031890	0.034394	0.035432	0.042417	0.044783	0.045717	0.046685	0.051838
0.00145	0.033951	0.036785	0.037972	0.045249	0.047939	0.049009	0.049600	0.055404
0.00150	0.036055	0.039245	0.040595	0.048150	0.051192	0.052411	0.052564	0.059069
0.00155	0.038200	0.041774	0.043303	0.051116	0.054540	0.055924	0.055576	0.062831
0.00160	0.040383	0.044396	0.046093	0.054147	0.057984	0.059547	0.058632	0.066687
0.00165	0.042603	0.047030	0.048966	0.057238	0.061520	0.063280	0.061728	0.070635
0.00170	0.044858	0.049754	0.051921	0.060389	0.065149	0.067122	0.064864	0.074673

APPENDIX 8-1 Data of Béliveau Table Tails Processing

1 Test 1: Knelson Concentrator with Table Tails 1 Diluted with 212 μm Silica (4:1)

CONCENTRATE

Size (μm)	Mass (g)	Mass (%)	Grade (g.t^{-1})	Recovery (%)
+300	12.5	10.89	76	20.2
212-300	20.4	17.83	30	48.0
150-212	25.5	22.26	423	48.6
106-150	17.0	14.82	831	64.4
75-106	18.2	15.92	1557	68.8
53-75	11.1	9.69	3314	73.0
38-53	6.6	5.79	11834	82.9
25-38	2.2	1.95	73116	90.6
-25	1.0	0.85	498239	85.3
Total	114.5	100.00	7183	82.6

TAILS

Size (μm)	Mass (g)	Mass (%)	Grade (g.t^{-1})	Recovery (%)
+300	34.3	6.39	11	79.8
212-300	1271.7	23.81	6	52.0
150-212	1529.2	28.63	7	51.4
106-150	801.7	15.01	10	35.6
75-106	605.7	1.34	21	31.2
53-75	358.9	6.72	38	27.0
38-53	261.2	4.89	62	17.1
25-38	122.3	2.29	138	9.4
-25	49.1	0.92	1695	14.7
Total	5341.2	100.00	32	17.4

FEED

Size (μm)	Mass (g)	Mass (%)	Grade (g.t^{-1})	Distribution (%)
+300	353.8	6.48	13	0.5
212-300	1292.2	23.68	11	1.4
150-212	1554.7	28.50	14	2.2
106-150	818.7	15.01	27	2.2
75-106	623.9	11.44	66	4.1
53-75	370.0	6.78	136	5.1
38-53	267.8	4.91	353	9.5
25-38	124.5	2.28	1445	18.1
-25	50.1	0.92	11307	56.9
Total	5455.7	100.00	182	100.0

2 Test 2: Knelson Concentrator with Table Tails 2 Diluted with 212 μm Silica (4:1)

CONCENTRATE

Size (μm)	Mass (g)	Mass (%)	Grade (g.t^{-1})	Recovery (%)
+300	12.5	11.07	4557	48.9
212-300	20.3	18.04	4724	51.7
150-212	28.1	24.97	6254	68.1
106-150	21.1	18.74	10241	85.1
75-106	19.5	17.33	15882	94.4
53-75	7.5	6.52	28237	96.1
38-53	2.8	2.50	56367	94.8
25-38	0.7	0.59	169158	92.6
-25	0.3	0.24	428490	82.1
Total	112.6	100.00	12916	81.1

TAILS

Size (μm)	Mass (g)	Mass (%)	Grade (g.t^{-1})	Recovery (%)
+300	388.4	6.89	153	51.1
212-300	1338.6	23.75	67	48.3
150-212	1688.7	29.96	49	31.9
106-150	942.4	16.72	40	14.9
75-106	738.9	13.11	25	5.6
53-75	318.5	5.65	27	3.9
38-53	143.2	2.54	63	5.2
25-38	56.4	1.00	159	7.4
-25	21.4	0.38	1177	17.9
Total	5636.4	100.00	60	18.9

FEED

Size (μm)	Mass (g)	Mass (%)	Grade (g.t^{-1})	Distribution (%)
+300	400.8	6.97	290	6.5
212-300	1359.0	23.64	137	10.4
150-212	1716.8	29.86	150	14.4
106-150	963.5	16.76	264	14.2
75-106	758.5	13.19	433	18.3
53-75	325.8	5.67	663	12.0
38-53	146.0	2.54	1187	9.7
25-38	57.0	0.99	2128	6.8
-25	21.7	0.38	6503	7.9
Total	5749.0	100.00	312	100.0

3 Test 3: Knelson Concentrator with Original Total Table Tails

CONCENTRATE

Size (μm)	Mass (g)	Mass (%)	Grade (g.t^{-1})	Recovery (%)
+300	16.5	9.91	4263	63.2
212-300	15.1	9.11	8484	68.5
150-212	22.3	13.41	11367	81.8
106-150	24.0	14.44	9804	86.4
75-106	36.1	21.72	7629	85.7
53-75	25.6	15.40	8479	87.8
38-53	16.4	9.89	11839	90.1
25-38	7.5	4.53	32345	89.9
-25	2.6	1.59	163698	74.8
Total	166.1	100.00	12335	81.5

TAILS

Size (μm)	Mass (g)	Mass (%)	Grade (g.t^{-1})	Recovery (%)
+300	104.7	4.81	391	36.8
212-300	144.1	6.62	410	31.5
150-212	247.7	11.38	228	18.3
106-150	289.0	13.69	125	13.6
75-106	506.1	23.25	91	14.4
53-75	403.2	18.52	75	12.2
38-53	279.5	12.84	77	9.9
25-38	140.8	6.47	195	10.2
-25	52.7	2.42	2764	25.1
Total	2176.9	100.00	213	18.5

FEED

Size (μm)	Mass (g)	Mass (%)	Grade (g.t^{-1})	Distribution (%)
+300	121.1	5.17	917	4.4
212-300	159.3	6.80	1178	7.5
150-212	270.0	11.52	1147	12.3
106-150	322.0	13.74	846	10.8
75-106	542.2	23.15	593	12.8
53-75	428.7	18.30	576	9.8
38-53	296.0	12.63	730	8.6
25-38	148.4	6.33	1825	10.8
-25	55.3	2.36	10444	23.0
Total	2343.0	100.00	1073	100.0

4 Test 4: Falcon Concentrator with Original Total Table Tails

CONCENTRATE

Size (μm)	Mass (g)	Mass (%)	Grade (g.t^{-1})	Recovery (%)
+300	29.8	8.22	1740	30.7
212-300	35.4	9.75	1750	18.3
150-212	54.8	15.10	1350	13.6
106-150	64.2	17.70	1290	15.0
75-106	71.1	19.59	1160	14.2
53-75	47.0	12.95	1270	14.4
38-53	39.9	10.99	2840	19.1
25-38	11.2	3.08	15870	46.6
-25	9.5	2.62	84460	85.6
Total	362.8	100.00	4153	33.4

TAIL A

Size (μm)	Mass (g)	Mass (%)	Grade (g.t^{-1})	Recovery (%)
+300	5.7	3.38	1001	3.4
212-300	8.4	5.00	984	2.4
150-212	15.1	9.02	963	2.7
106-150	24.1	14.42	644	2.8
75-106	37.6	22.48	471	3.1
53-75	33.7	20.17	415	3.4
38-53	31.1	18.59	603	3.2
25-38	7.9	4.71	1053	2.2
-25	3.7	2.23	3298	1.3
Total	167.2	100.00	688	2.6

TAIL B

Size (μm)	Mass (g)	Mass (%)	Grade (g.t^{-1})	Rec. (%)
+300	4.8	4.61	414	1.2
212-300	6.2	5.95	1033	1.9
150-212	10.2	9.76	1044	2.0
106-150	15.5	14.91	727	2.0
75-106	22.9	21.94	521	2.1
53-75	19.6	18.79	463	2.2
38-53	18.8	18.02	563	1.8
25-38	4.6	4.38	811	1.0
-25	1.7	1.64	407	0.1
Total	104.2	100.00	636	1.5

TAIL C

Size (μm)	Mass (g)	Mass (%)	Grade (g.t^{-1})	Recovery (%)
+300	175.1	5.29	622	64.7
212-300	235.3	7.11	1112	77.3
150-212	378.7	11.44	1174	81.7
106-150	515.7	15.58	861	80.2
5-106	706.4	21.34	664	80.7
53-75	520.0	15.71	636	80.0
38-53	569.0	17.19	788	75.9
25-38	133.1	4.02	1438	50.3
-25	76.8	2.32	1595	13.1
Total	3310.0	100.00	852	62.6

FEED

Size (μm)	Mass (g)	Mass (%)	Grade (g.t^{-1})	Distribution (%)
+300	215.4	5.46	782	3.7
212-300	285.3	7.23	1186	7.5
150-212	458.7	11.63	1185	12.1
106-150	619.6	15.71	894	12.3
75-106	837.9	21.24	694	12.9
53-75	620.3	15.73	666	9.2
38-53	658.7	16.70	897	13.1
25-38	156.7	3.97	2429	8.4
-25	91.7	2.33	10228	20.8
Total	3944.2	100.00	1143	100.0

APPENDIX 8-2 Data of Meston Table Tails Processing

1 Test 1: Knelson Concentrator with Original Meston Resources Table Tails

CONCENTRATE

Size (μm)	Mass (g)	Mass (%)	Grade (g.t^{-1})	Recovery (%)
+850	27.12	17.78	9519	81.0
600-850	19.92	13.06	17892	55.5
425-600	14.95	9.80	9991	42.4
300-425	20.38	13.36	8504	45.5
212-300	18.46	12.10	9157	44.6
150-212	18.43	12.08	16075	61.7
106-150	11.12	7.29	20380	61.4
75-106	6.99	4.58	32948	51.7
53-75	4.21	2.76	61393	38.1
38-53	4.22	2.77	181225	33.0
25-38	2.05	1.34	620750	37.0
-25	4.72	3.09	787067	50.0
Total	152.57	100.00	51584	45.64

TAILS

Size (μm)	Mass (g)	Mass (%)	Grade (g.t^{-1})	Recovery (%)
+850	479.79	9.62	126	19.0
600-850	537.64	10.78	532	44.5
425-600	495.75	9.94	410	57.6
300-425	464.77	13.73	303	54.5
212-300	643.37	12.90	326	55.4
150-212	766.56	15.37	240	38.3
106-150	571.56	11.46	249	38.6
75-106	397.99	7.98	541	48.3
53-75	224.43	4.50	1869	61.9
38-53	149.62	3.00	10365	67.0
25-38	24.94	0.50	87037	63.0
-25	10.97	0.22	339466	50.2
Total	4987.00	100.00	1880	54.4

FEED

Size (μm)	Mass (g)	Mass (%)	Grade (g.t^{-1})	Distribution (%)
+850	506.91	9.86	628	1.9
600-850	557.56	10.84	152	3.7
425-600	510.70	9.94	690	2.0
300-425	705.15	13.72	540	2.2
212-300	661.83	12.87	573	2.2
150-212	784.99	15.27	612	2.8
106-150	582.68	11.34	634	2.1
75-106	404.98	7.88	1101	2.6
53-75	228.64	4.45	2965	3.9
38-53	153.84	2.99	15052	13.4
25-38	26.99	0.53	127579	20.0
-25	15.69	0.31	474098	43.1
Total	5139.97	100.00	3355	100.0

2 Test 2: Knelson Concentrator Meston Resources Total Table Tails Diluted with 212 μm Silica (3:1)

CONCENTRATE

Size (μm)	Mass (g)	Mass (%)	Grade (g.t^{-1})	Recovery (%)
+850	20.51	13.93	9861	60.3
600-850	11.52	7.82	9833	25.1
425-600	7.92	5.38	11011	52.3
300-425	12.70	8.63	8133	65.4
212-300	21.91	14.88	4465	68.5
150-212	28.89	19.62	4593	63.9
106-150	15.81	10.74	7754	69.0
75-106	11.30	7.67	13295	65.1
53-75	6.28	4.27	30876	59.3
38-53	4.93	3.35	139904	58.4
25-38	2.03	1.38	508997	59.4
-25	3.44	2.34	765571	65.6
Total	147.24	100.00	37760	60.9

TAILS

Size (μm)	Mass (g)	Mass (%)	Grade (g.t^{-1})	Recovery (%)
+850	226.68	2.31	588.6	39.8
600-850	263.96	2.69	1278.9	74.9
425-600	262.00	2.67	303.9	47.7
300-425	554.42	5.65	98.5	34.6
212-300	1683.88	17.16	26.8	31.5
150-212	2871.23	29.26	26.1	36.1
106-150	1739.81	17.73	31.7	31.1
75-106	1193.24	12.16	67.5	34.9
53-75	554.42	5.65	240.0	40.7
38-53	323.82	3.30	1514.6	41.6
25-38	76.54	0.78	9240.7	40.6
-25	62.80	0.64	22007.8	34.4
Total	9812.80	100.00	364.2	39.1

FEED

Size (μm)	Mass (g)	Mass (%)	Grade (g.t^{-1})	Distribution (%)
+850	247.19	2.48	1358	3.7
600-850	275.48	2.77	1637	4.9
425-600	269.92	2.71	618	1.8
300-425	567.12	5.69	278	1.7
212-300	1705.79	17.13	84	1.6
150-212	2900.12	29.12	72	2.3
106-150	1755.62	17.63	101	2.0
75-106	1204.54	12.09	192	2.5
53-75	560.70	5.63	583	3.6
38-53	328.75	3.30	3590	12.9
25-38	78.57	0.79	22153	19.1
-25	66.24	0.67	60622	44.0
Total	9960.04	100.00	917	100.0

3 Test 3: Knelson Concentrator with Meston Resources -150 μm Table Tails

CONCENTRATE

Size (μm)	Mass (g)	Mass (%)	Grade ($g.t^{-1}$)	Recovery (%)
106-150	39.78	32.98	13309	78.4
75-106	25.28	20.97	24292	76.6
53-75	15.70	13.02	36624	68.8
38-53	16.10	13.35	123665	56.2
25-38	6.97	5.78	510588	58.0
-25	16.75	13.90	967742	64.7
Total	120.60	100.00	194813	63.4

TAIL

Size (μm)	Mass (g)	Mass (%)	Grade ($g.t^{-1}$)	Recovery (%)
106-150	1065.42	42.44	137	21.6
75-106	625.18	24.90	300	23.4
53-75	370.55	14.76	703	31.2
38-53	357.88	14.26	4350	43.8
25-38	63.16	2.52	40800	42.0
-25	28.18	1.12	313779	35.3
Total	2510.37	100.00	5405	36.6

FEED

Size (μm)	Mass (g)	Mass (%)	Grade ($g.t^{-1}$)	Distribution (%)
106-150	1105.20	42.01	611	1.8
75-106	650.47	24.72	1233	2.2
53-75	386.24	14.68	2163	2.3
38-53	373.98	14.21	9495	9.6
25-38	70.13	2.67	87518	16.6
-25	44.94	1.71	557670	67.5
Total	2630.97	100.00	14088	100.0

4 Test 4: Knelson Concentrator with Meston Resources -150 μm Table Tails with Magnetite Pre-fed

CONCENTRATE

Size (μm)	Mass (g)	Mass (%)	Grade (g.t^{-1})	Recovery (%)
106-150	4.30	2.58	178	0.7
75-106	2.44	1.46	207591	74.4
53-75	1.43	0.86	343220	62.0
38-53	3.12	1.87	599975	49.8
25-38	4.07	2.44	820579	45.3
-25	9.25	5.55	936140	48.5
Magnetite	142.07	85.24	1805	100.0*
Total	166.68	100.00	90746	49.1
Gold Distribution in Concentrate				
Component	**Mass (g)**	**Mass (%)**	**Grade (g.t^{-1})**	**Recovery (%)**
Enriched	24.61	14.76	604188	98.3
Magnetite	142.07	85.24	1805	1.7
Total	166.68	100.00	90746	100.0
To Original Table Tails +			604188	41.1

* The magnetite used did not contain gold, but the magnetite separated from bulk concentrate contained some gold due to the entrainment.

\+ The recovery referred to the entire size range of the original table tails.

TAIL

Size (μm)	Mass (g)	Mass (%)	Grade (g.t^{-1})	Recovery (%)
106-150	939.31	41.75	114	99.3
75-106	588.46	26.16	296	25.6
53-75	336.41	14.95	895	38.0
38-53	308.89	13.73	6117	50.2
25-38	54.29	2.41	74390	54.7
-25	22.26	0.99	412825	51.5
Magnetite *	33.75		0	0.0
Total	2249.63	100.00	6605	50.9

* 33.75 g of magnetite was collected from the overflow when feeding 200 g of magnetite; 24.18 g of magnetite was mixed in the Knelson Concentrator tails (200.00 - 142.07 - 33.75 = 24.18)

FEED

Size (μm)	Mass (g)	Mass (%)	Grade (g.t^{-1})	Distribution (%)
106-150	943.61	38.51	114	0.4
75-106	590.90	24.12	1152	2.2
53-75	337.84	13.79	2344	2.6
38-53	312.01	12.73	12055	12.2
25-38	58.36	2.38	126429	23.9
-25	31.51	1.29	566461	57.9
Magnetite	175.82	7.18	1459	0.8
Total	2450.06	100.00	12581	100.0

APPENDIX 8-3 Data of Hemlo Table Tails Processing

1 Test 1: Knelson Concentrator with Hemlo Total Table Tails

CONCENTRATE

Size (μm)	Mass (g)	Mass (%)	Grade (g.t^{-1})	Recovery (%)
+1700	11.98	8.06	668	8.9
850-1700	6.96	4.68	1572	4.0
600-850	7.40	4.98	1428	5.0
425-600	13.28	8.93	2222	8.0
300-425	20.60	13.85	4718	14.0
212-300	24.27	16.32	11845	22.6
150-212	27.19	18.28	32734	35.1
106-150	19.59	13.17	74180	49.9
75-106	10.99	7.39	109550	57.5
53-75	4.31	2.90	123450	59.9
38-53	1.65	1.11	317252	58.9
25-38	0.2689	0.18	514755	53.3
-25	0.2124	0.14	394599	38.7
Total	148.7031	100.00	35431	41.5

TAILS

Size (μm)	Mass (g)	Mass (%)	Grade (g.t^{-1})	Recovery (%)
+1700	85.81	1.91	951	91.1
850-1700	147.72	3.28	1779	96.0
600-850	167.45	3.72	1207	95.0
425-600	329.76	7.33	1029	92.0
300-425	543.56	12.08	1103	86.1
212-300	700.10	15.56	1407	77.4
150-212	937.00	20.83	1756	64.9
106-150	749.50	16.66	1948	50.1
75-106	510.52	11.35	1743	42.5
53-75	232.89	5.18	1531	40.1
38-53	84.53	1.88	4324	41.1
25-38	5.75	0.13	21126	46.7
-25	3.58	0.08	37077	61.3
Total	4498.15	100.00	1654	58.6

FEED

Size (μm)	Mass (g)	Mass (%)	Grade (g.t^{-1})	Distribution (%)
+1700	97.79	2.10	916	0.7
850-1700	154.68	3.33	1770	2.2
600-850	174.85	3.76	1216	1.7
425-600	543.04	7.38	1075	2.9
300-425	564.16	12.14	1235	5.5
212-300	724.37	15.59	1757	10.0
150-212	964.19	20.75	2630	19.9
106-150	769.09	16.55	3788	22.9
75-106	521.51	11.22	4015	16.5
53-75	237.20	5.10	3746	7.0
38-53	86.18	1.85	10316	7.0
25-38	6.02	0.13	43185	2.0
-25	3.79	0.08	57127	1.7
Total	4646.85	100.00	2735	100.0

2 Test 2: Knelson Concentrator with Hemlo -212 μm Table Tails

CONCENTRATE

Size (μm)	Mass (g)	Mass (%)	Grade (g.t^{-1})	Recovery (%)
150-212	52.78	36.66	60660	85.9
106-150	46.43	32.25	95492	92.5
75-106	29.56	20.53	123593	95.6
53-75	10.85	7.54	111782	96.1
38-53	3.67	2.55	337369	96.1
25-38	0.46	0.32	753401	93.3
-25	0.2036	0.14	617800	58.6
Total	143.9536	100.00	98727	91.8
To the Original Table Tails**			98727	70.8

APPENDIX 8-3 DATA OF HEMLO TABLE TAILS PROCESSING

TAIL

Size (μm)	Mass (g)	Mass (%)	Grade (g.t^{-1})	Recovery (%)
150-212	1323.81	35.01	396	14.1
106-150	1176.21	31.11	305	7.5
75-106	839.29	22.20	199	4.4
53-75	328.63	8.69	152	4.0
38-53	103.84	2.75	481	3.9
25-38	8.01	0.21	3118	6.7
-25	1.22	0.03	73059	41.4
Total	3781.01	100.00	334	8.2

FEED

Size (μm)	Mass (g)	Mass (%)	Grade (g.t^{-1})	Distribution (%)
150-212	1376.59	35.07	2707	24.1
106-150	1222.64	31.15	3919	31.0
75-106	868.85	22.14	4398	24.6
53-75	339.48	8.65	3719	8.2
38-53	107.51	2.74	11981	8.3
25-38	8.47	0.22	43850	2.4
-25	1.42	0.04	151134	1.4
Total	3924.96	100.00	39 43	100.0

3 Test 3: Knelson Concentrator with Hemlo -212 μm Table Tails with Magnetite Pre-fed

CONCENTRATE

Size (μm)	Mass (g)	Mass (%)	Grade ($g.t^{-1}$)	Recovery (%)
+150	3.31	2.03	608365	50.5
106-150	4.73	2.90	650407	64.7
75-106	4.59	2.82	571429	83.5
53-75	2.12	1.30	581897	95.3
38-53	1.63	1.00	748129	92.0
25-38	0.3852	0.24	761905	88.5
-25	0.1753	0.11	765957	64.1
Magnetite	145.92	89.60	290	100.0
Total	162.8605	100.00	65308	70.5

Gold Distribution in Concentrate

Component	Mass (g)	Mass (%)	Grade ($g.t^{-1}$)	Recovery(%)
Enriched	16.94	10.40	625354	99.6
Magnetite	145.92	89.60	290	0.4
Total	162.86	100.00	65308	100.0
To the Original Table Tails **			625354	54.1

* The magnetite used did not contain gold, but the magnetite separated from the bulk concentrate contained some gold due to the entrainment.

** The recovery referred to the whole size of the original table tails.

TAIL

Size (μm)	Mass (g)	Mass (%)	Grade (g.t^{-1})	Recovery (%)
150-212	1357.57	34.34	1450	49.4
106-150	1245.11	31.50	1350	35.3
75-106	827.70	20.94	628	16.5
53-75	386.78	9.78	157	4.7
38-53	126.09	3.19	840	8.0
25-38	7.25	0.18	5273	11.5
-25	2.29	0.06	32727	35.9
Magnetite #	34.34			0.0
Total	4006.88	100.00	1058	29.5

\# 34.34 g of magnetite was collected from the overflow when feeding 200 g magnetite, 19.74 g of magnetite was mixed in the KC tails (200.00 - 145.92 - 34.34 = 19.74)

FEED

Size (μm)	Mass (g)	Mass (%)	Grade (g.t^{-1})	Distribution (%)
150-212	1360.88	32.79	2926	26.4
106-150	1249.84	30.12	3806	31.5
75-106	932.29	20.06	3776	20.8
53-75	388.09	9.37	3328	8.6
38-53	127.72	3.08	10377	8.8
25-38	7.63	0.18	43449	2.2
-25	2.47	0.06	84768	1.4
Magnetite	180.26	4.34	235	0.3
Total	4150.00	100.00	3635	100.0

APPENDIX 8-4 Data of Snip Table Tails Processing

1 Test 1: Knelson Concentrator with Snip Coarse Table Tails (+212 μm 83.3%, -212 μm 16.7%)

CONCENTRATE

Size (μm)	Mass (g)	Mass (%)	Grade ($g.t^{-1}$)	Recovery (%)
+850	6.27	5.77	1707	37.1
600-850	6.20	5.71	2651	22.9
425-600	12.16	11.19	471	4.8
300-425	24.54	22.59	381	5.3
212-300	9.61	8.84	329	1.3
150-212	37.66	34.66	174	7.1
106-150	6.28	5.78	8522	52.0
75-106	3.68	3.39	14154	66.9
53-75	1.37	1.26	24039	70.3
38-53	0.74	0.66	79133	76.7
25-38	0.1230	0.11	122106	84.5
-25	0.0186	0.02	309516	35.2
Total	106.6516	100.00	2483	24.9

TAILS

Size (μm)	Mass (g)	Mass (%)	Grade ($g.t^{-1}$)	Recovery (%)
+850	198.41	1.68	91	62.9
600-850	621.50	5.26	89	77.1
425-600	1513.28	12.82	75	95.2
300-425	2974.92	25.20	57	94.7
212-300	4089.66	34.64	61	98.8
150-212	1078.15	9.13	80	92.9
106-150	614.18	5.20	81	48.1
75-106	411.89	3.49	63	33.2
53-75	153.65	1.30	91	29.7
38-53	70.16	0.59	254	23.3
25-38	12.48	0.11	221	15.5
-25	66.71	0.57	159	64.8
Total	11805.09	100.00	69	75.1

FEED

Size (µm)	Mass (g)	Mass (%)	Grade (g.t^{-1})	Distribution (%)
+850	204.68	1.72	141	2.7
600-850	627.70	5.27	114	6.7
425-600	1525.44	12.80	78	11.0
300-425	2999.46	25.18	59	16.4
212-300	4099.27	34.41	62	23.4
150-212	1115.81	9.37	83	8.6
106-150	620.46	5.21	166	9.5
75-106	415.57	3.49	188	7.2
53-75	155.02	1.30	302	4.3
38-53	70.90	0.60	1077	7.1
25-38	12.6046	0.11	1410	1.6
-25	66.7305	0.56	245	1.5
Total	11913.65	100.00	91	100.0

2 Test 2: Knelson Concentrator with Snip -212 µm Table Tails

CONCENTRATE

Size (mm)	Mass (g)	Mass (%)	Grade (g.t^{-1})	Recovery (%)
150-212	59.36	43.23	2732	51.8
106-150	41.02	29.87	5205	56.2
5-106	23.73	17.26	8917	68.7
53-75	8.42	6.13	16025	77.5
38-53	4.10	2.99	69029	88.8
25-38	0.5685	0.41	157754	84.1
-25	0.1156	0.08	203348	67.6
Total	137.3141	100.00	8145	68.4

TAIL

Size (μm)	Mass (g)	Mass (%)	Grade (g.t^{-1})	Recovery (%)
150-212	2729.04	34.72	55	48.2
106-150	2409.62	30.66	69	43.8
75-106	1646.31	20.95	59	31.3
53-75	654.00	8.32	60	22.5
38-53	280.32	3.57	128	11.2
25-38	51.60	0.66	329	15.9
-25	89.10	1.13	126	32.4
Total	7860.00	100.00	66	31.6

FEED

Size (μm)	Mass (g)	Mass (%)	Grade (g.t^{-1})	Distribution (%)
150-212	2788	34.87	112	19.2
106-150	2451	30.64	155	23.2
75-106	1670	20.88	184	18.8
53-75	662	8.26	262	10.7
38-53	284	3.56	1121	19.5
25-38	52	0.65	2045	6.5
-25	89	1.12	390	2.1
Total	7996	100.00	205	100.0

3 Test 3 Knelson Concentrator with Snip -212 μm Table Tails with Magnetite Pre-feed

CONCENTRATE

Size (μm)	Mass (g)	Mass (%)	Grade (g.t^{-1})	Recovery (%)
150-212	5.47	3.95	15610	28.1
106-150	5.41	3.91	35607	51.8
75-106	3.55	2.57	60215	66.6
53-75	0.89	0.64	150234	76.9
38-63	0.6258	0.45	413926	87.1
25-38	0.1704	0.12	445863	79.8
-25	0.0480	0.03	630896	72.4
Magnetite *	122.21	88.32	277	100.0
Total	138.3742	100.00	7405	62.5

Gold distribution in concentrate

Component	Mass (g)	Mass (%)	Grade (g.t^{-1})	Recovery (%)
Enriched	16.16	11.68	61295	60.5
Magnetite	122.21	88.32	277	2.1
Total	138.37	100.00	7405	62.5

* The magnetite did not contain gold. but the magnetite separated from bulk concentrate contained some gold due to the entrainment.

TAIL

Size (μm)	Mass (g)	Mass (%)	Grade (g.t^{-1})	Recovery (%)
150-212	2790.25	35.65	78	71.9
106-150	2376.23	30.36	76	48.2
75-106	1565.21	20.00	69	33.4
53-75	605.97	7.74	66	23.1
38-53	277.85	3.55	138	12.9
25-38	54.47	0.70	354	20.3
-25	156.08	1.99	74	27.6
Magnetite #	34.89			0.0
Total	7860.94	100.00	78	37.5

\# 34.89 g of magnetite was collected from the overflow when feeding 200 g magnetite, 42.90 g of magnetite was mixed in the KC tails (200.00 - 122.21 - 34.89 = 42.90)

FEED

Size (μm)	Mass (g)	Mass (%)	Grade (g.t^{-1})	Distribution (%)
150-212	2795.72	34.95	109	18.5
106-150	2381.64	29.77	156	22.7
75-106	1568.76	19.61	205	19.6
53-75	606.86	7.59	286	10.6
38-53	278.47	3.48	1068	18.1
25-38	54.64	0.68	1744	5.8
-25	156.12	1.95	268	2.6
Magnetite	157.10	1.96	215	2.1
Total	7999.31	100.00	205	100.0

APPENDIX 8-5 Data of Casa Berardi Table Tails Processing

1 Test 1: Knelson Concentrator with Casa Berardi Total Table Tails

CONCENTRATE

Size (μm)	Mass (g)	Mass (%)	Grade ($g.t^{-1}$)	Recovery (%)
+850	24.46	17.14	106	36.7
600-850	8.18	5.73	476	29.6
425-600	10.26	7.19	822	34.7
300-425	14.69	10.29	2360	64.4
212-300	18.63	13.05	4832	37.0
150-212	23.69	16.60	12500	48.5
106-150	19.79	13.86	36000	58.3
75-106	11.52	8.07	70300	55.1
53-75	6.18	4.33	78200	51.7
38-53	4.41	3.09	98500	42.6
25-38	0.69	0.48	103000	30.9
-25	0.2459	0.17	187304	19.9
Total	142.75	100.00	20966	49.4

TAILS

Size (μm)	Mass (g)	Mass (%)	Grade ($g.t^{-1}$)	Recovery (%)
+850	373.51	7.74	12	63.4
600-850	289.83	6.01	32	70.4
425-600	257.81	7.42	44	65.3
300-425	478.43	9.92	40	35.6
212-300	657.46	13.63	233	63.0
150-212	864.30	17.91	364	51.5
106-150	806.01	16.71	632	41.7
75-106	487.32	10.10	1356	44.9
53-75	270.79	5.61	1666	48.3
38-53	198.41	4.11	2946	57.4
25-38	30.82	0.64	5149	69.1
-25	9.81	0.20	18866	80.1
Total	4824.50	100.00	636	50.6

FEED

Size (μm)	Mass (g)	Mass (%)	Grade (g.t^{-1})	Distribution (%)
+850	397.97	8.01	18	0.1
600-850	296.01	6.00	44	0.2
425-600	368.07	7.41	66	0.4
300-425	493.12	9.93	109	0.9
212-300	676.09	13.61	360	4.0
150-212	887.99	17.88	688	10.2
106-150	825.80	16.62	1480	20.2
75-106	498.84	10.04	2948	24.2
53-75	276.97	5.58	3374	15.4
38-53	202.82	4.08	5024	16.8
25-38	31.51	0.63	7292	3.8
-25	10.06	0.20	22984	3.8
Total	4967.25	100.00	1220	100.0

2 Test 2: Knelson Concentrator with Casa Berardi -212 μm Table Tails

CONCENTRATE

Size (μm)	Mass (g)	Mass (%)	Grade (g.t^{-1})	Recovery (%)
150-212	37.60	28.74	16190	75.3
106-150	42.09	32.17	46860	87.2
75-106	27.64	21.12	82650	87.6
53-75	13.97	10.68	103000	84.1
38-53	8.40	6.42	186000	78.4
25-38	0.81	0.62	281000	59.9
-25	0.339	0.26	511000	47.1
Total	130.85	100.00	63185	81.6
To the Original Table Tails**			63185	77.0

APPENDIX 8-5 DATA OF CASA BERARDI TABLE TAILS PROCESSING

TAIL

Size (μm)	Mass (g)	Mass (%)	Grade (g.t^{-1})	Recovery (%)
150-212	1329.54	27.43	150	24.7
106-150	1480.98	30.55	196	12.8
75-106	975.79	20.13	331	12.4
53-75	564.58	11.65	481	15.9
38-53	418.29	8.63	1030	21.6
25-38	58.26	1.20	2620	40.1
-25	20.28	0.42	9600	52.9
Total	4847.71	100.00	384	18.4

FEED

Size (μm)	Mass (g)	Mass (%)	Grade (g.t^{-1})	Distribution (%)
150-212	1367.14	27.46	591	8.0
106-150	1523.07	30.59	1486	22.3
75-106	1003.43	20.15	2599	25.7
53-75	578.55	11.62	2956	16.9
38-53	426.69	8.57	4671	19.7
25-38	59.07	1.19	6437	3.8
-25	20.62	0.41	17844	3.6
Total	4978.56	100.00	2035	100.0

3 Test 3: Knelson Concentrator with Casa Berardi -150 μm Table Tails

CONCENTRATE

Size (μm)	Mass (g)	Mass (%)	Grade (g.t^{-1})	Recovery (%)
106-150	41.21	33.14	26400	72.7
75-106	40.81	32.83	46400	75.6
53-75	24.20	19.46	51800	76.1
38-53	15.57	12.52	93500	76.6
25-38	1.90	1.53	183200	72.9
-25	0.6515	0.52	333100	55.7
Total	124.34	100.00	50313	74.3
To the Original Table Tails**			50313	62.7

TAIL

Size(μm)	Mass (g)	Mass (%)	Grade (g.t^{-1})	Recovery (%)
106-150	1176.66	37.76	346	27.4
75-106	937.62	30.09	651	24.4
53-75	519.41	16.67	757	23.9
38-53	400.56	12.85	1113	23.4
25-38	60.10	1.93	2151	27.1
-25	21.89	0.70	7881	44.3
Total	3116.25	100.00	693	25.7

FEED

Size (μm)	Mass (g)	Mass (%)	Grade (g.t^{-1})	Distribution (%)
106-150	1217.87	37.58	1230	17.8
75-106	978.43	30.19	2559	29.8
53-75	543.61	16.78	3029	19.6
38-53	416.13	12.84	4570	22.5
25-38	62.00	1.91	7700	5.7
-25	22.55	0.70	17279	4.6
Total	3240.59	100.00	2597	100.0

4 Test 4: Knelson Concentrator with Casa Berardi -212 μm Table Tails with Magnetite Pre-feed

CONCENTRATE

Size (μm)	Mass (g)	Mass (%)	Grade (g.t^{-1})	Recovery (%)
150-212	0.77	0.48	198000	23.9
106-150	4.63	2.90	346000	64.9
75-106	4.16	2.61	443000	73.0
53-75	2.51	1.57	471000	71.7
38-53	2.24	1.40	712000	74.9
25-38	0.40	0.25	621000	61.1
-25	0.38	0.24	609000	60.3
Magnetite	144.54	90.55	273	100.0
Total	159.63	100.00	43185	67.3

Gold Distribution in Concentrate

Component	Mass (g)	Mass (%)	Grade (g.t^{-1})	Recovery(%)
Enriched	15.09	9.45	454220	99.4
Magnetite	144.54	90.55	273	0.6
Total	159.63	100.00	43185	100.0
To the Original Table Tails **			454220	63.2

* The magnetite used did not contain gold, but the magnetite separated from bulk concentrate contained some gold due to the entrainment.

** The recovery referred to the whole size of the total table tails.

TAIL

Size (μm)	Mass (g)	Mass (%)	Grade ($g.t^{-1}$)	Recovery (%)
150-212	1439.08	28.74	337	76.1
106-150	1603.09	32.01	541	35.1
75-106	934.46	18.66	731	27.0
53-75	544.11	10.86	856	28.3
38-53	405.14	8.09	1317	25.1
25-38	62.17	1.24	2530	38.9
-25	20.00	0.40	7660	39.7
Magnetite #	33.35			
Total	5041.41	100.00	664	32.7

33.35 g of magnetite was collected from the overflow when feeding 200 g magnetite, 22.11 g of magnetite was mixed in the tails of the Knelson Concentrator (200.00 - 144.54 - 33.35 = 22.11)

FEED

Size (μm)	Mass (g)	Mass (%)	Grade ($g.t^{-1}$)	Distribution (%)
150-212	1439.85	27.68	443	6.2
106-150	1607.72	30.91	1536	24.1
75-106	938.62	18.05	2691	24.7
53-75	546.62	10.51	3015	16.1
38-53	407.38	7.83	5225	20.8
25-38	62.57	1.20	6468	4.0
-25	20.38	0.39	18915	3.8
Magnetite *	177.89	3.42	222	0.4
Total	5201.04	100.00	1969	100.0

APPENDIX 8-6 Data of Aurbel Division Table Tails Processing

1 Test 1: Knelson Concentrator with Aurbel Division Total Table Tails

CONCENTRATE

Size (μm)	Mass (g)	Mass (%)	Grade ($g.t^{-1}$)	Recovery (%)
+1700	13.20	7.08	78	21.5
850-1700	45.38	24.35	3732	94.0
600-850	24.94	13.38	7757	34.4
425-600	23.40	12.56	6040	17.1
300-425	24.33	13.06	7499	23.6
212-300	22.27	11.95	10779	30.6
150-212	16.65	8.93	16037	27.7
106-150	8.69	4.66	39554	37.2
75-106	4.22	2.26	98177	47.5
53-75	1.74	0.93	225318	60.6
38-53	1.20	0.64	546313	64.0
25-38	0.2860	0.15	739708	56.2
-25	0.0517	0.03	734570	71.2
Total	186.3577	100.00	22309	46.4

TAILS

Size (μm)	Mass (g)	Mass (%)	Grade ($g.t^{-1}$)	Recovery (%)
+1700	54.85	1.05	69	78.5
+850-1700	810.75	15.52	84	6.0
600-850	657.40	12.58	560	65.6
425-600	727.64	13.93	942	82.9
300-425	860.42	16.47	688	76.4
212-300	863.60	16.53	631	69.4
150-212	722.29	13.82	966	72.3
106-150	344.34	6.59	1677	62.7
75-106	134.29	2.57	3416	52.4
53-75	35.62	0.68	7158	39.4
38-53	12.26	0.23	30034	36.0
25-38	0.72	0.01	228875	43.8
-25	1.06	0.02	14439	29.0
Total	5225.25	100.00	919	53.6

FEED

Size (μm)	Mass (g)	Mass (%)	Grade ($g.t^{-1}$)	Distribution (%)
+1700	68.05	1.26	71	0.1
850-1700	856.13	15.82	1338	12.8
600-850	682.34	12.61	823	6.3
425-600	751.04	13.88	1101	9.2
300-425	884.75	16.35	875	8.6
212-300	885.87	16.37	886	8.7
150-212	738.94	13.65	1305	10.8
106-150	353.03	6.52	2610	10.3
7 5-106	138.51	2.56	6303	9.8
53-75	37.36	0.69	17319	7.2
38-53	13.46	0.25	76045	11.4
25-38	1.01	0.02	373989	4.2
-25	1.12	0.02	47820	0.6
Total	5411.61	100.00	1655	100.0

2 Test 2: Knelson Concentrator with Aurbel Division -212 μm Table Tails with Magnetite Pre-feed

CONCENTRATE

Size (μm)	Mass (g)	Mass (%)	Grade (g.t^{-1})	Recovery (%)
150-212	9.34	5.16	64577	19.0
106-150	8.79	4.86	117150	32.3
75-106	7.90	4.37	97899	38.1
53-75	4.44	2.45	349294	85.1
38-53	3.98	2.20	558442	95.5
25-38	0.6616	0.37	630667	94.0
-25	0.0921	0.05	901759	83.2
Magnetite	145.67	80.54	632	100.0
Total	180.8737	100.00	37441	51.8
Gold Distribution in Concentrate				
Component	**Mass (g)**	**Mass (%)**	**Grade (g.t^{-1})**	**Recovery(%)**
Enriched	35.2037	1 9.46	189754	98.6
Magnetite	145.67	80.54	632	1.4
Total	180.8737	100.00	37441	100.0
To the Original Table Tails **			454220	28.1

* The magnetite used did not contain gold, but the magnetite separated from bulk concentrate contained some gold due to the entrainment.

** The recovery referred to the whole size of the total table tails.

TAIL

Size (μm)	Mass (g)	Mass (%)	Grade (g.t^{-1})	Recovery (%)
150-212	2203.66	55.52	1168	81.0
106-150	1116.77	28.14	1851	66.8
75-106	499.31	12.58	2505	61.8
53-75	116.58	2.94	2331	14.9
38-53	30.46	0.77	2477	4.6
25-38	1.42	0.04	18913	6.0
-25	0.84	0.02	19957	16.9
Magnetite #				
Total	3969.04	100.00	1590	48.2

39.42 g of magnetite was collected from the overflow when feeding 200 g magnetite, 14.91 g of magnetite was mixed in the tails of the Knelson Concentrator (200.00 - 145.67 - 39.42 = 14.91)

FEED

Size (μm)	Mass (g)	Mass (%)	Grade (g.t^{-1})	Distribution (%)
150-212	2213.00	53.33	1435	24.3
106-150	1125.56	27.12	2752	23.6
75-106	507.21	12.22	3990	15.5
53-75	121.02	2.92	15060	13.9
38-53	34.44	0.83	67605	17.8
25-38	2.08	0.05	213748	3.4
-25	0.94	0.02	106754	0.8
Magnetite*	145.67	3.51	631	0.7
Total	4149.91	100.00	3153	100.0

APPENDIX 8-7 Data of MSV Table Tails Processing

Knelson Concentrator with Aurbel Division Total Table Tails

CONCENTRATE

Size (μm)	Mass (g)	Mass (%)	Grade ($g.t^{-1}$)	Recovery (%)
+850	30.51	31.26	136	88.4
600-850	23.58	24.16	24	12.5
425-600	19.08	19.55	46	15.5
300-425	12.48	12.79	84	28.4
212-300	6.09	6.24	387	58.3
150-212	2.67	2.74	711	78.3
106-150	1.30	1.33	1961	79.7
75-106	0.81	0.83	11354	93.9
53-75	0.5499	0.56	9340	93.2
38-53	0.3688	0.38	67980	91.0
25-38	0.0531	0.05	205104	85.0
-25	0.1245	0.13	220908	90.0
Total	97.6143	100.00	933	79.7

TAILS

Size (μm)	Mass (g)	Mass (%)	Grade (g.t^{-1})	Recovery (%)
+850	195.94	15.14	3	11.7
600-850	217.38	16.80	18	87.6
425-600	236.70	18.29	20	84.5
300-425	232.35	17.95	11	71.6
212-300	177.63	13.73	10	41.7
150-212	116.88	9.03	5	21.7
106-150	61.43	4.75	11	20.4
75-106	34.29	2.65	17	6.1
53-75	14.54	1.12	26	6.8
38-53	6.13	0.47	404	9.0
25-38	0.52	0.04	3685	15.0
-25	0.43	0.03	7081	10.0
Total	1294.21	100.00	18	20.3

FEED

Size (μm)	Mass (g)	Mass (%)	Grade (g.t^{-1})	Distribution (%)
+850	226.45	16.27	21	4.1
600-850	240.96	17.31	19	4.0
425-600	255.78	18.38	22	5.0
300-425	244.83	17.59	15	3.2
212-300	183.72	13.20	22	3.5
150-212	119.55	8.59	20	2.1
106-150	62.73	4.51	51	2.8
75-106	35.10	2.52	279	8.6
53-75	15.09	1.08	365	4.8
38-53	6.50	0.47	4217	24.0
25-38	0.57	0.04	22343	11.2
-25	0.55	0.04	55064	26.7
Total	1391.82	100.00	82	100.0

IMAGE EVALUATION
TEST TARGET (QA-3)

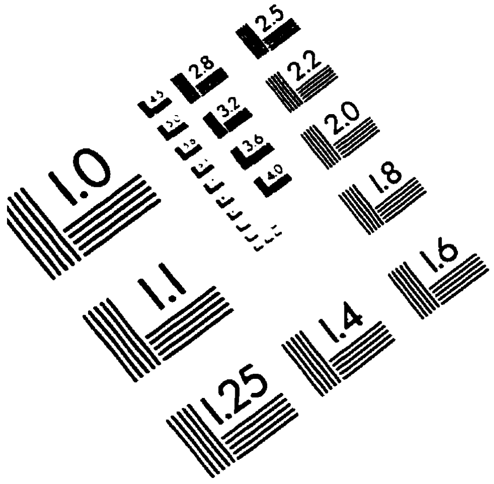

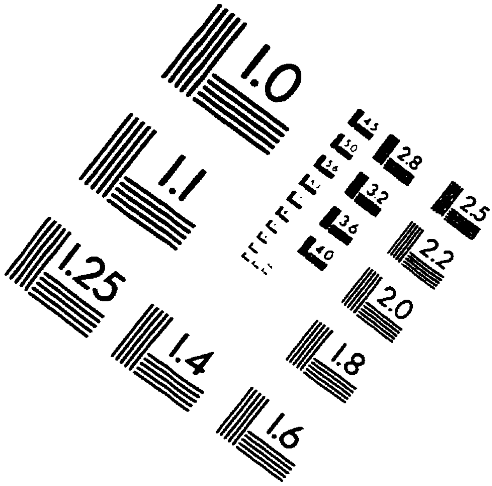

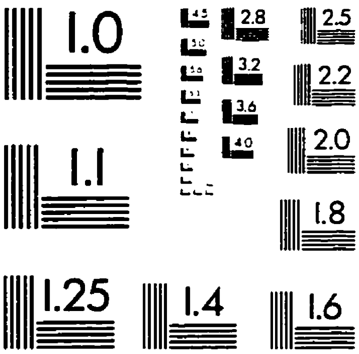

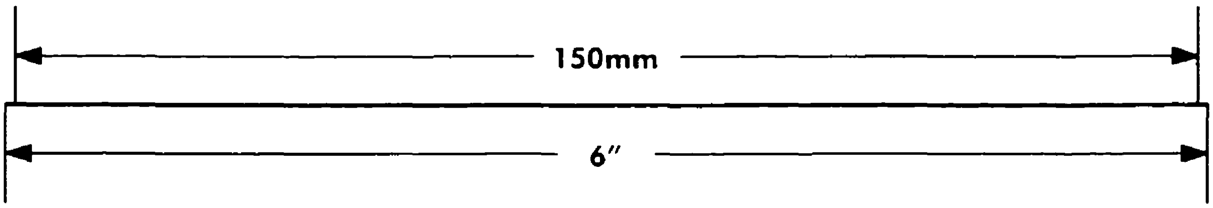

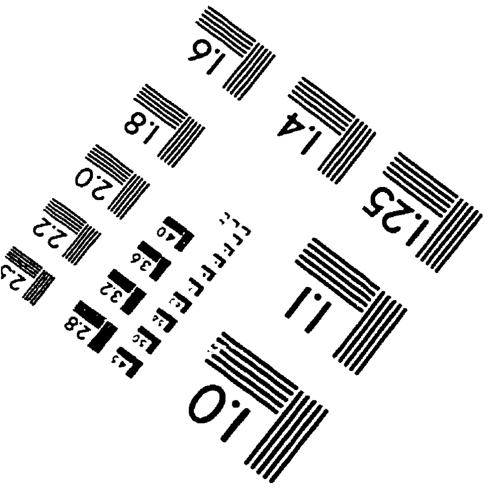

APPLIED IMAGE . Inc
1653 East Main Street
Rochester, NY 14609 USA
Phone: 716/482-0300
Fax: 716/288-5989